Mechanisms of Neurodegeneration and Neuronal Cell Loss in the Hippocampus in Murine Scrapie

Deborah A. Brown

A thesis submitted in partial fulfilment of the requirements of the University of Edinburgh for the degree of Doctor of Philosophy

The programme of research was carried out at the Neuropathogenesis Division (Unit)
The Roslin Institute and R (D) SVS, University of Edinburgh

March 2010

Declaration

I declare that the work presented in this thesis is my own, except where otherwise stated. All experiments were designed by myself, in collaboration with my supervisors Professor James Ironside and Professor Jean Manson. No part of this work has been, or will be submitted for any other degree, diploma, or qualification.

Deborah Brown

February 2009

Acknowledgements

I would initially like to thank my supervisors **Professor James Ironside** and **Professor Jean Manson** for their help and support during my PhD research. Thank you for the continual support, guidance and critical reading of the manuscript.

I would like to acknowledge members of the neuropathogenesis group, **Dr Jan Fraser**, **Janice Barr, Wing Gee Liu**, **Aileen Boyle and Gary Clarke.** In particular **Dr Jan Fraser**, who's work in the field of neurodegeneration in TSEs provided the basis for these studies presented here.

I would also like to thank **Pedro Piccardo** for his helpful discussions and guidance during the course of this project.

I would like to thank all of my friends in the Neuropathogenesis division especially **Sandra Coupar, Karen Brown** and of course the girls in the office **Alison Marshall** and **Karen Fernie** for their constant support, morale boosting, friendship, and encouragement during the preparation of this thesis.

I would like to thank the following people for excellent technical support during the course of this study:

To **Tricia Matheison** in the NPD animal facility for taking care of my experimental animals.

To the NPU histology group, especially **Gillian McGregor** for the excellent preparation of paraffin sections.

To **Karen Brown** for assistance with FACS analysis.

To **Janice Barr** for excellent advice and assistance with western blot analysis.

To **Barry Horne** in the IT department for his assistance with Adobe photoshop and preparation of Figures within this manuscript.

To all the staff at NPD who I enjoy working with and have all been supportive throughout the course of these studies

Finally thanks to my wonderful family, my sister **Janis** for listening on the phone and my sister-in-law **Lynda** for the visits to Grogport.

To my wonderful children **Alana, Adrian** and **Anthony** who mean the world to me, thanks for keeping me laughing and for making the dinner.

Last but not least thanks to my partner **Garry** for the support and love during the preparation of this manuscript.

Table of contents

Chapter 4 : Apoptosis and the caspase dependent pathway in TSE induced neuronal loss

Abbreviations

ABC	Avidin Biotin Complex
AD	Alzheimer's disease
AIF	Apoptosis-inducing factor
ALS	Amyotrophic lateral sclerosis
AMPA	α-amino-3-hydroxyl-5-methyl-4-isoxazole-propionate
Apaf-1	Apoptotic protease activating factor 1
ATP	Adenosine triphosphate
BASE	Bovine amyloidotic spongiform encephalopathy
BCA	Bicinchoninic acid
BSA	Bovine serum albumin
BSE	Bovine spongiform encephalopathy
CC	Corpus collosum
CDK	Cyclin dependent kinase
CNS	Central nervous system
CJD	Creutzfeldt-Jakob disease
CSF	Cerebrospinal fluid
CWD	Chronic wasting disease
DAB	Diaminobenzidine
DG	Dentate gyrus
DISC	Death-inducing signalling complex
dLGN	Dorsal lateral geniculate nucleus
DNA	Deoxyribonucleic acid
Dpi	Days post injection
ER	Endoplasmic reticulum
ERK	Extracellular regulated kinase
FACS	Fluorescence activated cell sorting
Fas-L	Fas ligand
Fas-R	Fas receptor
fCJD	Familial Creutzfeldt-Jakob disease
FDC	Follicular dendritic cell
FFI	Fatal familial insomnia
FITC	Fluorescein isothiocyanate
FSE	Feline spongiform encephalopathy
GFAP	Glial fibrillary acidic protein
GSK	Glycogen synthase kinase
GTP	Guanosine triphosphate
GSS	Gerstmann-Straussler-Scheinker syndrome
HD	Huntington's disease
HMWT	High molecular weight
ic	Intracerebral
iCJD	Iatrogenic Creutzfeldt-Jakob disease
ip	Intraperitoneal
JNK	Jun N-terminal kinase
kDa	Kilo daltons
LMWT	Low molecular weight
LTP	Long term potentiation
MAP	Microtubule associated protein

MEK	Mitogenic extracellular kinase
NB	Normal brain
NMDA	N-methyl-D-aspartic acid
NPU	Neuropathogenesis unit
PBS	Phosphate buffered saline
PCL	Pyramidal cell layer
PDZ	Acronym of post synaptic density protein (PSD95), Drosophila disc large tumor suppressor (DlgA), and zonula occludens-1 protein (zo-1)
PMCA	Protein misfolding cyclic amplification
PNS	Peripheral nervous system
Prion	Proteinaceous infectious particle
Prnp$^{o/o}$	PrP null
PRNP	Human prion protein gene
Prnp	Murine prion protein gene
PrP	Protease resistant protein
PrP^{c}	Normal cellular isoform of PrP
PrP^{Sc}	Abnormal disease-specific isoform of PrP
PrP$^{-/-}$	PrP null
PSD	Post synaptic density
PVDF	Polyvinylidine fluoride
RNA	Ribonucleic acid
SAF	Scrapie associated fibrils
sCJD	Sporadic Creutzfeldt-Jakob disease
SDS-PAGE	Sodium dodecyl sulfate polyacrylamide gel electrophoresis
SFV	Semliki forest virus
SINC	Scrapie incubation period
SO	Stratum oriens
SR	Stratum radiatum
TME	Transmissible mink encephalopathy
TNF	Tumour necrosis factor
TRAIL	TNF related apoptosis inducing ligand
TSE	Transmissible spongiform encephalopathy
TUNEL	Terminal deoxynucleotidyl transferase dUTP nick end labelling
vCJD	Variant Creutzfeldt-Jakob disease

Abstract

Transmissible spongiform encephalopathies (TSEs) or prion diseases are defined by infectivity and by the pathological damage they produce in the central nervous system (CNS), typically involving spongiform degeneration or vacuolation, deposition of abnormal PrP (PrP^{Sc}), glial activation and neuronal loss. Much of our understanding of the TSEs has derived from the study of murine scrapie models. The molecular basis of pathological changes is not clear, in particular the relationship between the deposition of PrP^{Sc} and neuronal dysfunction. A typical feature of TSE disease is neuronal loss, although the mechanisms leading to this loss are poorly understood. Apoptosis has been proposed as an important mechanism of TSE associated cell death, but which pathways are involved are still to be determined. The main aims of this thesis are to investigate the progression of the characteristic neuropathological changes observed in the TSE infected brain and to analyse the mechanisms involved in neuronal loss. In this study two contrasting scrapie mouse models were used : the ME7/CV model , and the 87V/VM model in which neuronal loss is targeted to different areas of the hippocampus, the CA1, and CA2 respectively. The role of the caspase-dependent pathway of apoptosis in the neuronal loss was investigated. The results of analysis of pro-apoptotic markers of disease in the two scrapie mouse models differed. The results observed in the ME7/CV scrapie mouse model suggest that apoptosis may not be the main mechanism of neuronal loss, whereas the 87V/VM model showed some indication that apoptosis may be involved.

Detailed studies in the progression of neurodegenerative changes in the ME7/CV scrapie mouse model revealed that the initial pathological change observed in the hippocampus was the deposition of PrP^{Sc} followed by a glial response, spongiform change and subsequent neuronal degeneration.

The role of the cytoskeleton and synaptic dysfunction in the neuronal damage observed in the CA1 of the ME7 infected hippocampus was analysed. Cytoskeletal disruption was observed in the post-synaptic dendritic spine, and the apical dendrites of CA1 neurons at 160days, a time point at which neurons are known to be lost. Changes in the expression of the pre-synaptic protein, synaptophysin and the post-synaptic protein PSD-95 were not observed until the terminal stage of disease when the neuronal loss is profound.

In conclusion, this research suggests that the mechanisms of neuronal loss may follow different biochemical pathways, which might not necessarily involve an apoptotic mechanism. Cytoskeletal disruption in the post-synaptic dendritic spine plays a major role in the neuronal dysfunction observed in ME7 infected CA1 neurons, although the post synaptic density does not seem to be involved .Pre-synaptic changes and disruption to the innervation of CA1 neurons is not apparent until the end stages of disease. The trigger for this cytoskeletal disruption and the subsequent neuronal loss may be the early deposition of PrP^{Sc} in the extracellular space but the precise mechanisms involved are still to be elucidated. The identification of the key events involved in the mechanisms of neruodegeneration in TSE diseases may lead to the development of therapeutic strategies to inhibit the neurodegenerative process.

Chapter 1 : Introduction and background

1.1. Transmissible spongiform encephalopathies

The transmissible spongiform encephalopathies (TSEs), or prion diseases, are fatal infectious, non-inflammatory neurodegenerative diseases of the central nervous system (CNS). They are characterised by the pathological changes observed in the CNS, which include vacuolation (Fraser, 1976; Fraser & Dickinson, 1967) gliosis and the accumulation of an abnormal form of the host sialoglycoprotein, prion protein (PrP) (Bolton et al, 1982; Bruce et al, 1989; McBride et al, 1992).

Scrapie, which naturally affects sheep and goats, is the most extensively studied member of the group of TSE diseases that affect a range of animal species and man (Table 1). These include Creutzfeldt-Jakob disease (CJD), Gerstmann-Straussler-Scheinker disease (GSS), fatal familial insomnia (FFI) and kuru in humans, bovine spongiform encephalopathy (BSE) in cattle, chronic wasting disease (CWD) in captive or free-ranging deer, feline spongiform encephalopathy in cats (FSE) and transmissible mink encephalopathy (TME) in captively-reared mink.

Over the years these diseases have been widely studied and much debate on their origins and aetiology has ensued. They share many characteristic features that can be problematic when studying the disease. They have extremely long incubation periods (up to several decades in humans), although the time from onset of the clinical illness to death of a human or animal host can be short (several weeks); they are resistant to standard decontamination methods (Taylor, 2000; Taylor, 2004); the nature of the infective agent is still uncertain (Chesebro, 1998) and the absence of a pre-mortem diagnostic test.

One of the features of these diseases is transmissibility, both within a host species, such as scrapie from sheep to sheep (Cosseddu et al, 2007) and Kuru from man to man (Gajdusek & Zigas, 1957), and across species, such as cattle BSE to humans, emerging as variant CJD (vCJD) (Hill et al, 1997). Several factors control the transmissibility of these diseases including the route of infection, (Eklund et al, 1967; Kimberlin & Walker, 1979) the infectious dose, age of host (Ierna et al, 2006; Outram et al, 1973) and the infecting strain.

Table 1. TSE diseases in humans and animals

Disease	Species	Cause
Scrapie	Sheep and goats	Transmission of infection either horizontal or maternal
BSE	Cattle	Ingestion of infected MBM in animal feed
CWD	Mule deer and elk	Unknown, appears to be spread by horizontal transmission
TME	Mink	Unknown, possible infection from animal feed containing material from infected sheep/cattle
FSE	Cats	Ingestion of infected MBM in animal feed
TSE not specifically named	Zoo animals (includes ungulates and wild cats)	Ingestion of infected MBM in animal feed
sCJD	Human	Unknown
fCJD	Human	PrP gene mutation
iCJD	Human	Surgical/medical contamination
vCJD	Human	Accidental transmission possibly from oral ingestion of BSE contaminated tissues
Kuru	Human	Ritual cannibalism
GSS	Human	PrP gene mutation
FFI	Human	PrP gene mutation
Atypical scrapie	Sheep	Not known, but observed in genotypes associated with resistance to classical scrapie
BASE	Cattle	Possibly sporadic, distinguished from classical BSE by deposition in the brain of Kuru-like plaques

Abbreviations: BSE; Bovine Spongiform Encephalopathy, CWD; Chronic Wasting Disease, TME; Transmissible Mink Encephalopathy, FSE; Feline Spongiform Encephalopathy, GSS; Gerstmann-Strausler Syndrome, FFI; Fatal Familial Insomnia BASE; bovine amyloidotic spongiform encephalopathy

1.2 The history of TSEs

1.2.1. TSEs in animals

Scrapie has been recognised for hundreds of years as a disease of sheep and goats, with the first record in the UK reported in 1732 (McGowan., 1922). Scrapie is discussed in greater detail below. Other TSEs of animals have not been documented for as long as scrapie; TME has been recognised for more than 50 years, CWD for more than 30 years and BSE for over 20 years.

TME

Transmissible mink encephalopathy (TME) is a rare disease only occurring in farmed mink, which are an end host. This disorder was first reported in 1965 by Hartsough and Burger (Hartsough & Burger, 1965) , although the disease had been recognised on mink ranches since 1947. There have been outbreaks recorded in Idaho; Wisconsin; Ontario, Canada; Finland; Germany and Russia, but it has never been recorded in the UK. The simultaneous occurrence of TME on several farms sharing the same feed firmly established it as a source of the infectious agent. The occurrence of the disease in Russia is said to have been traced to feeding carcasses of sheep affected with scrapie (Gorham J., 1991). TME has been experimentally transmitted to many other species including racoons (Eckroade et al, 1973), ferret, Syrian and Chinese hamster, rhesus monkey, sheep, goat and cattle (Barlow, 1972; Marsh & Hadlow, 1992). Attempts to transmit TME to mice usually fail (Taylor et al, 1986) although Barlow and Rennie claim success (Barlow & Rennie, 1970).

CWD

Chronic wasting disease (CWD) is a naturally occurring TSE disease of mule deer, white-tailed deer, and Rocky mountain elk. The disease is found in both captive and free ranging deer and elk populations, the latter being under much less human control

and therefore difficult to manage. CWD was first identified as a fatal wasting syndrome of captive mule deer in the late 1960s in research facilities in Colorado and was recognised as a TSE in 1978 (Williams & Young, 1980; Williams & Young, 1992). The disease was first recognised in the wild in 1981, when it was diagnosed in a free-ranging elk in Colorado (Williams & Miller, 2002). By the mid-1990s surveillance studies had confirmed that CWD was endemic in North America and apparently spreading through both wild and captive cervid populations. The exact mechanism of natural transmission of CWD in the wild is not known. Nonetheless, some form of direct or indirect horizontal transmission apparently sustains epidemics (Miller & Williams, 2003). Concentrating deer in captivity or by feeding them artificially may facilitate transmission. Maternal transmission made little, if any, contribution to the occurrence of CWD. Environmental contamination may be a possible source of transmission, excreta or decomposed carcass remains may harbour some infectivity for years (Miller et al, 2004).

Although CWD does not appear to occur naturally outside the cervid family, it has been transmitted experimentally by intracerebral injection to a number of animals, including mice, ferrets, mink, squirrel monkeys and goats (Bartz et al, 1998). More recently transgenic mice expressing PrP from mule deer, referred to as tg (Cer PrP) have been used successfully as a model for experimental transmission of CWD (Angers et al, 2006; Browning et al, 2004). Whether CWD is transmissible to humans, as has been shown for BSE, is unknown. Intracerebral infection with CWD of two lines of “humanized” transgenic mice that are susceptible to human TSE, failed to develop disease (Kong et al, 2005), suggesting there is a species barrier between CWD and humans.

BSE

In the late 1980s a new TSE emerged in cattle, bovine spongiform encephalopathy (BSE),(Wells GAH, 1987) which has accounted for the majority of TSE cases in the UK. The BSE epidemic has had devastating and far-reaching consequences for agriculture and man. It seems likely that BSE was transmitted to cattle by ingestion of TSE-contaminated protein supplements derived from rendered carcasses of sheep and cows (meat and bone meal). The exact source of this TSE and the conditions under which it emerged are unclear, although the evidence points towards the rendering processes involved in the production of meat and bone meal fed to cattle during the 1970s and 80s, playing a major role (Wilesmith et al, 1991; Wilesmith et al, 1992). The BSE agent was also subsequently found to have been transmitted to other species including domestic cats, wild felines, ungulates such as kudu and oryx (Kirkwood et al, 1990) and American bison (Kirkwood and Cunningham 1999). Surprisingly, dogs that where fed a similar commercially available diet to cats, and would have been exposed to contaminated meat and bonemeal (MBM) feed, did not seem to be naturally susceptible to the BSE agent (Bradley, 1996; Wells et al, 2003).

Transmission studies of BSE to mice consistently produced a characteristic pattern of incubation periods and neuropathology that served as a 'signature' for the BSE strain (Bruce, 2003). This same signature was observed in primary transmissions of TSE from domestic cats (Doherr, 2003) and exotic ungulate species (Cunningham et al, 2004), confirming the suspected link with BSE and providing evidence for the accidental spread of a TSE between species.

Natural and experimental scrapie

Scrapie is the most studied of the group of TSE diseases. The name 'scrapie' is an old Scottish word that describes the infected animal's tendency to scrape or scratch itself against fence posts and similar objects, resulting in the loss of fleece. Scrapie has been studied in depth for more than 50 years and for many years the aetiology of the disease was far from obvious.

The first report of intra-species transmissibility was in 1939 by two French workers, Cuille and Chelle, who inoculated healthy sheep with spinal cord from infected sheep. (Cuille' J & Chelle PL, 1936). The success rate for transmission to sheep was only 25%; further studies in goats which gave 100% transmission rate (Cuille' J & Chelle PL, 1939) convinced the research community that this was an infectious, transmissible disease.

In the natural disease, death occurs most frequently in sheep between 2 and 5 years old. Scrapie has a long incubation period, ranging from several months to years, the onset is slow and there are no visible indicators of early infection. The clinical phase of the disease is short in comparison to the protracted asymptomatic period, the symptoms of which are ataxia (abnormal gait), puritis (itching) and recumbency (inability to stand). Natural scrapie is transmissible both horizontally among the flock and vertically from ewe to lamb (Andreoletti et al, 2002). To date there is no cure and no therapeutic intervention that affects the lethal outcome.

Genetic influence on scrapie pathogenesis

Although there is no evidence for a genetically inherited TSE in animals, studies with natural and experimental scrapie of sheep have shown that the prion protein gene (*prnp*) is an important factor in disease susceptibility (Hunter et al, 1997b; Hunter et al, 1997c) . In sheep and goats polymorphisms of the PrP gene have

been strongly associated with the incidence of natural and experimental scrapie. Studies of natural scrapie have confirmed the importance of three codons (136, 154 and 171) that can encode one of two alternative amino acids , giving a range of possible variants or alleles (Hunter, 1997). Based on the variation found in the UK sheep population originally 15 three-codon genotypes were defined (Dawson et al, 1998). In this standard model, codon 136 has two possible amino acids, A and V, codon 154 has also two, R and H and codon 171 has three possible amino acids, Q, R and H (table 2). These polymorphisms are combined to form five alleles (ARQ,VRQ, AHQ,ARR,ARH), ARR and AHQ are associated with resistance; ARQ, ARH and VRQ are associated with susceptibility. These alleles can be arranged into 15 genotypes e.g. ARR/ARR, VRQ/ARQ, or ARH/AHQ (Goldmann, 2008). A five group risk classification system has been developed based on these fifteen genotypes which was modified to be applied in breeding and eradication programmes like the National Scrapie Plan of Great Britain and equivalent plans in other member states of the European Union (Dawson et al, 1998; Detwiler & Baylis, 2003).

The 15 genotypes differ widely in their susceptibility to scrapie, ranging from complete resistance for the ARR/ARR genotype to extreme susceptibility for the VRQ/VRQ genotype. There are subtle effects of specific allele pairings, generally more susceptible genotypes have younger ages at death from scrapie, different strains of scrapie occur which may attack genotypes differently. Different sheep breeds vary in the assortment of the five alleles that they predominantly encode. Furthermore, certain genotypes may be susceptible to scrapie in some breeds and resistant in others. The explanation for this is not known, but may relate to different scrapie strains circulating in different breeds, or there may be effects of other genes which modulate the effect of PrP (Baylis et al, 2004; Baylis & Goldmann, 2004)

It is still a matter of some debate whether natural scrapie is a genetic disease arising from the PrP alleles , or whether PrP controls susceptibility to an infecting agent. There is strong evidence to support the fact that scrapie is not solely a genetic disease, as not only are VRQ/VRQ sheep found in countries such as Australia and New Zealand, which do not have endemic natural scrapie (Bossers et al, 1999; Hunter et al, 1997a), it has also been shown that VRQ/VRQ sheep from the NPU Cheviot flock can survive into old age when their environment is free of scrapie infection (Foster et al, 2006; Hunter et al, 1997a).

Table 2. Sheep PrP gene – the three most important disease-related polymorphisms

Codon	Amino Acid alternatives	Single-letter code
136	Valine	V_{136}
	Alanine	A_{136}
154	Arginine	R_{154}
	Histidine	H_{154}
171	Arginine	R_{171}
	Glutamine	Q_{171}
	Histidine	H_{171}

Atypical TSEs in ruminants: Atypical scrapie, Nor98 and BASE

In 1998, an unusual type of scrapie was diagnosed in Norwegian sheep and was subsequently designated Nor98 scrapie. Active surveillance of small ruminants throughout the European Union (EU) to detect these "atypical" cases of scrapie has identified the presence of atypical forms of scrapie in a number of countries including Germany, Belgium and France (Baron et al, 2007; Buschmann et al, 2004). The

neuropathological, molecular and biochemical characteristics of Nor98 differ from those of classical scrapie. The primary structure affected in the brains of sheep infected with classical scrapie, the dorsal motor nucleus of the vagus (DMNV), is not a target in Nor98 scrapie. In western blotting analysis of protease-resistant PrP, an unusual band of low molecular weight (10-12KDa) is observed, in contrast to that of "classical" scrapie where the protease-resistant form of PrP is detected as three bands between 18 and 29 kDa corresponding to the un-, mono- and di-glycosylated forms of PrP (Baron et al, 2007). Evidence so far indicates that atypical scrapie affects animals with different PrP genotypes to those associated with classical scrapie, such as those with the $A_{136}H_{154}Q_{171}$ or $A_{136}R_{154}R_{171}$ genotypes (Benestad et al, 2008; Buschmann et al, 2004).

Experimental transmission studies of atypical scrapie material into inbred mice were unsuccessful (Benestad et al, 2008). Later the development of lines of transgenic mice expressing ovine VRQ PrP were used successfully to transmit the disease, proving that atypical/Nor98 was an infectious TSE agent (Arsac et al, 2007).

An increase in the active surveillance for detection of TSEs in ruminants identified a number of atypical TSE cases in cattle. These included the identification of a novel TSE in cattle from Italy with unusual pathology in the form of amyloid plaques in the CNS (Casalone et al, 2004). Classical cattle BSE is not associated with PrP plaque deposition in the brain. Therefore this new form of BSE was termed bovine amyloidotic spongiform encephalopathy (BASE). Further surveillance identified other apparently novel BSE phenotypes, cases were reported in Japan (Nakamitsu et al, 2006; Yamakawa et al, 2003) and other European countries (Buschmann et al, 2006); (Biacabe et al, 2004). Transmission of BASE isolates to wild-type mice produced a neuropathological and molecular disease phenotype

indistinguishable from that of BSE-infected mice, whereas the characteristics of the BASE strain were preserved in transmissions to transgenic mice expressing bovine PrP (Capobianco et al, 2007). Strikingly, the glycoform patterns of PrP^{Sc} BASE isolates and the PrP^{Sc} deposition observed in the CNS closely resembled those found in some cases of sCJD (Casalone et al, 2004)

1.2.2 Human TSEs

Kuru

During the 1950s, when research into scrapie was growing, there was an increased interest in kuru, an epidemic disease amongst the Fore-speaking people of Papua New Guinea (Zigas & Gajdusek, 1957). The clinical signs and neuropathology of the disease was strikingly similar to scrapie; this was particularly noted by Hadlow (1959), who suggested that kuru may be a transmissible disease just like scrapie (Hadlow WJ, 1959). It was discovered that the Fore tribe of Papua New Guinea participated in endocannibalism; a ritualistic form of cannibalism involving the consumption of deceased relatives (Alpers, 1965; Gajdusek, 1963). This cannibalistic ritual was shown to be responsible for the transmission of kuru (Collinge et al, 2006; Mathews et al, 1968). It was noted that a higher percentage of females than males contacted the disease, due to the predominant consumption of brain material, containing high levels of infectivity, by women and infants (Gajdusek, 1966). In comparison, the male members of the tribe mainly consumed muscle from the deceased (Hornabrook & Moir, 1970).

The initial transmission studies of kuru to wild-type mice were unsuccessful (Gajdusek & Gibbs, 1964), this may have been due to the fact that the studies were terminated as early as 3 months, which would not have been long enough to produce disease in rodent models. Experimental inoculation of kuru infected brain into

chimpanzees resulted in a spongiform encephalopathy remarkably similar to kuru in humans (Gajdusek et al, 1966); (Beck et al, 1966). Studies by Klatzo *et.al.* also revealed neuropathological similarities between kuru and CJD (Klatzo et al, 1959). These studies in the 1960s were the first to demonstrate the infectious nature of kuru and its transmissibility.

Creutzfeldt-Jakob disease (CJD)

A peculiar progressive neurological disease termed spastic pseudosclerosis and its neuropathology were first described by Hans Gerhard Creutzfeld (Creutzfeldt, 1920) and Alfons Maria Jakob (Jakob, 1921). This disease was later named Creutzfeldt-Jakob disease after its first two observers, Creutzfeldt and Jakob and is recognised to occur in several different aetiological forms: Sporadic CJD (sCJD), familial CJD (fCJD), iatrogenic CJD (iCJD) and variant CJD (vCJD)

Sporadic CJD

The sporadic form of CJD is the most common subtype of CJD, corresponding to about 80% of cases. The disease most commonly occurs in the seventh decade of life, with an average duration of illness of approximately 4-5 months. sCJD is thought to originate de novo and in terms of the prion hypothesis may be a spontaneous disease. The naturally occurring polymorphism at position 129 of the human prion protein gene (*PRNP*), which can encode either a methionine (M) or valine (V) allele, clearly influences susceptibility to sporadic CJD; there is also evidence of a strong influence of codon 129 genotype on the clinicopathological phenotype in sCJD.

Genetic or familial CJD

Familial CJD occurs as an autosomal dominant inherited disorder, associated with point mutations, deletions, or insertions in the coding sequence of the *PRNP* gene (Kovacs et al, 2002). Other familial forms of human TSE are Gerstmann-Straussler-

Scheinker disease (GSS) and fatal familial insomnia (FFI). These familial diseases are also associated with mutations in the *PRNP* gene; the most common mutation observed in GSS is the P102L mutation (Kretzschmar et al, 1991). GSS is characterised by prominent ataxia, dementia in late stages of disease, and numerous kuru and multicentric PrP amyloid plaques in the brain (Hainfellner et al, 1995; Kretzschmar, 1993).

FFI is associated with a D178N mutation of the *PRNP* gene in association with methionine at codon 129. Clinically, FFI frequently begins with disturbances of vigilance and sleep that are often neglected. The patients go on to develop hallucinatory states, autonomic disturbances such as high blood pressure and hyperthermia, disturbances of gait, disequilibrium and myoclonus. The onset of disease is between 36 and 62 years and the disease duration varies from 8 to 72 months (Krasnianski et al, 2008; Provini et al, 2008). Pathologically, FFI is characterised by severe Thalamic gliosis and neuronal loss, with little spongiform change and very scantly deposited PrP in the brain.

iCJD

This infectious form of CJD comprises cases transmitted following a range of medical and surgical procedures. The over-whelming majority of iCJD cases have been caused either by the parenteral administration of contaminated growth hormone preparations from the pituitary gland of the deceased (Caboclo et al, 2002; Cordery et al, 2003), or by contaminated grafts of dura mater (Croes et al, 2001). A few cases occurred after neurosurgery including insertion of deep brain electrodes, and corneal transplantations (Brown et al, 2006).

vCJD

This new form of human TSE was discovered in 1996 and occurred in younger individuals than those with sCJD, with distinctive clinical features and neuropathology characterised by the presence of 'florid' PrP amyloid plaques in the brain. Unlike sCJD, in vCJD the peripheral lymphoid system becomes infected early in the disease (Hill et al, 1999b; Hill et al, 1997). Transmission of brain material from vCJD affected individuals into mice produced a "signature" undistinguishable from that of BSE (Bruce et al, 1997). Incubation periods observed in specific mouse strains (Figure 1), lesion profiles in the brain and PrP^{Sc} glycoform profiles were identical to that of BSE. The most likely cause of transmission was suspected to be through dietary exposure (Bruce et al, 1997; Collinge et al, 1996; Hill et al, 1997). To date approximately 300 cases of vCJD have been identified worldwide, the majority of which have occurred in the UK (http://www.cjd.ed.ac.uk/). All cases tested were of the same *PRNP* genotype i.e. homozygous for methionine (M) at codon 129 (Colm H & knight R, 2002). Three cases of vCJD have occurred in recipients of packed red blood cells from donors who subsequently developed and died from vCJD (Llewelyn *et al*, 2004 ;Wroe *et al*, 2006). All three recipients were methionine homozygotes at codon 129 in the *PRNP* gene. A case of asymptomatic vCJD infection was detected following autopsy in a fourth recipient of packed red blood cells from a vCJD infected donor. However, this recipient was a heterozygote (methionine/valine) at codon 129 in the *PRNP* (Peden *et al*, 2004). This raised fears of the possibility of a second epidemic in MV heterozygote individuals, with an estimated 300 to 350 victims.

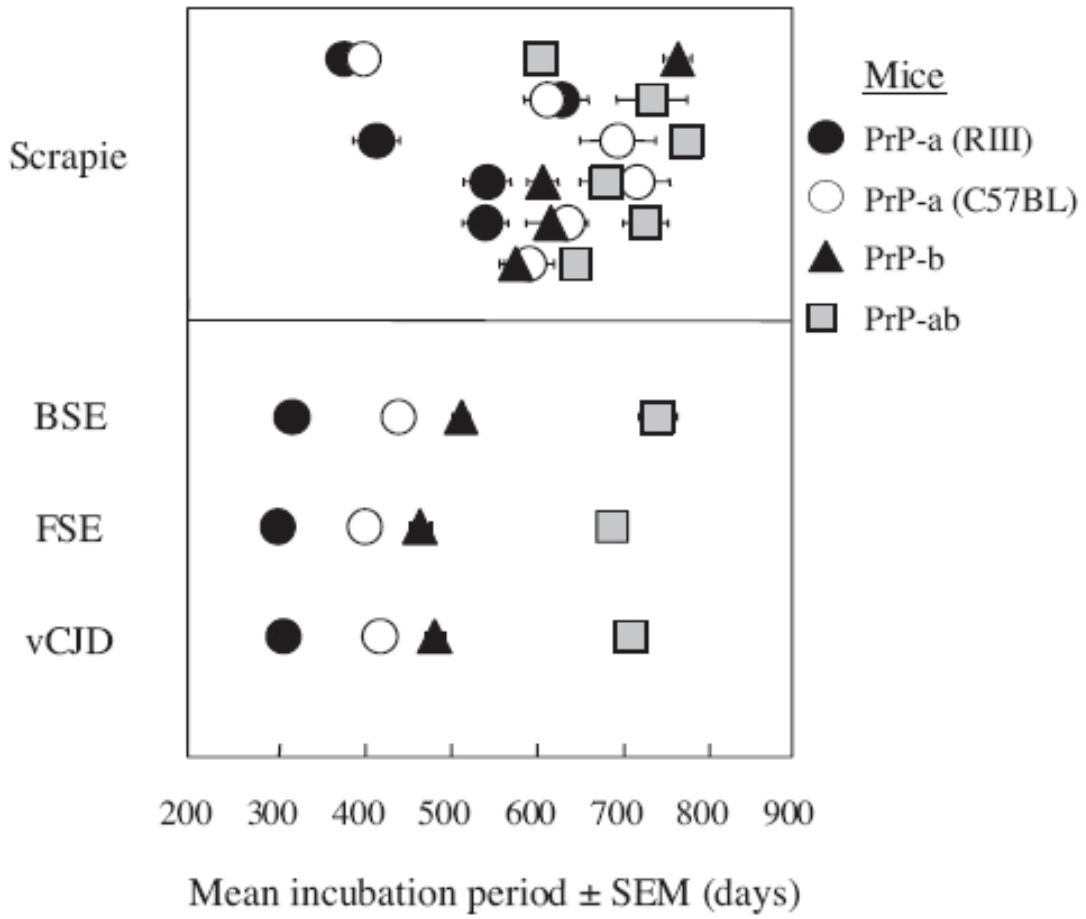

Figure 1. Incubation periods in mice injected with TSEs from naturally infected hosts. Results are shown for transmissions from six individual scrapie sheep. Pooled data from several transmissions are shown for cattle, feline spongiform encephalopathy (FSE) and human vCJD. Transmission of BSE, FSE and vCJD to inbred mice with different *prnp* genotypes show identical incubation periods, indicating that they are all from the same TSE strain. In comparison the six sheep scrapie transmissions all differ in the incubation period observed on transmission to mice. Diagram from Bruce *et.al.* 2003 British Medical Bulletin

1.3 The nature of the infectious agent

1.3.1 Viruses, viroids, virinos and SAF

The nature of the infectious agent is perhaps one of the most extensively studied aspect of TSE research and to this day remains a matter of passionate controversy. During the 20th century, different theories on the nature of the causative agent were put forward. Ranging from a sarcosporidia (1914) (M'Gowan J, 1914), a DNA-polysaccharide complex (1968) (Adams D, 1968) and a holoprion, consisting of PrP^{Sc} and a nucleic acid (Weissmann, 1991).

The properties of the scrapie agent did not fit with established criteria for how infectious diseases were known to behave i.e. the TSE pathogen is transmissible, replicates and exists as many strains with genetically stable phenotypes (Dickinson & Outram, 1979). These properties are consistent with the activity of viruses and initially the agent was thought to be a "slow virus" because of the unusually long incubation periods between time of exposure to the pathogen and the onset of symptoms (Cho, 1976). However in 1966, Alper and colleagues reported that the minimum molecular weight of the scrapie agent that still maintained infectivity was too small ($\approx 2x10^5$) to possibly be a virus (Alper et al, 1966). Later the same group demonstrated that the infectious agent was extremely resistant to treatments that normally destroy nucleic acids, such as ultraviolet and ionization radiation (Alper et al, 1967). Over the past 30 years despite extensive biochemical and electron microscopy analysis, no convincing evidence of an associated viral agent has emerged. Over the years several theories were proposed for the agent. One theory was that the infectious agent could be encoded by a viroid and, as in plants, could be a simple nucleic acid of very small size (Diener, 1973). One of the hypothese that gained some scientific support was the virino hypothesis, which was a modification of

the viral theory, in which a virino was defined as a small informational molecule, possibly a nucleic acid, that was associated with a host protein that serves as a coat (Carp et al, 1994; Kimberlin, 1982).

Any hypothesis about the nature of the agent would have to take into account a number of diverse observations, including the infectious, familial and sporadic forms of the disease and the physiochemical properties of the agent. It would also have to explain the occurrence of multiple strains or isolates of infectious agent. It has been proposed that the only way that strain differences can be accounted for is to assume that there is nucleic acid associated with the agent (Dickinson & Outram, 1988). The virino hypothesis proposes that the infectious particle is comprised of a nucleic acid that is bound to and protected by PrP host protein. The presence of a nucleic acid is key to the virino hypothesis as this is the only molecule known to biology that is capable of replication and transfer of genetic information. To explain the lack of detection, the nucleic acid must be small and around 100-1000 base pairs in size, or infact does not exist.

Scrapie associated fibrils (SAF)

Electron microscopy techniques had been used successfully to detect viruses and viroid structures, therefore this technique was used to try and identify the scrapie agent. Amyloid-like fibrillar structures termed scrapie associated fibrils (SAF) were observed in membrane fractions from infected brain after treatment with mild detergents. These SAFs were observed in brains from animals affected with the disease (Merz et al, 1981) and from CJD in humans (Merz et al, 1983) and never observed in unaffected tissue. These fibrils were identified as paired or quadruple fibrillar structures 4-6 nm in size, resembling amyloid observed in some TSE strains (Isomura et al, 1991). Prusiner identified similar structures and named them ‘prion

rods' (Prusiner et al, 1983). It is now accepted that SAF and 'prion rods' are the same structural entity, varying only in their length. Co-isolation of SAF and infectivity from spleens and brain of scrapie infected mice suggested a close association with infectivity (Rubenstein et al, 1991). The relationship between SAF and infectivity is hard to determine. Difficulties in isolating the infective agent restrict studies to crude preparations, and it is not known if the treatments used actually destroy any nucleic acid or protein components of the infectious agent. In order to properly identify the infectious agent further techniques need to be developed to isolate the agent to a high degree of purity.

1.3.2 Prions

The suggestion that the unconventional properties of the infectious TSE agent might be accounted for in a protein-only model was first proposed in 1967 by JS Griffith (Griffith, 1967), who believed that the agent was a self-replicating protein derived from a normal cellular protein. It was not until the early 1980s that progress was made furthering this hypothesis. During purification for the scrapie agent it was found that infectivity was associated with a protein that was partially resistant to proteolytic degradation and had a molecular mass of around 27-30 kDa on SDS polyacrylamide gels (Prusiner, 1982; Prusiner et al, 1982). This protein was associated with infectivity from all scrapie fractions, but not from control samples. As this was the only molecule that could be linked with infectivity, Prusiner proposed the term 'prion' to describe the scrapie agent implying that it was a proteinaceous infectious agent. The prion protein that had been isolated was found to be the product of a cellular gene on the short arm of chromosome 20 in humans and in mice located on chromosome 2 (Liao et al, 1986; Sparkes et al, 1986).

1.3.3 The prion hypothesis

The prion hypothesis suggested by Stanley Prusiner in the early 1980s claims that scrapie and related diseases were caused by prions, novel proteinaceous infectious particles that lacked a nucleic acid (Prusiner, 1982). These prion proteins (PrP) were the sole component of the infectious agent (McKinley et al, 1983). It was suggested that some insult triggers host neuronal PrP (PrP^c) to refold from the normal largely α-helical form to the predominantly β-pleated sheet disease-causing form (PrP^{Sc}). Progressively more of the cellular PrP^c being sequestered into the abnormal, protease resistant isoform which accumulates and may form amyloid.

A number of studies have produced evidence which favour the prion hypothesis. These include the generation of infectivity in neuroblastoma cells (Race et al, 1987) and the cell free conversion of PrP^c into PrP^{Sc} by Caughey and colleagues (Caughey et al, 1995). One of the most controversial studies in this field was the study by Legname. They demonstrated that a recombinant truncated fragment of mouse PrP^c can misfold *in vitro* into β sheet rich fibrils and cause a prion disease after intracerebral (ic) inoculation (Legname et al, 2004). However, a major flaw in this work is that they only produced disease in transgenic mice overexpressing PrP, but not in wild type mice, although subsequent passage of brain material from the transgenic mice produced disease in wild-type mice.

Protein misfolding cyclical amplification (PMCA)

Another approach used in an attempt to prove the prion hypothesis was the use of PMCA (protein misfolding cyclical amplification). This technique was designed to mimic PrP^{Sc} autocatalytic replication. In a cyclic manner, similar to PCR cycling, a tissue homogenate "seed" containing PrP^{Sc} is incubated with excess PrP^c, which is converted to PrP^{Sc}. The new PrP^{Sc} aggregates are then sonicated to generate multiple

smaller units for the continued formation of new PrP^{Sc} (Saa et al, 2006; Saborio et al, 2001). This technology has been used successfully to replicate the misfolded protein from diverse species (Soto et al, 2005), and to prove that the newly generated protein exhibits the same biochemical, biological and structural properties as brain derived PrP^{Sc} and is infectious to wild-type animals, producing a disease with similar characteristics as the illness produced by brain-isolated prions (Castilla et al, 2005). In the studies by Castilla *et al* only the one strain of hamster PrP^{Sc} was used, and also the *in vitro*-generated infectious agent produced disease with a delay in the incubation period. This may be associated with a loss of infectivity in the de novo produced hamster PrP^{Sc}. Further work analysing the apparent discrepancy between the amount of PrP^{Sc} produced and infectivity related these changes to the differences in the size distribution of PrP aggregates that changed their clearance rate (Weber et al, 2007).

One of the main difficulties of the prion hypothesis has been to provide a molecular explanation for the TSE strain phenomenon. The prion hypothesis suggests that different strains of TSE agent could be attributed to different conformations of PrP^{Sc}, and that each conformation would interact differently with PrP^{c} to determine strain characteristics (Bessen *et al*, 1995). Recent work has shown that PrP^{Sc} generated *in vitro* by PMCA from five different mouse TSE strains, maintains the strain-specific properties. Wild type mice inoculated with the *in vitro* generated PrP^{Sc} showed disease characteristics indistinguishable from those of the parental strains (Castilla et al, 2008). Biochemical features were also maintained upon replication of four human TSE strains. Similar studies with CWD combining the use of PMCA with transgenic mouse models demonstrated the amplification of CWD prions with unaltered strain properties (Green et al, 2008). Also revealed in this study was the ability of the PMCA technique to abrogate the inter species barrier, although the

adaptation of mouse prions to form novel cervid prions required several hundred days and subsequent stabilisation in transgenic mice (Agrimi et al, 2008). These studies provide additional support for the prion hypothesis and also that strain variation may be dependent on PrP^{Sc} properties.

However, all these studies rely on the conversion of PrP^{c} into the abnormal protease resistant form, PrP^{Sc} and that PrP^{Sc} is the infectious agent. In other conversion studies proteinase K resistant PrP was generated but this did not result in infectivity (Hill et al, 1999a). It has been suggested that the PMCA technique may be useful as a diagnostic tool to identify pre clinical cases of TSE disease. However, some studies have shown that transmission of infectivity can occur in the absence of detectable PrP^{Sc} (Barron et al, 2007; Lasmezas et al, 1997). Moreover, the detection of PrP^{Sc} in the absence of clinical symptoms of disease or infectivity has been demonstrated in transgenic mice inoculated with brain material from a case of GSS (Piccardo et al, 2007).

Although it is widely accepted that both the normal and abnormal forms of PrP are intrinsic to the disease process, the precise mechanisms by which PrP^{c} is converted into PrP^{Sc} is still not fully understood. While major improvements in the PMCA technology have provided further evidence to support the protein only hypothesis, it still remains a controversial subject within the field of TSE research.

1.4 The prion protein (PrP)

1.4.1 PrP^{c} and the PrP gene

PrP^{c} plays a key role in the pathogenesis of TSEs. PrP^{c} is a 33-35KDa sialoglycoprotein and is the product of a single host gene, *PRNP* in humans and *prnp* in mice. The gene is found on chromosome 20 in humans and chromosome 2 of mice (Liao et al, 1986; Sparkes et al, 1986) and consists of 2 or 3 exons, a single open

reading frame and a cytidine/guanidine rich promoter. The structure of the gene and the sequence of the protein are highly conserved in various mammals. Primarily, transcription of the PrP gene is found in neurons of the central and peripheral nervous system (Bendheim et al, 1992; Kretzschmar et al, 1986; Manson et al, 1992). PrP^c is also found in lower levels in heart, lung, kidney, spleen, liver, and lymphocytes (Caughey *et al*, 1988;Cashman *et al*, 1990;Mabbott *et al*, 1997).

Human and mouse genetics have made major contributions to TSE disease research, one of these being the discovery of mutations in the *PRNP* gene in families with fCJD, GSS and FFI. All familial forms of TSE disease are associated with mutations, deletions or insertions in the *PRNP* gene. Over 30 different mutations have been described (Figure 2), not all of which appear to be pathogenic (Gambetti et al, 2003; Goldfarb et al, 1991). However, it is not known whether the presence of the pathogenic mutations alone cause disease or if they influence the susceptibility to infection.

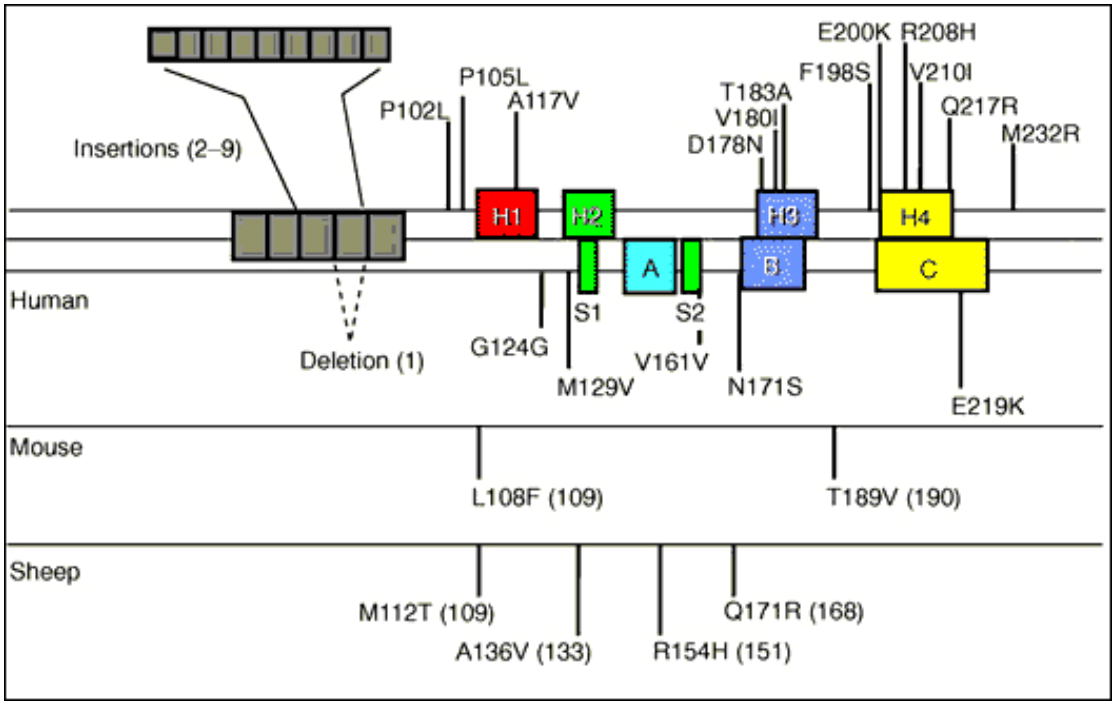

Figure 2. Mutations observed in the human, mouse and sheep *PRNP* gene

1.4.2 Structural features of the cellular (PrP^{c}) and scrapie form of PrP (PrP^{Sc})

PrP^{c} is the product of a single gene, called *Prnp*, that directs synthesis of a 254-residue protein, which contains a signal peptide for secretion, five octapeptide repeats near the amino-terminus, two glycosylation sites, and one disulphide bridge (Cohen, 1999) (Figure 3) A glycosylphosphatidylinositol (GPI) anchor attaches the protein to the outer surface of the cell membrane. PrP^{c} is constitutively expressed in the brain and other tissues of healthy individuals as three glycoforms, mono-,di- and unglycosylated, the proportions of which differ in different species (Ermonval et al, 2003). PrP^{c} has a molecular weight of 33-35 kDa and is sensitive to digestion with proteinase K. The abnormal form of the protein, PrP^{Sc} is synthesised from the normal cellular isoform PrP^{c} by a post translational process that probably occurs in endosomes (Griffiths et al, 2007; Porto-Carreiro et al, 2005). PrP^{Sc} has many

properties that differ from those of PrP^{c} ; PrP^{Sc} is insoluble in detergents, while PrP^{c} is readily solubilised under non denaturing conditions (Meyer et al, 1986). PrP^{Sc} is partially hydrolysed by proteases to form a fragment designated PrP 27-30, while PrP^{c} is completely degraded under the same conditions (Oesch et al, 1985), and PrP^{Sc} accumulates within and around cells, whereas PrP^{c} has a short half life and turns over rapidly in cells (Borchelt et al, 1990).

Differences between the normal and abnormal isoforms of the protein occur in the secondary and tertiary structures that determine conformation. Fourier transformation infrared and circular dichroism experiments have shown that the structure of PrP^{c} comprises around 43% α-helix and only 3% β-sheet, while PrP^{Sc} has 34% α-helix but incorporates a greatly increased, 43% β-sheet (Pan et al, 1993).
The protease-resistant core of PrP^{Sc} designated PrP 27-30 was originally identified as being the major component of fibrillar structures, initially termed scrapie-associated fibrils (SAF) (Merz et al, 1981) that were isolated from detergent-treated tissue extracts of scrapie infected brains.

In the brains of some animals and humans that have died of TSE diseases, amyloid plaques are found, which contain PrP^{Sc}. Amyloid is known to have a β-pleated sheet structure (Glenner et al, 1974). The secondary structure of PrP 27-30 is 50% β sheet, which on aggregation could develop into amyloid plaques.

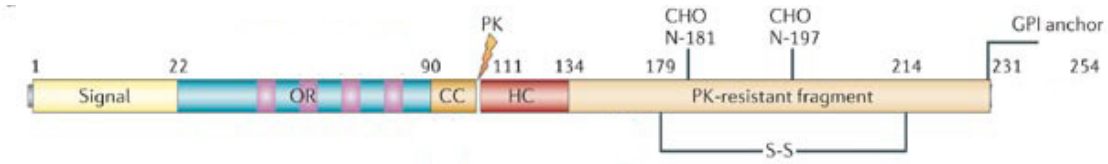

Figure 3. Structure of PrP. An outline of the primary structure of cellular PrP(PrP^c).A secretory signal peptide resides at the extreme N terminus. The numbers describe the position of the respective amino acids. CC defines the charged cluster, HC the 'hydrophobic' core. S-S indicates the single disulphide bridge. The proteinase K (PK) resistant core of PrP^{Sc} is depicted in gold and the approximate cutting site of PK within PrP^{Sc} is indicated by the lightning symbol. Figure adapted from Aguzzi *et.al.* 2008)Molecular mechanisms of prion pathogenesis. Annu.Rev.Pathol.Mech.Dis. 3: 11-40

1.4.3 The function of PrP^c

Investigating the biological activity of PrP^c is likely to be crucial for understanding the pathogenesis of TSE diseases, since alteration of its function may play a role in the disease process. PrP^c is expressed early in embryogenesis, and in the adult it is present at highest levels in neurons of the brain and spinal cord (Harris et al, 1993; Manson et al, 1992). PrP^c is also found at lower levels in glial cells of the CNS as well as in a number of peripheral cell types (Ford et al, 2002b; Moser et al, 1995). Although the function of PrP^c is not yet known, there is an abundant amount of literature describing the properties of the protein. The location of PrP^c in lipid rafts, a membrane fraction specialised in signalling, pointed towards a potential role for PrP^c in signal transduction (Taylor & Hooper, 2006). Yeast two hybrid screens have identified several signalling molecules that bind to PrP, including a neuronal phosphoprotein synapsin Ib, the adapter protein Grb2, and the still uncharacterised PrP^c interactor protein Pint1 (Spielhaupter & Schatzl, 2001), although there is no evidence for the physiological relevance of these interactions. Most of these interactors are primarily cytoplasmic proteins and are therefore unlikely to associate directly with PrP^c, which is localised to the outer surface of the plasma membrane. A

more likely candidate for interaction with PrP, would be a cell surface receptor. Both the laminin receptor (LRP/LR) (Martins, 1999) and heparin sulphate have been identified as possible cell surface receptors of PrP^c. Different isoforms corresponding to different maturation states of the laminin receptor have been identified, the main 67KDa LR being the major receptor form expressed in the brain, found within the cytoplasm and plasma membrane in most neurons and a subset of glia cells (Baloui *et al*, 2004). Heparin sulphate proteoglycan functions as a co-factor/co-receptor, mediating the binding of PrP^c to the laminin receptor (Caughey et al, 1994; Hundt et al, 2001) and may also act as a receptor for PrP^{Sc} (Horonchik et al, 2005).

There are a number of studies suggesting that PrP^c can activate transmembrane signalling pathways involved in several different phenomena, including neuronal survival, neurite outgrowth (Taylor & Hooper, 2006), and neurotoxicity. Recent studies have suggested a potential role for the P13 Kinase/AKt signalling pathway in the neuroprotective effects of PrP^C (Satoh et al, 2009; Schmalzbauer et al, 2008). In one of these studies AKt activity was found to be diminished in neurons and brain tissue from PrP deficient mice ($PrP^{-/-}$) in comparison to wild type mice. Moreover, pharmacological inhibition of AKt reduced the ability of PrP^c to protect cells against oxidative damage (Vassallo et al, 2005).

A major role for PrP^c may be in promoting neuronal survival by suppressing programmed cell death. Support for this comes from *in vitro* experiments showing that PrP^c can protect human neurons from Bax-induced apoptosis (Bounhar et al, 2001).Furthermore, the C-terminal end of Bcl-2 protein interacts with PrP^c in a yeast two-hybrid system (Kurschner & Morgan, 1995; Kurschner & Morgan, 1996). Therefore it is possible that PrP^c actually acts as a member of the Bcl-2 family. The anti-apoptotic activity of PrP^c was demonstrated in a human breast carcinoma cell line

(Diarra-Mehrpour et al, 2004).PrP^c plays a role in neuronal survival by protecting neurons in culture against oxidative stress, and brain tissue against ischemia, hypoxia, or trauma (Lo et al, 2007; McLennan et al, 2004; Weise et al, 2004)

PrP^c has been shown to be involved in the binding and metabolism of copper (Brown, 2001) (Viles et al, 1999). The octapeptide repeat region of PrP^c is able to bind copper within the physiological concentration range (Todorova-Balvay et al, 2005) , suggesting that PrP^c may have a role in normal brain metabolism of copper (Brown et al, 1997; Kramer et al, 2001). Copper interaction with PrP may also modulate the conversion of the normal protein into the pathological isoform; it has been shown that binding of copper causes a change in both the secondary and tertiary structure of PrP^c, leading to the formation of a protease resistant form (Qin et al, 2000).

Several strains of PrP-null mice have been generated to aid the search for possible biological functions of PrP^c. However, differences in the way gene disruption was achieved led to conflicting conclusions. A consistent finding in all mice devoid of PrP^c is their resistance to scrapie, and their inability to propagate infectivity. Two lines generated, referred to as $Prnp^{0/0}$ Zurich I and $Prnp^{-/-}$ Edinburgh, were viable and had no obvious neurological abnormalities (Bueler et al, 1992; Manson et al, 1994), although some minor electrophysiological and circadian rhythm defects were observed (Tobler et al, 1996). In another 2 lines, ICM $Prnp^{-/-}$ (Moore et al, 1995) and Japan $Prnp^{-/-}$ (Sakaguchi et al, 1996) the mice developed cerebellar Purkinje cell degeneration and demylination of peripheral nerves, causing late-onset ataxia. This phenotype was later discovered to be due to overexpression of a gene located downstream of PrP, termed *Prnd* whose product is a protein called doppel (Moore *et al*, 1999). These findings led to the suggestion that some of the TSE

clinical symptoms such as ataxia might be due to increased expression of doppel in the brain during disease. This was subsequently found not to be the case; TSE infection does not alter the levels of *Prnd* in the CNS and doppel expression in the brain had no influence on the incubation period, spongiform degeneration, or PrP^{Sc} deposition in TSE-infected mice (Tuzi et al, 2002).

1.4.4 A role for PrP^{c} at the synapse

Several experimental observations suggest that PrP^{c} may play a role in synaptic structure, function or maintenance. This hypothesis is consistent with the fact that synaptic pathology is often a prominent feature of TSE diseases (Jeffrey et al, 2000). Light and electron microscopic immunohistochemical studies, as well as localisation of PrP-EGFP fusion protein, indicate that PrP^{c} is preferentially concentrated along axons and in presynaptic terminals (Barmada et al, 2004; Ford et al, 2002a; Ford et al, 2002b; Laine et al, 2001; Mironov et al, 2003; Moya et al, 2000; Sales et al, 2002). Incubation of cultured hippocampal neurons with recombinant PrP induces rapid elaboration of axons and dendrites, and increases the number of synaptic contacts (Kanaani et al, 2005). This suggests that PrP^{c} may play a regulatory role in synapse formation. PrP^{c} expression has also been observed in peripheral synapses, and is concentrated at the neuromuscular junction where it is localised in the sub-synaptic sarcoplasm (Gohel et al, 1999).

Electrophysiological recordings from brain slices of $Prnp^{0/0}$ mice also support a functional role for PrP in synaptic transmission. Initially, it was reported that LTP was impaired and receptor mediated fast inhibition involving GABA-A receptors was decreased (Collinge et al, 1994; Manson, 1995), however this result has been disputed (Lledo et al, 1996). Other studies have demonstrated a positive correlation between the expression level of PrP^{c} and the overall strength of glutamatergic transmission in

the hippocampus, the range of synaptic responses increasing with the level of PrP expression (Carleton et al, 2001). *Prnp*$^{0/0}$ mice have also been shown to display several other neurobiological abnormalities that may also relate to the participation of PrP^{c} in synapse formation and function. These include alterations in nerve fibre organisation (Colling et al, 1997), circadian rhythm (Tobler et al, 1996), and spatial learning (Criado et al, 2005).

1.5 Experimental TSE strains

1.5.1 Identification of strains

Strain variation in scrapie was first recognised over 40 years ago, when experimental sheep scrapie, designated SSBP/1, was transmitted to and serially passaged in goats. Two separate passage lines were maintained which produced strikingly different clinical signs in unselected goats from the same herd, either a "drowsy" or a "scratching" syndrome (Pattison & Millson, 1961). This difference between the two isolates remained constant on repeated goat-to-goat passage which suggested that two different scrapie strains had been isolated from the original study (Chandler R L, 1961; Pattison & Millson, 1961; Pattison & Smith, 1963). The SSBP/1 inoculum was originally produced from a brain pool of 3 cheviot sheep with symptoms of natural scrapie. Serial passage of this brain material was continued in cheviot sheep with very little deviation from the original disease characteristics, incubation periods and clinical features of disease remained stable. The inoculum used in the goat transmission studies was acquired from the 18th passage of this brain pool (Pattison & Millson, 1961; Pattison & Smith, 1963).

Further studies in mice discovered that the two strains isolated from the goat studies actually contained a mixture of strains. The "drowsy" or "Chandler" isolate (Chandler R L, 1961) contained the 139A, 79A and 79V scrapie agent strains,

and the "scratching" isolate contained the 22C and 22H strains (Dickinson *et al*, 1986). Further passage of the Chandler isolate at the Rocky Mountain Laboratory in Montana USA, led to what is now know as the RML isolate, which may be a mixture of 139A and 79A strains. Most of the studies described in this thesis were performed using the ME7 strain of scrapie. This strain was originally isolated from experiments of intragastric transmission, to mice, of pooled spleen material from cases of natural scrapie (Zlotnik & Rennie, 1965). These transmission studies resulted in TSE disease initially in a group of mice termed mouse experiment 7 (ME7), subsequent passage of brain material from these mice led to the isolation of the strain that is now called ME7. In contrast, the 87V strain of scrapie has been isolated from many different breeds of sheep infected with natural scrapie following passage in VM mice (Bruce, 1985; Bruce *et al*, 1987)

Most studies into strain variation in TSEs have been carried out in mouse models of disease. Long-term studies in mice started by Alan Dickinson in the 1960s, analysing different isolates of scrapie, revealed that there were numerous strains of the scrapie agent that produce distinct patterns of disease in the infected host (Bruce & Fraser, 1991; Bruce et al, 1991). There are many strains of scrapie, each with its own distinct, reproducible disease characteristics which are stable on repeated experimental passage. Murine scrapie strains are identified on the basis of these disease characteristics, in particular the incubation periods produced in mice of defined genotypes (Figure 4) and the severity and distribution of vacuolar pathology in the brains of these mice. Additional useful indicators of disease are the particular clinical signs displayed at the end stage of the disease, changes in locomotor activity and posture and the physico chemical properties of the agent e.g. susceptibility to thermal inactivation (Dickinson & Taylor, 1978).

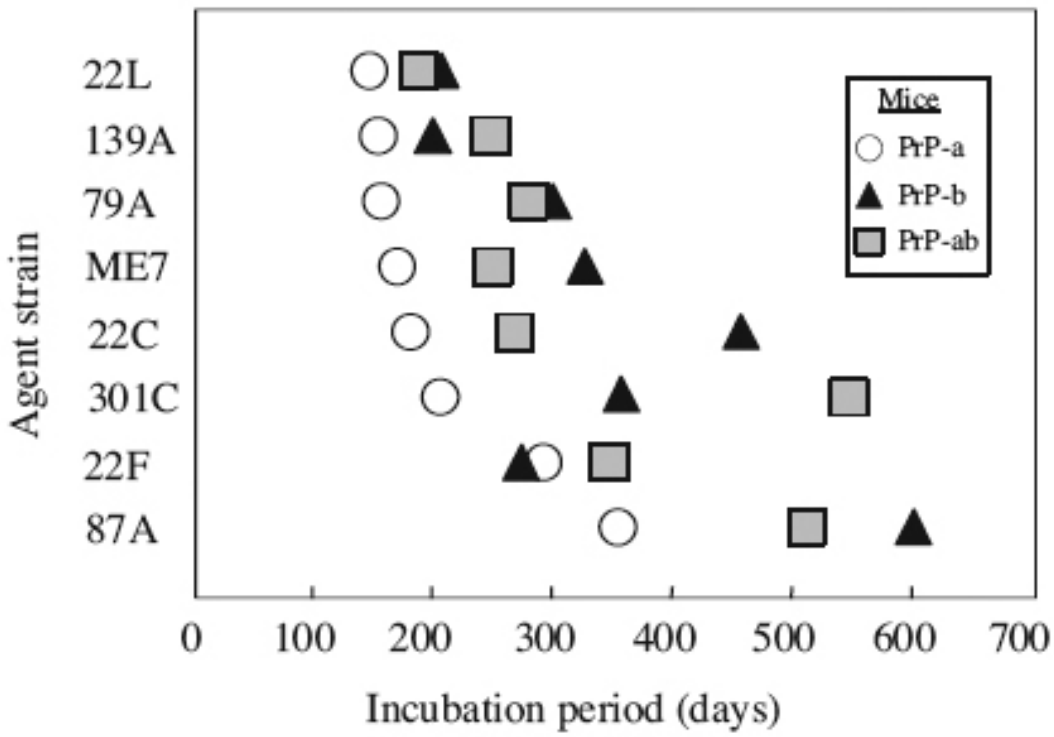

Figure 4. Incubation period data from the different strains of scrapie in the three PrP genotypes of mice. Incubation periods between intracerebral injection and the development of clinical disease for eight TSE strains in mice showing different incubation periods. All of these TSE strains had been propagated in mice of the PrP^{a} genotype. Diagram from Bruce *et.al* 2003 British Medical Bulletin.

1.5.2 Incubation periods of disease

The incubation period of TSEs is defined by the interval between initial infection of the host and the development of clinical signs of disease. Each murine scrapie strain, under standard conditions of dose, route of infection and mouse genotype, has a characteristic, highly reproducible pattern of incubation period (Figure 4). The major influence on the length of the incubation period is exerted by the *sinc* (scrapie incubation) gene. The action of the *sinc* gene was first described over 20 years ago (Dickinson et al, 1968), due to the fact that in any experimental rodent model, the period of time from infection to death was extremely predictable. The action of the *sinc* gene was first recognised in mice infected with the ME7 strain of scrapie. Two

alleles of this gene were identified, designated s7 and p7, which gave respectively, short or prolonged incubations periods with ME7. Later, it was shown that the *sinc* gene controlled the incubation period of all strains of scrapie. Since these early studies further evidence has came to light that the host encoded protein PrP is the major gene involved in the control of scrapie pathogenesis. Mice with *Sinc* s7 and p7 genotypes encoded PrP^c proteins that differed at residues 108 and 189 of the *Prnp* gene. Gene targeting experiments have now proved that *Sinc* and *Prnp* are the same (Moore et al, 1998) and that PrP^c is the product of sinc. This discovery and the importance of the *Prnp* gene and PrP^c in TSE research has overshadowed Dickinson's early work and usage of the *sinc* terminology is now obsolete. In current literature the $sinc^{s7}$ and ^{p7} alleles are more commonly referred to as $Prnp^a$ and $Prnp^b$, respectively.

1.5.3 Vacuolar pathology and lesion profiles

TSE strains can be distinguished on the pathological changes they produce in the brains of infected mice. The most obvious change observed in routine histological sections is a vacuolation of the neuropil. This vacuolation appears as tiny holes in both the white and grey matter of the brain (Figure 1&2A). This vacuolar degeneration gave rise to the terminology spongiform degeneration or spongiosis, that describes the microscopic appearance but not the texture of the brain.

Vacuolation of the brain is one of the classical lesions associated with TSE pathology. These vacuoles are defined as small round or oval empty spaces in the neuropil. Ultrastructural examination of vacuoles within brains of mice infected with the ME7 strain of scrapie showed that they contained a limiting double membrane which showed protrusion or proliferation of the inner most lamella. Sometimes whorled membrane configurations were also seen. This vacuolation was observed in neuronal perikarya, myelinated fibres, dendrites and axonal presynaptic terminals (Jeffrey et al,

1991). It is suggested that some scrapie vacuoles arise as a result of incorporation of abnormal membrane into organelles, possibly mitochondria, in neuronal perikarya and neurites (Liberski et al, 2002a). Another suggestion is that the vacuoles may develop through the process of autophagy (see mechanisms of neuronal loss – autophagy) (Liberski, 2004).

TSE strains show dramatic and reproducible differences in the severity and distribution of this vacuolar degeneration in the brains of genetically uniform mice. This forms the basis of a semiquantitative method of strain discrimination in which the severity of pathology is scored from coded sections in nine grey matter and three white matter brain areas. Grey matter vacuolation is scored on a scale of 0-5 and white matter vacuolation is scored on a scale of 0-3, where 0 represents no lesion and 5 the most severe (Bruce, 1996). The resulting lesion profile is formed by the line that joins the points of the average of the scores from the individual areas. Each combination of agent strain and mouse genotype has a characteristic lesion profile. This method of strain typing has been used at NPU for more than 30 years resulting in a 'tried and tested' reliable system. Using this methodology Bruce *et.al* showed that vCJD victims died from an agent that was indistinguishable from BSE (Figure 5) and concluded that the most likely scenario for developing the disease was from dietary exposure to BSE (Bruce et al, 1997).

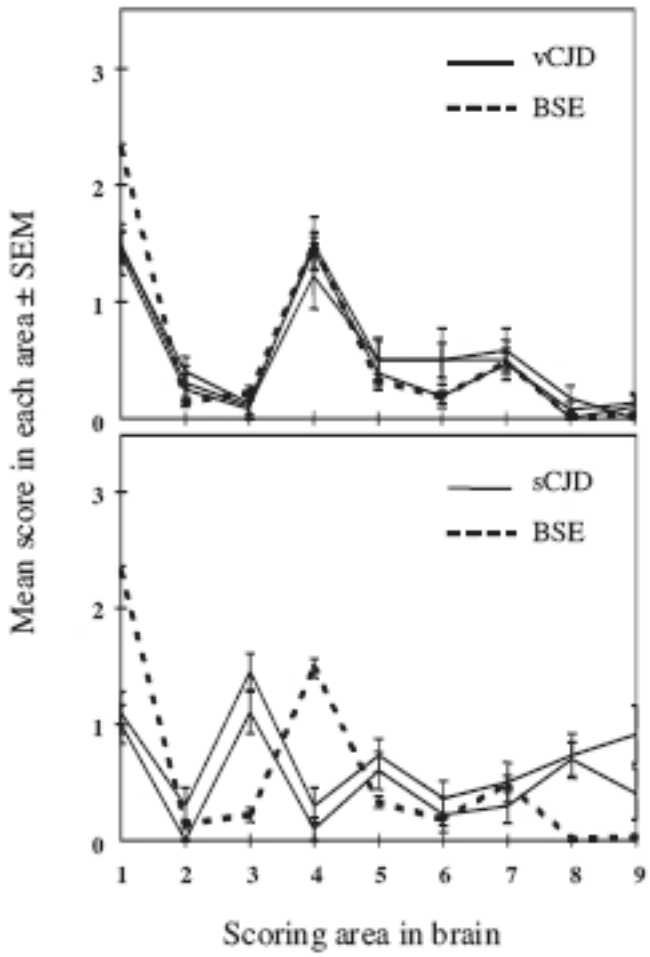

Figure 5. Comparison of lesion profiles in wild type mice infected with vCJD, sCJD and BSE. Lesion profiles for PrP^a mice infected with vCJD from three patients and sCJD from two patients. In each case these are compared with the lesion profile for BSE in the same mouse strain. Lesion profiles constructed from the mean vacuolation scores in nine areas of the brain. BSE and vCJD profiles are almost identical, there are no similarities between the sCJD and BSE profile.

1.5.4 PrP^{Sc} isoform analysis

PrP is a host-encoded glycoprotein involved in the pathogenesis of TSEs. PrP has two N-glycosylation sites and can exist as mono, di or unglycosylated forms. PrP^{c} is glycosylated at both sites but PrP^{Sc} varies in its degree of glycosolation, which can be influenced by the strain of TSE (Somerville et al, 1997). PrP^{Sc} may also vary independently in the amount and pattern of glycosylation in different brain regions. (Somerville,1999). PrP^{Sc} glycoform analysis has been used in the differential diagnosis of human TSEs. The biochemical characteristics of PrP^{Sc} were studied in 19 cases of sCJD. Four groups of subjects defined by the genotype at codon 129 of the *PRNP* gene, and two types of protease-resistant PrP^{Sc} that differed in size and glycosylation were discovered. The four Creutzfeldt-Jakob disease groups showed distinct clinicopathological features that corresponded to previously described variants. The typical Creutzfeldt-Jakob disease phenotype or myoclonic variant and the Heidenhain variant were linked to methionine homozygosity at codon 129 and to "type 1" protease-resistant PrP^{Sc}. The atypical and rarer variants such as that with dementia of long duration, the ataxic variant, and the variant with kuru plaques were linked to different genotypes at codon 129 and shared the "type 2" protease-resistant PrP^{Sc}. (Parchi *et al*, 1996).

The significance of PrP glycosolation and its role in TSE susceptibility and strain identification is not yet fully understood. Gene targeting studies using PrP glycosylation knockout mice infected with strains of TSE revealed that differences in host PrP glycosylation can alter TSE strain and disease targeting characteristics (Tuzi et al, 2008). Although this may be the case, glycoform analysis is not universally accepted as an ideal method to distinguish between strains. Differences in PrP^{Sc} glycoform ratios have been observed between CNS and lymphoid tissues from

infected individuals, between brain and spleen of scrapie infected mice (Rubenstein et al, 1991) and within brain and tonsil of vCJD patients (Hill et al, 1999b) This technique has been successfully used as a biochemical tool to differentiate sporadic from vCJD (Collinge et al, 1996) and to support the finding that BSE and vCJD (Hill et al, 1997) were due to the same agent strain, and can provide useful supporting data in strain-typing experiments.

1.5.5 The 87V/VM and ME7/CV scrapie models

The 87V/VM and ME7/CV combinations are two contrasting murine scrapie models which differ in their sequence of pathological hallmarks, incubation periods of disease and targeting of neuronal populations when infected by intracerebral (i.c.) inoculation. PrP^{Sc} in both models was located within neurons and the surrounding neuropil. Deposition of PrP^{Sc} in both models is targeted to the hippocampus, although to different neuronal populations (Figure 6B &7B)

The VM mice (*Prnp*^{b}) inoculated with the 87V agent of scrapie results in an incubation period of disease of approximately 320 days post injection (dpi). Pathology is targeted to the CA2 of the hippocampus, the dorsal lateral geniculate nucleus, and the thalamus. PrP^{Sc} is first detected in this model in the red nucleus of the medulla at 80dpi and is not detected in the hippocampus until 200dpi (Bruce et al, 1989) (Figure 6B). This deposition is preceded by dendritic dysfunction, astrogliosis, vacuolation and neuronal damage (Belichenko et al, 2000; Jeffrey et al, 1994a). Dendritic abnormalities are observed at 70dpi and are restricted to the CA2 pyramidal neurons (Jamieson et al, 2001b). A common pathological feature observed in this model is the deposition of amyloid plaques within the hippocampus and cerebral cortex (Bruce et al, 1989). These plaques contain amyloid fibrils and are surrounded by microglia (Wisniewski et al, 1975).

The CVF1 cross (*Prnp*^{ab}) infected with the ME7 strain of scrapie results in consistently severe pathology of the hippocampus and an incubation period of approximately 250 days (Scott & Fraser, 1984). PrP^{Sc} deposition is widespread within the hippocampus (Figure 7B), whereas vacuolation and neuronal loss are specifically targeted to the CA1 of the hippocampus. At the terminal stage of disease, vacuolation, gliosis and diffuse granular deposits of PrP^{Sc} are widespread in all brain areas. Using immunohistochemistry, PrP^{Sc} is first detected in the hippocampus at 70 dpi (Jeffrey et al, 2001), followed by vacuolation at 90 dpi. Infectivity in this model is detected at 50 dpi, before the detection of PrP^{Sc}, this would suggest a lack of correlation between infectivity and PrP^{Sc} in this model. By 100 dpi astrogliosis is evident in the hippocampus and a decrease in long term potentiation is observed in CA1 neurons infected with ME7. Also observed at this time point is the loss of axon terminals and synapses from the dendrites of CA1 neurons (Jeffrey et al, 2000). This correlates with dendritic damage observed in these neurons; dendritic spine loss is detected at 100 days, becoming marked by the terminal stage of disease (Brown et al, 2001). The few remaining neurons show a grossly altered morphology, with irregularly swollen dendrites containing varicosities (Belichenko et al, 2000). In contrast to the 87V/VM model PrP^{Sc} deposition in the form of plaques is rare. PrP^{Sc} deposition in the ME7/CV model can be seen in an aggregated fibrillar (Jeffrey et al, 2000) form or as a widespread diffuse labelling throughout the neuropil (Figure 7B).

Both these scrapie mouse models target the hippocampus, a brain structure in which neuronal connections have been well characterised (Freund, 2002), providing a useful tool to study the mechanisms of neuronal loss in TSE diseases.

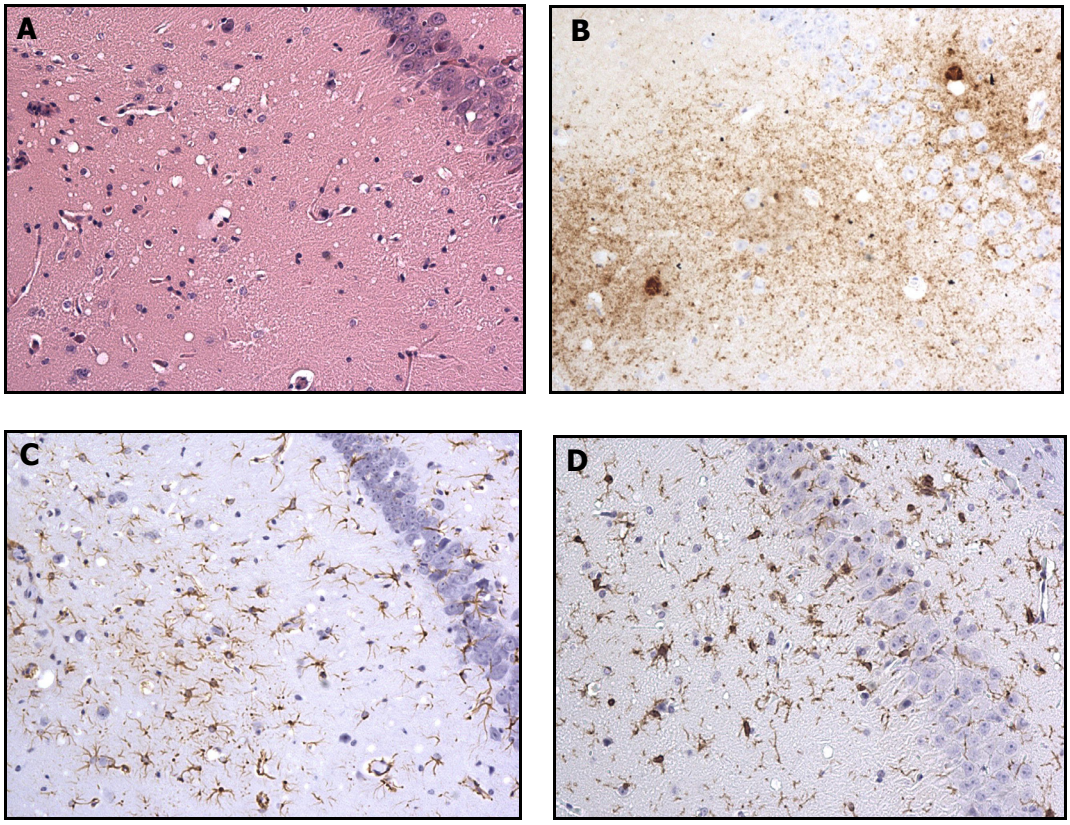

Figure 6. 87V/VM scrapie mouse model :- neuropathological changes observed in the hippocampus of VM mice infected with 87V. A) haematoxylin and eosin staining showing vacuolation in the CA2 of the hippocampus. B) 6H4 labelling of PrP^{Sc} in the CA2 of the hippocampus. C) GFAP labelling of reactive astrocytes in the CA2 of the hippocampus. D) Iba1 labelling of microglia in the CA2 of the hippocampus. (Magnification x 20)

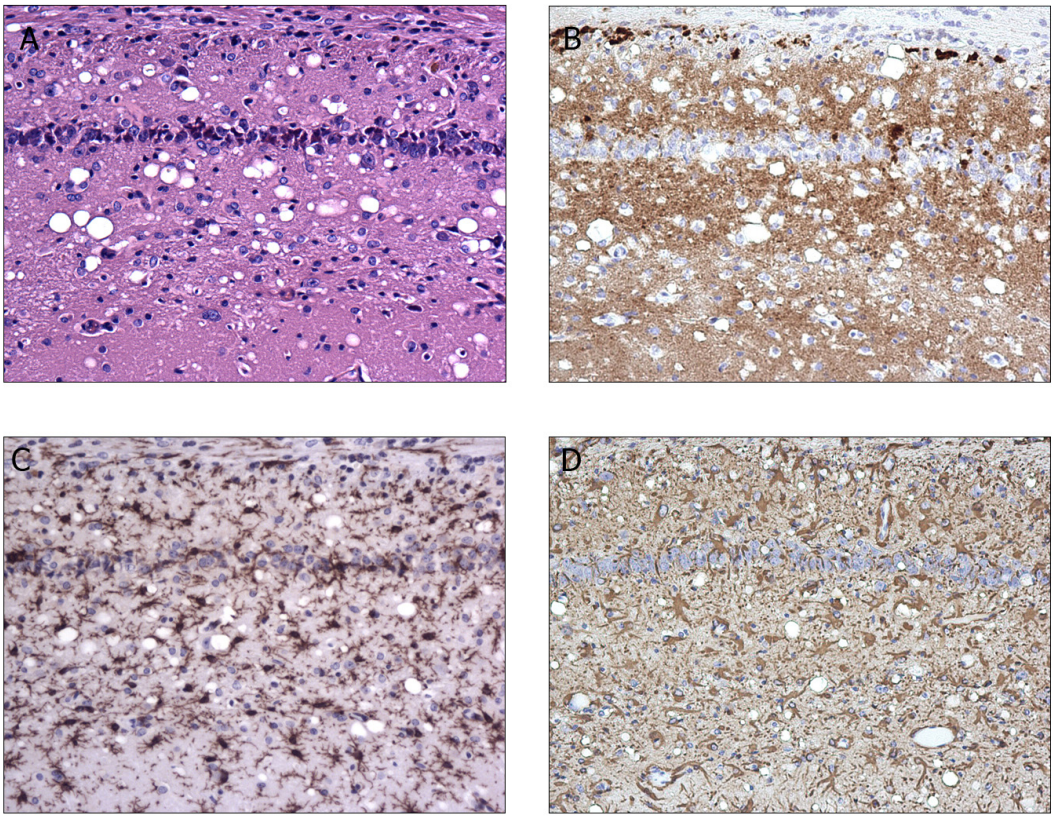

Figure 7. ME7/CV scrapie mouse model :-neuropathological changes observed in the hippocampus of CV mice infected with ME7. A) Haematoxylin and eosin staining showing vacuolation in the neuropil of the hippocampus and neuronal loss in the CA1. B) 6H4 labelling of diffuse PrP^{Sc} in the CA1 of the hippocampus. C) GFAP labelling of reactive astrocytes in the CA1 of the hippocampus. D) Iba1 labelling of microglia in the CA1 of the hippocampus. (x20 magnification)

1.6 Peripheral pathogenesis of TSE

Introduction

Although the ultimate target of TSE infection is the CNS, there is evidence that both the lymphoreticular system (LRS) and the peripheral nervous system (PNS) may be involved in the disease pathogenesis prior to CNS invasion. Initial studies in rodent models analysing the pathogenesis of the TSEs were performed using the intracerebral (ic) route of infection. This route is not a natural route of infection and it was soon recognised that more biologically relevant routes of infection should be examined i.e. oral and peripheral routes. The identity of the source and mode of transmission of many TSE diseases is unclear. However strong evidence indicates that BSE in cattle and vCJD and kuru in humans occurred through the oral route of transmission. Also transmission of TSEs via the skin (scarification) is known to be an effective route of peripheral transmission (Mohan et al, 2004; Mohan et al, 2005; Taylor et al, 1996). Following exposure, many of the acquired TSE agents accumulate in lymphoid tissues such as the spleen, lymph nodes, tonsil, appendix and Peyer's patches before spreading to the CNS, a process termed neuroinvasion (Mabbott & MacPherson, 2006). This occurs in sheep with natural scrapie (van Keulen et al, 1996), mule deer with CWD (Sigurdson et al, 1999), mink with TME (Hadlow et al, 1987) and humans with vCJD (Hilton et al, 1998); (Hill et al, 1999b)

1.6.1 The lymphoreticular system in TSE pathogenesis

After oral or peripheral routes of infection, several TSE agents replicate in the LRS prior to neuroinvasion (Ehlers et al, 1984; Farquhar et al, 1994; Fraser, 1992; Kimberlin & Walker, 1979; Kimberlin & Walker, 1989; Kimberlin, 1988; Mabbott et al, 1998) (Figure 8). Early studies measuring infectivity levels after intraperitoneal (i/p) infection of mice with the Chandler strain (Eklund et al, 1967) or in natural

scrapie (Hadlow et al, 1982) showed that, outside the CNS, the highest titres of infectivity are found in the spleen and lymph nodes. During this period of infection there are no clinical signs of disease and detection of infectivity in the spleen precedes that of the CNS by many weeks or longer (Dickinson & Fraser, 1969; Dickinson et al, 1975). Following splenectomy the incubation period of disease was extended, although this was dependent on route of infection, time of splenectomy (Fraser & Dickinson, 1978) and was strain and species dependent. Splenectomy had no effect on hamsters i/p infected with the 263K strain of scrapie (Kimberlin & Walker, 1989)

Studies to identify which cell types in the LRS may play a role in the peripheral pathogenesis of TSE have demonstrated the importance of the follicular dendritic cell (FDC) (Figure 8). These cells are radiation resistant and support scrapie replication in the spleen of mice (Brown et al, 1999; Montrasio et al, 2000). They are non-lymphoid cells, which are found within germinal centres of secondary lymphoid follicles where they trap antigens in the form of antigen antibody complexes (Kosco et al, 1992). In mice, PrP^{c} is expressed by FDCs in both uninfected and TSE infected mice (McBride et al, 1992; Ritchie, 1999). These PrP^{c} expressing FDCs may be key players in the mechanisms of peripheral infection but the uptake and transfer of the TSE agent by these cells, has still to be elucidated (Mabbott & MacPherson, 2006).

Some TSEs do not appear to involve or depend on the peripheral lymphoid system for pathogenesis. In cattle experimentally inoculated with BSE, accumulation of PrP^{Sc} is observed in the tonsil and distal ileum (Terry et al, 2003), which contrasts with its abundant lymphoid-tissue distribution following transmission to humans (Wadsworth et al, 2001) and sheep (Foster et al, 2001; van Keulen et al, 2008). Very low levels of PrP^{Sc} have been observed in the spleen in a minority of sCJD cases with a lengthy history (Glatzel et al, 2003). Involvement of the LRS is not observed in

humans suffering from iCJD (Head et al, 2004) or kuru (Brandner et al, 2008). The lack of involvement of the LRS in kuru is consistent with the hypothesis that kuru originated from the chance consumption of an individual with sCJD (Alpers & Rail, 1971). Although the transmission of kuru to humans is through the oral route, the peripheral pathogenesis resembles that of sCJD and not vCJD (Brandner et al, 2008), suggesting that the pathogenesis of vCJD may be determined by the strain type rather than the route of infection.

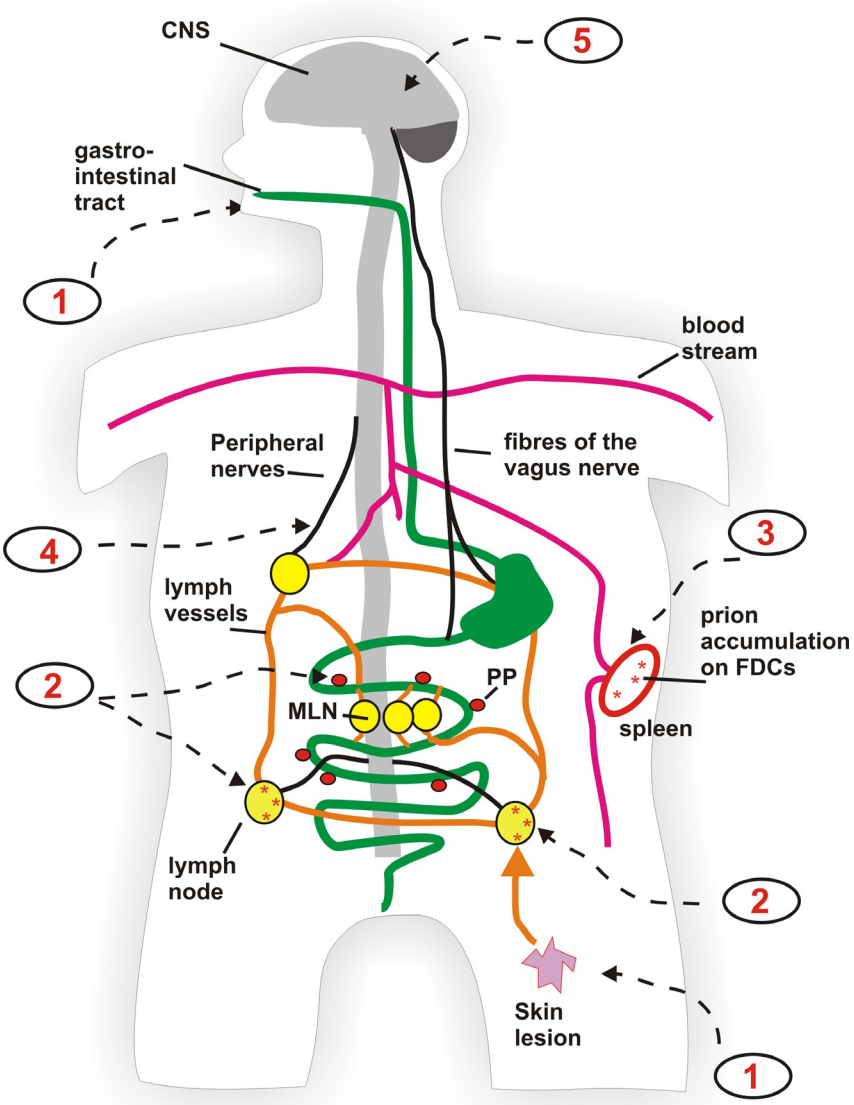

Figure 8. Route of TSE neuroinvasion following peripheral exposure. 1. Natural TSE diseases are often acquired by peripheral exposure such as orally or through skin lesions. 2. Following exposure the TSE agent often first accumulates in follicular dendritic cells (FDC) in local lymphoid tissue i.e. lymph node, Peyer's patches and mesenteric lymph nodes. 3. shortly afterwards the TSE agent is disseminated to most other lymphoid tissues including the spleen. 4. After accumulating in FDCs the TSE agent infects the sympathetic nerves and fibres of the vagus nerve, and spread along these to the CNS. 5. Accumulation of the TSE agent (PrP^{Sc}) in the brain is accompanied by neurodegeneration and the death of the host. Diagram from Mabbott *et.al.* (2005) Prions and the blood and immune systems. Haematoligica; 90:542-548

1.6.2 Peripheral nervous system in TSE pathogenesis

The involvement of the peripheral nervous system in the pathogenesis of TSEs was first demonstrated in experiments involving sciatic nerve transection. If the infectious agent was injected directly into nerves the extraneural involvement could be bypassed (Kimberlin et al, 1987; Kimberlin et al, 1983a; Kimberlin et al, 1983b; Kimberlin & Walker, 1980). Substantial amounts of infectivity have been found in a number of fore and hind limb peripheral nerves of scrapie infected sheep (Groschup et al, 1996).

Numerous findings indicate that after peripheral exposure, the peripheral nervous system plays an essential role in the spread of the agent to the brain and spinal cord. This holds true for scrapie in sheep (Groschup et al, 1996; van Keulen et al, 1996), experimental scrapie in mice (Fraser, 1982; Kimberlin, 1993; Kimberlin & Walker, 1982) and in hamsters (Baldauf et al, 1997; Beekes et al, 1996), as well as for experimental forms of CJD (Muramoto et al, 1993) and BSE (Wells et al, 1998) in animals. Studies in which the spatial-temporal course of replication of the infectious agent in parenterally infected mice and hamsters was investigated, showed that the infectious process spreads to the spinal cord at the thoracic level, and from there moves upwards into the brain (Kimberlin, 1993; Kimberlin et al, 1983b; Kimberlin & Walker, 1980; Kimberlin & Walker, 1982). In the 263K hamster model neuroinvasion appears to occur very rapidly, with extremely short incubation periods of approximately 65 days (Kimberlin & Walker, 1986).

How the infection reaches the CNS after oral infection with the scrapie agent has been systematically investigated in Syrian hamsters orally challenged with the 263K strain of scrapie. On the basis of a close quantitative association of infectivity and PrP^{Sc} in this experimental model (Baldauf et al, 1997; Beekes et al, 1996), PrP^{Sc} was used as a biochemical marker for tracing the spread of infection through the body

in a time course study. In this study PrP^{Sc} accumulated in a defined temporal sequence, in sites that accurately reflected known autonomic and sensory relays. The infectious agent primarily uses synaptically linked autonomic ganglia and efferent fibers of the vagus and splanchnic nerves to invade the initial target sites in the brain and spinal cord (Beekes et al, 1996; Beekes & McBride, 2000; Beekes et al, 1998; McBride et al, 2001).

Both the parasympathetic and sympathetic nervous system seem to play an important role in the infectious spread of the agent from the gut to the CNS (Figure 5). Studies in naturally occurring scrapie of sheep (van Keulen et al, 1996), in cattle BSE (Schulz-Schaeffer et al, 2000) and in CWD (Sigurdson et al, 1999; Williams, 2000) of deer have confirmed experimentally established parasympathetic pathways of infection.

Although most studies suggest that the spread of infection from peripheral sites to the brain occurs primarily along neural routes, haematogenous spread may also occur in TSE infection. Infectivity in the blood of hamsters i/p infected with the 263K strain of scrapie could be detected for 40 days after infection (Diringer, 1984). This hamster model has been used successfully in experimental studies of infectivity through blood transfusion, and hamster blood has been shown to be a good substitute for human blood for investigations of the component distribution of TSE infectivity in blood (Brown et al, 1998; Elliott et al, 2005). Infectivity has also been efficiently transmitted by blood transfusion in sheep. Both BSE and scrapie had unexpectedly high transmission rates (Houston et al, 2008; Hunter et al, 2002). Also the neuropathological phenotype of experimental ovine BSE was maintained after blood transfusion (Siso et al, 2006), suggesting that a change in the pathologic phenotype of vCJD would not be expected as a result of exposure to infected blood. Sheep blood

would be a more realistic substitute for human blood for investigations of the component distribution of TSE infectivity in blood.

1.6.3 The CNS and TSE pathogenesis

The CNS is the ultimate target for TSE infection. The characteristic neuropathological changes observed in the brain include vacuolation, gliosis, accumulation of PrP^{Sc} and neuronal loss. Neuronal loss is not due solely to differences in the susceptibility of different subsets of neurons to the disease process, but is influenced by the agent strain and the host genotype (Bruce, 1976). For example, in the ME7/CV model used in these studies, infection of CVF1 mice, an F1 cross between C57BL (*Prnp*^{a}) and VM (*Prnp*^{b}) mice, with the ME7 strain of scrapie produces severe pathology in the pyramidal cell layer of the CA1 sector of the hippocampus (Scott & Fraser, 1984). This pathology is not observed in the VM mouse strain when challenged with ME7.

Although neuronal loss is a classic feature of TSEs, the cellular pathways leading to this are still unclear. There are three mechanisms by which neurons may die: autophagy, necrosis and apoptosis. Apoptosis has become the most popular concept of cell death in neurodegeneration, and there is considerable evidence supporting a role for this type of cell death in TSEs (Giese et al, 1995; Gray et al, 1999; Lucassen et al, 1995; Williams et al, 1997a). Mechanisms of neuronal loss and their role in TSE-induced neurodegeneration are discussed below in section 1.7. The role that apoptosis plays in the neuronal loss is investigated further in Chapter 4.

It seems obvious that neuronal dysfunction must lie at the root of clinical disease, yet the extent and progression of neurodegeneration, and its relationship with the other pathological processes are not yet known. Using the ME7/CV scrapie mouse

model the relationship between neuronal loss, vacuolation, gliosis and the deposition of PrP^{Sc} in TSEs will be investigated. This is discussed fully in Chapter 3.

1.7 Mechanisms of neuronal loss

1.7.1 Autophagy

One of the suggested mechanisms of neuronal cell death in TSEs is autophagy. Cellular autophagy is a physiological degradative process involved, like apoptosis, in embryonic growth and development, cellular remodelling and the biogenesis of some subcellular organelles (Filonova et al, 2000; Hariri et al, 2000; Sattler & Mayer, 2000). Nascent immature autophagic vacuoles coalesce with lysosomes to form degradive autophagic vacuoles (Figure 9). Electron microscopy techniques revealed that these vacuoles were composed of areas of the cytoplasm sequestered with single, double or multiple membranes originated from the endoplasmic reticulum. Sequestered cytoplasm contained ribosomes, occasionally mitochondria, small secondary vacuoles with vesicles, or had a homogenously dense appearance (Liberski et al, 2002b; Liberski et al, 2004). Autophagy may co-exist with apoptosis or may precede it and the process may be induced by apoptotic stimuli (Xue et al, 1999). Autophagy has been observed in CJD and animal models of TSE. In CJD, autophagic vacuoles were formed within synapses and may contribute to the synaptic loss observed in brains affected in TSEs (Sikorska et al, 2004). These autophagic vacuoles were also observed in CJD and scrapie infected rodent brains (Boellaard et al, 1991; Boellaard et al, 1989; Liberski et al, 2002a). Although there is strong evidence that autophagy is a common ultrastructural feature of TSEs, it is still unclear how the autophagy contributes to the overall pathology and, especially, to the neuronal loss underlying TSE diseases.

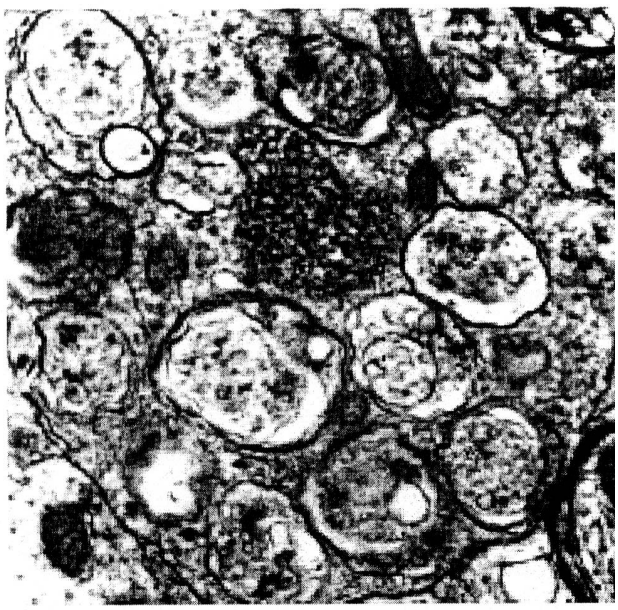

Figure 9. Autophagic neuron. Many characteristic autophagic vacuoles observed within an autophagic neuron of a hamster brain infected with the 263K strain of scrapie. Some vacuoles have single membranes and others are surrounded by double membranes. Image from Liberski *et.al.* Acta. Neuropathol. 2002

1.7.2 Necrosis

When stressed beyond their tolerance cells undergo necrosis, an acute, non-apoptotic form of cell death. A wide range of factors can trigger necrotic cell death. Both extrinsic and intrinsic signals can initiate necrotic cell death; for example, hostile environmental conditions or mutated genes (Walker et al, 1988). Acute energy depletion is one of the most potent necrosis-triggering conditions in neurons (Ankarcrona et al, 1995; Leist et al, 1997). Energy depletion can rapidly develop during ischaemic or hypoglycaemic episodes. Cells undergoing necrosis display gross morphological and ultra structural features that contrast sharply with those exhibited by cells undergoing apoptosis. Death is accompanied by extensive swelling of the cell, distension of various cellular organelles, clumping and random degradation of nuclear DNA, extensive plasma membrane endocytosis and autophagy

(Figure 10) (Ferri & Kroemer, 2001; Hall et al, 1997; Syntichaki & Tavernarakis, 2002).

Neurodegenerative disorders such as Alzheimer's, Parkinson's, Huntington's, motor neuron and prion diseases all share a conspicuous common feature: aggregation and deposition of abnormal proteins in the brain (although the nature and site of deposition of these abnormal proteins varies according to the disease). Neurons are particularly vulnerable to the toxic effects of mutant or misfolded proteins (Taylor et al, 2002) ; these toxic effects may contribute to the neuronal cell death observed in these diseases which may be a combination of apoptosis and necrosis (Martin, 1999; Martin, 2001). There is little evidence in the literature about the involvement of necrosis in TSE diseases. In one study were hamsters were treated with the 139H strain of scrapie, these animals developed a generalized endocrinopathy, including lesions in the hypothalamus, pituitary and pancreas. Further observations using EM techniques revealed that the cellular death observed in the islets of Langerhans in 139H infected hamsters was due to necrosis (Ye et al, 1997). The role of necrosis in the neuronal cell death observed in TSE diseases is still unclear, evidence so far for its involvement in the disease indicates that it may not play an important role in the cell death observed in these diseases.

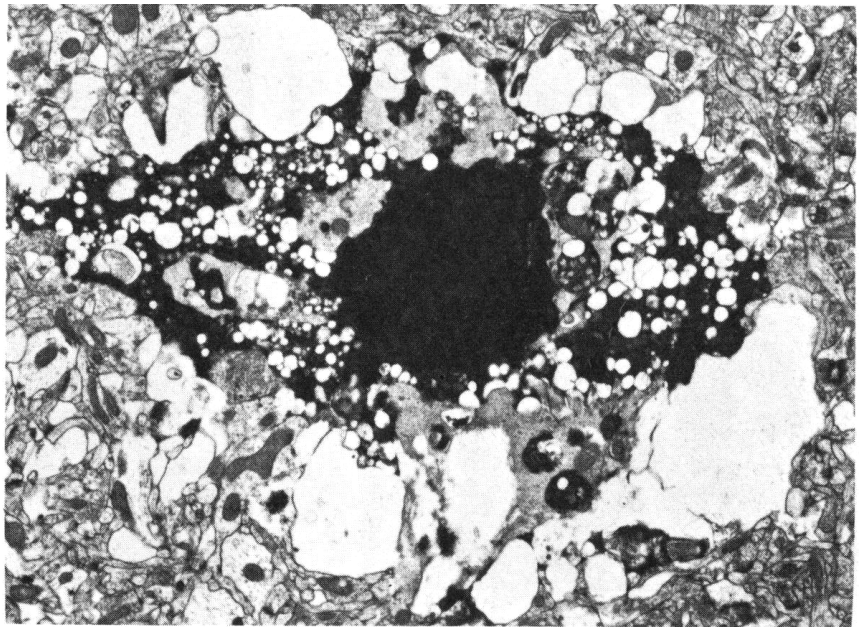

Figure 10. Necrotic neuron. Neuron observed in the advanced stages of ischemia showing swelling of the cell, clumping and random degradation of nuclear DNA, extensive plasma membrane endocytosis. Vacuoles within the cytoplasm represent dilated cisternae and vesicles of smooth and granular endoplasmic reticulum and the remains of swollen mitochondria. Image from Greenfield's Neuropathology, third edition, Edward Arnold publishers Ltd (1976)

1.7.3 Apoptosis

Apoptosis is a programmed cell death regulated by a series of events. It is essential for cell development, maturation, normal tissue turnover and regulation of immune systems (Wyllie et al, 1980). The identification of apoptotic cells is based upon the morphological detection of cellular and nuclear membrane shrinkage, condensation and fragmentation of nuclear chromatin (Figure 11), and biochemically by endonuclease-mediated internucleosomal fragmentation of DNA into multiple oligosomal sub-units of 180 bp (DNA laddering). Apoptosis can be induced by cell surface receptor engagement, growth factor withdrawal, and DNA damage triggered by toxic compounds and exposure to γ– and UV-irradiation. The involvement of apoptosis in the neuronal cell death observed in TSE diseases has been well documented, although the exact mechanisms in which this occurs is still not fully

understood. *In vitro* studies using the toxic peptide PrP 106-126 in cell culture have shown the upregulation of pro-apoptotic markers of disease i.e. caspase-3, 6 and 8 (White et al, 2001) and the induction of multiple transduction pathways such as the JNK c-jun pathway (Carimalo et al, 2005), P38 MAP Kinase (Corsaro et al, 2003) and the glycogen synthase kinase pathway (Perez et al, 2003), which lead to apoptotic cell death, and may be involved in prion induced neurodegeneration. *In vivo*, neuronal apoptosis has been observed in scrapie mouse models of disease (Giese et al, 1995; Lucassen et al, 1995; Siso et al, 2002; Williams et al, 1997a), in sheep infected with scrapie (Fairbairn et al, 1994) and humans affected by CJD (Ferrer, 2002).

Several families of proteins and specific biochemical signal transduction pathways regulate cell death. Caspases are a family of proteins involved in apoptosis that will be discussed further in Chapter 4, along with their role in the caspase dependent pathway of apoptosis.

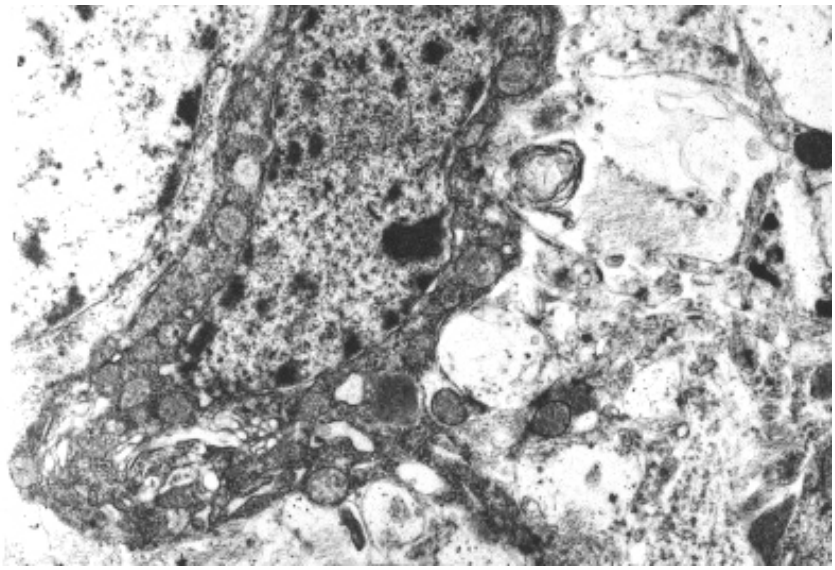

Figure 11. Apoptotic neuron. Apoptotic neuron from the brain of an ME7 terminally infected CV mouse. Showing the characteristic chromatin clumping within the nucleus and blebbing of the cell membrane. Image courtesy of Dr Martin Jeffrey

1.8 Aims of this study

Neuronal loss is one of the characteristic neuropathological features observed in TSE induced neruodegeneration, the mechanisms leading to the death of these neurons is not yet fully elucidated. The aims of this study are to investigate the fundamental mechanisms of neurodegeneration in the TSEs. Using murine scrapie models of disease, the relationship of neuronal loss with the deposition of PrP^{Sc}, gliosis and synapse loss will be investigated. Considerable evidence in the literature suggests that neuronal cell death in TSEs occurs through an apoptotic mechanism, although the trigger for this event is unknown. In this thesis the role of apoptosis and the caspase-dependent pathway in the neuronal cell death observed in TSEs will be investigated.

The relationship between the pathological changes occurring in the brain and the development of clinical disease in the TSEs is not known ; however any strategy aimed at intervening to halt the degenerative process must be aimed at the fundamental lesion and not its sequelae.

Therefore the specific aims of this thesis are to :

- Perform a time course study of the neuropathological changes observed in the hippocampus of the ME7/CV scrapie mouse model and to identify at which time point in the progression of the disease, these changes initially occur.
- Identify the relationship between these neuropathological changes and the loss of CA1 neurons observed in the hippocampus.
- Establish whether apoptotic mechanisms play a role in the neuronal cell death observed in the CA1 sector of the hippocampus.
- Investigate the role of the neuronal cytoskeleton and synaptic changes in the neuronal damage observed in the CA1 sector of the hippocampus, and to establish their relationship with the subsequent neuronal loss.

Chapter 2 : Materials and methods

2.1 Experimental animal procedures

2.1.1 Experimental animal groups and murine strain combinations

Animals were taken from the specified pathogen free colony maintained at the Neuropathogenesis Unit. Animal related procedures comply with the Animals (scientific) Act of 1986 in accordance with Home Office regulations. The two inbred mouse strains intracerebrally (ic) inoculated in these experiments were the VM/Dk (VM, *Prnp*^{b} genotype) inoculated with the 87V murine scrapie strain (87V/VM model), and the F1 cross between C57BL/Dk and VM/Dk (CV, *Prnp*^{ab} genotype), inoculated with the ME7 murine scrapie strain (ME7/CV model). For the ME7/CV model a serial kill study was also set up were brains were taken at intervals as described in table 1 below. The incubation period and neuropathological details of these mouse and scrapie strain combinations have been detailed in chapter 1 section 1.5.5.

Dpi	ME7	NB
69	4	3
102	4	3
130	4	3
160	4	3
200	4	3
term	4	3

Table 1. ME7/CV serial kill time points taken and numbers of animals analysed. Dpi = days post injection, ME7= ME7 infected brains, NB= normal brain injected controls

2.1.2 Scrapie inoculation and tissue collection procedures

Inoculum for injection was prepared from the brains of animals which had reached the terminal stages of disease. Brains were removed using aseptic techniques and stored at -20^{o}C, or below, until required. Mice under halothane anaesthesia were injected by intracerebral inoculation into the right frontal cortex with a 25 gauge needle fitted with a 2mm needle guard to prevent penetration of the needle beyond the outer cortical layers. Mice were inoculated with 20µl of 1% brain homogenates prepared in 0.9% sterile saline. Cohorts of control animals were inoculated with equivalent volumes of normal brain homogenates. Mice in these experiments were inoculated by the trained staff of the animal facility.

2.1.3 Mouse brain collection

All experimental animals were culled by cervical dislocation by the experienced staff of the animal handling facility. Brains for histopathological anlaysis were removed and placed into formol saline, fixed for 48 hours, then trimmed as Figure 1 below and processed through to paraffin wax. Brains for biochemical analysis (western blot) were snap frozen in liquid nitrogen and stored in the -70^{o}C freezer. Brains for FACS analysis were taken fresh into Hanks balanced salt solution and prepared as FACS method in appendix 3.

2.2 Histopathological techniques

2.2.1 processing of tissue for pathological analysis

Mouse brains were processed for pathological analysis as shown below in Figure 1

The hippocampal block was the main area analysed in this study as the pathology observed in both the 87V/VM and the ME7/CV mouse models targeted the hippocampus. In the ME7/CV mouse model neuronal loss was targeted to the CA1 sector of the hippocampus. In the 87V/VM mouse model neuropathological changes

were targeted specifically to the CA2 sector of the hippocampus. A diagram showing the main areas of the hippocampus analysed is shown below (Figure 2).

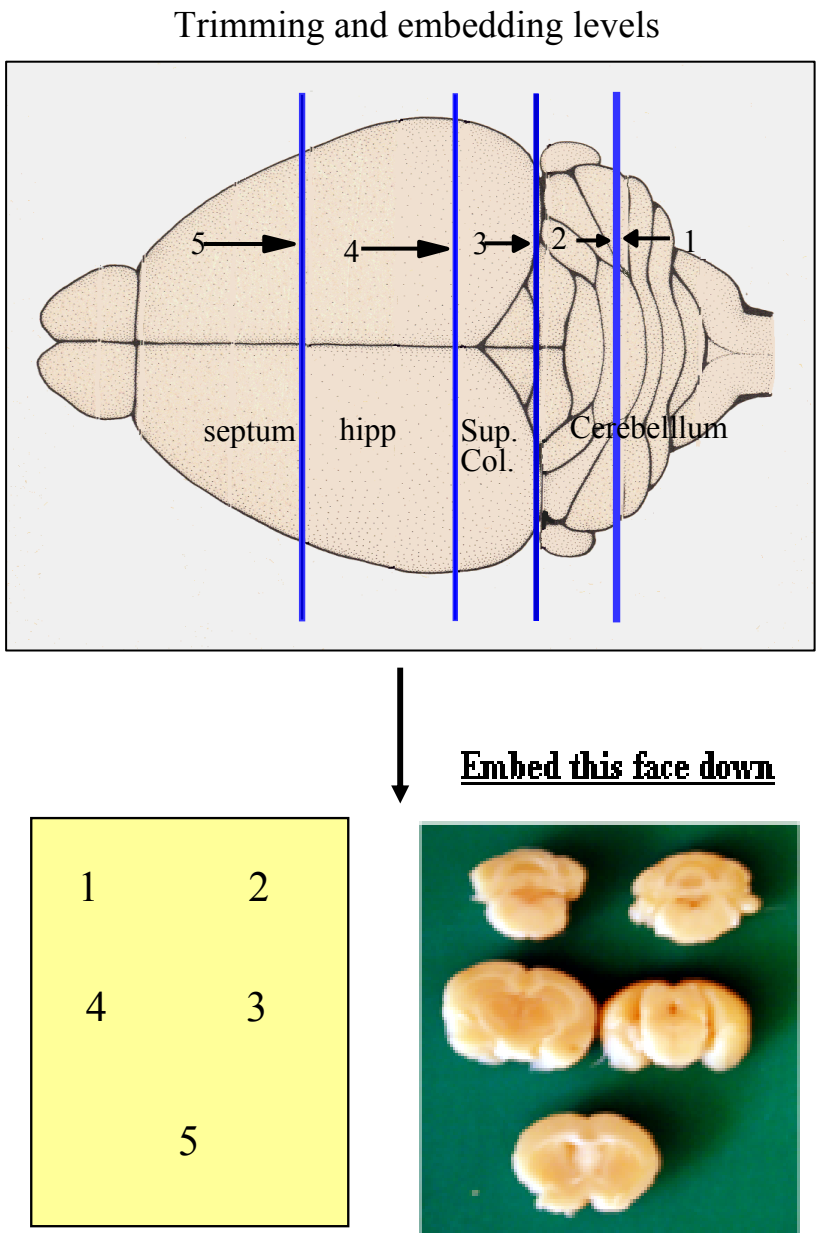

Figure 1. Mouse brain sectioning levels for immunohistochemistry and Haematoxylin and Eosin staining
Brains are cut coronally and sectioned at the 5 levels used routinely for histopathological analysis. Hippo=hippocampus, Sup.Col.=superior colliculus

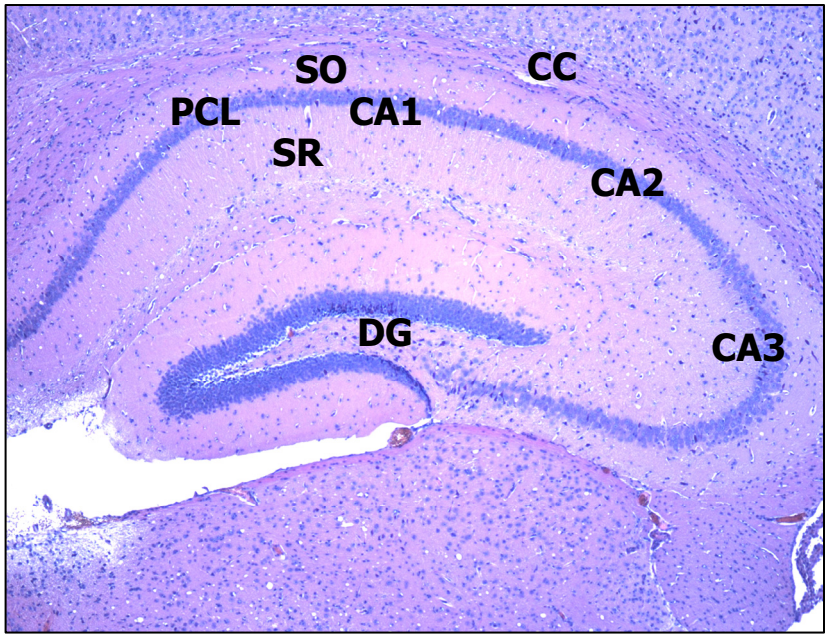

Figure 2. Diagram of the mouse hippocampus. Haematoxylin and Eosin stained hippocampus section showing main areas analysed. PCL – pyramidal cell layer, CA1- CA1 sector of the pyramidal cell layer, SO – stratum oriens, SR- stratium radiatum, CC- corpus collosum, CA2 – CA2 sector of the pyramidal cell layer CA3 – CA3 sector of the pyramidal cell layer, DG – dentate gyrus. Magnification x4

2.2.2 Immunohistochemical analysis of paraffin-embedded samples

Paraffin-embedded 6µm tissue sections were hydrated by passage through alcohols to water prior to immunocytochemical analysis. A generic immunocytochemical method was used as per appendix 1 and a list of antibodies used plus pretreatments required can be found in table 1.2 in appendix 1. To analyse vacuolation and neuronal loss haematoxylin and eosin labelling was performed using a Leica autostainer.

The serial kill time points taken (table 1.) were chosen in line with previous results using the ME7/CV scrapie mouse model. The first time point of 69 days was chosen because previous experiments had suggested that this was the earliest time point at which PrP^{Sc} could be detected. The other time points were evenly distributed throughout the incubation period of disease. Incubation period data from the mice at the terminal stage of disease in this experiment were at approximately 240dpi., consistent with previous experiments. All comparisons discussed in the results were

performed analysing the four infected and three normal brain controls in each time point. Three normal brain control section were included at every time point but only one example from a single time point is shown in the immunolabelling figures. A table of all antibodies used, pretreatments required and source can be found in appendix 1.

In these studies IHC analysis had its limitations. This methodology has been used successfully for years as a technique to analyse the characteristic neuropathological changes observed in the brains of both animals and humans with TSE disease. In this case IHC is a useful tool used in both research and the diagnosis of TSEs. In the apoptosis studies performed in this thesis IHC was used to analyse which brain areas and cells were involved in TSE induced cell death. Western blot analysis was also used as a confirmatory tool in some of these studies. In the cytoskeletal and synapse studies IHC was used in serial kill studies to identify at which time point throughout the course of disease that cytoskeletal changes and synapse loss is first observed. In the cytoskeletal studies IHC was not sensitive enough to pick up the early cytoskeletal changes observed with the lucifer yellow studies i.e. dendritic spine loss observed at 109 days post infection. Therefore the Lucifer yellow microinjection technique was a more appropriate technique to use in order to identify subtle changes in dendritic spine loss.

2.2.3 Analysis of vacuolation and neuronal loss

6μm paraffin sections were stained with Haematoxylin and Eosin using the Leica Autostainer. Vacuolation was analysed using the Nikon E800 microscope. Neuronal loss was quantified using image pro plus software. Neuronal cell numbers were counted in single sections from two serial kill time points in the ME7/CV scrapie mouse model; 160dpi and 200dpi. Two measurement tools were used within the

image pro plus software; the trace tool was used to measure the length of each CA1, and the tag point tool was used to count the neuronal cell bodies (Figure 3). All data is then exported to Excel for analysis

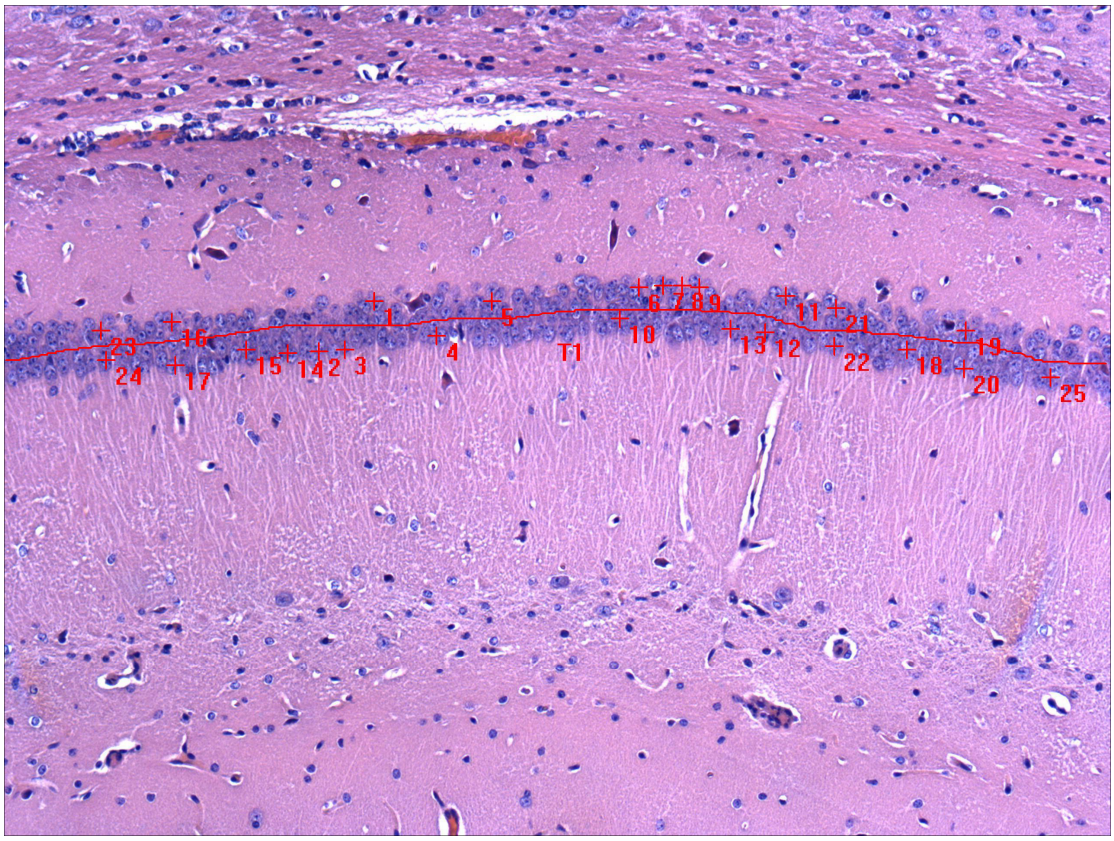

Figure 3. Neuronal counts and image pro-plus Image showing how both measurement tools within the image pro-plus software where used to analyse the length of the CA1 and perform neuronal counts. The trace is performed first and then removed from the image and then neuronal cell bodies are counted using the tag point technique.

2.2.4 Thioflavin labelling of amyloid plaques

Thioflavin S (Sigma) labelling was performed to identify if the plaque like deposits observed in the ME7/CV scrapie mouse model contained amyloid. 6µm paraffin sections were dewaxed and taken down to water. Sections were counterstained with haematoxylin prior to Thioflavin S staining, 1minute in haematoxylin solution followed by 30 seconds in Scotts tap water. Sections were washed in running tap water then stained with 1% Thioflavin S solution made up in distilled water for 5

minutes. Sections were then quickly taken through three changes of 70% alcohol, washed in running tap water then mounted in aquamount (Dako).

Thioflavin staining was imaged using a Nikon E800 microscope attached to a Hamamatsu fluorescent camera.

2.3 Western blot analysis of murine brain samples

2.3.1 Sample preparation

2.3.1.1 87V/VM whole brain sample preparation

A 10% homogenate was prepared in Tris lysis buffer (Appendix 2) and total protein analysed (section 3.3.3.5). Samples were diluted in x1 sample buffer to contain 10,5 and 2.5mg/ml of total protein per 20µls of sample. Immediately prior to running gel 2µls sample reducing agent was added, vortexed and denatured at 98^{o}C for 5 mins and spun at 120g for 5 mins. Continued with generic western method in Appendix 2.

2.3.1.2 Micro-dissection of mouse hippocampus

The micro-dissection procedure for obtaining the hippocampal samples was performed following a published protocol (Barr et al, 2004). Briefly brains were removed from -70^{0}C storage and allowed to partially thaw on -20^{0}C cold plate. Each brain was cut using disposable scalpel blades (Swann Norton No 11) at the level of the hippocampus (Figure 1). The hippocampus was excised using a punch technique involving the hollow cannula of a biopsy needle (Scottish Medical) (Figure 4). Several punches were required to remove each hippocampi, and tissue was expelled into an eppendorf tube from the cannula using an empty 5ml syringe attached at one end. Samples were then snap-frozen in liquid nitrogen and stored in a -70^{0}C freezer.

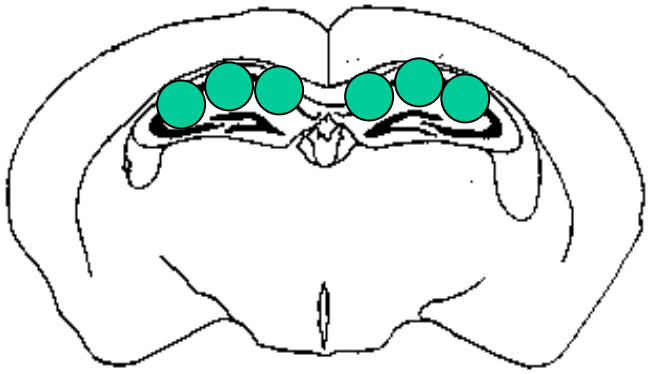

Figure 4. Micro-dissection of hippocampus for western blot analysis
Frozen (-70^{0}C) mouse brains are thawed on a -20^{0}C cold plate and cut at the level of the hippocampus (Figure 3). A hollow bore of a biopsy needle was used to gently collect both hippocampi (green circles).

2.3.1.3 Sample preparation of dissected hippocampus

A 10% homogenate was prepared in Tris lysate buffer. If subcellular fractionation required, tissue was lysed in sample buffer 1 using a proteome extraction kit (Calbiochem), continued with sub-cellular separation of cytosol, nuclear, organelle and cytoskeletal fractions (section 2.3.2). Total protein analysis of samples was performed, where necessary samples were concentrated using a methanol precipitation technique. To methanol precipitate samples, a x4 volume of ice-cold methanol/2% acetic acid was added to each sample, the tube was gently inverted twice and precipitated overnight at -20^{o}C. Samples were centrifuged at 16,000g for 10 minutes, methanol/2% acetic acid supernatants were carefully removed and the protein pellet dried for up to 2 hours in a centrifugal vacuum concentrator (Therm Savant Speed-Vac). Dried samples were each re-suspended in 20µl 1x sample buffer, sample-reducing agent added at 1x, and samples gently vortexed. Samples were heated at 98^{o}C for 5 minutes prior to SDS-PAGE.

2.3.2 Subcellular fractionation

Subcellular fractionation was performed using the ProteoExtract subcellular proteome extraction kit (Calbiochem). Briefly, extraction buffers I-IV and centrifugation steps are used sequentially to isolate the four cell fractions. I- cytosolic, II – membrane/organelle, III – nucleic protein and IV – cytoskeletal matrix , from dissected hippocampus. The four subcellular fractions were stored in a -70^{o}C freezer and protein estimations performed on each sample.

2.3.3 BCA total protein determination assay

Total protein estimation was determined using the microplate protocol of the bicinchoninic acid (BCA) assay (Pierce). This assay uses BCA to detect cuprous ions generated from cupric ions by reaction with protein in the samples under alkaline conditions. Bovine serum albumin (BSA) standards (Pierce) and samples to be analysed were diluted in the lysis buffer used to produce the original tissue homogenate. BSA standards were prepared (1500µg/ml, 1000µg/ml, 750µg/ml, 250µg/ml, 100µg/ml and 50µg/ml) and samples to be analysed were diluted in the ratio of 1:5 and 1:10 to calculate the total protein content in each sample as derived from the standard curve. 25µl of each standard and diluted sample were added in duplicate to wells of a 96 well microplate. 200µl of BCA working solution was added to plate and also used as a blank. Microplate was incubated at 37^{o}C for 30mins and absorbance values at 570nm were read and analysed on a V-max microplate reader (Molecular devices). Protein concentrations for each sample were derived from the BSA standard curve.

2.3.4 Western blot procedure

All biological reagents and experimental equipment were purchased from invitrogen, unless otherwise stated. Proteins were transferred from 4-12% Bis-Tris gels to polyvinylidine difluoride (PVDF) membranes using the Novex Transblot module; 3MM filter paper and PVDF membranes were purchased pre-cut. PVDF membranes were blocked with 20ml 3% non-fat dried milk (Upstate) in TBS for 2 hours prior to incubation with primary antibody of choice (Appendix 2 table 2.2.). PVDF membranes were then incubated overnight at $4^{o}C$ in 20ml of antibody solution in freshly prepared 3% non-fat dried milk in TBS. Rest of method as Appendix 2.

Western blot analysis has its limitations it can be used semi-quantitatively to analyse the expression of proteins within specific brain areas and can inform on expression levels and up or down regulation of specific proteins. This technique cannot identify specific cell types involved and is therefore normally backed up by IHC analysis in brain sections.

2.4 Fluorescent activated cell sorter (FACS) analysis

FACS analysis as a tool to analyse cells in the CNS is predominantly used in *in vitro* cell culture systems. This study was set up to determine whether FACS analysis could be used successfully *ex vivo* and also to establish if it could be used to analyse apoptotic cell loss. The initial pilot study was set up to analyse microglial cells within the mouse brain. As there is a marked upregulation of microglia in the ME7/CV scrapie mouse model at the terminal stage of disease this was an ideal candidate cell to initially use to test the suitability of the method.

FACS analysis was performed on brain tissue using a method adapted from one used for analysis of spleen tissue. Briefly brains were removed and placed into growth medium without buffers, RPMI or HBSS can be used. Brains were dissected

into three parts: frontal lobe, mid and hind brain. Single cell suspension was prepared for each sample as protocol in Appendix 3.

2.4.1 Cell viability

One ME7 infected and one NB control (CV mouse) were analysed. Brains were dissected into three parts as above, and single cell suspensions prepared. Cell viability was analysed by using both trypan blue and FACS analysis. A one in four dilution of the cells was prepared in trypan blue and cells analysed and counted. Cell suspension was made up to a $1x10^6$ dilution for FACS analysis. Cells were then put through the FACS machine without any markers to analyse numbers of cells viable in solution. (Results in chapter 4).

2.4.2 Microglial study

One ME7 infected and one NB control (CV mouse) were analysed. Brains were dissected into three parts, as above and single cell suspensions prepared. Cells were labelled with F4/80 conjugated to FITC and FACS analysis performed. F4/80 is a mouse macrophage marker that is expressed on microglia.

2.4.3 Neuron study

One normal mouse brain was taken and a single cell suspension was prepared. One step was added to this methodology, as the cells seemed to be prone to clumping. The brain was crudely dissected and placed into dissociation medium in the incubator at 37^o C for 30mins. At 15 mins the pieces of brain were disaggregated by sucking them up through a syringe and placing the suspension back into the incubator for 15mins. The rest of the method as in Appendix 3 was followed. Neurons were identified using the NeuN antibody conjugated to Alexa 488 at 1/100. NeuN is a neuron specific nuclear protein observed in CNS and PNS neurons.

A cytospin preparation was made from cells labelled with NeuN conjugated to Alexa 488. A cell suspension containing $1x10^6$ cells was spun in the cytospin centrifuge (Shandon). These cells where analysed using the Zeiss pascal 5 confocal microscope. Single scanned images were produced using an Argon 488 laser and an FITC filter. Images were prepared from the cytospin preparations at x20 and x60 oil magnification.

In these studies FACS analysis had its limitations. The technique was applied successfully to the analysis of microglia and could be used in the future in time course studies to investigate the timing of the microglial response in TSE infected mouse brains. On the other hand FACS may not be the method of choice for analysis of neurons ex vivo. Neurons seemed to be more prone to clumping and have a complex morphology, the crude FACS methodology may sheer of their dendrites and axons which may initiate cell death. This could make it impossible to distinguish between cell death due to the disease or that produced in the preparation of the single cell suspension.

Chapter 3: Time course study of the neuropathological changes observed in the hippocampus of the ME7/CV scrapie mouse model

3.1 Introduction

TSE diseases of animal and man cause a progressive degeneration of the central nervous system (CNS) that is eventually fatal. Neuropathological changes characteristic of these diseases include vacuolation, gliosis, accumulation of the disease specific form of the normal cell-surface sialoglycoprotein, PrP and neuronal loss. Much of our understanding of the TSEs has come from the study of murine scrapie models. The strain of scrapie and the strain of mouse infected produces distinct patterns of disease (Bruce & Fraser, 1991). Vacuolation of the brain also known as spongiform change is one of the classical lesions associated with TSE pathology. It appears as tiny holes in the neuropil of the grey matter and can also be observed within the cytoplasm of neurons (Fraser, 1993). TSE strains show dramatic and reproducible differences in the severity and distribution of this vacuolar degeneration in the brains of genetically uniform mice (Fraser & Dickinson, 1967). This pathological feature has been historically used as a method of strain typing and is discussed in chapter 1.

Another characteristic pathological features observed in these mouse models of disease is the deposition of disease specific PrP (PrP^{Sc}). PrP is a normal cellular membrane-bound sialoglycoprotein (PrP^{c}), which when converted to its abnormal form (PrP^{Sc}), undergoes a conformational change to a predominantly β-pleated structure. Ultrastructural studies have shown that it is localized to amyloid fibrils, accumulates on the plasmalema of neurite membranes and coincided with intense vacuolation of the neuropil (Ersdal et al, 2004; Jeffrey et al, 1994b). Visualised

immunohistochemically, PrP^{Sc} deposition in the TSE infected brain takes several different forms: amyloid plaques, fine granular or synaptic deposits, and coarser deposits including perineuronal and perivacuolar forms (Bruce et al, 1989). Experimental studies in scrapie mouse models have revealed that the pattern of PrP deposition within the brain depends on the strain of agent used, route of injection and the mouse genotype (Bruce et al, 1989) (Figure 1). The isolation of PrP allows for the production of many PrP epitope specific antibodies and with the developing technique of immunohistochemistry, can be used as a diagnostic tool and to define phenotypes. Several PrP antibodies are available from a number of donor species that recognise the full length protein or that recognise different epitopes on the PrP molecule. The mouse monoclonal antibody used in this study, 6H4, recognises the epitope DWEDRYYRE (amino acids 143-151) and has been used successfully to immunolabel PrP^{Sc} in the brains of mice infected with scrapie (Jamieson et al, 2001b; Liu et al, 2003). The diagnosis of scrapie strains is usually performed using a scoring system for vacuolation observed in specific areas of the mouse brain (lesion profile).

One of the other pathological features observed in mouse models of TSE is glial activation. The gliosis observed in TSE infected brains involves a lesion-related increase in size and number of astrocytes and microglia (Figure 2). Glial activation within the brain can occur generally in response to neurological disease or trauma and is not a specific indicator of TSE disease. However the role of the glial response in the development of TSE disease in the brain is still to be elucidated. Although there is no evidence for a classical immune response in the CNS in TSEs, microglial activation and recruitment of CD8 T cells has been shown to occur early in the incubation period (Betmouni et al, 1996). There is a marked activation of both microglia and astrocytes observed in the brains of both humans and animals at the terminal stage of TSE

disease (Rezaie & Lantos, 2001). This activation parallels the temporal and spatial patterns of PrP^{Sc} deposition, precedes neuronal cell death *in vivo* and displays characteristic patterns in different models of CJD (Baker et al, 1999; Giese et al, 1998). Studies in mouse models of disease have shown that microglial activation correlates with the accumulation of disease specific PrP (Williams et al, 1997a; Williams et al, 1997b; Williams et al, 1994). Microglial processes have been observed around vacuoles and at the periphery of amyloid plaques (Wisniewski et al, 1990), it is not yet known if microglia are involved in the formation or phagocytosis of amyloid fibrils. In both *in vivo* and *in vitro* studies, activated microglia have been shown to be neurotoxic, secreting potentially harmful mediators such as nitric oxide, reactive oxygen intermediates, excitatory amino acids, proteases, chemokines and cytokines, exacerbating the damage observed in TSE disease (Burwinkel et al, 2004; Fabrizi et al, 2001; Veerhuis et al, 2002).

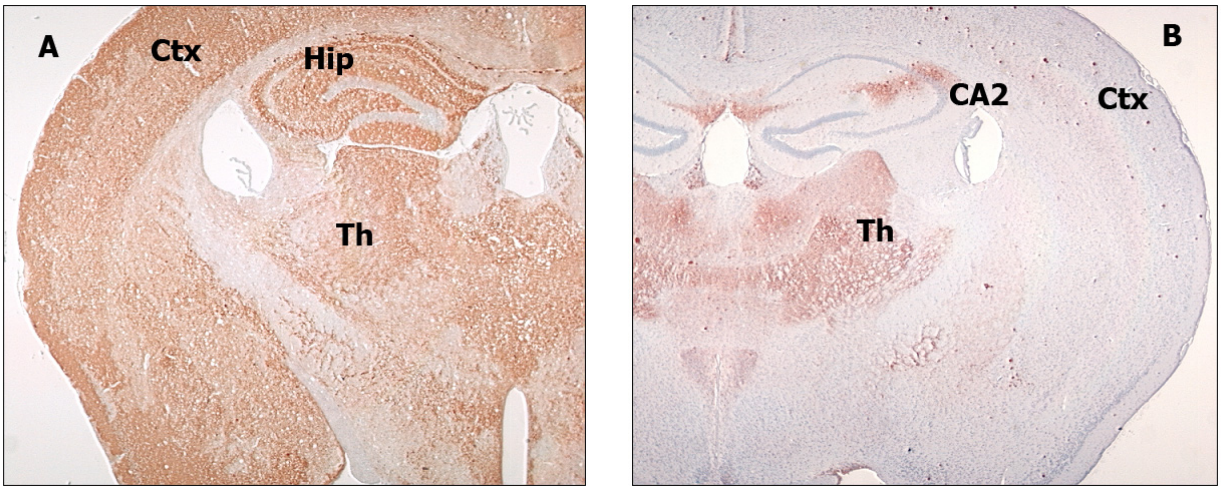

Figure 1. Pattern of disease specific PrP^{Sc} in two scrapie mouse models (A) ME7/CV : the deposition of PrP in the brain is diffuse, targeting the hippocampus (Hip), thalamus (Th) and cortex (Ctx) and (B) 87V/VM : diffuse accumulations are observed in the thalamus (Th) and also precisely targeted to the CA2 of the hippocampus. Plaques are also typically numerous with this strain, observed throughout the cortex (Ctx). Magnification x2

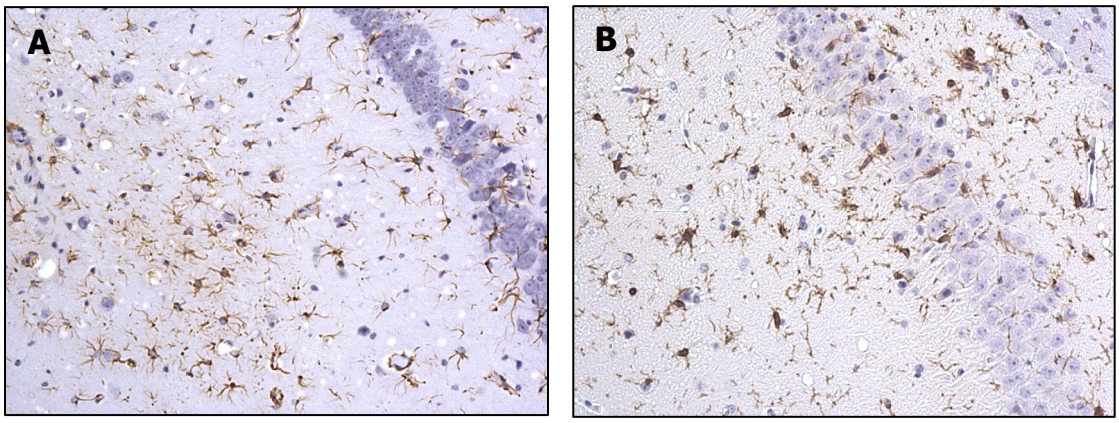

Figure 2. 87V/VM scrapie mouse model :- targeting of the glial response in the CA2 of the hippocampus in VM mice infected with the 87V strain of scrapie.
(A) GFAP labelling of reactive astrocytes in the CA2 of the hippocampus.
(B) Iba1 labelling of microglia in the CA2 of the hippocampus. (Magnification x 20)

Reactive astrocytosis observed in prion diseases is most apparent in areas where severe spongiform change and neuronal loss occur. Reactive astrocytes are also closely associated with the deposition of PrP^{Sc} (Bruce et al, 1994), which has been shown to accumulate within astrocytes in both mouse and hamster models of scrapie (Diedrich et al, 1991; Ye et al, 1998) This is not always the case and depends on the TSE model studied. In C57BL and CV mice infected with vCJD, the pattern of astrocytosis within the hippocampus differed from the distribution of PrP^{Sc} (Brown et al, 2003b)

In the past, the neuronal network was considered the most important system in the brain, and astrocytes were looked upon as "gap fillers". Now they are thought to play a number of active roles in the brain including structural and metabolic support, transmitter reuptake and release, regulation of ion concentration in the extracellular space, modulation of synaptic transmission, vasomodulation and nervous system repair (Farfara et al, 2008; Gibbs et al, 2008; Schwab & McGeer, 2008; Taber & Hurley, 2008).

The exact role of astrocytes in the propagation and pathogenesis of the TSE agent is still uncertain. In the model studied here astrocytosis and microglial activation occurs after the deposition of PrP^{Sc} which may be the trigger for this glial response.

Neuronal loss is another characteristic hallmark of TSE disease. Neuronal loss has been identified and quantified in BSE infected cattle. The vestibular nuclei from BSE cattle had an approximately 50% reduction in total numbers of neurons when compared with controls (Jeffrey et al, 1992a). Neuronal loss has also been observed in scrapie mouse models of disease, in an intra-ocularly infected murine scrapie model a significant loss of neurons in the dorsal lateral geniculate nucleus (dLGN) was

observed (Jeffrey et al, 1995a). In the model used in this study, the ME7/CV mouse model, neuronal loss was observed in the CA1 of the hippocampus, in this model 50% of neurons died by day 160 of a 250 day incubation period. Murine scrapie models target many different brain areas but due to the well characterised nature of the neuronal connections of the hippocampus, a large quantity of research has concentrated on the effects of these strains on this area. The targeted neuronal loss observed in the CA1 field of the hippocampus in the ME7/CV scrapie mouse model makes it an ideal model to study the mechanisms involved in the neuronal loss observed in TSEs.

The ME7/CV mouse model was used in these studies. The CVF1 (C57BLxVM) cross (*Prnp*^{ab}) intracerebrally infected with the ME7 strain of scrapie results in consistently severe pathology of the hippocampus and an incubation period of approximately 250 days (Scott & Fraser, 1984). Previous studies performed using this mouse model observed early changes in CA1 neurons of the hippocampus. At 100 days post infection synapse loss, axon terminal degeneration was observed (Jeffrey et al, 2000), and the ability of these neurons to maintain LTP was disrupted (Johnston et al, 1998b). Also observed at this time point was the loss of dendritic spines from the apical dendrites of CA1 neurons (Brown et al, 2001).

The relationship between pathological changes and the development of clinical disease in the TSEs is not known; however any strategy aimed at intervening to halt the degenerative process must be aimed at the fundamental lesion and not at its sequelae. Previous studies on specific aspects of the neuropathological changes observed in the ME7/CV scrapie mouse model have been performed. For the first time all of the characteristic neuropathological changes observed in this model have been analysed and compared in a single study. The time course study performed in

this thesis using the ME7/CV scrapie mouse model was used to analyse the relationship between the deposition of PrP^{Sc}, vacuolation, activated microglia and astrocytes, and the subsequent neuronal loss observed in this mouse model.

3.2 Aims of Chapter

The principal aims of the work in this chapter are to perform a time course study of the neuropathological changes observed in the hippocampus of the ME7/CV scrapie mouse model, to identify at which time point in the progression of the disease, these changes initially occur, and to relate these changes to the loss of CA1 neurons observed in the hippocampus. The identification of the key events involved in the mechanisms of neurodegeneration in TSE diseases may lead to the development of therapeutic strategies to inhibit the neurodegenerative process.

Specific aims

- To analyse the deposition of PrP^{Sc} in the hippocampus of the ME7/CV mouse model throughout the incubation period of disease (Table 1. time points analysed)
- To analyse the astrocytic and microglial response in the ME7 infected hippocampus throughout the incubation period of disease
- To investigate at which stage in the disease process do the first signs of vacuolation occur.
- To relate the above pathological changes with the neuronal cell loss observed in the CA1 of the hippocampus

3.3 Materials and Methods

3.3.1 Immunohistochemical analysis of PrP^{Sc}, astrocytes and microglia

Immunohistochemical (IHC) labelling was performed for PrP^{Sc} using 6H4 , a mouse monoclonal antibody that recognises the epitope DWEDRYYRE (amino acids 143-151) on the PrP gene. This antibody was chosen as it has been used successfully on mouse brain with excellent staining results with no non specific background (Jamieson et al, 2001a; Liu et al, 2003). Astrocytes were labelled using the cytoskeletal marker glial fibrilliar acidic protein (GFAP), this antibody specifically labels intermediate filaments found within astrocytes only. For microglia labelling Iba1 was used, this is a calcium binding protein found within resident microglia. Historically microglia have been difficult to label in paraffin sections, with citrate buffer pretreatment Iba1 is an excellent marker that labels both resting and reactive microglia. For methodology see Chapter 2 materials and methods and appendix 1.

3.4 Results

3.4.1. First PrP^{Sc} deposition in the ME7 infected hippocampus is observed at 69dpi, increasing in intensity throughout the incubation period of disease.

In the ME7/CV mouse model of disease the first neuropathological changes observed in the hippocampus is the deposition of disease specific PrP (PrP^{Sc}) at 69 dpi, observed as punctuate deposits in the pyramidal cell layer (PCL) of the CA1 sector and in the corpus callosum (CC) (Figure 3A). By 102 dpi, both the intensity and distribution of PrP^{Sc} has increased, revealing a widespread diffuse labelling throughout the CA1 of the hippocampus in both the stratum oriens (SO) and the stratum radiatum (SR). Also observed was an increase in the punctate deposition of PrP^{Sc} observed in the pyramidal cell layer and the corpus callosum (Figure 3B). PrP^{Sc} deposition increased in intensity throughout the incubation period of disease, but in some brains unexpected lower levels were observed. In two brains inspected at 130

days post ME7 infection the deposition of PrP^{Sc} in the hippocampus was low compared with earlier time points and other brains at the same time point. (Figure 3C). From 160 dpi (Figure 3D) onwards diffuse and punctuate forms of PrP^{Sc} increase in amount and intensity until the terminal stage of disease. At the terminal stage of disease the deposition of PrP^{Sc} in the hippocampus is widespread and intense, a dramatic loss in CA1 neurons is observed and there is shrinkage of both the SO and SR (Figure 5F). In TSE models of disease PrP^{Sc} deposition is observed in different forms; in the ME7/CV scrapie mouse model diffuse labelling is prominent in the hippocampus (Figure 3D). Plaque like deposits, which contain amyloid (Figure 5), are observed in the corpus callosum increasing in number by the terminal stage of disease (Figure 4), and neurons encircled by PrP^{Sc} are also observed at this stage in the hypothalamus.

Thioflavin labelling was performed on sections containing the plaque like deposits to identify if they contained amyloid. A terminally infected 87V/VM mouse brain was included as a positive control, as a characteristic pathological feature of this model is amyloid plaques observed throughout the cortex (Figure 5A). The PrP plaque like deposits observed in the corpus callosum labelled with thioflavin, revealing that they contain amyloid (Figure 5).

The PrP^{Sc} deposition within some of the groups of animals was variable, in the 200 dpi group the intensity of PrP^{Sc} deposition, but not the distribution varied. (Figure 6A&B). Differences in the intensity of PrP^{Sc} immunolabelling was also observed in serial sections from the same brain that had been immunolabelled with 6H4 on different days (Figure 7A&B). Therefore comparison of PrP^{Sc} immunolabelling was performed within the same IHC run and not between them.

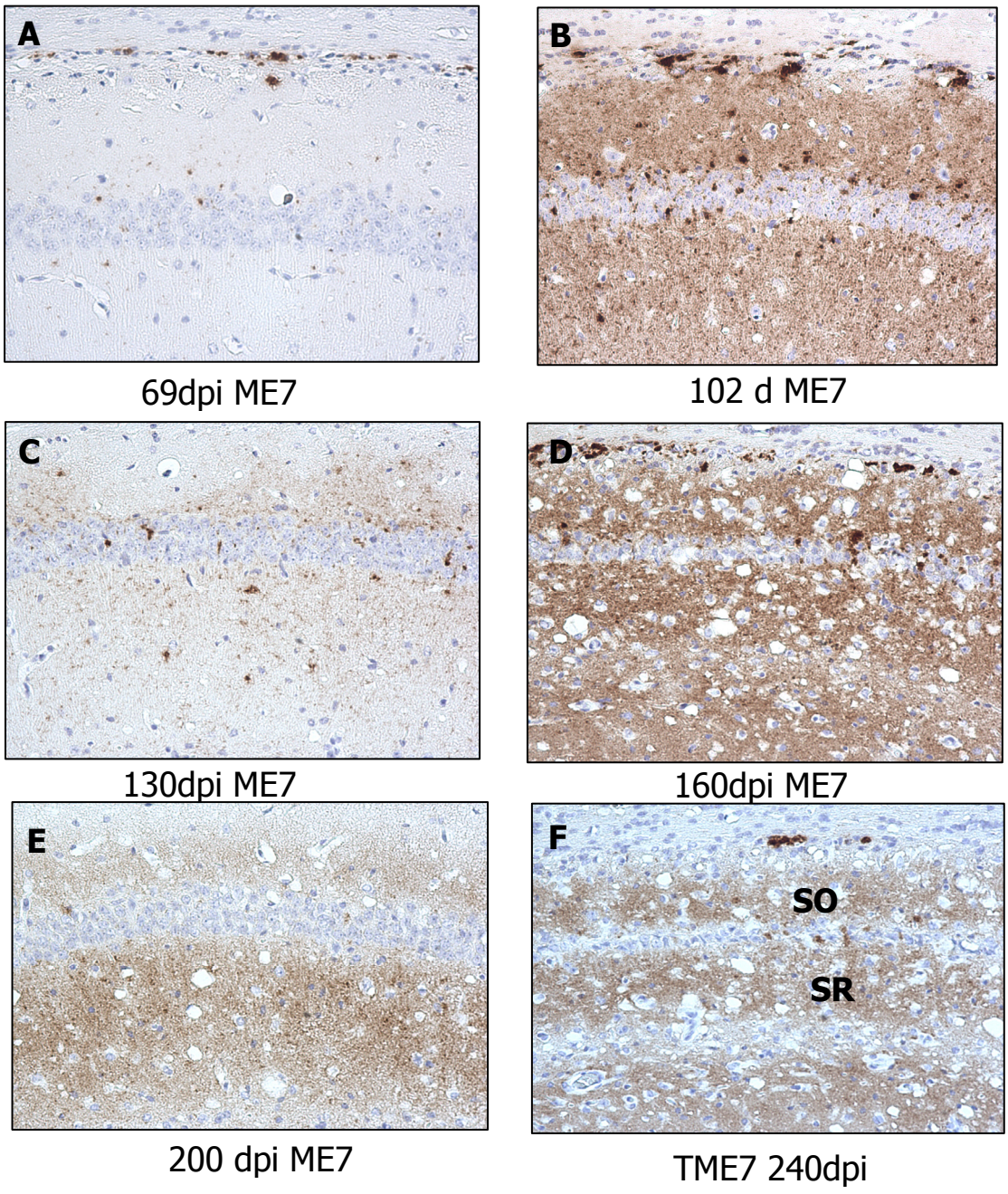

Figure 3. Time series of the PrP^{Sc} deposition in the CA1 of the hippocampus in the ME7/CV mouse model. (A) First PrP^{Sc} deposition observed as punctate deposits in the pyramidal cell layer and the corpus collosum. (B) Increase in amount and intensity of PrP^{Sc} deposition at 102 dpi. (C) Decrease in amount and intensity of PrP^{Sc} labelling observed at 130 dpi. (D) Marked increase in intensity of the PrP^{Sc} labelling observed at 160 dpi. (E) Widespread PrP^{Sc} deposition in the CA1 at 200 dpi.(F) PrP^{Sc} deposition observed at the terminal stage of disease (note shrinkage of the Stratum radiatum (SR) and Stratum oriens (SO) Magnification x20

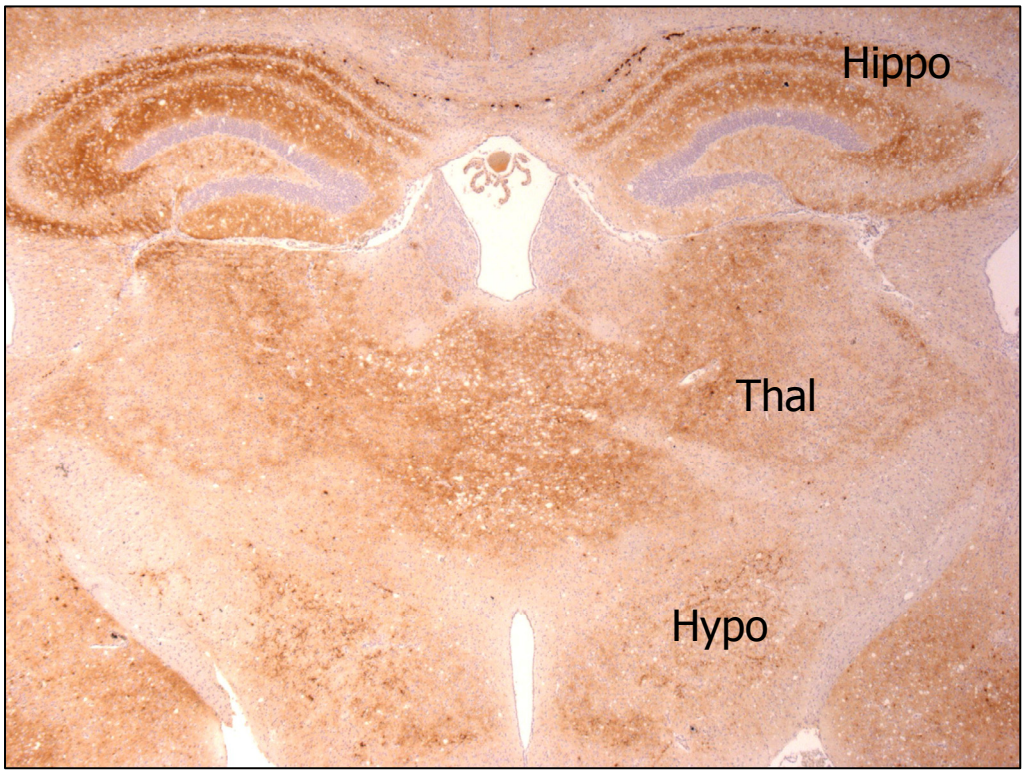

Figure 4. PrP^{Sc} deposition in the ME7/CV mouse model at the terminal stage of disease. Widespread distribution of PrP^{Sc} observed throughout the hippocampus (Hippo) thalamus (Thal) and hypothalamus (Hypo). Magnification x2

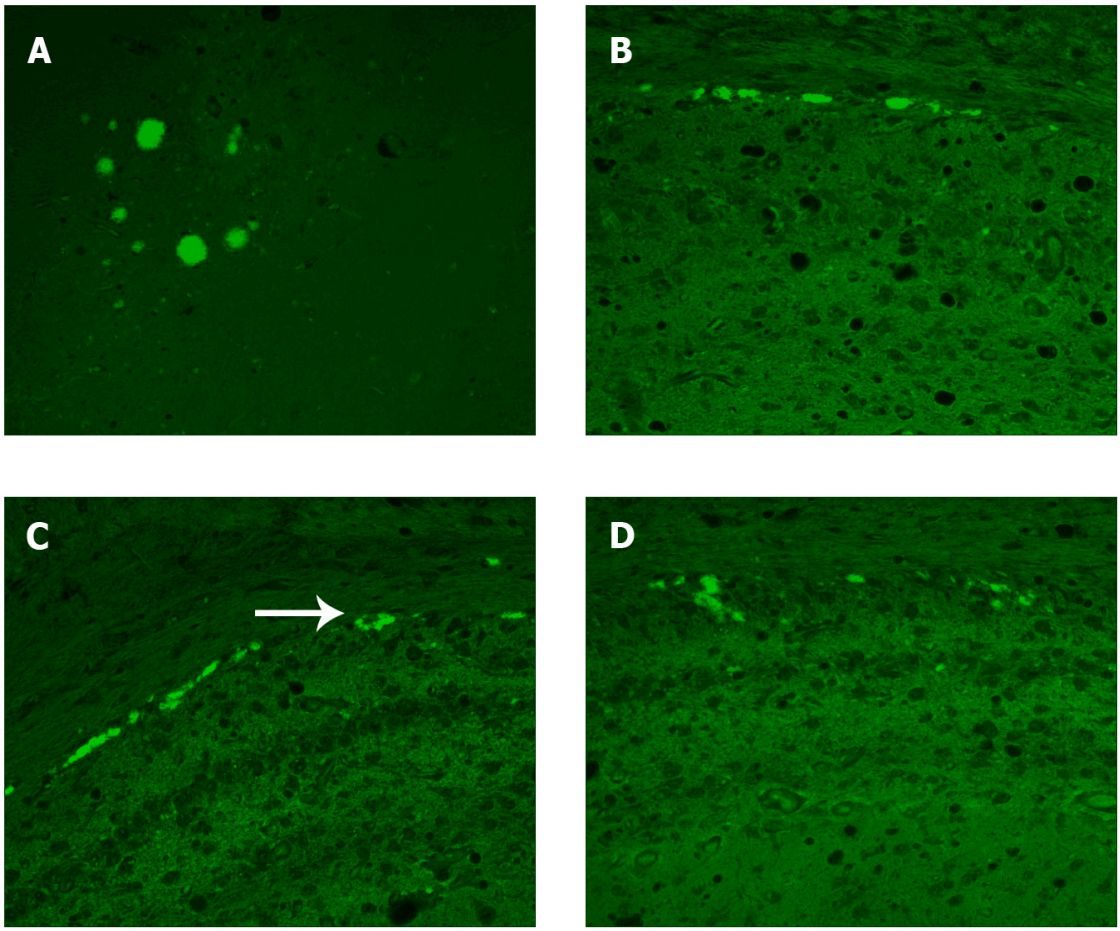

Figure 5. Thioflavin labelling of amyloid deposits observed within the ME7 infected hippocampus. (A) 87V/VM terminal brain showing amyloid plaques labelled with thioflavin. (B) thioflavin labelling of amyloid in the corpus callosum (CC) of 160dpi ME7 infected hippocampus. (C) thioflavin labelling of amyloid in the CC of 200dpi ME7 infected hippocampus, arrow indicating an amyloid plaque. (D) thioflavin labelling of amyloid in the CC of the hippocampus at the terminal stage of disease.

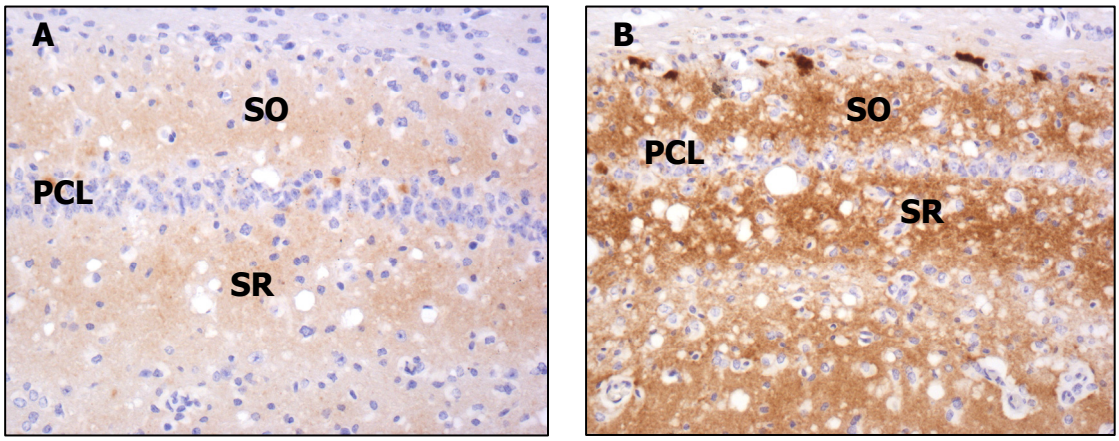

Figure 6. Difference in PrP^{Sc} deposition between animals in the 200 dpi group. 6H4 labelling was performed in the same IHC run. (A) Diffuse labelling observed in the Stratum radiatum (SR) and Stratum oriens (SO) in the CA1 of the hippocampus. (B) More intense labelling of PrP^{Sc} observed in the CA1 also showing an increase in the cell loss from the pyramidal cell layer (PCL) and shrinkage of the SR and SO. Magnification x20

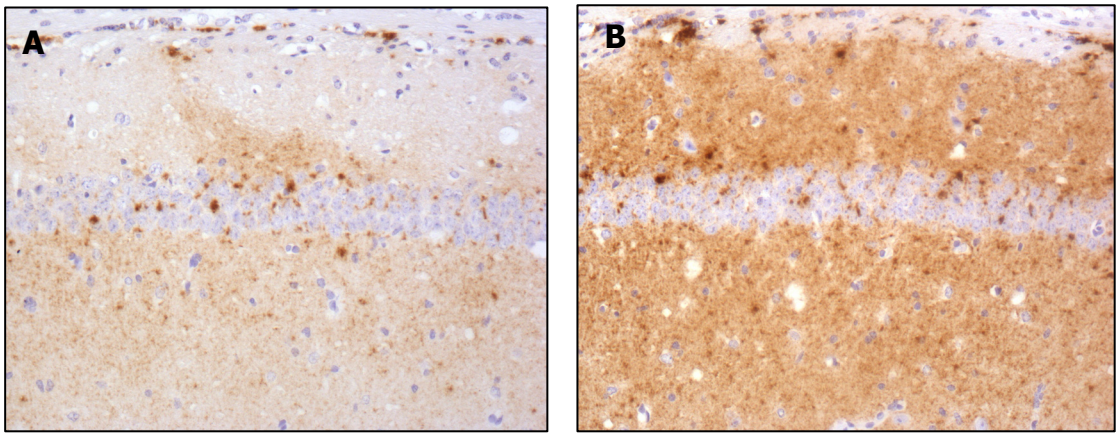

Figure 7. Differences observed between IHC runs in serial sections from the same brain. PrP^{Sc} staining of serial sections from the same brain in the hippocampus at 102 dpi (A) 6H4 labelling performed on 25-10-07 and (B) 6H4 labelling performed on 31-10-07. Magnification x20

3.4.2 Increase in astrocytes observed from 102 dpi ME7. Morphologically astrocytes appear reactive from 160 dpi ME7.

Astrocytes are observed in the ME7 infected hippocampus as early as 69 dpi. Morphologically they appear normal, with fine processes extending into the neuropil (Figure 8A) similar to those observed in the 102 dpi NB injected control (Figure 10C). At 102 days post ME7 infection slight astrocytic hypertrophy and hyperplasia is observed with a thickening of astrocytic processes (Figure 8B). By 130 days post infection astrocytic hyperplasia is evident but morphologically astrocytes appear similar to those observed in NB infected controls (Figure 8C). From 160 dpi onwards astrocytic hypertrophy and hyperplasia increases, morphologically astrocytes show a thickening of processes, some having lost their processes entirely and show glial fibrillary acid protein (GFAP) labelling of cell bodies only (Figure 8F&9A). Also from 160 dpi astrocytes appear to increase in numbers in the PCL of the hippocampus, surrounding the cell bodies of the CA1 neurons (Figure 8E&F). Variation in astrocytic labelling was observed within the groups of animals which correlates with the deposition of PrP^{Sc}. For example the 102 and 130 days ME7 infected brains labelled with GFAP in figure 8 have also been labelled with 6H4, the marked PrP^{Sc} deposition observed in the 102d infected ME7 brain (Figure 3B) corresponds with the activation of astrocytes observed at this time point (Figure 8B).

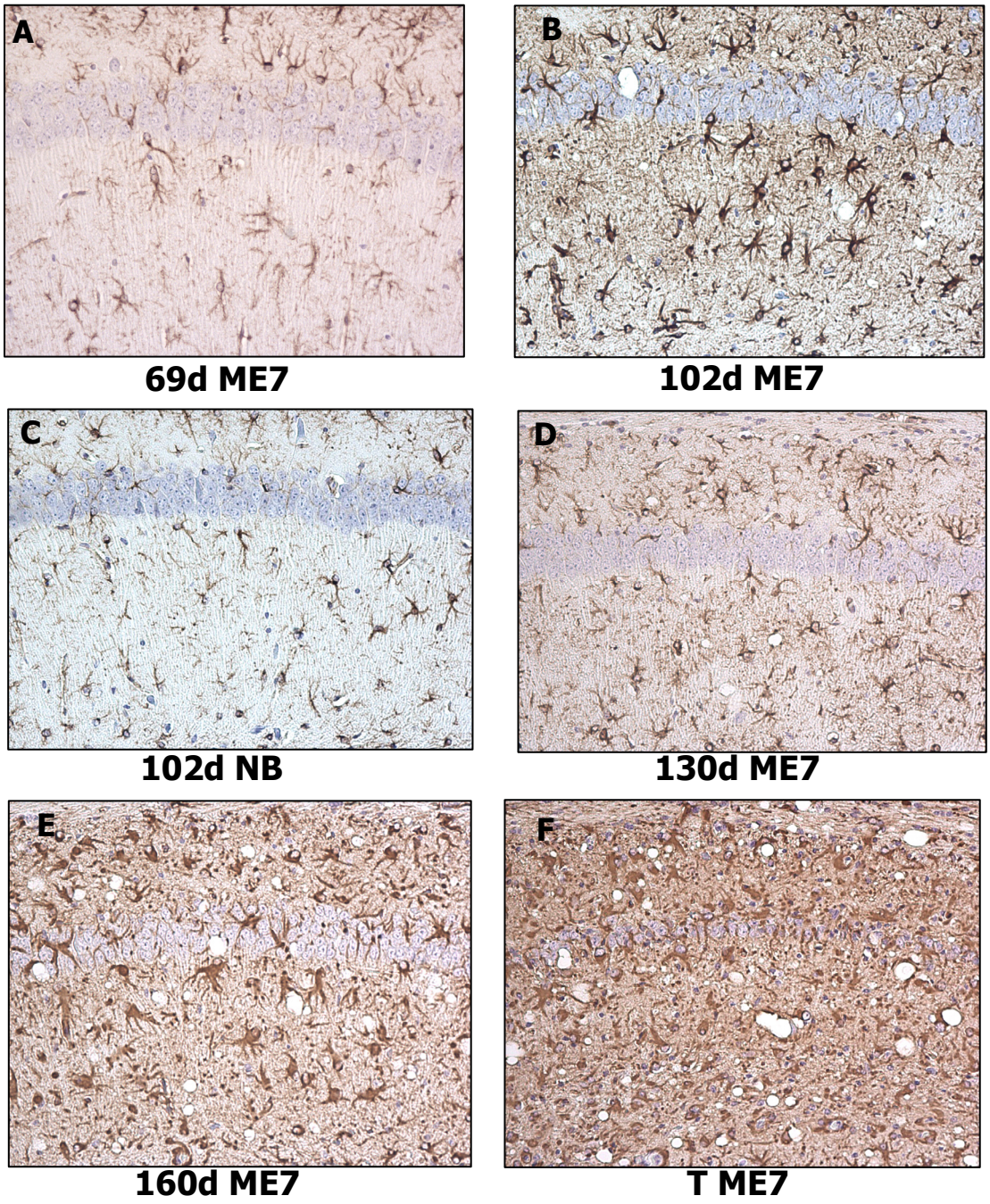

Figure 8. Time series of astrocytosis in the hippocampus in the ME7/CV mouse model . GFAP labelling of astrocytes throughout the incubation period of disease.(A) 69 days post ME7 infection showing normal morphology (B) Astrocytes at 102 dpi slight hypertrophy but no apparent hyperplasia. (C) Astrocytes in a NB control at 102 dpi showing normal morphology. (D) Astrocytes at 130dpi appearing similar to the NB injected control. (E) At 160 dpi astrocytic hyperplasia and hypertrophy was observed, also astrocytes surrounding the cell bodies of the CA1 neurons, this was also observed at the terminal stage of disease (F). (F) Marked astrocytic hypertrophy and hyperplasia at the terminal stage of disease. Magnification x20

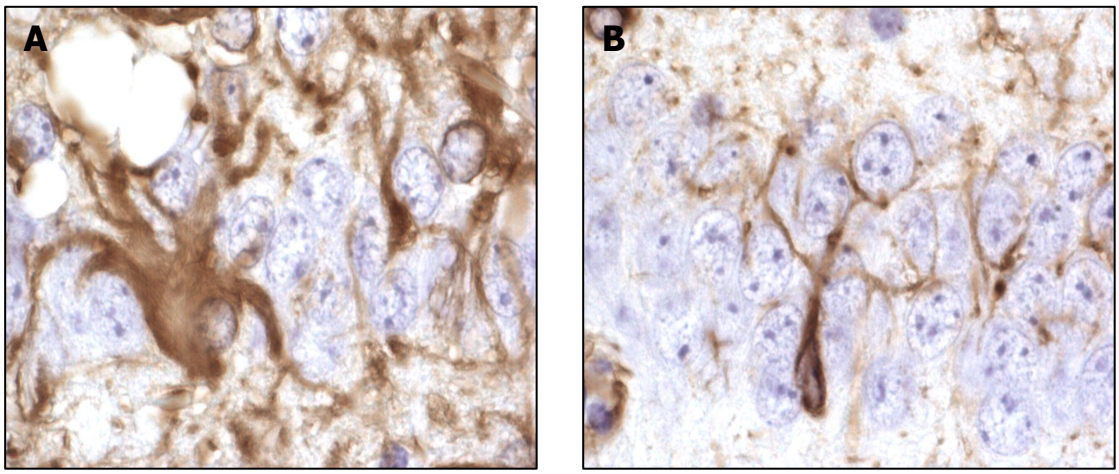

Figure 9. Morphology of astrocytes in ME7 infected and normal brain injected controls. (A) Morphology of an astrocyte observed in the hippocampus of an ME7 infected brain at the terminal stage of disease.(B) Astrocyte morphology observed in a NB injected control. Processes from both types of astrocytes surrounding the cell bodies in the pyramidal cell layer. Magnification x100 oil

3.4.3 Increase in microglia and change in morphology observed from 102dpi ME7

Microglia are the brain's intrinsic immune cells and serve as damage sensors of the brain. Under normal conditions they are in a resting state, but when activated the morphology of microglia change from a highly branched, ramified resting morphology , with retraction of cell processes and eventually transformation into cells with an amoebiod appearance (Perry et al, 2007). These morphological changes are observed in the brains of mice infected with ME7 (Figure 11).

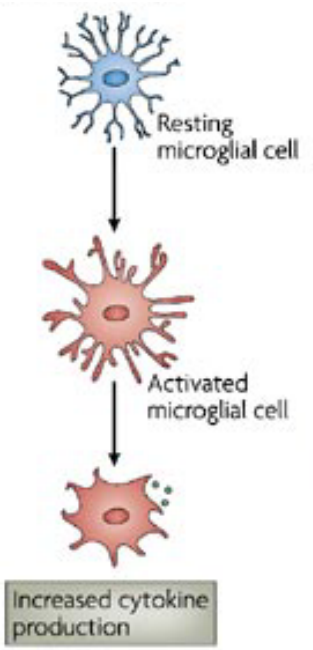

Figure 10. Morphology of microglia Changes in morphology of microglia cells from resting to amoeboid. Taken from Perry *et.al Nat Rev Immunol* **7:** 161-167

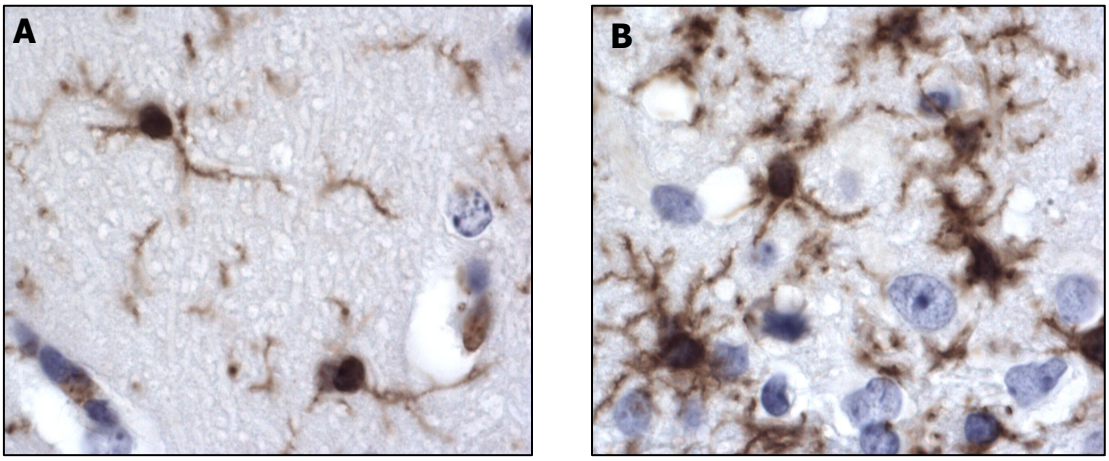

Figure 11. Morphology of microglia observed in the ME7/CV scrapie mouse model. (A) Microglia in a normal brain injected control showing the normal resting morphology. Fine processes are observed branching throughout the neuropil (B) Microglia in an ME7 infected brain at the terminal stage of disease, showing an increase in numbers of microglia and an activated state. Magnification x100 oil

In the ME7/CV scrapie mouse model microglia are observed in their resting state at 69dpi in both the ME7 and NB infected mice (Figure 12A&B). By 102 dpi a dramatic increase in numbers of microglia are observed in the hippocampus in both the stratum oriens and stratum radiatum. The morphology has also changed and microglia are observed in the active state (Figure 12C). At 130 dpi similar changes are observed (Figure 12D). From 160 dpi numbers of microglia are shown to increase and show morphological characteristics of the reactive type (Figure 12E). By the terminal stage of disease microglia are reactive and a few are observed in the amoeboid form (Figure 12F)

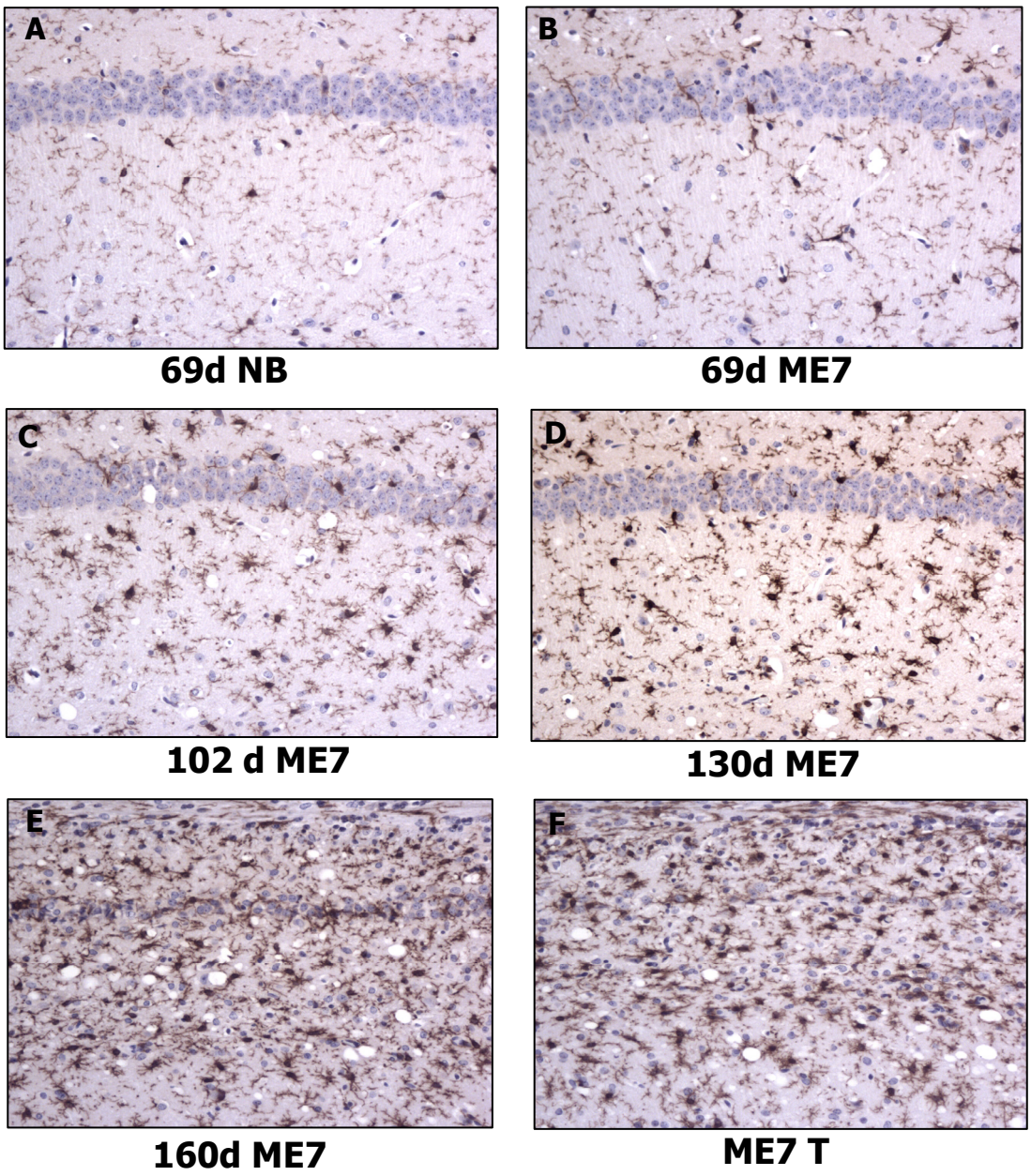

Figure 12. Time series of microglial response observed in the ME7/CV scrapie mouse model. Resting microglia observed at 69dpi NB (A) and ME7 (B). Increase in numbers of microglia and change in morphology at both102 (C) and 130 dpi (D). From 160dpi (E) an increase in numbers of microglia and reactive and amoeboid morphology is observed (F). Magnification x20

3.4.4 First signs of vacuolation in the CA1 of the hippocampus are observed at 102 dpi

Vacuolation was first observed in the CA1 of the ME7 infected hippocampus at 102 dpi (Figure 13B). At 130 dpi number of vacuoles observed in the hippocampus increased (Figure 13C). From 160 dpi, vacuolation observed in the hippocampus increased in numbers, and in some cases, size of vacuoles (Figure 13D). Considerable variability was observed within the groups. Vacuolation was observed in the hippocampus around 40 days after the first signs of PrP^{Sc} deposition and increased in severity throughout the incubation period of disease.

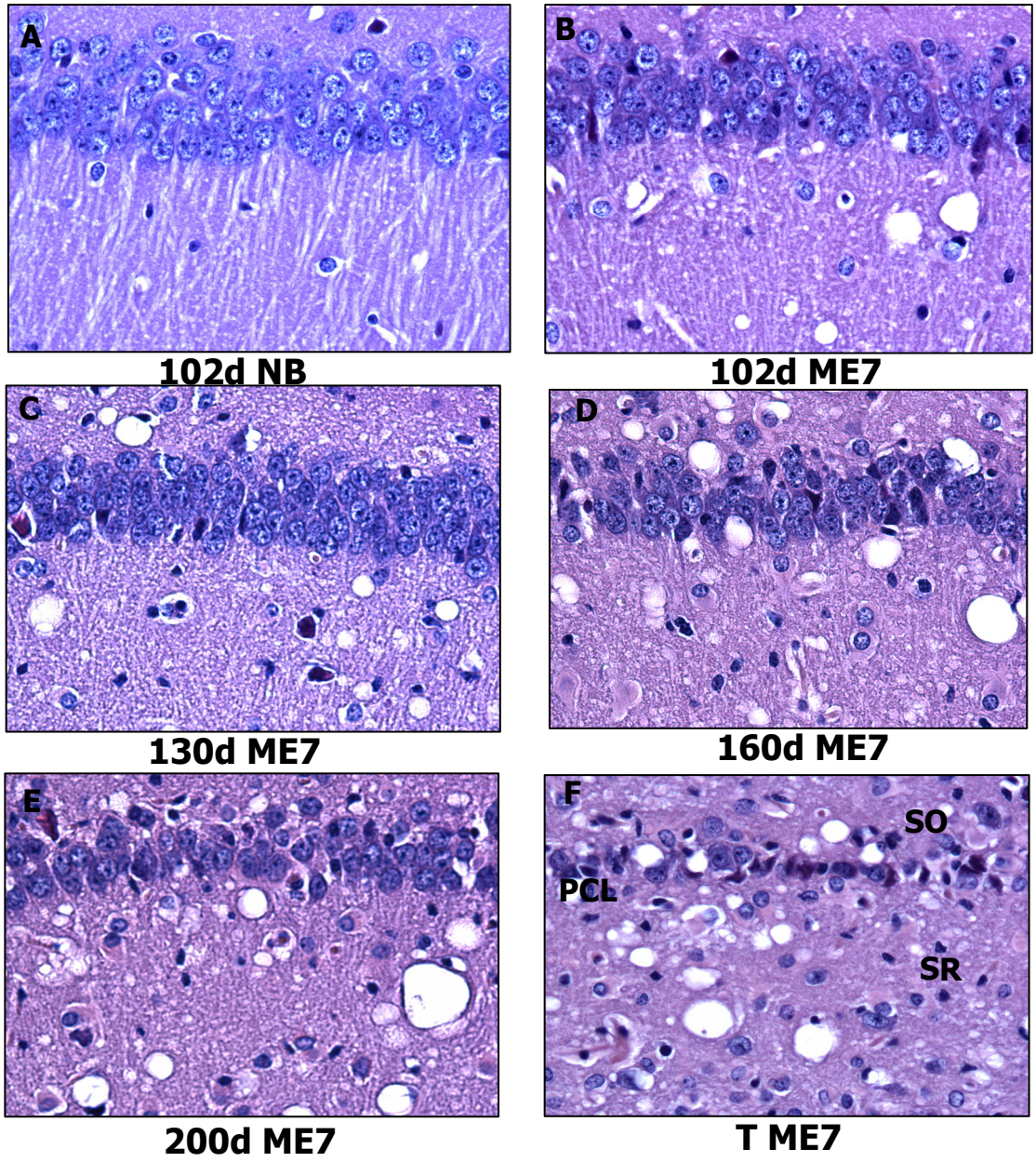

Figure 13. Time series of vacuolation observed in the hippocampus of the ME7/CV scrapie mouse model (A) 102dpi normal brain showing no vacuolation (B) First signs of vacuolation observed in the 102 dpi ME7 infected hippocampus. (C) increase in vacuolation observed at 130dpi. (D) Vacuolation observed at 160 dpi, larger vacuoles observed at this time points. Amount of vacuolation increases at 200 dpi (E) numerous vacuoles observed at the terminal stage of diseases appear smaller due to shrinkage of stratum radiatum (SR) (F) PCL=pyramidal cell layer, SO= stratum oriens, SR= stratum radiatum

3.4.5 Neuronal loss in the CA1 of the hippocampus is observed from 160 dpi ME7 infection

Neuronal loss is one of the main pathological features observed in the hippocampus of the ME7/CV scrapie mouse model. When injected with the ME7 strain of scrapie, the CV mouse strain produces a targeted loss of neurons in the CA1 sector of the hippocampus. Previous studies in the ME7/CV mouse model, using morphometric analysis, discovered that the first significant neuronal loss was observed at 160 dpi. (Jeffrey et al, 2000)

In this study, the neuronal cell loss observed in the CA1 of the hippocampus was analysed using haematoxylin and eosin stained sections. The number of cell bodies in the pyramidal cell layer of the hippocampus at each time point were analysed by light microscopy. Differences were observed in the thickness of the cell layers between animals in the same group, and in some cases, between the left and right side of the hippocampus (Figure 14C&D). This observation was found predominantly in the 160 and 200 day time points. Morphometric analysis of neuron cell numbers was performed on all animals in both these time points (Figure 15&17). A difference in neuronal cell numbers was observed between the infected and control animals in each group. A dramatic difference was observed in the one animal (number 2) between the left and right side of the hippocampus; the right side had a more severe neuronal loss, which appeared to relate to the injection site, the right side of the mid cortex. To check that the length of the pyramidal cell layer was not affected by the shrinkage observed in the hippocampus the length of each CA1 area used for counting was measured, there were no major differences between animals in the length of the CA1 sector measured. Microscopically, neuronal loss could be observed at 160dpi, but as seen previously this differed between animals, although there was neuronal loss in all the ME7 infected animals in comparison to the NB controls (Figure 15), only

one showed a dramatic loss at this time point (Figure 14C). Dark neurons were also observed in the pyramidal cell layer of this animal (Figure 18C arrow), this feature is an artefact produced by removal of the unfixed brain at autopsy, and has been observed in both ME7 infected and normal brain controls (Figure 18A). This artefact can be resolved by perfusion fixation of the brain (Cammermeyer, 1961). At 200 dpi there was considerable variation in the amount of neuronal cell loss observed in the CA1 pyramidal cell layer two out of the four ME7 infected animals showed a dramatic loss of neuronal cell bodies (Figure 16D&17), the other two animals differed in the numbers of cells lost (Figure 16B&C). Neuronal loss increased in severity throughout the incubation period of disease (Figure 19), although some differences were observed between animals the main trend observed throughout the incubation period of disease was an increase in the loss of CA1 neurons.

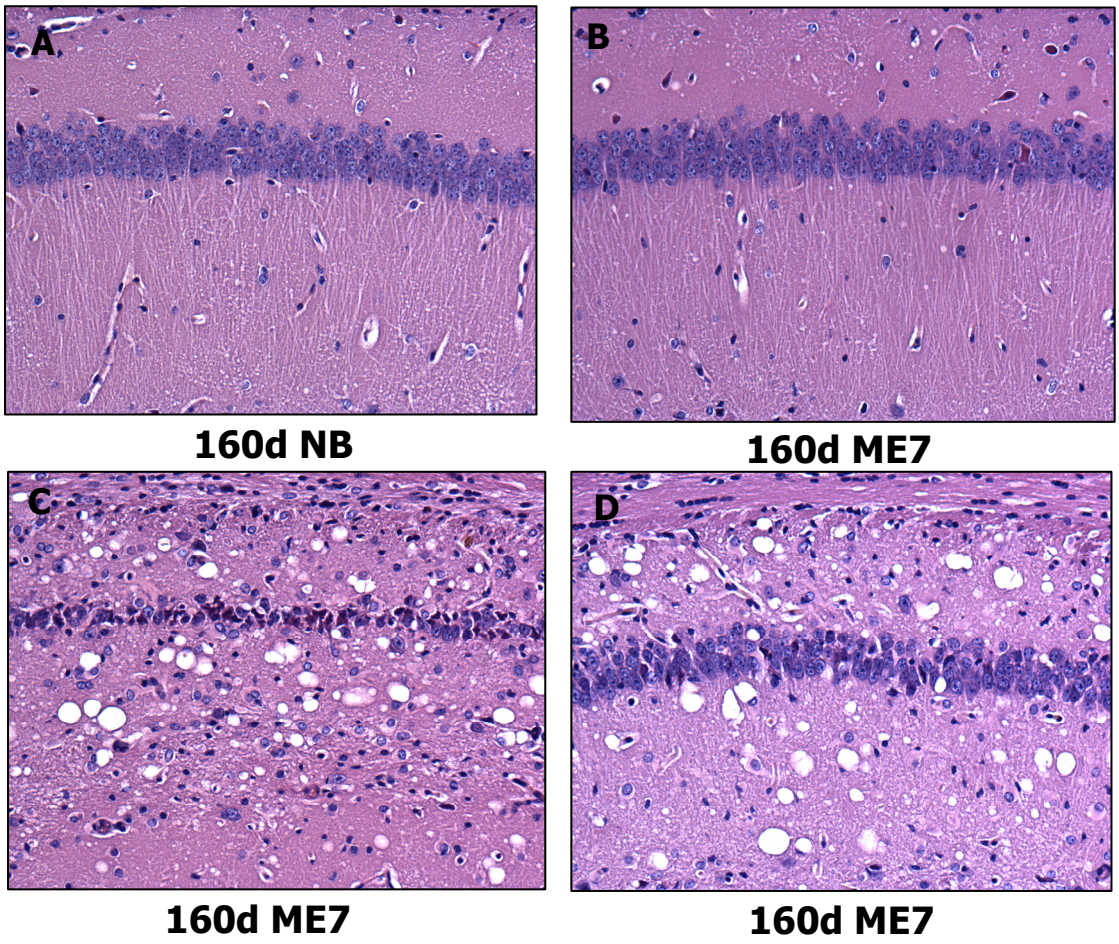

Figure 14. Neuronal cell loss observed in animals at 160 dpi ME7. (A) Pyramidal cell layer in the CA1 of the hippocampus of a 160dpi NB. (B) Pyramidal cell layer from one of the ME7 infected animals at 160dpi. (C) Marked neuronal loss observed in one animal at 160dpi (D) pyramidal cell layer from a third animal at 160 dpi. In (C) and (D) vacuolation in the neuropil of both the stratum radiatum and stratium oriens is observed. Magnification x40

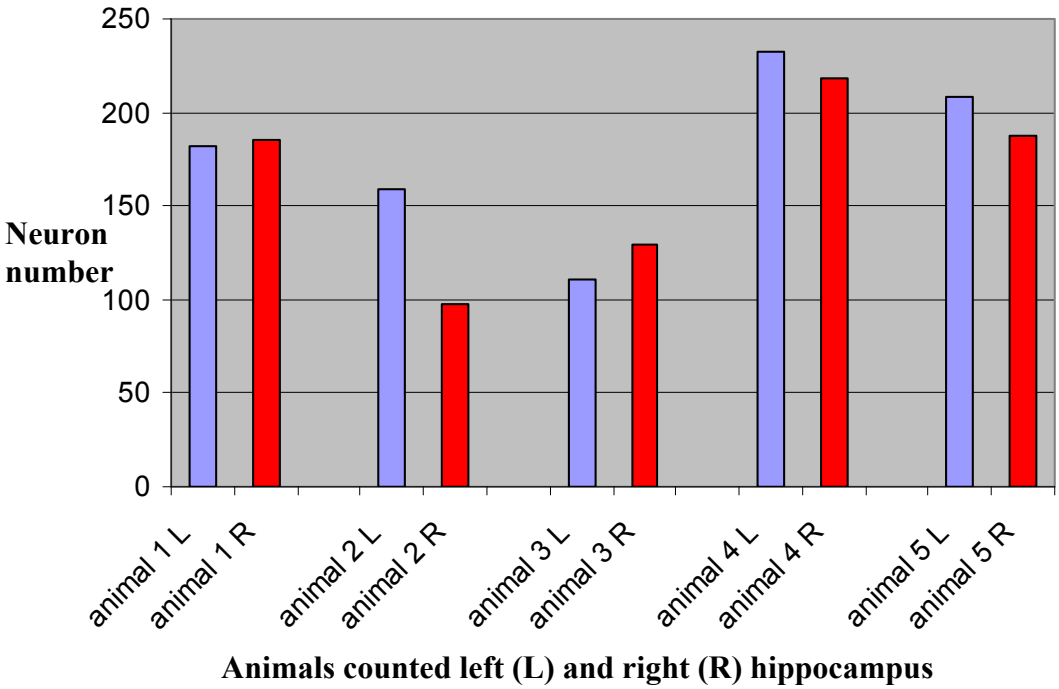

Figure 15. Neuronal counts from 160dpi ME7 and NB CA1 sector of the hippocampus. Animals 1-3 are from the left (L) and right (R) of the 160dpi ME7 infected CA1, 4&5 are normal brain controls. Difference observed in neuron number in animal 2 between the left and right hippocampus, and differences observed between animals in neuron number as shown in Figure 16.

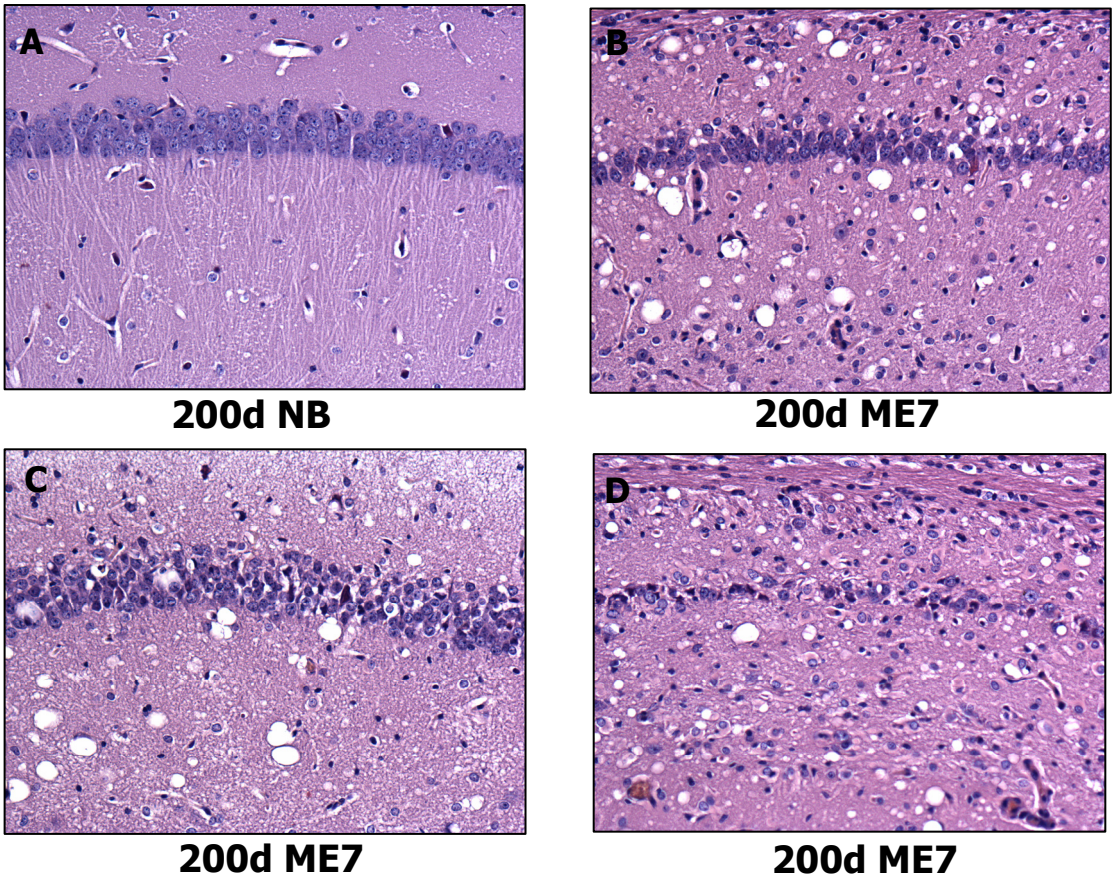

Figure 16. Neuronal cell loss observed in animals at 200dpi ME7. (A) Pyramidal cell layer in the CA1 of the hippocampus in a 200 dpi NB. (B) Pyramidal cell loss observed in an ME7 infected brain at 200dpi. (C) No pyramidal cell loss observed in this ME7 infected brain at 200 dpi. (D) Obvious pyramidal cell loss observed in this ME7 infected animal at 200 dpi. Magnification x40

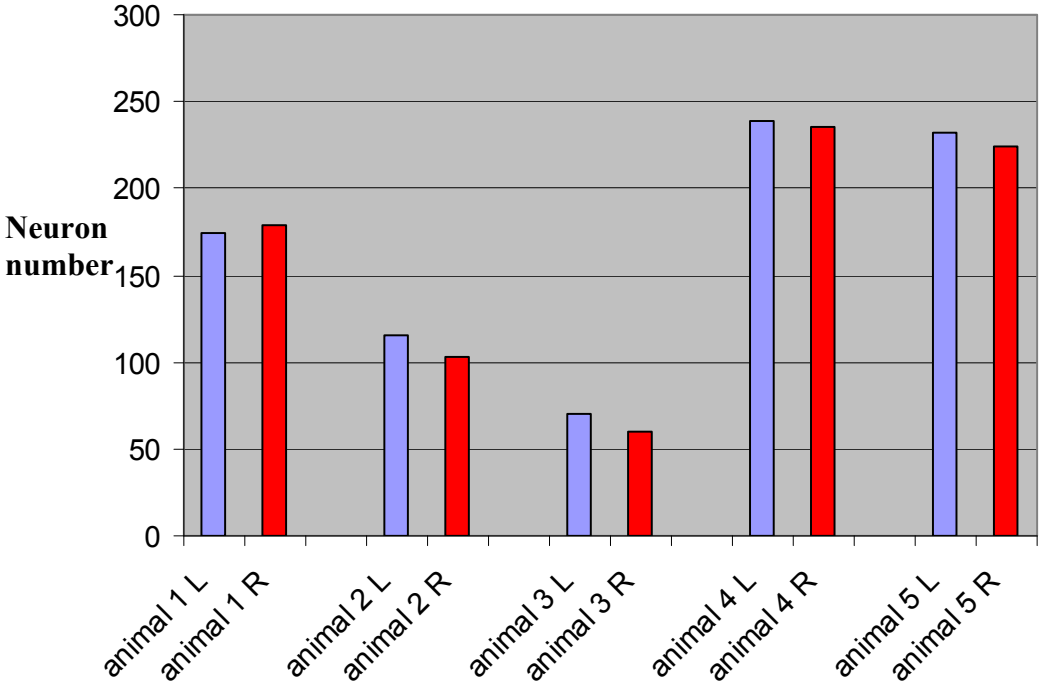

Figure 17. Neuronal counts from 200 dpi ME7 and NB CA1 sector of the hippocampus. Animals 1-3 are from the left (L) and right (R) of the 200dpi ME7 infected CA1, 4&5 are normal brain controls. No major difference is observed between the left and right of the hippocampus, but differences in neuron number observed between animals in the ME7 infected brains as shown in Figure 18

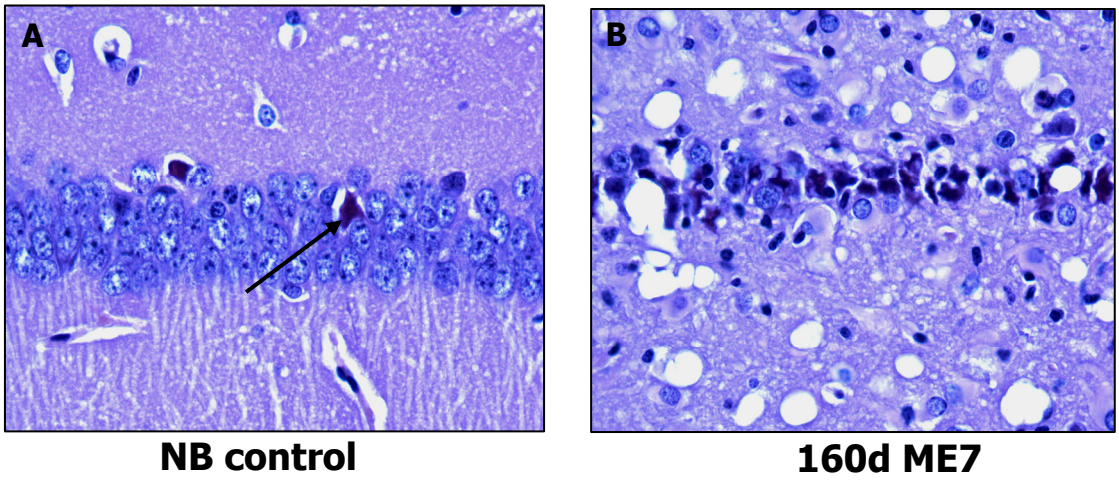

Figure 18. Dark neurons observed in both a NB control and an ME7 infected brain (A) Two dark neurons (arrow) observed in the 102d NB control. (B) increase in dark neurons in the 160d ME7 infected hippocampus. Magnification x 40

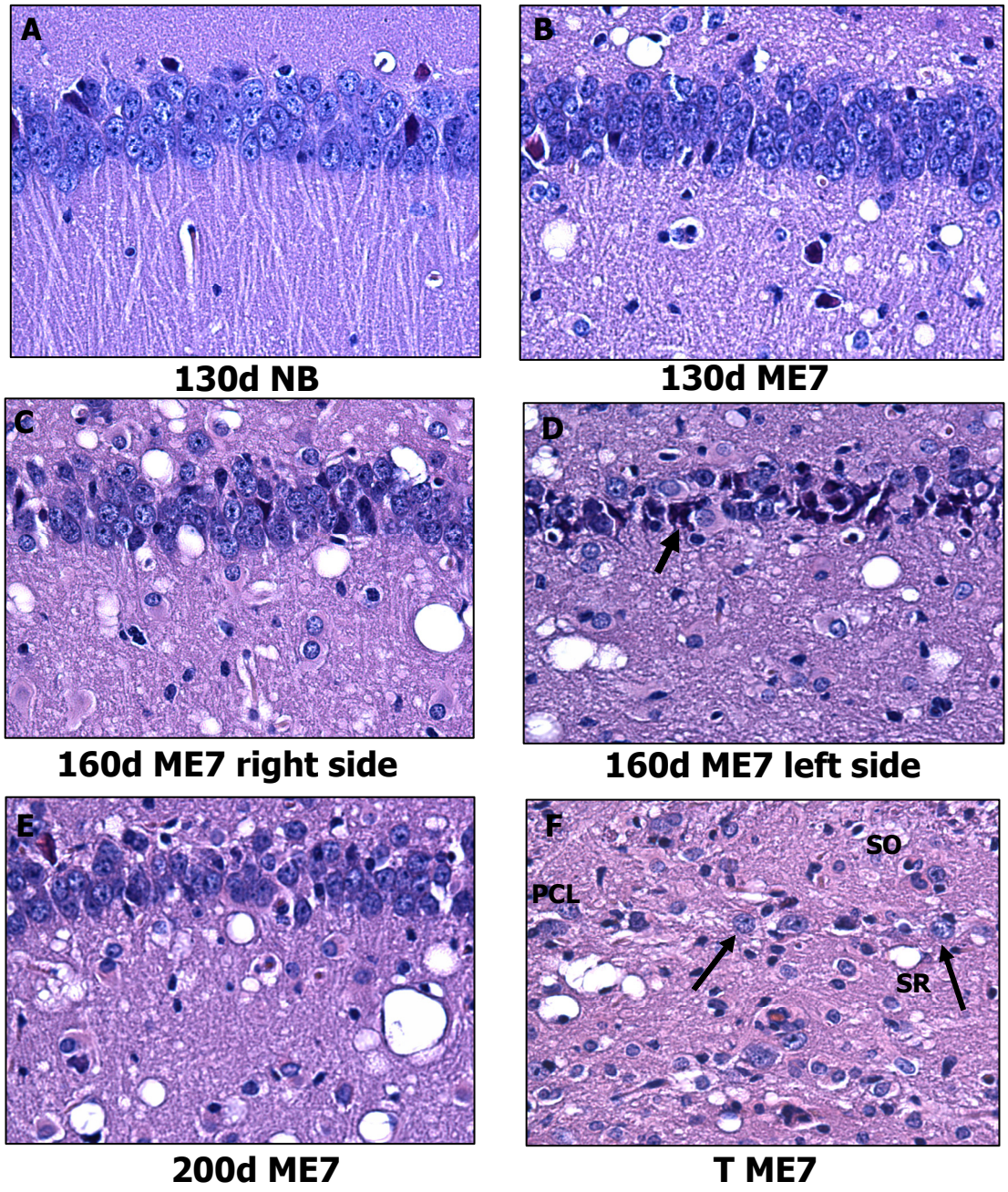

Figure 19. Time series of neuronal cell loss observed in the ME7/CV scrapie mouse model. (A) pyramidal cell layer in a 130 dpi NB injected animal. (B) 130 dpi ME7 infected animal showing no apparent pyramidal cell loss (C) 160 dpi ME7 infected animal the right side of the hippocampus (D) The left side of the hippocampus from the same 160 dpi infected animal showing a marked pyramidal cell loss. Also showing dark neurons (arrow) (E) Pyramidal cell loss observed at 200 dpi. (F) Single pyramidal cell neurons in the CA1 in the ME7 infected hippocampus at the terminal stage of disease (arrows). Also observed is shrinkage of the stratum oriens (SO) and stratum radiatum (SR) T= terminal. Magnification x20

Summary of results

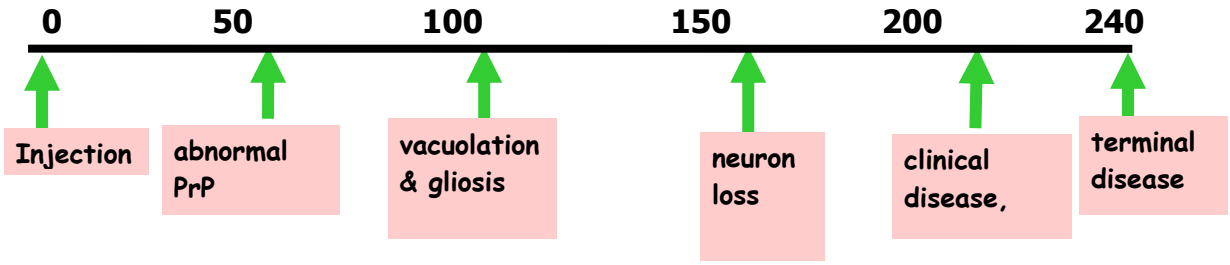

Figure 20. Sequence of development of neurodegeneration in the hippocampus of the ME7/CV scrapie mouse model. Time line of days post injection from injection at day 0 to terminal disease at 240 days. Summary of results from the study on the neuropathological changes observed in the ME7/CV mouse model, results depicted as a time line of events.

3.5 Discussion

In the ME7/CV scrapie mouse model neuronal loss is not observed until 160 days of a 240 day incubation period. A fundamentally important question is what happens to these neurons prior to their loss? It is important to establish the key neurodegenerative events that contribute to the loss of neurons as any strategy aimed at intervening to halt the degeneration would be better aimed at the initial insult rather than the final event.

The first neuropathological change observed in the CA1 of the hippocampus in the ME7/CV mouse model is deposition of PrP^{Sc} at 69 dpi, followed by the first signs of vacuolation and a glial response at 102 dpi. Neuronal loss, although variable, was not observed until 160 dpi, which correlates with previous morphometric analysis in this model (Jeffrey et al, 2000).

The initial pathological insult observed in the CA1 of the hippocampus in the ME7/CV mouse model, is PrP^{Sc} deposition, followed closely by vacuolation and then a glial response. The extent of microglial and astrocytic activation increased with disease progression and paralleled increases in PrP^{Sc} deposition. In the ME7/CV scrapie mouse model the deposition of disease specific PrP in the CA1 of the hippocampus may be the trigger for the activation of both microglia and astrocytes and the consequent damage to CA1 neurons. The type of PrP^{Sc} deposition observed in the ME7/CV model is mainly in the diffuse form and intense accumulations are observed in the stratum radiatum, the area within the hippocampus where the apical dendrites of the CA1 neurons lie. Although there was some differences in deposition of PrP^{Sc} observed within the brains of animals in the same group the main trend observed throughout the incubation period of disease was an increase in PrP^{Sc} deposition, becoming widespread at the terminal stage of disease (Figure 4). In this study the amount of PrP^{Sc} observed at 69 dpi was increased in comparison to that observed in previous studies at this time point. Therefore an earlier time point included in this study may have revealed the initial deposition of PrP^{Sc} even earlier in the incubation period of disease.

The role that PrP^{Sc} deposition plays in the neuronal loss observed in TSE diseases is still to be determined. In contrast, in the 87V/VM scrapie mouse model, where targeted neuronal loss is observed in the CA2 of the hippocampus, cytoskeletal damage is observed in the CA2 neurons long before the deposition of PrP^{Sc} (Jamieson et al, 2001b). The differences observed in PrP^{Sc} toxicity in these two models may relate to the type of PrP^{Sc} deposited in the brains of these mice. In the 87V/VM model PrP^{Sc} is observed mainly in the form of amyloid plaques, whereas a diffuse form of PrP^{Sc} predominates in the ME7/CV model.

A glial response is first observed in the hippocampus of the ME7/CV model at 102 dpi. Prior to this is the deposition of PrP^{Sc} which may initiate the upregulation of microglia and astrocytes. Microglia in their normal resting state are known to be motile, extending their processes into the neuropil scanning the brain for damage. Astrocytic signalling in the brain may lead microglia to the sites in need of inspection (Raivich, 2005).

In the ME7/CV scrapie mouse model activated microglia were observed in the hippocampus after the deposition of abnormal PrP and co-exists with the upregulation of astrocytes. This corresponds with previous studies in TSE mouse models were PrP^{Sc} deposition initiates a glial response (Bruce et al, 1994; Williams et al, 1997a; Williams et al, 1997b). The role of microglia in the TSE infected brain is not fully understood. The results observed here reveal the activation of microglia as early as 100 days, although variation between animals is observed, this activation increases throughout the incubation period of disease, and parallels the deposition of PrP^{Sc}. In contrast, previous results analysing microglial activation in this model revealed activation at a much later stage in the diseases process (Fraser, 2002).The earlier activation of microglia observed in this study may be due to the increase in the amounts of PrP^{Sc} observed at the earlier time points. The glial response observed in the ME7/CV mouse model may be due to the initial damage caused by the increase in PrP^{Sc} deposition and could be playing a protective role in the brain. As this glial activation occurred after PrP^{Sc} deposition this indicates that astrocytes and microglia were responding to rather than initiating the related pathology. This is enforced by the fact that in this model microglia are shown to have an anti-inflammatory phenotype .

Most studies concerning the activation of microglia by PrP have been performed using the amyloid fibril-forming PrP-derived peptide, PrP 106-126. In cell

culture this peptide activates microglia (Brown et al, 1996), and supernatants from these stimulated cells are also known to induce the proliferation of astrocytes and are toxic for neuronal cells (Brown & Mohn, 1999; Hafiz & Brown, 2000). These cell culture studies also revealed that PrP^{Sc} mediated neurotoxicity requires activation of microglia in combination with the expression of PrP on neuronal cells (Giese et al, 1998). However the rapid addition of PrP peptides to microglia in culture does not represent the progression of PrP^{Sc} as observed in the brains of mice infected with ME7. Therefore the relevance of these *in vitro* studies and the role of the microglial response to the deposition of PrP^{Sc} observed *in vivo*, are limited.

An increase in astrocytes along with microglia are also observed in the brains of mice infected with ME7. Activated astrocytes in the ME7/CV scrapie mouse model are first observed at 102 days in both the stratum radiatum and stratum oriens of the ME7 infected hippocampus. Astrocytic hypertrophy is observed at this time point but no apparent hyperplasia is observed until 160 days, a time point at which CA1 neurons are known to be lost. Also observed at this time point is an increase in the numbers of astrocytes observed surrounding the neuronal cell bodies, which increases with severity of neuronal loss (Figure 10F). Astrocytes perform many functions in the brain that mainly involve the support of neurons. The distribution of the astrocytic response observed in the ME7 infected hippocampus corresponds with the progression of degeneration observed in CA1 neurons. A marked astrocytic response is observed in the stratum radiatum of the hippocampus where the initial damage observed in CA1 neurons is detected. Observed prior to this neuronal damage is the accumulation of PrP^{Sc}. In rodent models of TSEs, astrocytes have been shown to be associated with (Bruce et al, 1994) and accumulate PrP^{Sc} (Brown et al, 2003b Diedrich, 1991; Ye et al, 1998) This phenomenon is strain dependent and astrocytosis

is not always observed in association with PrP^{Sc} deposition (Aoki et al, 1999; Brown et al, 2003b; Van Everbroeck et al, 2002). In the ME7/CV scrapie mouse model PrP^{Sc} deposition is observed prior to the activation of astrocytes, and ultrastructurally has been shown to be released by neurons, suggesting that in this mouse model astrocytes do not play a role in the production of PrP^{Sc}. The role astrocytes play in the production of PrP^{Sc} in TSE disease is uncertain. In mice devoid of murine PrP, but expressing hamster PrP transgenes driven by the astrocyte-specific GFAP promoter, astrocytes produced and expelled PrP^{Sc} into the neuropil, where it caused neuronal damage (Jeffrey et al, 2004; Raeber et al, 1997).

An emerging role for astrocytes in the nervous system is in synaptogenesis. Astrocytes form an intimate association with synapses throughout the adult CNS, where they help regulate ion and neurotransmitter concentrations. (Theodosis et al, 2008). *In vivo* astrocytes are involved in activity-dependent structural and functional synaptic changes throughout the nervous system (Slezak et al, 2006; Ullian et al, 2004). The astrocytosis observed in the ME7/CV scrapie mouse model may play a role in controlling synaptic plasticity and synaptic loss observed in the CA1 neurons of the hippocampus.

Vacuolation of the ME7 infected hippocampus was first observed at 102 dpi, as small holes in the pyramidal cell layer and larger holes in the stratum radiatum (Figure 13B). Vacuolation occurs over 30 days after the first deposition of PrP^{Sc}, and is observed firstly in the stratum radiatum, the area of the hippocampus that contains the apical dendrites of the CA1 neurons. This vacuolation increases rapidly towards the terminal stage of disease and is more widespread throughout the hippocampus (Figure 13). The vacuolation observed in the ME7 model appears to be associated with the deposition of diffuse PrP^{Sc} and increases throughout the incubation period of

disease. Ultrastructural studies have shown that vacuoles are mainly contained within dendrites with smaller numbers occurring in axons, axon terminals and the neuronal perikaryon (Jeffrey et al, 1995b; Jeffrey et al, 1991; Jeffrey et al, 1992b; Kim & Manuelidis, 1983; Kim & Manuelidis, 1986; Liberski et al, 1990). The vacuolation observed in the ME7/CV model may contribute to the neuronal damage and eventual loss of CA1 neurons in the hippocampus. Furthermore, the varicosities observed within the apical dendrites of CA1 neurons at the terminal stage of disease (Belichenko et al, 2000; Brown et al, 2001) may actually be a product of vacuolation within these dendrites (Figure 21).

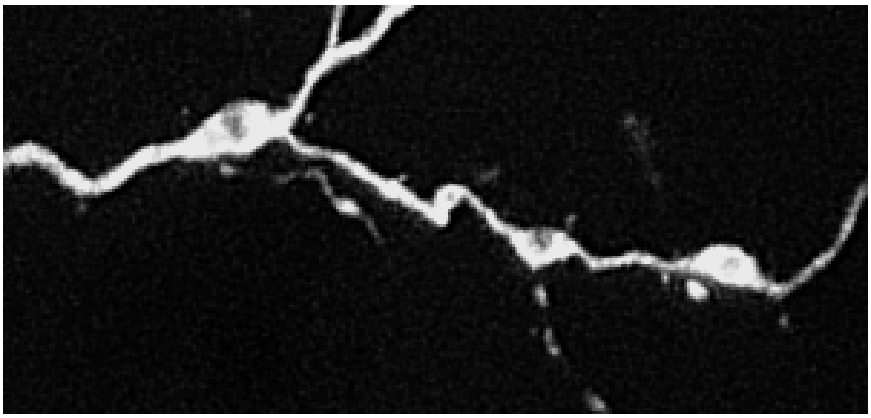

Figure 21. Varicosities observed within the apical dendrite of an ME7 infected CA1 neuron at the terminal stage of disease. Confocal z-series of an ME7 infected CA1 neuron injected with Lucifer yellow.

The loss of CA1 neurons in the ME7 infected hippocampus was observed from 160 dpi this correlates with previous morphometric analysis of neuronal loss in this model (Jeffrey et al, 2000). The neuronal loss observed in this scrapie mouse model is preceded by the deposition of abnormal PrP from 69 days, synapse loss and axon terminal degeneration at 100 days. The dendrites of the CA1 neurons become shrunken and contorted by the end of the incubation period, and lose most of their

spines, a process which starts around 100 days post infection (Brown et al, 2001). The evidence from this model suggests that abnormal PrP is the primary trigger for neurodegeneration, and that the subsequent damage is part of a cascade of events involving glial activation. As in some mouse models of Alzheimers disease (Shankar et al, 2008; Viola et al, 2008) the deposition of abnormal protein produces a synaptotoxicity which leads to the loss of synapses and neuronal function, which is exacerbated by a glial response. By the terminal stage of disease the CA1 hippocampal layer can be reduced to just one cell thick with almost total loss of neurons.

Neuronal loss is observed in the ME7 infected hippocampus but the mechanisms involved in this cell loss are still to be determined. Apoptosis is the suggested mechanism of neuronal loss in TSEs, but which apoptotic pathways are involved have still to be elucidated. In chapter 4 the role of apoptosis in the neuronal loss observed in TSEs will be investigated.

Chapter 4: Apoptosis and the caspase dependent pathway in TSE induced neuronal loss

4.1 Introduction

Apoptosis

Apoptosis has been proposed as an important mechanism of cell death involved in neurodegeneration. Apoptosis is a programmed cell death regulated by a series of events. It is essential for cell development, maturation, normal tissue turnover and regulation of immune systems (Wyllie et al, 1980). Identification of apoptotic cells is morphologically based upon the detection of cellular and nuclear membrane shrinkage, condensation and fragmentation of nuclear chromatin, and biochemically by endonuclease-mediated internucleosomal fragmentation of DNA into multiple oligosomal sub-units of 180 bp (DNA laddering). Most of the evidence in the literature indicates that apoptosis may play a role in the neuronal loss observed in TSE diseases, but it is not clear which pathways are involved in this apoptotic loss.

Caspases

Caspases are a family of cysteine proteases that have been identified as being key regulators and effectors of the apoptotic response in a variety of species. The discovery of a role for the caspases in apoptosis has its origins in observations made by Horvitz's group on the regulation of programmed cell death during development of the nematode worm *Caenorhabditis elegans (C. elegans)* (Ellis et al, 1991). Further work was instigated to try and identify similar proteases that could play a role in regulation of mammalian apoptosis, and several were soon discovered. To date, 14 human caspases have been identified and these proteases appear to comprise a complex proteolytic system, similar to the complement system (Salvesen & Dixit,

1997; Slee et al, 1999). Caspases can be subdivided on the basis of their activity into "initiator" (cell death signalling) caspases and "effector" (cell disassembly) caspases. The initiator caspases, such as caspases 8 and 9 appear to activate other caspases at the effector end of the cascade such as caspases – 3, 6 and 7 (Figure 1). It is the effector caspases that are largely responsible for the morphological and biochemical changes that are the hallmarks of apoptosis.

There are two different caspase-dependent mechanisms by which a cell commits itself to apoptosis: 1) The extrinsic or death receptor mediated pathway, and 2) The intrinsic or mitochondrial pathway (Figure 1). The role of these pathways in the neuronal loss observed in TSEs will be investigated in this chapter. A third pathway is involved in the induction of apoptosis, the caspase independent pathway, this pathway is initiated by the release of Apoptosis Inducing factor (AIF) from the mitochondrial membrane and is discussed below.

Caspase-independent pathway

This pathway of programmed cell death is initiated through a caspase independent mechanism. Upon induction of apoptosis, AIF (apoptosis inducing factor), a protein that normally resides in the intermembrane space of the mitochondria, is released from the mitochondria into the cytosol and translocates to the nucleus. When in the nucleus it binds to DNA triggering chromatin condensation and DNA fragmentation. The DNA fragmentation is not the characteristic 180-200bp observed in caspase cleaved apoptosis, it is in the form of high molecular weighted fragments of 50kB (Susin et al, 1999)

There is no evidence in the literature of a role for the caspase-independent pathway in TSE induced neurodegeneration. In Alzheimers, a disease analogous to TSEs , AIF was expressed in cortical and hippocampal neurons (Reix et al, 2007).

Studies in animal models of disease (Bertrand et al, 2001) and cell cultures treated with Aβ peptides (Giovanni et al, 2000) suggest a role for the caspase-independent pathway in cell death in AD.

Translocation of AIF from the mitochondria to the nucleus has been observed in ischemia induced apoptotic lesions in the rat brain (Chaitanya & Babu, 2008; Cho & Toledo-Pereyra, 2008; Ferrer et al, 2003), demonstrating the involvement of the caspase-independent pathway following transient focal ischaemia and reperfusion.

Further studies are required to identify which apoptotic pathways are involved in the neuronal loss observed in TSE diseases.

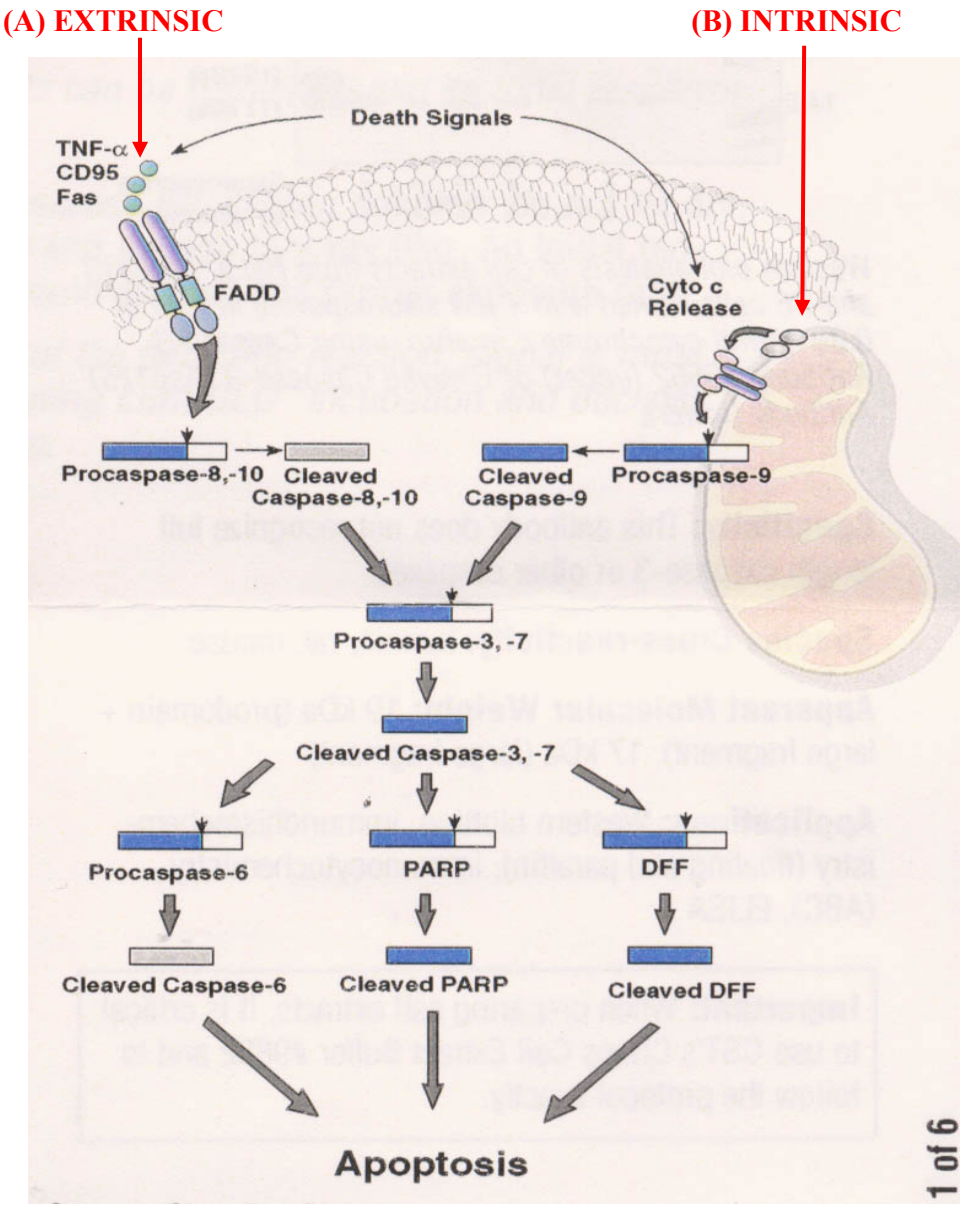

Figure 1. Caspase Cascade

This pathway shows the cascade of events that occur when apoptosis is initiated through a caspase dependent manner. This proteolytic system can be initated in two ways, either extrinsic (receptor mediated) (A) or intrinsic (mitochondrial from within the cell) (B) Diagram from Cell Signalling technology

4.1.1 The extrinsic or death receptor mediated pathway

Extrinsic or receptor mediated cell death is initiated by a TNF (tumour necrosis factor) superfamily of ligands which include, TNF, FasL and TRAIL (TNF related apoptosis inducing ligand). These ligands bind to their receptors to evoke the formation of a death inducing signalling complex (DISC) that is comprised of death receptors, adaptor molecules and initiator caspases. The assembly of a DISC results in the activation of caspase 8, which can activate downstream executioner caspases leading to apoptosis. The up-regulation of Fas and caspases as markers for neurodegeneration in TSE disease has been observed in the brains of mice infected with the 87V strain of scrapie (Jamieson et al, 2001a). However, this was not the case in mice infected with the RML strain of scrapie, where active caspase-3 was observed in the same areas of the brain as TUNEL expression, but no difference in Fas expression was shown (Siso et al, 2002) . Gene expression levels of both the Fas receptor (Fas) and active caspase-8 were increased in C57BL mice infected with ME7, but no difference was observed in the levels of Fas ligand (Fas-L) expression (Stobart et al, 2007). One study examining the expression of proteins linked with the signalling pathways involved in the cell death observed in the cerebellum in Creutzfeldt-Jakob disease (CJD) found no modifications in the expression of Fas, Fas-L, MEK, ERK, Bcl-2 or Bax, in vulnerable granule cells in this disease.. Although Purkinje cells of the cerebellum are relatively resistant to CJD, increased diffuse Fas, Fas-L, MEK, ERK and Bax expression, and enhanced granular active caspase-3 immunoreactivity was observed in the cytoplasm of these cells. The expression of these proteins did not lead to cell death suggesting that these proteins have functional roles differing from those related with apoptosis (Puig & Ferrer, 2001).

These studies have demonstrated that the role of the extrinsic receptor mediated pathway in the apoptosis observed in TSE disease is still unclear. In this study, the involvement of this apoptotic pathway, in the neuronal loss observed in the CA1 of the hippocampus in the ME7/CV model, will be analysed.

4.1.2 The intrinsic or mitochondrial pathway

The intrinsic or mitochondrial pathway of apoptosis is triggered by internal signals within the cell i.e. reactive oxygen species that in turn interact with a family of proteins, the Bcl-2 proteins that are located in the mitochondrial membrane. The Bcl-2 family consists of anti-apoptotic members, Bcl-2 and Bcl-X_L and pro-apoptotic members Bax and Bak. The anti-apoptotic members maintain the integrity of the mitochondrial membrane, preventing the release of cytochrome c (Kluck et al, 1997; Yang et al, 1997), while the pro-apoptotic members interact with the mitochondrial membrane resulting in membrane permeabilisation and the release of cytochrome c. Cytochrome c release is mediated through balanced interactions of pro- and anti-apoptotic members of the Bcl-2 family. When cytochrome c is released into the cytosol it interacts with apoptotic protease activating factor 1 (Apaf-1) to form the apoptosome, a complex consisting of cytochrome c, ATP, procaspase-9 and Apaf-1, resulting in the activation of caspase 9 and downstream effector caspases and therefore apoptotic cell death (Zou et al, 1999) (Figure 2).

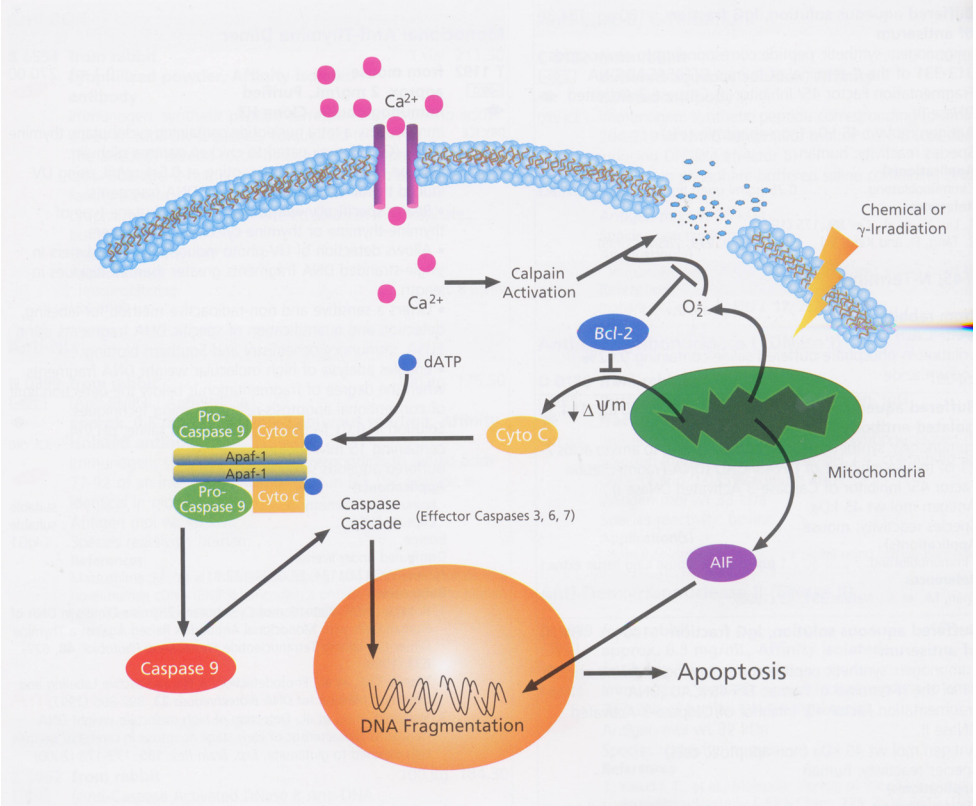

Figure 2. Intrinsic (mitochondrial) pathway of caspase dependent apoptosis
Increase in reactive oxygen species inside the cell interact with the Bcl-2 proteins to induce permeabilisation of the mitochondrial membrane releasing cytochrome C into the cytoplasm which initiates formation of the apoptosome leading to activation of the caspase cascade and apoptotic cell death

Both *in vivo* and *in vitro* studies into the role of these anti and pro-apoptotic proteins in TSE diseases have revealed conflicting results. In a study analysing the expression of Bcl-2 and Bax in the brains of hamsters infected with scrapie, Bcl-2 was significantly decreased, whereas the expression levels of Bax were significantly increased (Park et al, 2000). Over expressing Bcl-2 in GT1-7 neural cells protected against prion toxicity (Ferreiro et al, 2007), but this was not the case *in vivo*; Bcl-2 overexpression and Bax deletion did not protect against prion toxicity in mice infected with the RML strain of scrapie (Steele et al, 2007). ER stress induced by the 106-126 PrP peptide required functional mitochondria for the apoptotic cell death to occur (Ferreiro et al, 2008) . The differential expression of these proteins and their role in

the neuronal loss observed in TSE disease is still to be determined. In this study two scrapie mouse models will be used to analyse the role of the mitochondrial pathway in TSE induced neuronal loss.

4.1.3 FACS analysis as a method to identify apoptotic cells *in vivo*

FACS analysis is a tool that is predominantly used in *in vitro* cell culture systems and analysis of cell types in the blood. *In vivo* it is mainly used to analyse morphologically simple and small cell types like those found in the lymphoreticular system i.e. B cells in the spleen. In the brain most *in vivo* research using FACS as a tool is performed on brain tumours i.e. astrocytomas and gliomas (Rainov et al, 2000). To determine whether FACS analysis could be used as a tool to analyse, *in vivo*, cells in the CNS a pilot study on the analysis of microglia was performed. Microglia have been analysed successfully *in vivo* by FACS analysis in other rodent models of disease (Marques et al, 2008; Mensah-Brown et al, 2005), and are also known to be upregulated in the ME7 infected brain. Therefore this was an ideal candidate cell to initially use in a pilot study to test the suitability of FACS analysis as a tool to use for *in vivo* analysis of cells in the CNS. If successful analysis of neurons using the FACS methodology and its use in the analysis of apoptotic markers *in vivo* will be determined. FACS analysis has been used successfully in analysing pro-apoptotic markers in neuronal cell cultures (Awasthi et al, 2005,Igosheva, 2005 ; Boccellino et al, 2003), and *in vivo* to successfully identify neuronal cells within the CNS (Bowen et al, 2007). But this methodology has not been widely used *in vivo* to analyse pro-apoptotic markers in the CNS.

4.2 Aims of Chapter

- To establish through a variety of approaches if apoptotic mechanisms are involved in the loss of neurons in TSEs.
- To determine if the FACS analysis technique has the potential to be used in the analysis of apoptotic cells.

Specific aims and approaches

Using two scrapie mouse models of disease :- the 87V/VM and ME7/CV mouse models the following approaches were taken:-

- Analysis of TUNEL and active caspase-3 was performed on animals at the terminal stage of disease in both mouse models. Active caspase-3 analysis was also performed on a time series from the ME7/CV model.
- To investigate the role of both the extrinsic (receptor mediated) and the intrinsic (mitochondrial) apoptotic pathways several markers were analysed.

4.3 Materials and Methods

4.3.1 Immunohistochemical analysis of proapoptotic markers

Active caspase-3

Caspase-3 is observed within cells in two forms; the pro-form which is constitutively expressed in all cells, and the active form which is produced by the cleavage of the proform by upstream caspases in the caspase-dependent pathway of apoptosis. Once cleaved the cell is then destined for cell death via an apoptotic mechanism. Therefore it is essential that when trying to identify apoptotic cell death via a caspase-dependent mechanism that the antibodies used identify the cleaved form of caspase-3 and not the procaspase form.

Initial studies analysing active-caspase-3 expression were performed using the antibody from R&D systems used previously on the 87V/VM scrapie mouse model (Jamieson et al, 2001a). As both the ME7 and the NB infected sections showed similar staining patterns with this antibody another active caspase-3 antibody was used. The active caspase-3 antibody from Oncogene worked well and staining was observed in single cells in the infected samples only. This antibody was chosen on recommendation from another laboratory.

In addition suitable positive controls to include in the IHC studies were assessed. These included paraffin sections from a mouse model of Semliki Forest Virus (SFV), a mouse model of ischaemia, human tonsil tissue and mammary tissue.

TUNEL labelling

TUNEL labelling was performed on brains fixed in formol saline for a total of 48hrs. Brains were immersed in formol saline overnight, trimmed and left for a further 24 hours and then processed through to paraffin wax. When developing the TUNEL technique the best results were achieved by light fixation in formol saline and sections that were cut straight after processing to wax. Optimisation of proteinase K (PK) digestion of tissue sections was essential as over digestion can cause false positives. A concentration of 2.5µg/ml of PK for 15mins was used in these studies. Full TUNEL technique can be found in appendix 1 under immunohistochemical methods.

Fas receptor labelling

Two antibodies were used to assess the expression of the Fas receptor in both the 87V/VM and ME7/CV scrapie mouse models. Both antibodies were purchased from Santa Cruz, The C20 antibody was raised to the C terminus of the Fas protein and had been used previously on the 87V/VM mouse model (Jamieson et al, 2001a), the A20 antibody was raised to the N terminus of the Fas protein and had been used in a

previous study analysing Fas expression in the RML/C57BL scrapie mouse model (Giese et al, 1995). (see appendix 1 and table 1.2 for IHC method and concentration of antibodies)

Mitochondrial proteins Bax,Bcl-2 and cytochrome C

The expression of the mitochondrial proteins Bax, Bcl-2 and cytochrome c were analysed to identify the role,if any, of the intrinsic (mitochondrial) pathway in the apoptotic cell loss. Both the Bax and Bcl-2 antibodies were purchased from upstate as on their specification sheets they were shown to work well in both IHC and western blot analysis on mouse tissue. The cytochrome C antibody had been used successfully on human sections in huntington's disease (Kiechle et al, 2002) and from the specification sheet for the antibody, it also reacted well with mouse cytochrome C.

4.3.2 Western blot analysis of proapoptotic markers

In the identification of a suitable active caspase-3 antibody to use in western blot analysis, initially 87V infected whole brains were used as in the previous study by Jamieson et al. Further experiments analysed both scrapie mouse models. Dissected hippocampus (ME7) and thalamus (87V) was used in active caspase-3 analysis using the Cell Signaling antibody. The thalamus was used in the 87V/VM model as this area is also targeted in this model and more tissue could be collected in dissection. It was almost impossible to dissect out the CA2 sector of the hippocampus and to obtain enough tissue for western blot analysis. See Chapter 2 materials and methods for more details on sample preparation and Appendix 2 for western blot method and list of antibodies used.

4.4 Results

4.4.1. TUNEL labelling is detected in the hippocampus of the ME7/CV scrapie mouse model at the terminal stage of disease and not in the normal brain injected controls

Studies in the ME7/CV model revealed TUNEL labelling in the hippocampus in brains at the terminal stage of disease (Figure 3). Single cells were observed in the dentate gyrus in the hippocampus. A positive control of mammary tissue was included from the apoptag TUNEL kit. Apoptosis during lactation is a normal function of mammary tissue (Iizuka et al, 2006) and therefore a useful tissue to use as a positive control in the TUNEL technique (Figure 3B). Morphology of the cells labelled in the ME7 infected hippocampus resembled those labelled in the mammary tissue, cells looked shrunken and condensed nuclei stained intensely with TUNEL technique. The numbers of cells labelled with the TUNEL technique were similar in both the 87V/VM and ME7/CV model. However, whereas in the 87V/VM model the TUNEL labelling was observed in the nucleus of CA2 neurons, the sector of the hippocampus were neuronal damage is observed, here no TUNEL positive cells were observed in the CA1 of the ME7 infected hippocampus where neurons are known to be lost. TUNEL labelling in the ME7 infected hippocampus was confined to the dentate gyrus where there was no obvious neuronal loss. The morphology of the cells labelled with the TUNEL method in the ME7 infected brain (Figure 3C&D) was similar to that observed with the active caspase-3 labelling (Figure 9B).

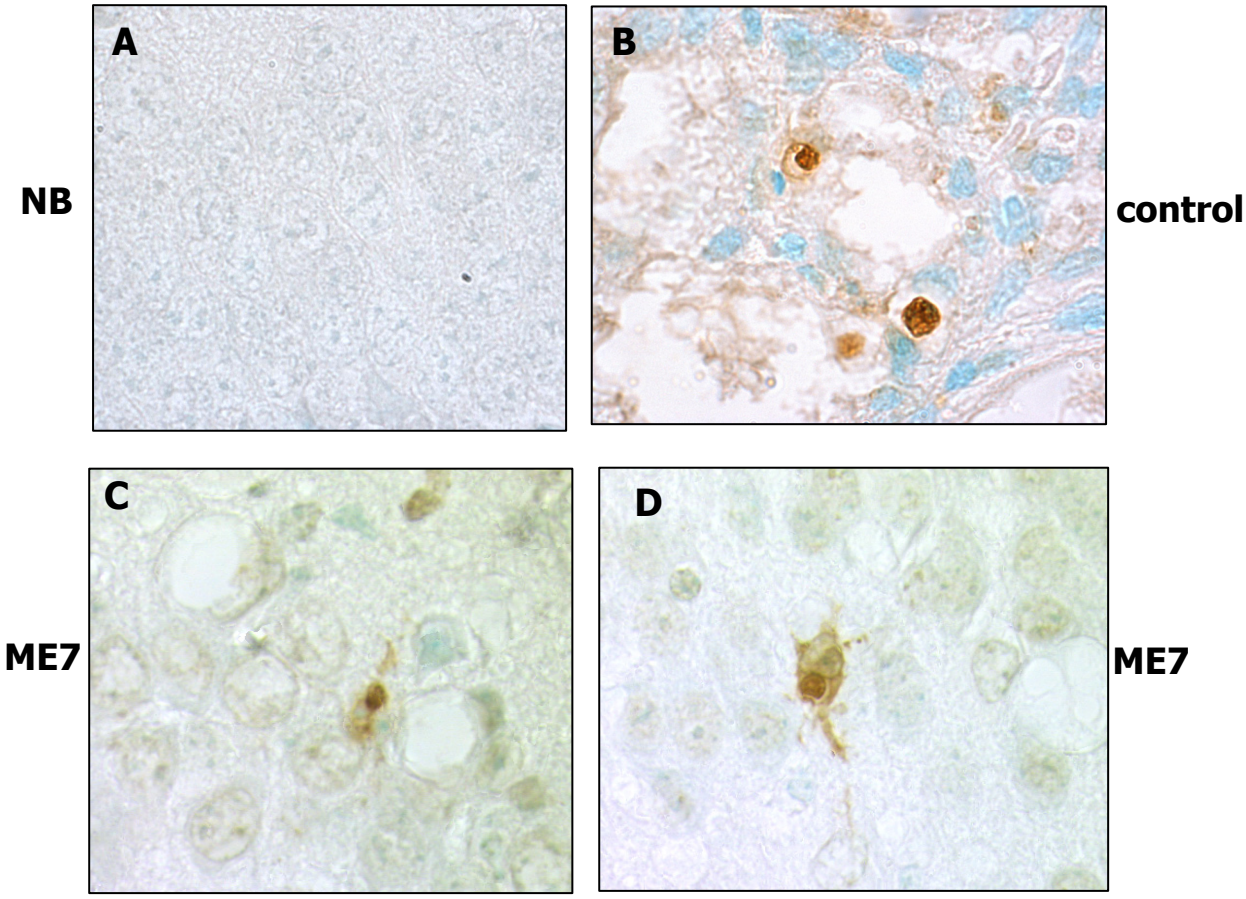

Figure 3. TUNEL labelling in the ME7/CV model at the terminal (ME7 T) stage of disease (A) Normal brain injected control with no TUNEL labelling (C)&(D) TUNEL labelling of single cells observed in the dentate gyrus of the hippocampus in ME7 infected animals at the terminal stage of disease. (B) TUNEL labelling in the positive control mammary tissue supplied with Apoptag TUNEL kit. Magnification x100 oil

4.4.2. Identification of antibodies that recognise the active form of caspase-3

Four antibodies were compared to identify a suitable antibody that will recognise the active form of caspase-3. All these antibodies claimed that they recognised the cleaved form of active caspase-3. A list of antibodies tested are shown in Appendix 1. In western blot analysis both the R&D system and the Pharmingen antibody detected the procaspase form of caspase-3 as a 32kDa band (Figure 4&6). IHC analysis using the R&D systems antibody revealed similar labelling in both ME7 infected and normal control brains (Figure 5). Two antibodies were identified that could be used successfully for the identification of active caspase-3 in immunohistochemical and western blot analysis. For IHC an active caspase-3 antibody was purchased from Oncogene. This active caspase-3 antibody was used successfully in immunohistochemical analysis of active caspase-3 in brains from both the 87V/VM and ME7/CV models at the terminal stage of disease (Figure 9), and also the time series analysis of the ME7/CV mouse model (Figure 10). An active caspase-3 antibody from Cell Signalling Technology was used successfully in western blot analysis of terminally infected brains from both the 87V/VM and ME7/CV mouse models (Figure 7), a positive control supplied with this antibody revealed active caspase-3 expression in every western blot application.

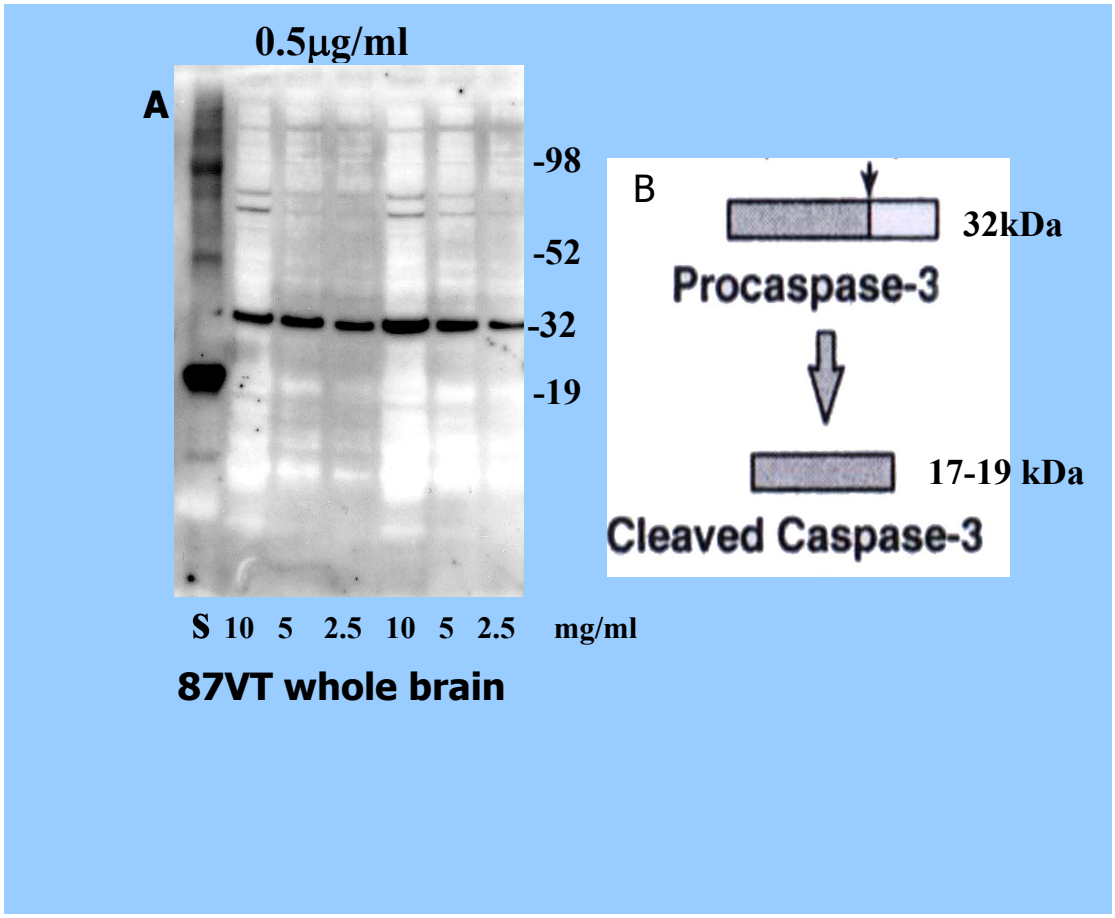

Figure 4. Western blot analysis of three different dilutions of 87V infected whole brains with the caspase-3 antibody from R&D systems. Results shown here reveal that this antibody recognised the procaspase form (32kDa) of caspase-3 (A) Western blot analysis of caspase-3 expression in two terminal 87V infected mouse brains added to gel at 2.5, 5& 10mg/ml. No bands were observed at 17-19 kDa, bands were observed at 32kDa, the molecular weight (MW) of the procaspase form of caspase-3. (B) Diagram showing MW of procasase-3 and its cleavage product active caspase-3

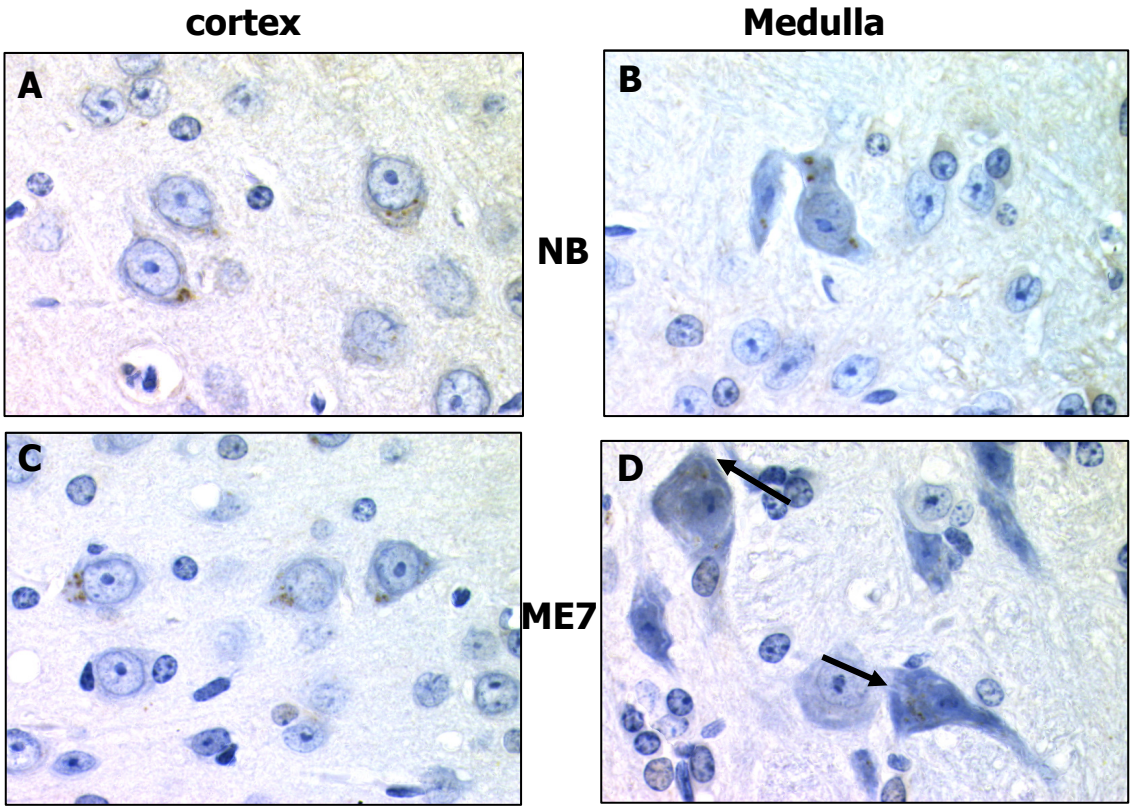

Figure 5. Casapse-3 imunolabelling of both ME7 infected and normal brain (NB) injected controls with R&D antibody used on westerns in Figure 4. (A) Punctate labelling observed in the cytoplasm of cortical neurons in the NB injected controls, and also in the medulla (B). Similar labeling was also observed in the ME7 infected brains in both the cortex and medulla (C) & (D) arrows. magnification x60 oil

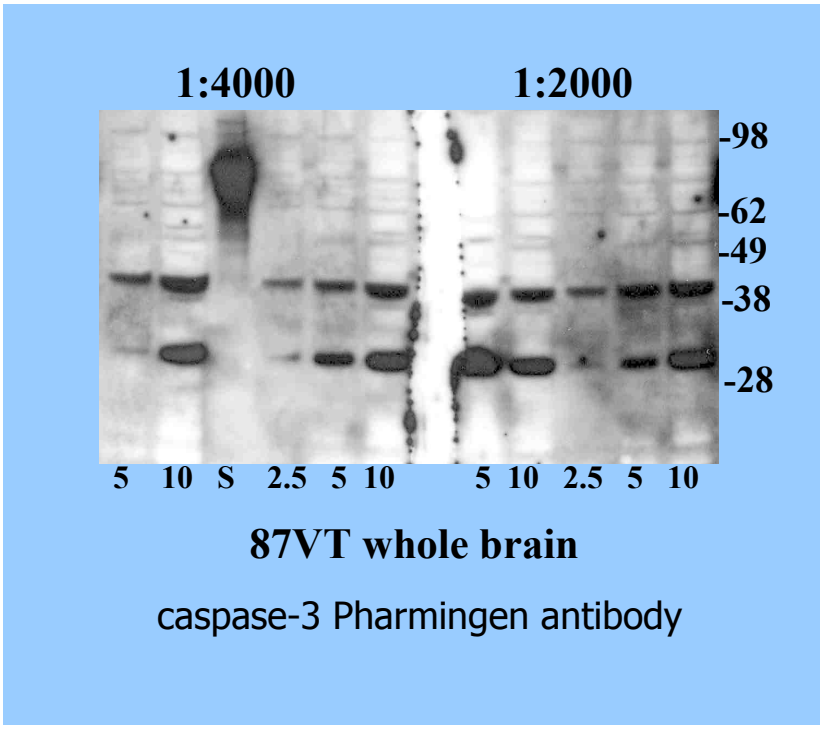

Figure 6. Western blot analysis of 87V T whole brains with the Pharmingen antibody. Results shown here reveal that it recognised the procaspase form only. Whole brain lysates were added at 2.5,5 and 10 mg/ml and the Pharmingen antibody was used at 1/2000 and 1/4000 concentration. Bands were observed at 32kDa recognising the procaspase form of active caspase-3 but nothing was observed between 17&19 kDa were bands would be observed if caspase-3 was cleaved.

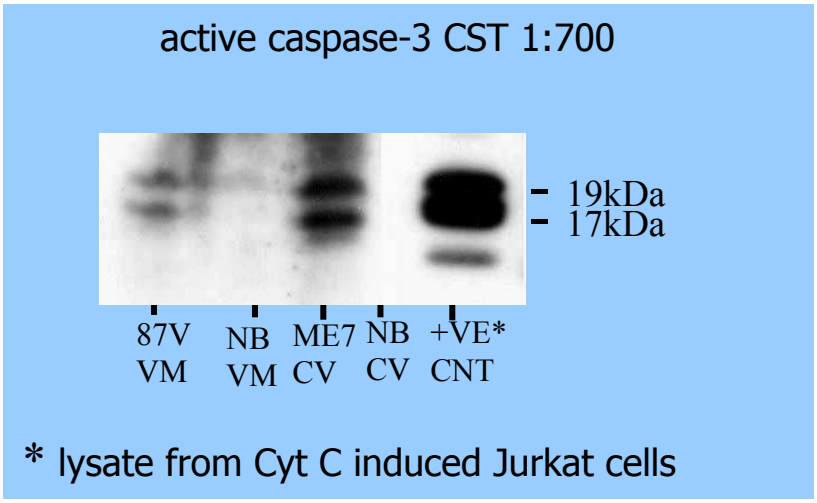

Figure 7. Western blot analysis of active caspase-3 in both the 87V/VM and the ME7/CV scrapie mouse models using an active caspase-3 antibody from cell signalling technology. Dissected hippocampus (ME7) and thalamus (87V) samples methanol precipitated and added to the gel. In both the 87V and ME7 infected samples two bands were recognised at 17 and 19 kDa denoting active caspase-3, no bands were recognised in the NB aged matched controls.

4.4.3 Identification of suitable controls to use in IHC anlaysis of active caspase-3

The most suitable positive control to use in the IHC studies was the SFV infected mouse model. Active caspase -3 labelling revealed intense labelling in cells within the olfactory bulb of the SFV infected mouse (Figure 8A). Single cells were labelled in the dentate gyrus in the ischaemia mouse model (Figure 8B), although active caspase-3 labelling is observed it was not as intense as that shown in the SFV mouse model. The human tonsil section stained well and was used in each IHC run as a positive control to ensure the IHC technique was successful. Mammary tissue was provided as a positive control to use with the TUNEL technique, positive cells were always observed in this tissue in every TUNEL run performed (Figure 8D).

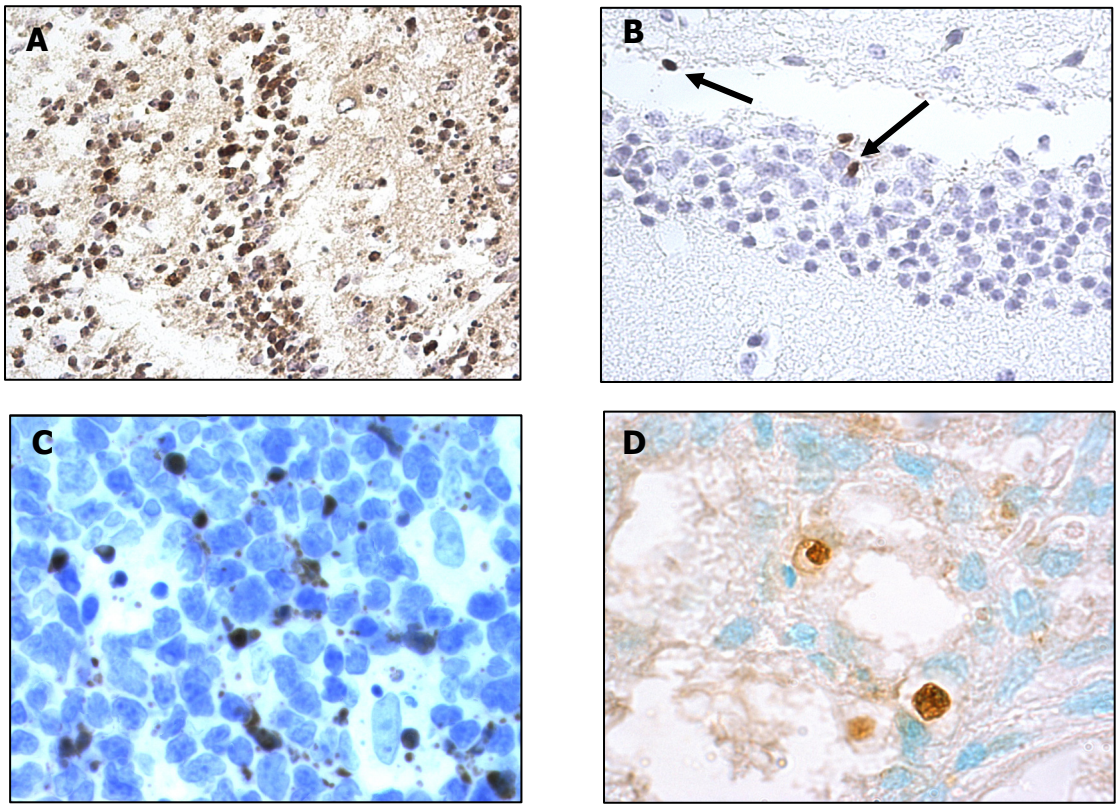

Figure 8. Positive controls to use in IHC analysis of active caspase-3 and TUNEL labelling

Figures (A)-(C) labelled with active caspase-3 Oncogene antibody and (D) TUNEL labelling (A) Olfactory bulb from Semliki Forest Virus infected mouse brain showing marked upregulation of active caspase-3 in SFV infected cells. (B) Mouse model of Ischaemia after 6 hours reperfusion, showing only single cells labelling in the dentate gyrus, not many cells dying through apoptosis in this model. (C) Active caspase-3 labelling of human tonsil, rapid turnover of B cells in the tonsil undergoing apoptosis. (D) TUNEL labelling of apoptotic cells observed in mammary tissue, the positive control provided with apoptag TUNEL labelling kit. Magnification (A)&(B) x40, (C)&(D) x 60 oil

4.4.4. Active caspase-3 labelling is observed in both the 87V/VM and ME7/CV mouse model at the terminal stage of disease

The Oncogene antibody was used to immunolabel active caspase-3 in terminally infected brains from both the 87V/VM and ME7/CV mouse models. This antibody labelled both positive control and experimental tissues. Active caspase-3 labelling was observed in single cells in the thalamus of the 87V infected brain (Figure 9D), and in the dentate gyrus of the ME7 (Figure 9B) infected brain at the terminal stage of disease. These cells had similar morphology to those labelled previously with the TUNEL technique. No labelling was observed in aged matched normal brain controls (Figure 9C). High expression of active caspase-3 was observed in the SFV infected positive control section (Figure 9A).

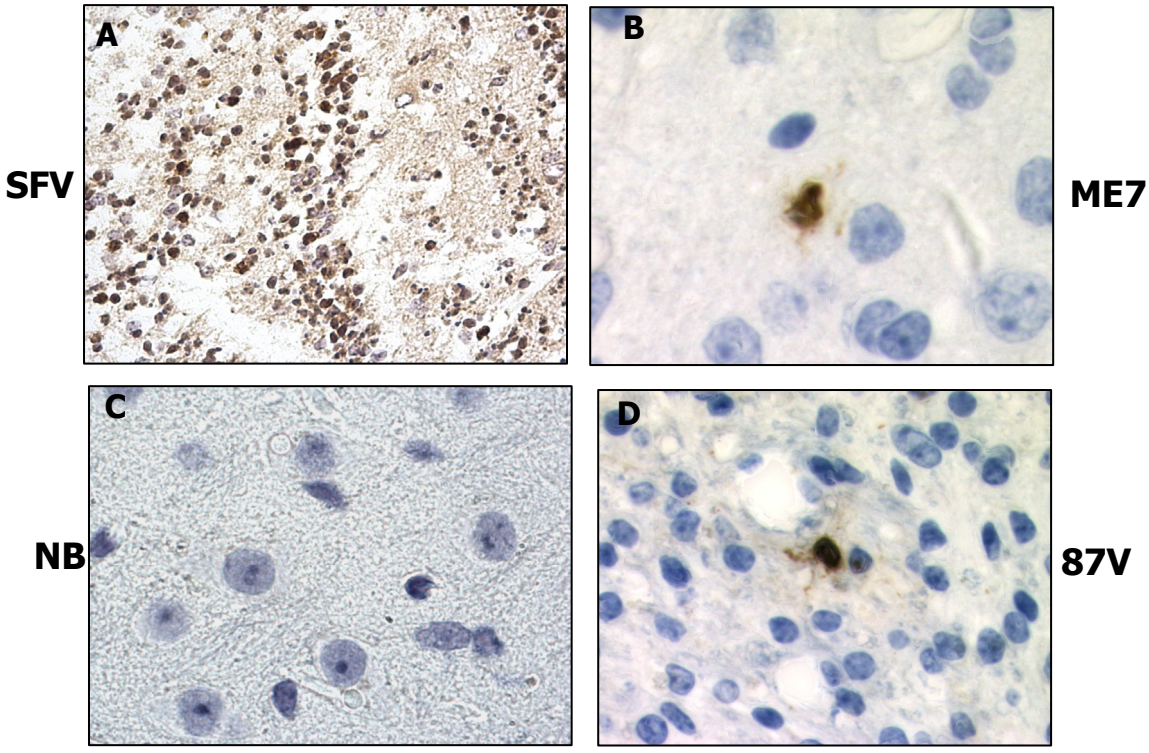

Figure 9. Active caspase-3 labelling in terminal brains from both the ME7/CV and 87V/VM model. (A) Olfactory bulb from a Semliki Forest Virus (SFV) infected mouse brain demonstrating upregulation of active caspase-3 labelling in SFV infected cells. (B) Active caspase -3 labelling of single cells in the ME7 infected hippocampus. (C) NB control showing no labelling with the active caspase-3 antibody. (D) Active caspase-3 labelling of single cells in the 87V infected thalamus. Magnification (A) x40 (B),(C)&(D) x100 oil

4.4.5. Analysis of active caspase-3 in the ME7/CV time series :- active caspase-3 is observed in single cells in all time points

Active caspase-3 labelling of single cells in the hippocampus was observed in all the ME7 infected serial kill time points. None of the cells labelled were in the CA1 of the hippocampus, where neuronal cell loss takes place. Active caspase-3 positive cells were observed in the dentate gyrus (Figure 10A&B), cortex (Figure 10C&E) and white matter tracts in the corpus collosum (Figure 10D). The cells labelled did show the characteristic morphological changes that are observed in cells undergoing apoptosis such as shrinkage of the cell and pyknotic nuclei. No labelling was observed in any of the aged matched control brains.

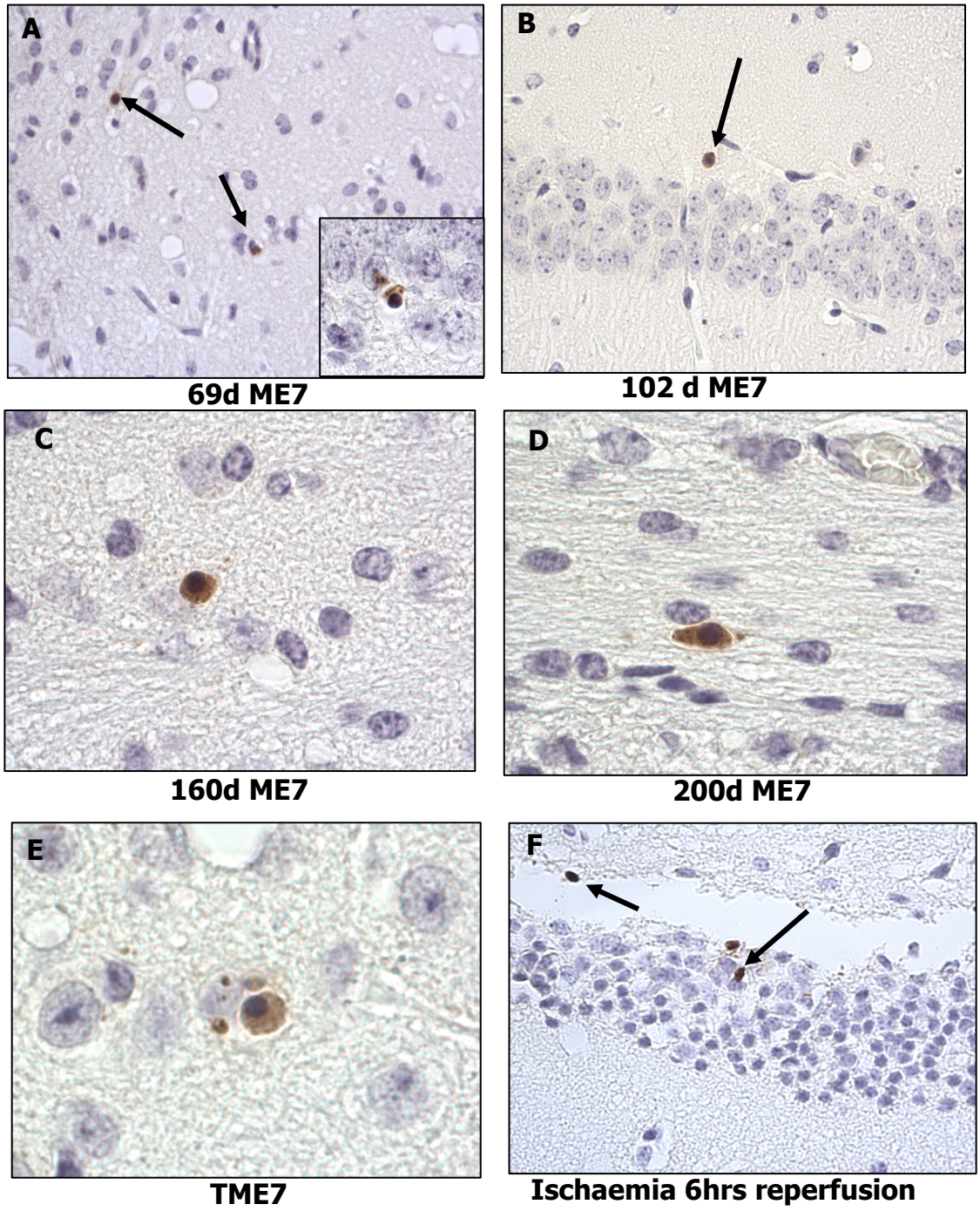

Figure 10. Active caspase-3 labelling in the time series of the ME7/CV scrapie mouse model. Single cells labelling in the hippocampus in the ME7 infected brains throughout the time series from 69dpi – terminal (A)-(E). (F) Single cells labelling in the dentate gyrus (arrows) in an ischaemia mouse model (positive control). Magnification (A), (B) and (F) x40, (C), (D) & (E) x 100 oil, insert in (A) is x100 oil

4.4.6. Fas is not upregulated in the brains of mice infected with the ME7 strain of Scrapie

To investigate the role of the extrinsic pathway in the neuronal loss observed in TSE disease the expression of the Fas receptor was analysed in the brains of two scrapie mouse models.

Using a Fas receptor antibody raised to the C terminus of the Fas protein, weak expression of Fas was observed in the CA2 of the 87V infected hippocampus (Figure 11A), an area that is a known pathological target in this model, but not in the NB injected control (Figure 11C). In the ME7/CV model only astrocytic like expression was observed in the CA3 of the hippocampus (Figure 11B), no labelling was observed in the NB control (Figure 11D). To confirm these results a second Fas antibody was acquired, this antibody was raised to the N-terminus of the Fas protein. A different staining pattern was observed with this antibody in infected brains from both the ME7/CV and 87V/VM scrapie mouse models (Figure 12). Fas expression was observed in the cytoplasm of neuronal cell bodies in both the CA2 (87V) and CA1 (ME7) of the hippocampus, a slight increase in intensity observed in the NB controls (Figure 12A&B). Fas expression was also observed within glial cells in the ME7 infected hippocampus (Figure 12D). Both these antibodies labelled glial cells in the ME7/CV model, although in different sectors of the hippocampus.

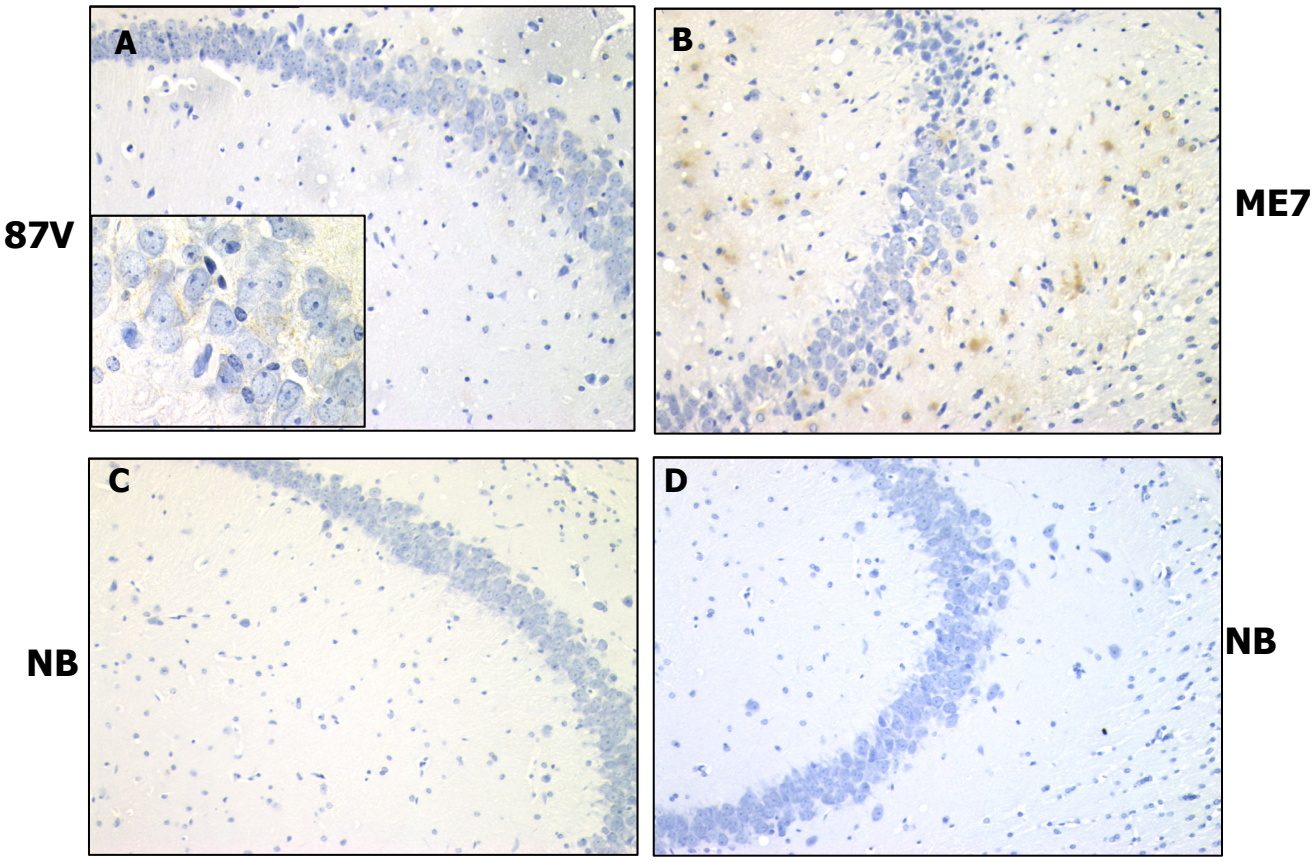

Figure 11. Fas expression in both the 87V/VM and ME7/CV scrapie mouse models using the antibody raised to the C terminus of the protein (A) Faint expression of Fas in the CA2 of the 87V infected hippocampus. (B) Fas expression observed in glial cells in the CA3 of the ME7 infected hippocampus. No labelling observed in the VM (C) or CV (D) normal brain injected controls. Magnification x20, insert in (A) x60 oil

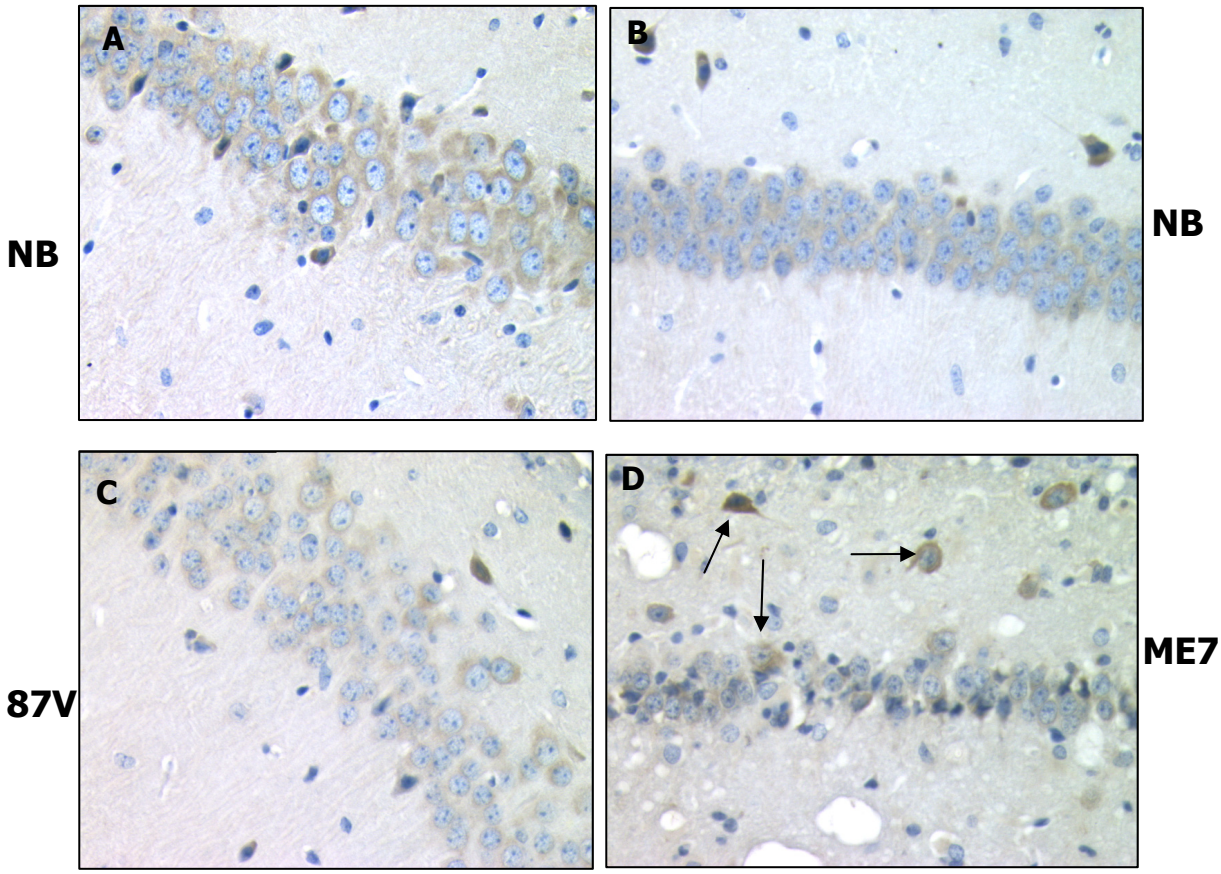

Figure 12. Fas expression in both the 87V/VM and ME7/CV scrapie mouse models using the antibody raised to the N-terminus of the protein (A) Fas expression in the CA2 in a VM normal brain control (B) Fas expression in a CV normal brain control. (C) Loss of expression observed in the CA2 of the 87V infected hippocampus. (D) Fas expression in the CA1 of the ME7 infected hippocampus observed in glial cells in the stratum oriens and pyramidal cell layer (arrows). Magnification x40

4.4.7. Cytochrome c deposition in the hippocampus of terminal stage murine scrapie infected brains and normal brain injected controls is similar

To investigate the role of the mitochondrial pathway in the neuronal loss observed in scrapie mouse models, the deposition of Cytochrome c was analysed in both the 87V/VM and ME7/CV models. Cytochrome c labelling in the 87V and NB injected controls was similar. Diffuse labelling was observed in the cytoplasm of CA2 neurons in the hippocampus in both the 87V infected and NB control. A slight difference was observed in the 87V infected CA2 (Figure 13A), in addition to diffuse labelling, single cells with intense labelling were also observed (Figure 14C). In the ME7/CV model diffuse labelling was observed in the cytoplasm of CA1 neurons in the NB controls (Figure 14C). Single cells with intense labelling were also observed within the pyramidal cell layer (Figure 14A arrow) these cells resembled the dark neurons observed in haematoxylin and eosin stained sections in Chapter 2. In the ME7 infected brain the type of deposition had changed and punctate intense cytochrome c labelling was observed in single neurons in the CA1 of the ME7 infected hippocampus (Figure 14D).

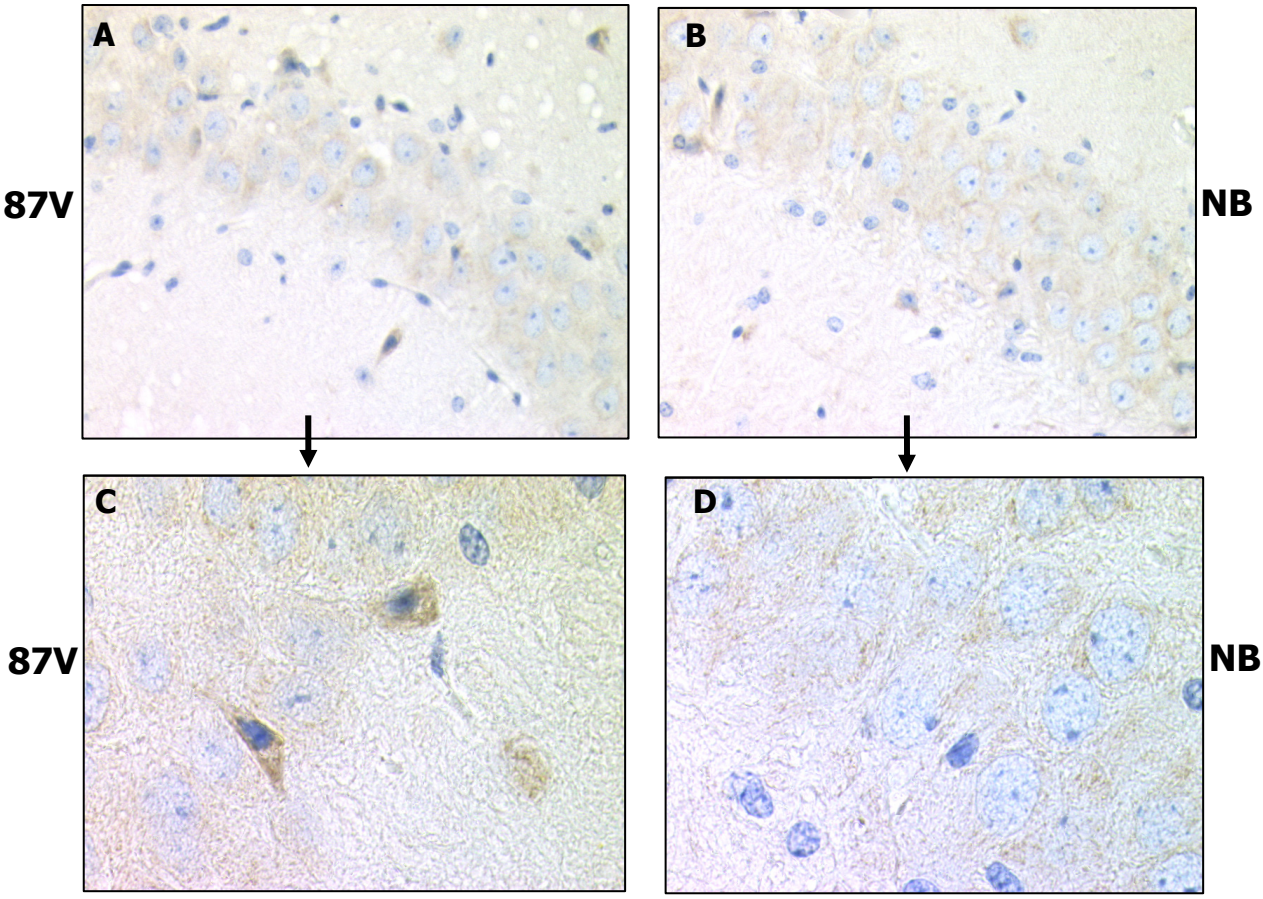

Figure 13. Cytochrome c expression in the 87V/VM scrapie mouse model. (A) CA2 of the hippocampus in the 87V infected mouse showing diffuse labelling in the cytoplasm of CA2 neurons, and single cells within the pyramidal cell layer (C). (B)&(D) CA2 of the hippocampus in a normal brain injected control, also showing diffuse labelling in the cytoplasm of CA2 neurons. Magnification (A)&(B) x40 and (C) &(D) x100 oil. Arrows between figures denotes a high power of the figure above.

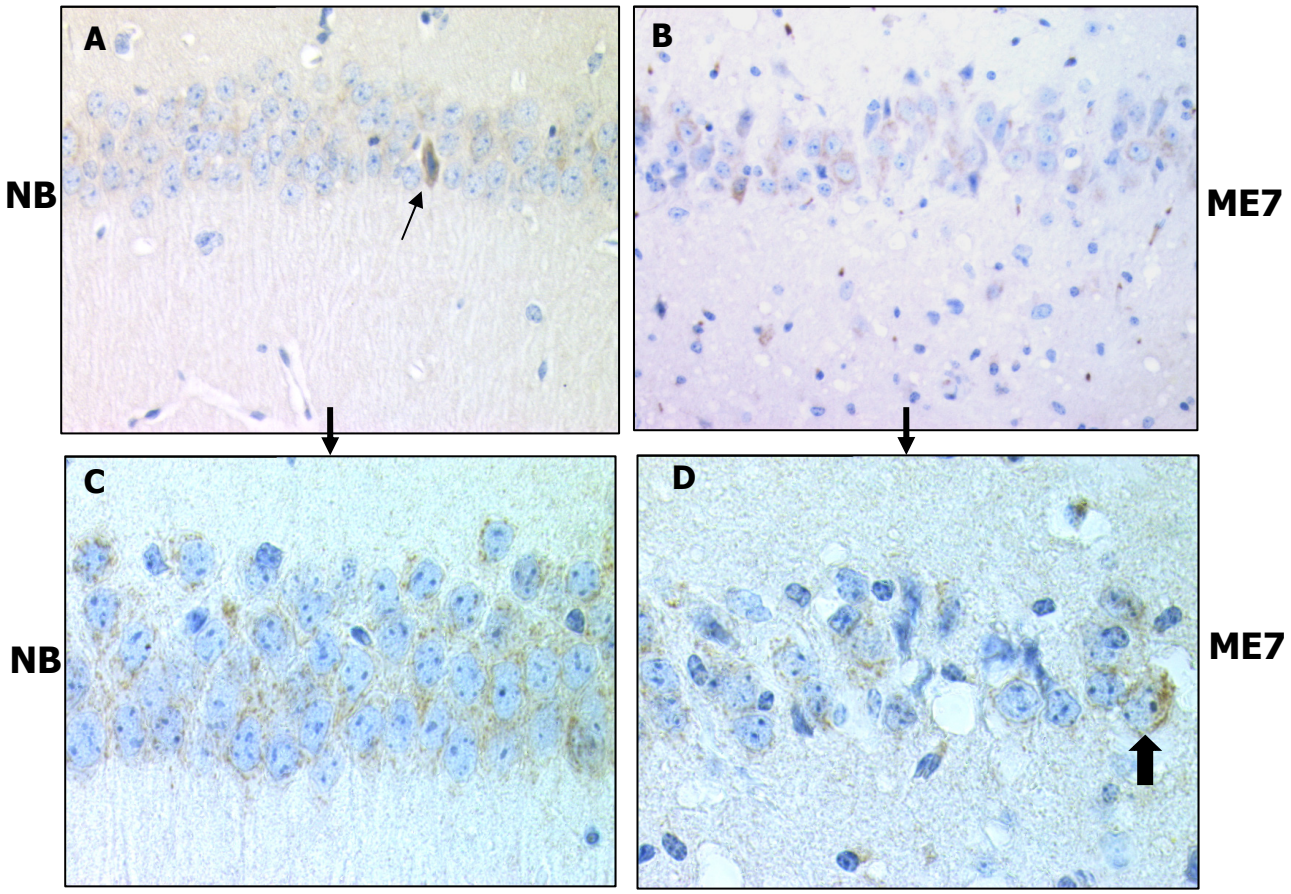

Figure 14. Cytochrome c expression in the ME7/CV scrapie mouse model. (A)&(C) Diffuse labelling observed in the cytoplasm of CA1 neurons in the hippocampus. (B)&(D) Diffuse labelling observed in the cytoplasm of CA1 neurons in the ME7 infected hippocampus. More intense labelling observed in a single neuron in the ME7 infected brain (block arrow in D). Arrows between figures denotes a higher power of the figure above.

4.4.8. Active caspase- 9 is upregulated in the brains of mice infected with 87V.

To investigate which pathway, the extrinsic or intrinsic, is involved in the activation of caspase-3 , the role of active caspase-8 and 9, caspases found upstream of caspase-3, was determined. Antibodies that react with both active caspase-8 & 9 were used to analyse the expression of these proteins in both the 87V/VM and ME7/CV mouse models. As both these caspases reside in the cytosol, subcellular fractionation was performed on dissected hippocampus from both the 87V/VM and ME7/CV model and the lysates from the cytosolic fraction used for analysis. The 87V infected samples showed a slight upregulation of active caspase-9 (Figure 15) in comparison with the NB controls. No active caspase-8 upregulation was observed in either model.

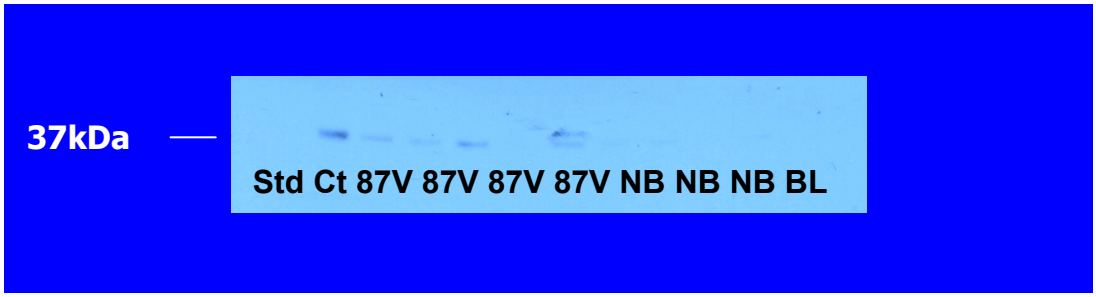

Figure 15. Expression of Active caspase-9 (37kDa) in cytosol fractions from 87V and NB/VMs. Active caspase-9 observed in terminal brains from 87V infected animals and not in the normal brain controls (87V- 87V infected brain, NB- normal brain, BL- blank Ct = +ve control Std = molecular weight markers) samples methanol precipitated and 60ug protein loaded on gel

4.4.9. Bax expression in the hippocampus of the ME7/CV and 87V/VM scrapie mouse models is similar in both infected and normal brain controls

Cytochrome c release from the mitochondria is mediated through the balance of pro and anti apoptotic members of the Bcl-2 family of proteins. To determine the role these proteins play in the scrapie infected mouse brain, the expression of Bax (pro-apoptotic) and Bcl-2 (anti-apoptotic) were analysed. Brains from both the ME7/CV and the 87V/VM scrapie mouse models at the terminal stage of disease were analysed and compared to aged matched NB controls. No difference in Bax expression was observed between the infected and NB controls in both scrapie mouse models. Diffuse cytoplasmic staining was observed surrounding cell bodies in the CA1 of both the NB control (Figure 16A) and the ME7 infected hippocampus (Figure 16B). Strong cytoplasmic labelling was observed surrounding cell bodies in the CA2 of both the NB/VM controls (Figure 16C) and the 87V infected (Figure 16D) hippocampus. A section from a human tonsil was included as a positive control. Bax expression was observed within tingible body macrophages, these cells phagocytose dying cells, and the Bax labelling observed within these cells may be due to the clearance of debri from apoptotic B cells. Non-specific (artefactual) Bax expression within the cells of the squamous epithelium surrounding the tonsil was also observed (Figure 16E).

Western blot analysis of Bax in subcellular fractions: cytosol, nuclear and organelle from ME7 and normal brain controls revealed expression of Bax in the cytosol fractions only (Figure 19). No difference was observed between the infected or control samples.

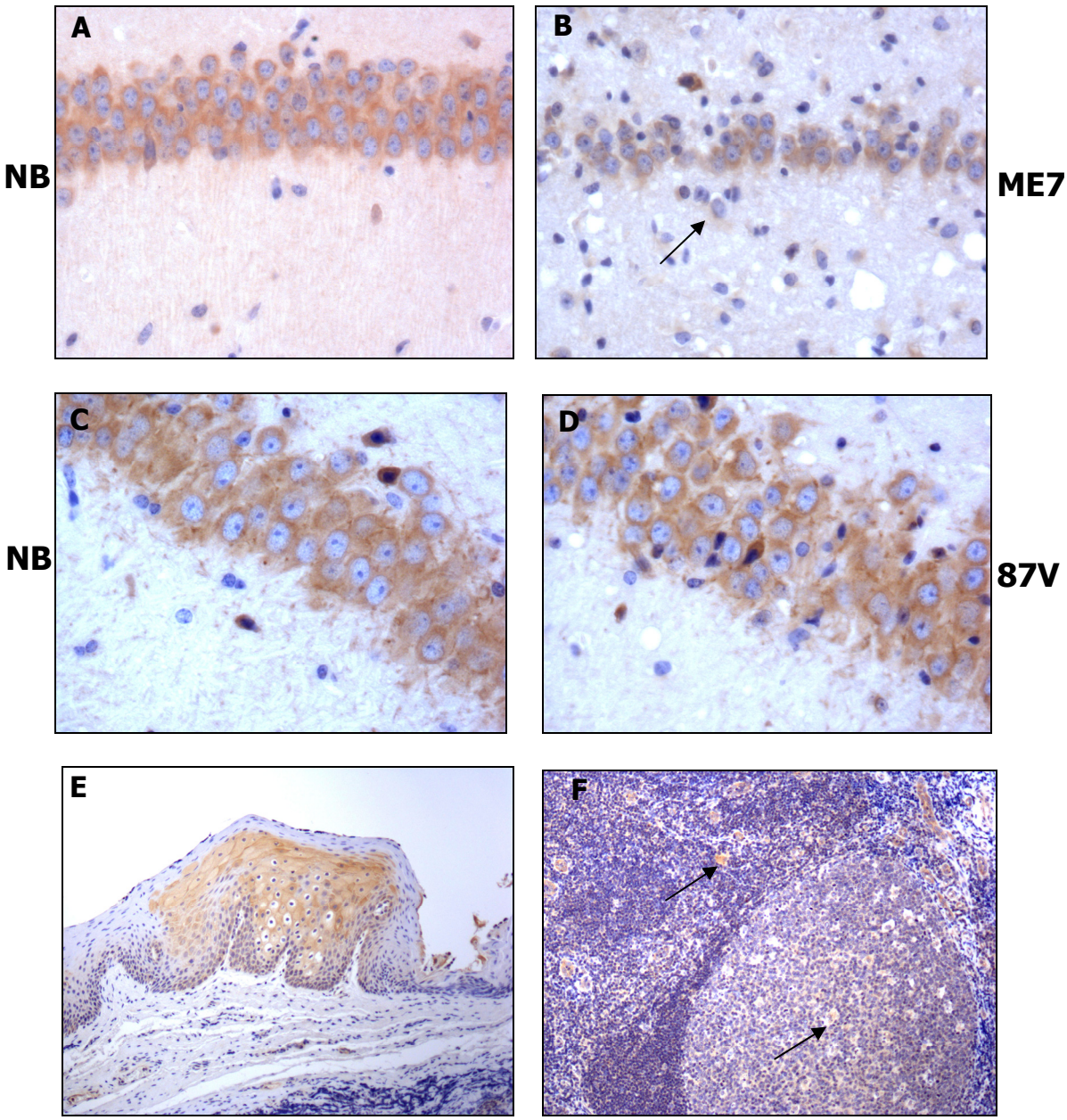

Figure 16. Bax expression in the CA1 (ME7) and the CA2 (87V) of the hippocampus. Bax expression observed in the cytoplasm of neuronal cell bodies in the CA1 of the hippocampus in the ME7/CV mouse model (A) NB control and (B) ME7 infected, faint expression observed in glial cells (arrow), and the CA2 of the hippocampus in the 87V/VM model (C) NB control. and (D) 87V infected. No differences were observed in Bax expression between the controls and infected in both mouse models. (E) Non-specific (artefactual) labelling of the squamous epithelium in the tonsil, and (F) Bax expression observed in tingible body macrophages within the follicles of the tonsil and surrounding T zone (arrows). Magnification A-D x40, E x4, F x20

4.4.10. Increase in Bcl-2 expression is observed in the infected hippocampus of the ME7/CV and 87V/VM scrapie mouse models

Bcl-2 is an anti-apoptotic member of the Bcl-2 family of proteins that resides in the mitochondrial, endoplasmic reticulum and nuclear membranes. Its main function is to maintain the integrity of the mitochondrial membrane preventing release of cytochrome c into the cytoplasm and apoptotic cell death. A Bcl-2 mouse monoclonal antibody from Upstate was used in both IHC and western blot analysis.

In the ME7/CV mouse model Bcl-2 expression was observed within glial cells in the pyramidal cell layer and the stratum radiatum of the hippocampus (Figure 17B). Faint expression was observed in the cytoplasm surrounding the pyramidal cell bodies in the NB control (Figure 17A). In the 87V/VM mouse model faint membranous labelling was observed surrounding the cell bodies of the CA2 neurons in both the NB control (Figure 16C) and the 87V infected hippocampus (Figure 17D). A slight increase in labelling was observed in the 87V infected cell bodies in the CA2.

Western blot analysis of Bcl-2 was performed on the organelle and nuclear subcellular fractions. Western blot analysis of Bcl-2 in the ME7 infected and NB controls at the terminal stage of disease revealed expression of Bcl-2 in the nuclear fractions only with an increased expression observed in the ME7 infected brains (Figure 18). There was no expression of Bcl-2 in the organelle fraction.

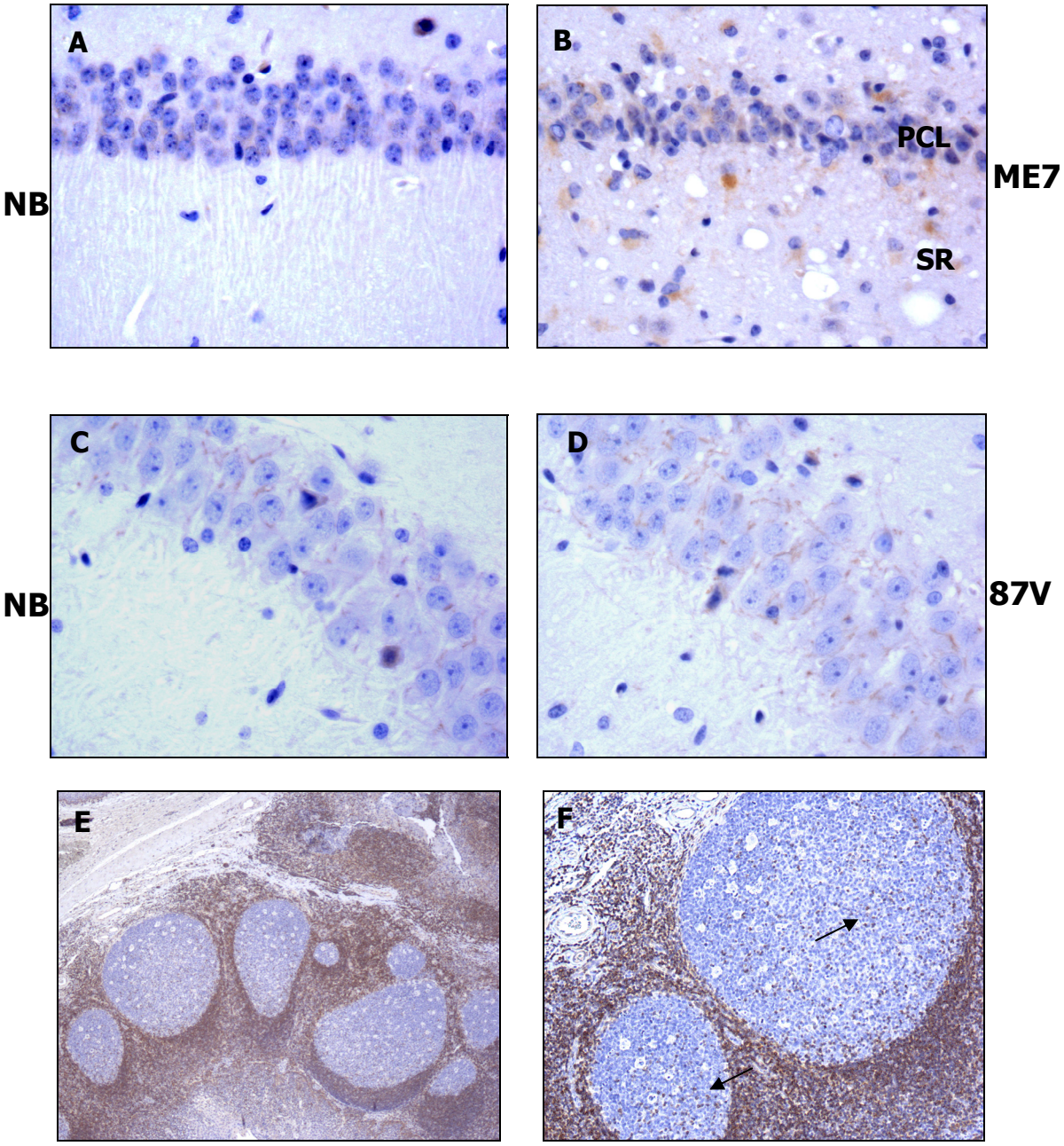

Figure 17. Bcl-2 expression in the CA1 (ME7) and the CA2 (87V) of the hippocampus Bcl-2 expression observed in the ME7/CV mouse model (A) faint labelling in the cytoplasm of pyramidal cell bodies in the NB control. (B) Bcl-2 expression observed within glial cells in the pyramidal cell layer (PCL) and stratum radiatum (SR) of the ME7 infected hippocampus. Bcl-2 expression in the CA2 of the hippocampus in the 87V model (C) faint cytoplasmic labelling observed around cell bodies in the CA2 of a NB control (D) increased expression in the 87V infected CA2. (E) Expression of Bcl-2 in tonsil mainly observed surrounding follicles in the T cell zone. (F) Bcl-2 labelling also observed in cells within the germinal centre (arrows). Magnification A-D x40, E x4 and F x20

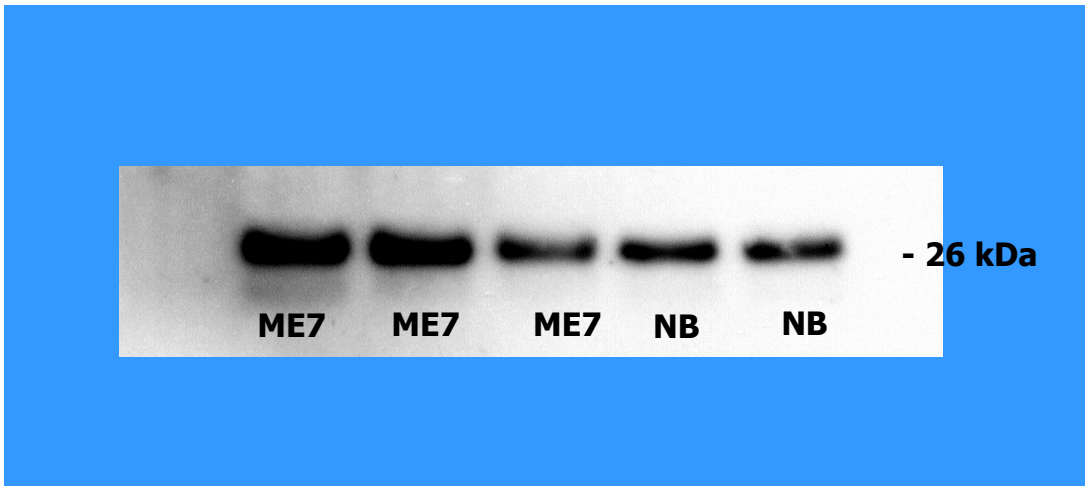

Figure 18. Bcl-2 expression in ME7 infected and normal brain control nuclear fractions. Each well was loaded with 20µg protein in 20µl. Protein estimation performed in each sample and an equivalent amount of protein added in each sample. Expression of Bcl-2 was increased in two of the three ME7 infected nuclear fractions in comparison to the normal brain control. Expression of Bcl-2 was only observed in the nuclear fraction.

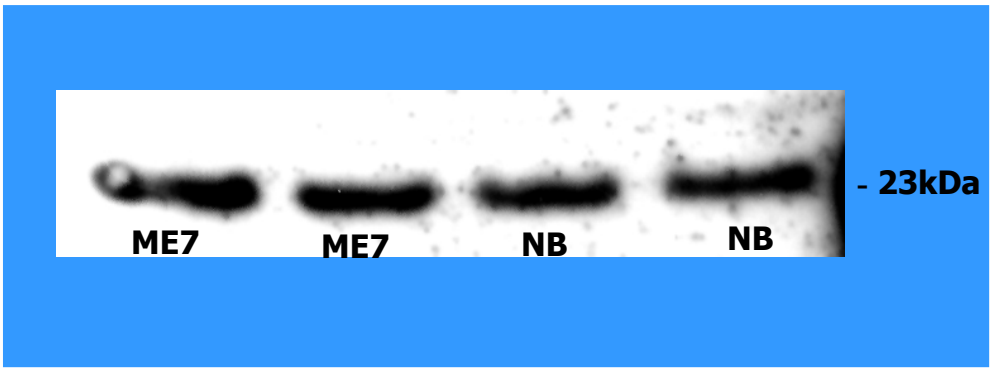

Figure 19. Bax expression observed in the Cytosol fractions only.
Each well was loaded with 20µg of protein in 20µl. Protein estimation performed in each sample and an equivalent amount of protein added in each sample. Expression of Bax was observed in both the NB controls and the ME7 infected samples from the cytosol fraction and no difference in amounts were observed.

4.5 Results of FACS analysis study

4.5.1 Brain cells are viable after FACS methodology

The viability of brain cells were tested after preparation using the FACS methodology. A high percentage of cells were viable in both the infected and control brains. Cell suspensions analysed with both trypan blue and FACS (Figure 20) revealed a high percentage of cells were viable. Not as many cells were observed in the ME7 infected brain specifically in the midbrain portion which contains the hippocampus, where neurons are known to be lost.

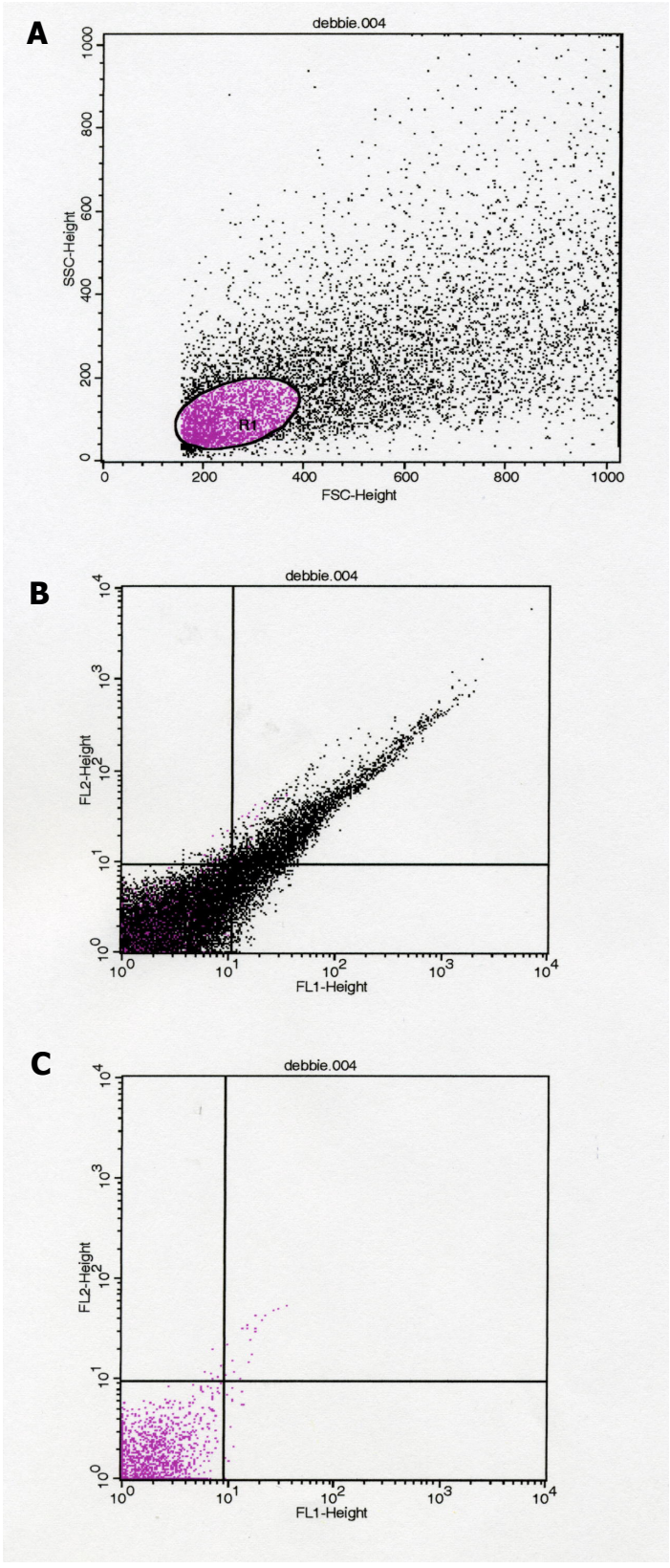

Figure 20. Testing cell viability by analysing cells in the FACS machine without a fluorescent label. Example of cell viability after preparation with FACS methodology. ME7 infected hind brain (A) Whole number of viable cells observed in FACS machine. (B) Total cell population observed in ungated sample. (C) Cell population observed in gate one (R1 from Fig. A).

4.5.2 FACS analysis of microglia labelled with F4/80

As a high percentage of brain cells were viable a further study was undertaken to analyse the microglial response in the ME7 infected brain.

A high percentage of cells labelled with the microglial marker F4/80. Two gates were applied to the cell suspension and most of the fluorescently labelled cells were observed in gate 1 (R1), where smaller less complex cells are observed (example Figure 21). In both the NB and ME7 infected cell suspensions F4/80 microglial labelling was increased in comparison with the control cells with no label (NB example Figure 22). In comparing the percentage of total cell numbers labelled in both the normal and ME7 infected cells in the three areas dissected, the area showing the greatest increase in microglia was the mid brain (Figure 23&25). This section of the brain contains the hippocampus an area in the ME7 infected brain were microglia are know to be activated and increase in numbers (see chapter 3 Figure 13F). On analysis of the gated cell suspension (R1) from both the normal and ME7 infected cells, differences were observed in both the forebrain and mid brain (Figure 24). This correlates with IHC analysis of the microglial response in the ME7 infected brain. FACS analysis of the microglial response in the ME7 infected brain successfully recognised the main areas of the brain involved in the increase in reactive microglia, corresponding with that observed in tissue sections.

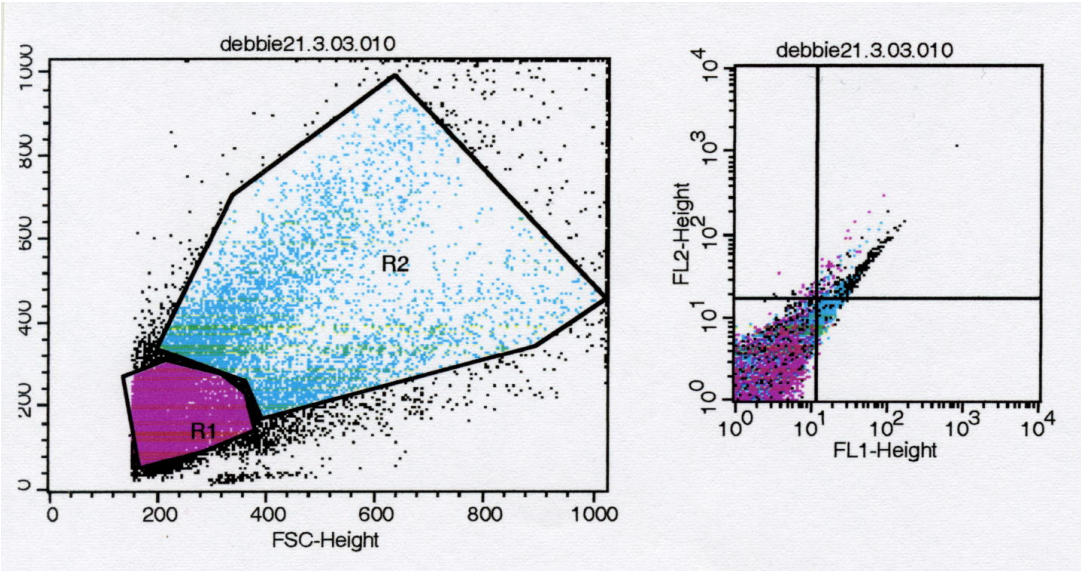

Figure 21. Example of FACS analysis of cell numbers labelled with F4/80 microglial marker. ME7 infected midbrain labelled with F4/80 two gates applied. R1 is the region where all smaller less complex cells would be observed and R2 represents the region where larger more complex cells would be observed. Most fluorescently labelled cells were found in gate 1 (R1).

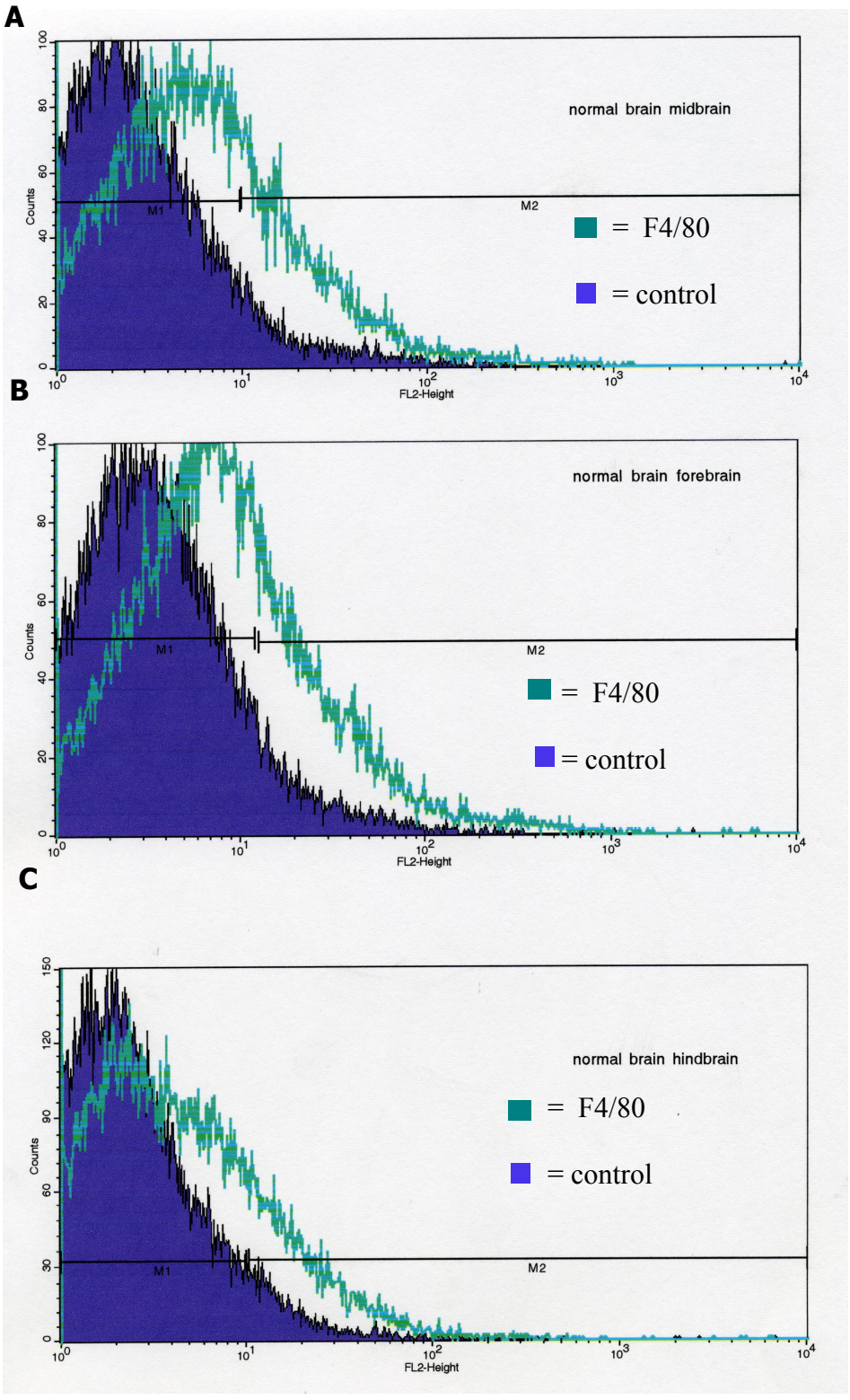

Figure 22. FACS analysis of microglia in normal brain versus control cells with no label. The blue filled in trace are the control cells with no label and the green line are cells labelled with F4/80 microglial marker. (A) midbrain (B) Forebrain and (C) hindbrain from normal brain. A marked difference was observed between control cells and those labelled with F4/80 in midbrain, forebrain and hindbrain.

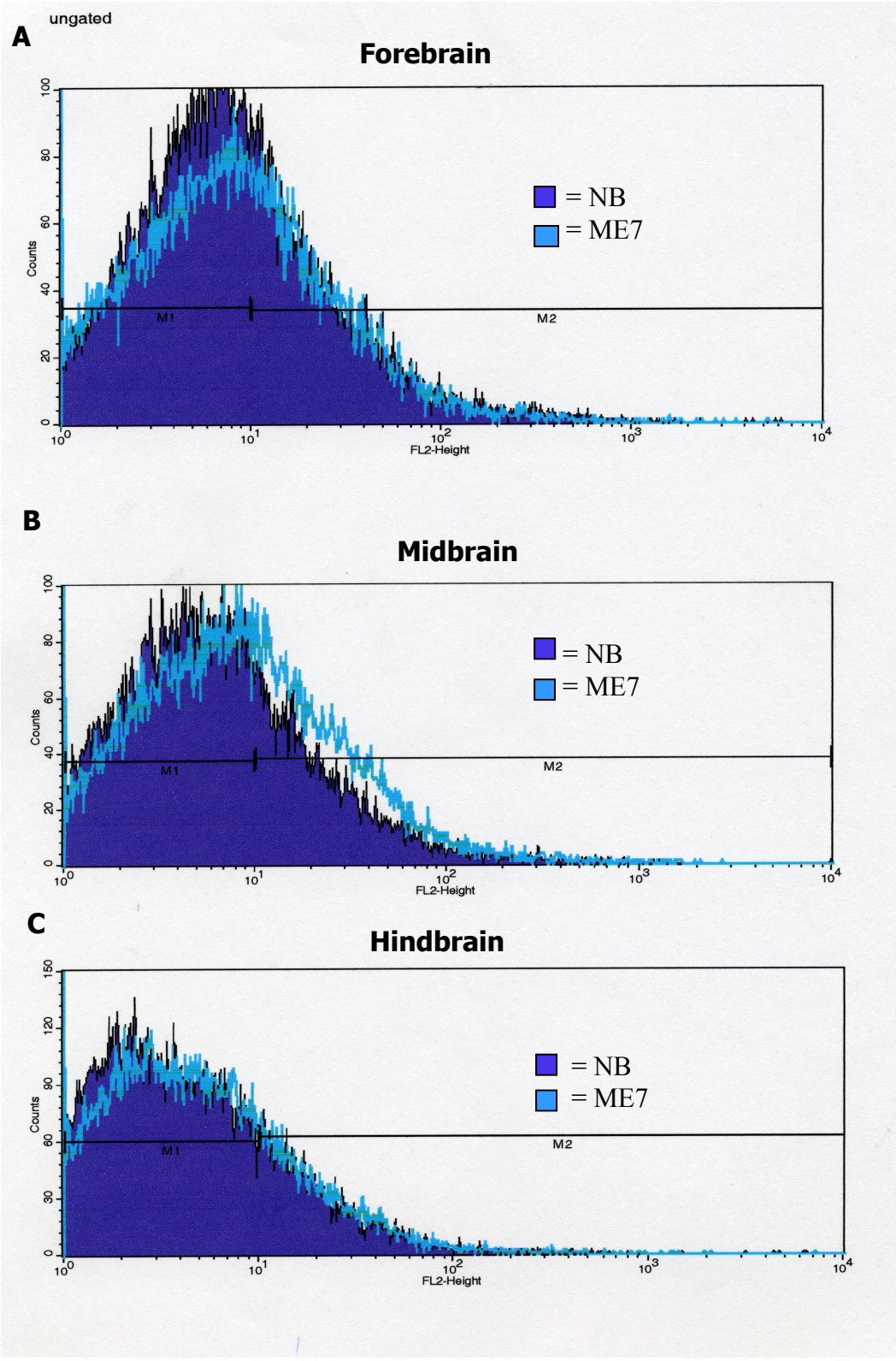

Figure 23. FACS analysis of normal brain and ME7 infected cells labelled with F4/80 microglial marker. Total numbers of cells analysed with no gate. (A) Forebrain showing no difference in numbers of microglia labelled in both the normal and ME7 infected brains. (B) Midbrain showing upregulation of microglia in the ME7 infected cells in comparison to the normal brain. (C) Hindbrain showing no difference in numbers of microglia labelled in both the normal and ME7 infected brains.

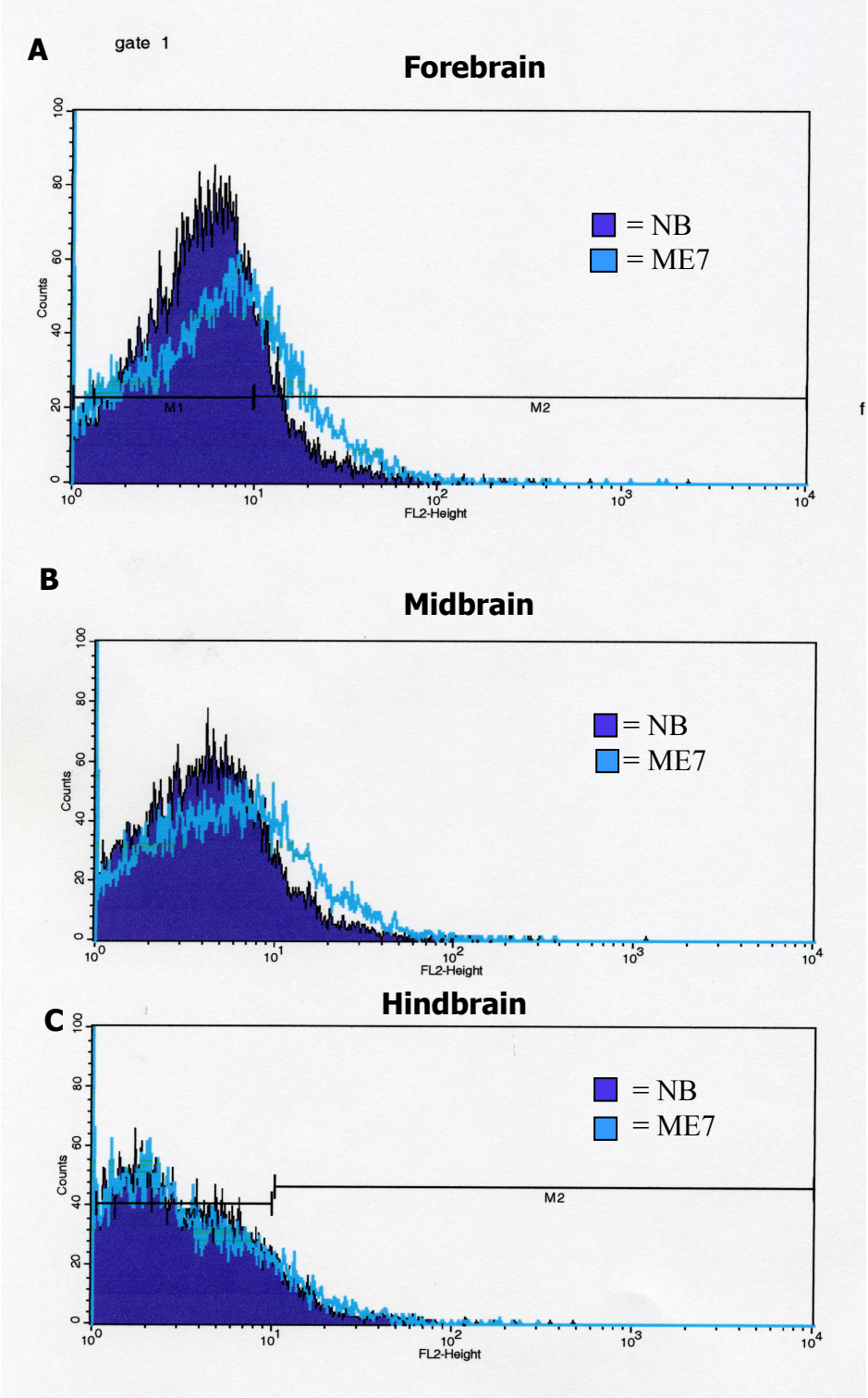

Figure 24. FACS analysis of normal brain and ME7 infected cells labelled with F4/80 microglial marker. Total numbers of cells analysed from gated sample. (A) Forebrain showing a difference in numbers of microglia labelled with F4/80 in the ME7 infected brains in comparison to the normal brains. (B) Midbrain showing upregulation of microglia in the ME7 infected cells in comparison to the normal brain. (C) Hindbrain showing no difference in numbers of microglia labelled in both the normal and ME7 infected brains.

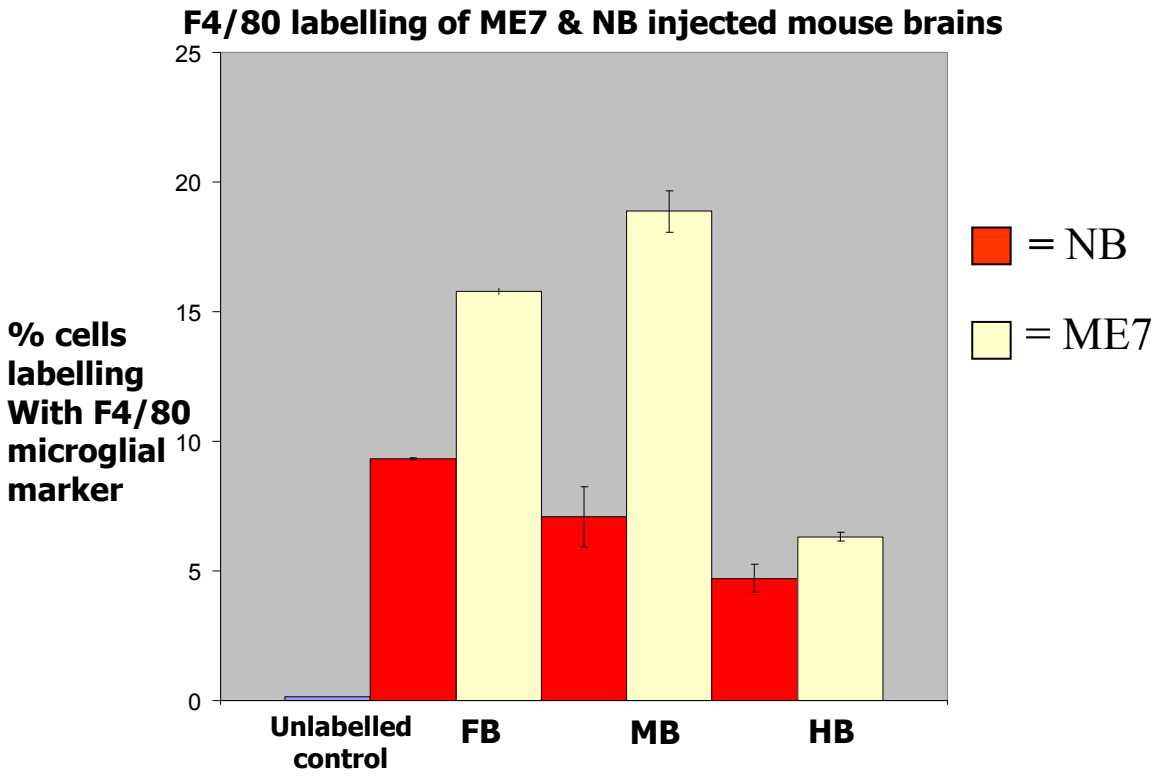

Figure 25. Percentage of cells labelling with the microglial marker F4/80 in both the normal brain and ME7 infected brain in the forebrain (FB), midbrain (MB) and hindbrain (HB). Graph from data in figure 24 above. The greatest increase in microglial response is observed in the ME7 infected midbrain which contains the hippocampus, an area known to have a marked upregulation of microglia.

4.5.3. FACS analysis of neurons in a normal mouse brain

Inspection of cell suspension when performing cell counts with trypan blue revealed less clumping of cells when tissue was treated with dissociation medium prior to FACS methodology.

FACS analysis of cells labelled with NeuN showed many cells labelling in the whole cell suspension (Figure 27). Most cells labelled with NeuN were observed in the R1 gate where the cells would be smaller in size and less complex (Figure 26). Cells in both gates 1 (R1) (Figure 28) and 2 (R2) (Figure 29) labelled with the Neu N antibody, with a higher proportion observed in gate 1 (R1). Analysis of a cytospin prepared from the cell suspension revealed that the cells labelled with NeuN were quite small and rounded up (Figure 30).

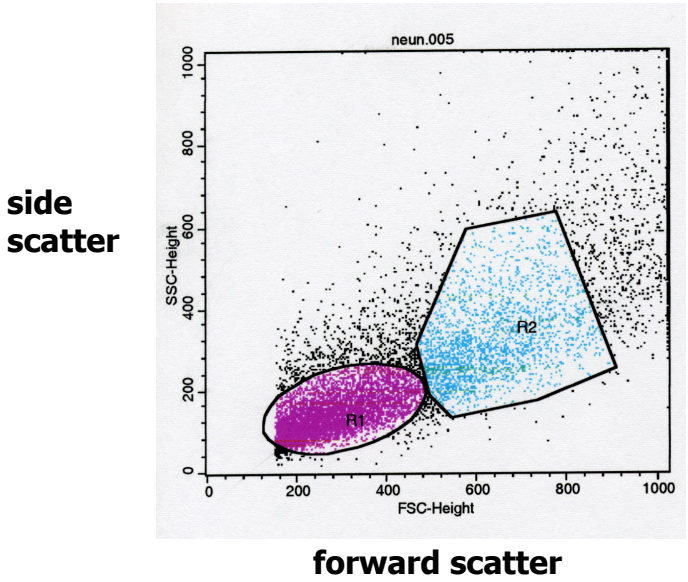

Figure 26. FACS analysis of cells labelled with NeuN. Most cells labelled with NeuN were observed in gate 1 (R1) where smaller and less complex cells would be observed. A cut off point just before 200 on the forward scatter was used to eliminate debris. Forward scatter = cells relative size, side scatter = cells relative granularity or internal complexity

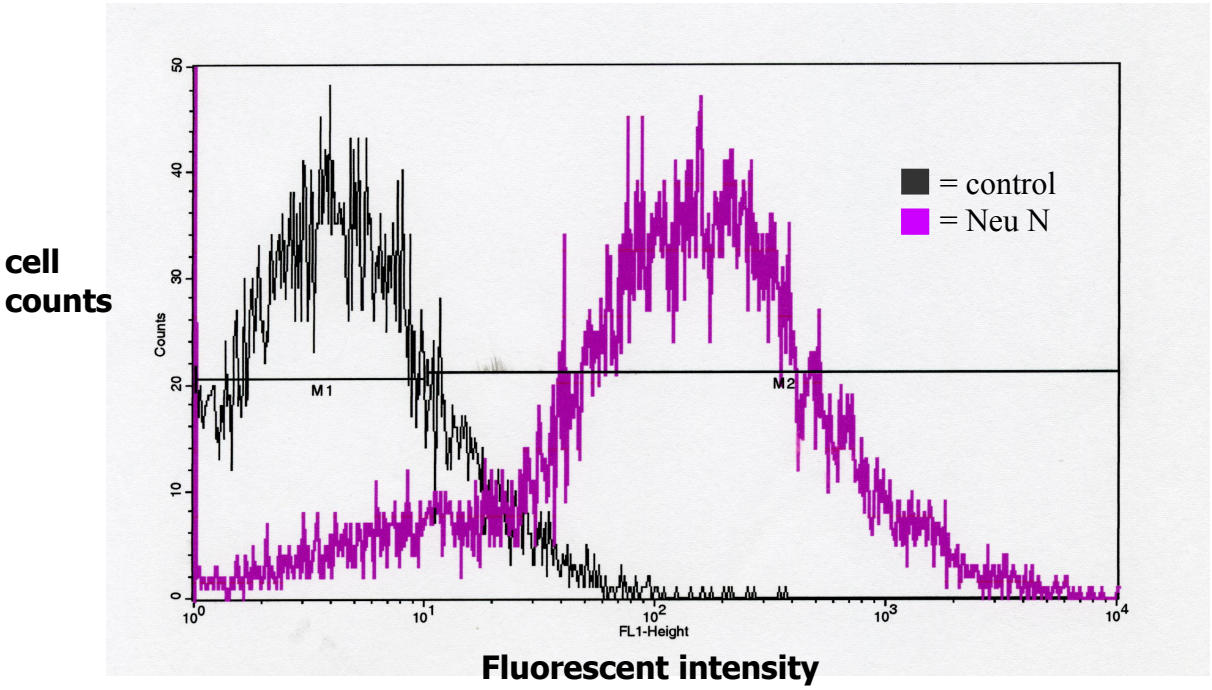

Figure 27. FACS analysis of control cells with no label and NeuN labelled cells with no gate. Comparison of total cell numbers in NeuN labelled and unlabelled control cells. Fluorescent intensity of NeuN labelled cells in purple trace in comparison with control cells with no label in the black trace

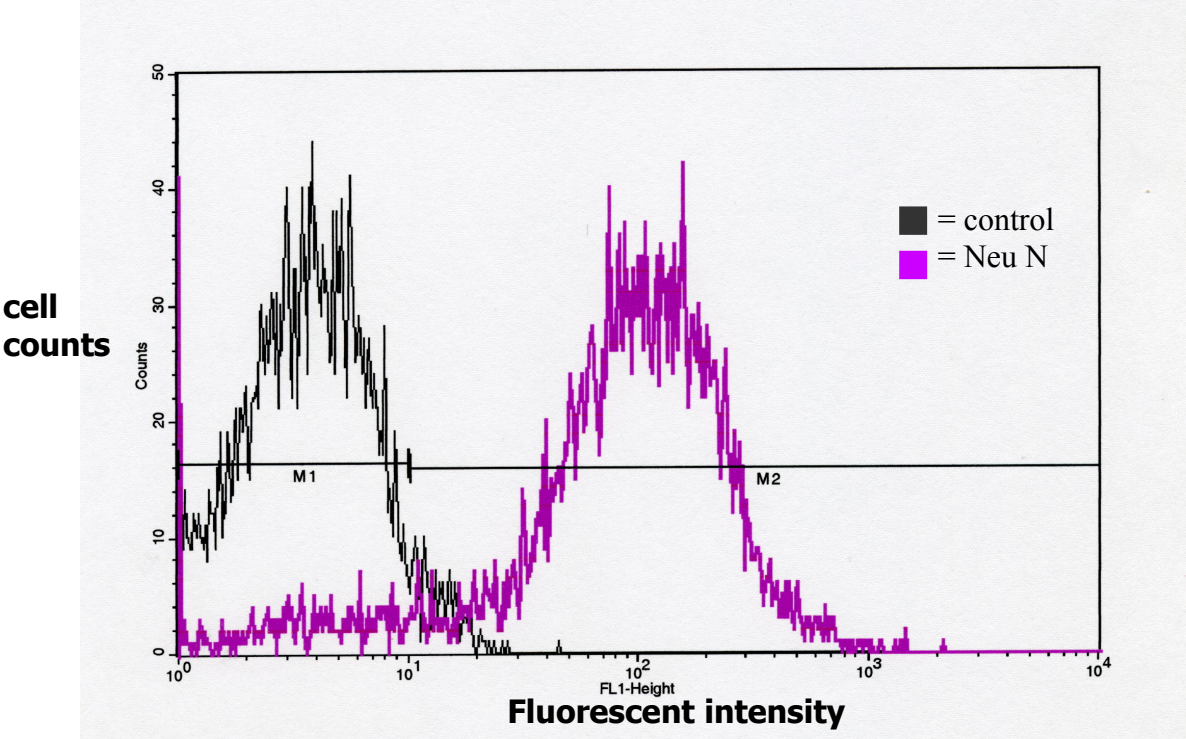

Figure 28. FACS analysis of control cells in comparison to NeuN labelled cells from gate 1. Increase in fluorescent intensity observed in NeuN labelled cells in comparison to control cells from gate 1 in Figure 26. Black trace are cells with no label and purple trace are fluorescing cells labelled with NeuN.

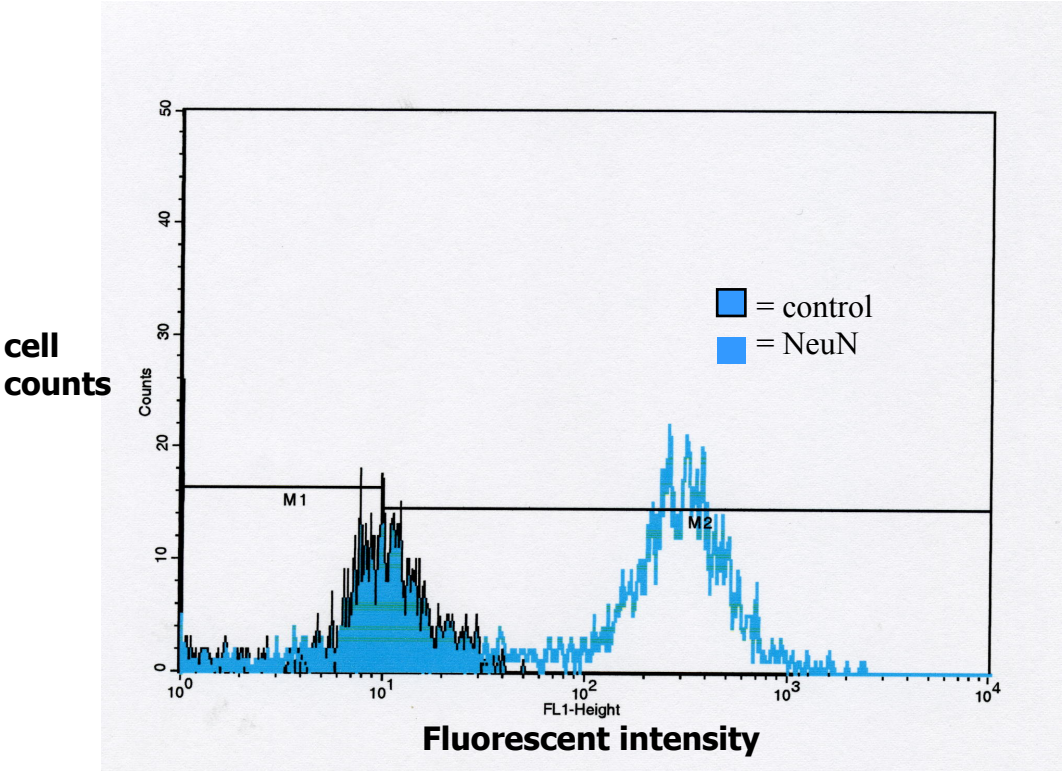

Figure 29. FACS analysis of control versus NeuN labelled cells in gate 2. Black trace filled in with blue are control cells with no label . Blue trace are NeuN labelled cells from R2 in Figure 26.

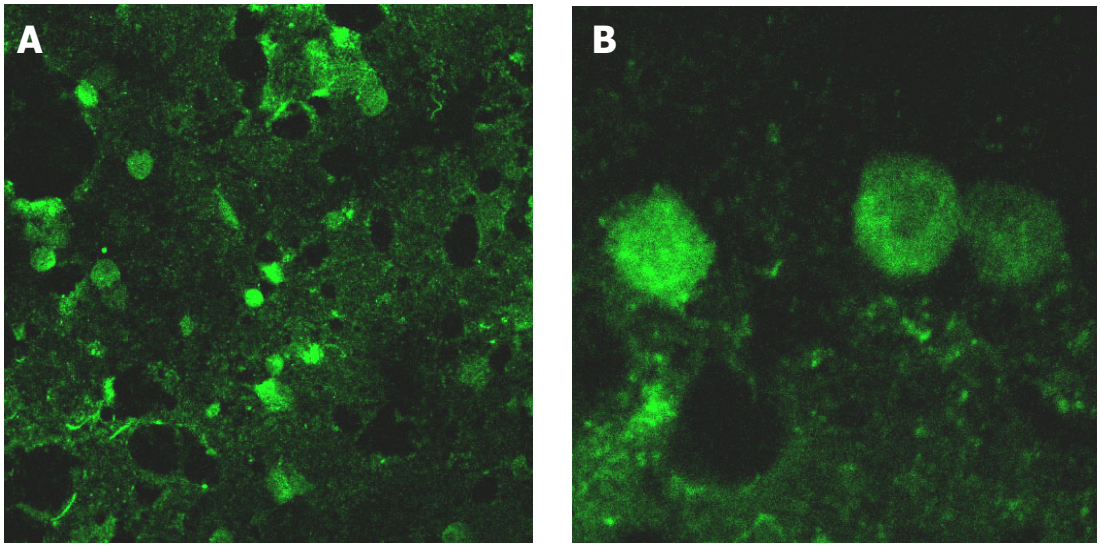

Figure 30. Confocal images of cytospin preparation of cells labelled with NeuN. (A) x20 magnification of cells labelled with NeuN. (B) x60 oil magnification of cells labelled with NeuN. Cells are rounded and do not show a typical neuronal morphology as would be observed in neuronal cell cultures.

4.6 Discussion

In the ME7/CV model both TUNEL and active caspase-3 labelling was observed in single cells in the hippocampus. These cells were not observed in the CA1 sector of the hippocampus, where the targeted neuronal loss is observed, and the numbers of apoptotic cells detected were very low. Single cells were observed in the dentate gyrus, cortex and white matter tracts in the corpus collosum. Also western blot analysis of active caspase-3 was only observed in dissected hippocampus samples following protein concentration with methanol precipitation.

The time course study performed in the ME7/CV scrapie mouse model did not show any increase in apoptotic cells throughout the incubation period of disease. Single active caspase-3 cells were observed in the brains of mice throughout the progression of the disease, and as in the terminally infected mice few cells were detected. This correlates with analysis of active caspase-3 in the brains of C57BL mice infected with the ME7 strain of scrapie (Cunningham et al, 2003). In this model single active caspase-3 cells were first observed in the dentate gyrus at 19 weeks post injection and not in the CA1 where cells are known to be lost.

The TUNEL labelling technique can produce false positives (Stahelin et al, 1998), and is also known to label cells undergoing necrotic cell death (Frankfurt & Krishan, 2001). Therefore TUNEL labelling on its own is not a reliable marker for the identification of apoptosis, this marker labels dead cells but cannot identify which type of cell death is occurring in the cell. Active caspase-3 is known as the central executioner of the apoptotic pathway (Cohen, 1997) and is a reliable marker that can be used in conjunction with the TUNEL method to positively identify cells dying through an apoptotic mechanism (Mazumder et al, 2008; Yakovlev & Faden, 2001).

Using both TUNEL methodology and active caspase-3 labelling, apoptotic neurons have been shown in both naturally occurring and experimentally induced TSEs (Dorandeu et al, 1998; Ferrer, 2002; Jamieson et al, 2001a; Jamieson et al, 2001b; Jesionek-Kupnicka et al, 1999; Puig & Ferrer, 2001; Williams et al, 1997a). In rodent models of TSE disease apoptotic cells have been identified using the TUNEL method and an inconsistency was observed between numbers of cells labelled with this technique (Jesionek-Kupnicka et al, 1997; Jesionek-Kupnicka et al, 2001). In the ME7/CV scrapie mouse model TUNEL labelling was observed in a few cells in the hippocampus at 170dpi (Brown et al, 2003a), labelling resembled that observed in this study. In C57BL mice infected with the 79A strain of scrapie, a marked retinopathy is observed along with degeneration in the cerebellum. In these mice a massive cell loss was observed in the retina, identified with TUNEL labelling, but only a few cells labelled in the cerebellum of terminally ill mice (Giese et al, 1995). In a BSE mouse model where neuronal loss is also observed in the CA1 of the hippocampus, a few TUNEL labelled cells were detected at the end stages of disease. TUNEL labelling and active caspase-3 are useful markers for detecting apoptosis *in vivo* when there is a marked induced cell death, like that observed within the retina of 79A infected mice. The lack of expression of these markers in the dramatic loss of neurons observed in the ME7 infected hippocampus may be due to a rapid clearance of these dying cells *in vivo*, or that the cell loss does not involve an apoptotic mechanism.

Previous studies in the 87V/VM scrapie mouse model revealed an increase in expression of the Fas receptor in 87V infected CA2 neurons, suggesting a role for the extrinsic mediated pathway of apoptosis in TSE induced cell death.

In the ME7/CV scrapie mouse model Fas expression was not upregulated in ME7 infected CA1 neurons, although expression of this pro-apoptotic marker was observed

in glial cells in the CA3 sector of the hippocampus. Fas is a member of the TNF family of receptors that regulate a large and diverse number of cellular processes, many of which involve the immune system. Fas is constitutively expressed on both microglia and astrocytes (Bonetti et al, 1997; Lee et al, 2000; White et al, 1998). In murine microglia Fas is expressed at low levels and up-regulated by TNF-α or IFN-γ. The expression of Fas observed on glial cells at the terminal stage of disease in the ME7 infected brain may be induced by the expression of the pro-inflammatory cytokine IL-1β, found upregulated in astrocytes at this stage of the disease (Brown et al, 2003a; Williams et al, 1997b) and not related to apoptosis. Conflicting results were observed when analysing the role of the Fas receptor in the 87V/VM scrapie mouse model. Previous documented results revealed upregulation in the CA2 sector as early as 100 days, increasing in intensity at the terminal stage of disease (Jamieson et al, 2001a). In the study performed here using the same antibody only a faint labelling of Fas could be observed in the CA2 at the terminal stage of disease. In a study using the RML strain of scrapie (Siso et al, 2002), no difference in Fas expression was observed between infected and control brains. Similar results were observed in both the 87V/VM and ME7/CV models using the same antibody from this study. Evidence from previous studies and the work performed in this study reveal inconsistent results and the role of the receptor mediated pathway via Fas induction in TSE disease is unclear. Fas expression is often observed in cells not undergoing apoptosis in TSE infected brains and may have other functions unrelated to the induction of apoptosis (Puig & Ferrer, 2001).

The role the extrinsic pathway of apoptosis via Fas induction plays in the cell death observed in TSEs is uncertain. Therefore induction of apoptosis via the intrinsic (mitochondrial) pathway was investigated. When mitochondria are damaged i.e.

through the increase in reactive oxygen species within the cell, they release cytochrome c from the mitochondrial membrane into the cytosol. The expression of cytochrome c was analysed in brains at the terminal stage of disease in both scrapie mouse models. No marked difference was observed in the expression of cytochrome c in the ME7 (CA1) and the 87V (CA2) infected hippocampus in comparison with the aged matched controls. Some subtle changes where observed in the infected brains, single cells resembling the dark neurons identified in haematoxylin and eosin stained sections in Chapter 2, expressed cytochrome c. An increase in dark neurons are observed in ischaemic conditions in the brain. Mitochondria are a primary target in hypoxic conditions and when damaged release cytochrome c into the cytosol (Christophe & Nicolas, 2006). In the ME7 infected CA1 neurons, an increase in punctate labelling in the cytoplasm of some neurons was observed. A similar pattern of staining was observed in the brains of Huntington's disease (HD) patients and in a transgenic model of HD, also shown in this study was a shift in the distribution of cytochrome c from the mitochondrial to the cytosolic fraction (Kiechle et al, 2002). The change in the pattern of staining observed in the ME7 infected CA1 neurons may relate to a shift in the distribution of cytochrome c from mitochondrial to cytosolic. The change in cytochrome c may not be due to an apoptotic mechanism, cytochrome c also plays a role in the antioxidant cascade and the changes observed here may be related to an increase in reactive oxygen species, which have been shown to be increased in TSE disease (Brazier et al, 2006; Choi et al, 1998; Guentchev et al, 2000; Kim et al, 2001; Milhavet & Lehmann, 2002). Gene expression studies in the hippocampus of the ME7/CV scrapie mouse model revealed upregulation of mitochondrial genes involved in the apoptotic pathway, suggesting a role for this pathway in the neuronal loss observed in this model (Brown et al, 2003a).

In the caspase-dependent pathway active caspase-3 can be activated by an extrinsic (receptor), or an intrinsic (mitochondrial) mediated pathway. Upstream of caspase-3 are two caspases which upon activation initiate caspase-3 cleavage through either the intrinsic or extrinsic mediated pathway. On initiation of the Fas receptor complex activation and cleavage of caspase-8 occurs leading to the cleavage of caspase-3. When cytochrome c is released from the mitochondria it activates caspase-9 resulting in its cleavage and the formation of the apoptosome complex (Figure 2). To analyse the role of both pathways in the cell loss observed in the two scrapie mouse models the expression of both active caspase-8 and active caspase-9 were examined.

Upregulation of active caspase-9 was observed in the 87V infected brains only (Figure 15). Active caspase-9 is involved in the mitochondrial pathway of apoptosis, and is cleaved by cytochrome c when it is released from the mitochondria into the cytoplasm. This result contradicts previous results in this model where Fas was found to be upregulated; induction of apoptosis through a Fas mediated mechanism activates caspase-8 resulting in its cleavage. The upregulation of active caspase-9 observed in this model indicates that there may be crossover between both the extrinsic and intrinsic pathways and that the activation of the caspase dependent pathway in the 87V/VM scrapie mouse model may involve both a receptor mediated and mitochondrial pathway. This phenomenon has been observed in disease states, crosstalk between extrinsic and intrinsic cell death pathways have been observed in a mouse model of amyotrophic lateral sclerosis (ALS) (Tokuda et al, 2007) and in pancreatic cancer (Basu et al, 2006).

The activation of caspase-9 observed in the 87V/VM scrapie mouse model is suggestive of a role for the mitochondrial pathway of apoptosis in this model. The

role that the mitochondria may play in the activation of the caspase-dependent pathway was further investigated. Residing in the mitochondrial membrane is a group of proteins, called the Bcl-2 family. There are both pro- and anti-apoptotic members of this family of proteins, in which the balance of, can determine whether the cell commits to apoptosis. Bcl-2 is an anti-apoptotic member of this family and Bax is a pro-apoptotic member. Bax translocation to the mitochondrial membrane induces the formation of the mitochondrial pore, releasing cytochrome c from the mitochondria into the cytosol. In both scrapie mouse models the expression of Bcl-2 and Bax was investigated.

No difference in Bax expression was observed in the CA1 sector (ME7) or CA2 sector (87V) of the hippocampus in both the infected and normal brain controls (Figure 15&18). The expression observed on immunohistochemical and western blot analysis was cytosolic. In a healthy cell Bax is expressed in the cytosol and on induction of apoptosis translocates to the mitochondrial membrane where it interacts with Bcl-2 and initiates mitochondrial pore formation. No Bax expression was observed in the organelle fraction from either the infected or normal brain controls revealing no translocation from the cytosol to the mitochondrial membrane and therefore no Bax induced initiation of the mitochondrial pathway. In a BSE mouse model Bax deletion did not protect neurons from TSE induced death and did not alter the development of disease (Coulpier et al, 2006). However, in a transgenic mouse model of inherited prion disease, Bax deletion rescued cerebellar granule neurons from apoptosis, although the clinical phase of disease was unaltered (Chiesa et al, 2005). The role that Bax plays in the cell loss observed in this transgenic mouse model may be related to the overexpression of mutant PrP in this model.

The increase in gene expression and protein levels of Bax were increased in the brains of sheep with natural scrapie, (Lyahyai et al, 2007) and correlates with PrP^{Sc} deposition (Lyahyai et al, 2006) but not with active caspase-3 labelling. In the sheep study active caspase-3 labelling was observed in glial cells and not within neurons labelling with Bax, revealing that neuronal dysfunction in natural scrapie and the upregulation of Bax is not related to apoptosis.

Bcl-2 expression in the CA1 sector of the ME7 infected hippocampus was observed in glial cells in and around the CA1 pyramidal cell layer. Changes in mitochondria and increased expression of Bcl-2 has been observed in astrocytes undergoing stress (Ouyang & Giffard, 2004). Upregulation of astrocytes is a feature observed in the CA1 sector of the ME7 infected hippocampus, and the stress induced upregulation of Bcl-2 observed in these cells may have a neuroprotective role for both the neuron and astrocyte in this model. In contrast, in the CA2 sector of the 87V infected hippocampus Bcl-2 labelling was observed surrounding the cell bodies of CA2 neurons and appeared to be increased in the 87V infected neurons. The slight increase in this anti-apoptotic protein in these neurons may be due to a survival role within these neurons, counteracting the cell death mechanisms. Bcl-2 is inserted into the mitochondrial, endoplasmic reticulum and nuclear membranes where it has anti-apoptotic functions. In the nucleus it interacts with nuclear lamins preventing breakage of DNA and neuronal cell death (Cassarino & Bennett, 1999). In the ME7 infected hippocampus the expression of Bcl-2 was observed in the nuclear fraction only, suggesting that the upregulation of this anti-apoptotic protein in the nucleus may play a protective effect in the nucleus trying to counteract DNA breakage due to apoptosis.

This study provides very limited evidence for a role of apoptosis in the neuronal cell loss observed in TSEs. Differences observed in the two scrapie mouse models studied may relate to differences in susceptibility of the neuronal populations targeted in the hippocampus in these models. The 87V strain of scrapie targets a smaller more precise sector of the hippocampus, the CA2, which may ease the detection of apoptotic cells *in vivo*. Also, although a microglial response is observed in the CA2 at the terminal stage of disease, it is not as extensive as that observed in the CA1 of the ME7/CV model, therefore clearance of apoptotic cell bodies may be minimal in the 87V/VM model.

Further studies analysing other cell death mechanisms i.e. autophagy, and their role in the neuronal cell loss observed in TSEs are required.

FACS analysis as a tool to identify apoptotic markers in vivo

The first FACS analysis study performed in this thesis was set up to identify if this technology could be used to identify a known phenomenon that is observed in the ME7 infected brains, a dramatic upregulation of microglia at the terminal stage of disease. This initial study was very successful revealing an upregulation of a microglial response in both the midbrain and forebrain but not in the hind brain. This result corresponds with immunohistochemical analysis of microglia in the ME7 infected brain, in which a marked upregualtion is observed in the hippocampus, an area found within the midbrain. FACS analysis may be a quick and useful technique to use in quantification studies of the microglial response in different brain areas throughout the course of the disease in scrapie mouse models.

In the second study in the analysis of neurons in the normal mouse brain *in vivo,* a population of cells where labelled with NeuN a neuronal marker. These cells where predominantly found within gate 1 (Figure 28) a region where smaller less

complex cells are observed. On further analysis of the neurons labelled with NeuN, morphologically these cells were quite small and round (Figure 30) and not as large and complex as neurons observed after days in cell culture or in situ within the brain. Neurons are larger and more complex cells than microglia and their processes may be sheared off in the methodology used to obtain a single cell suspension for FACS analysis. Also the methodology used and the major disruption to neurons may induce apoptosis in these cells, making it difficult to interpret results and true apoptosis due to the disease conditions. Future studies using FACS analysis of neurons *ex vivo* may have to include steps to ensure the minimal alteration to the *in vivo* conditions.

Further studies are required to determine the use of FACS analysis as a tool to study apoptotic cell loss *ex vivo*.

Chapter 5 : Cytoskeletal changes and synaptic loss observed in the CA1 neurons of the ME7 infected hippocampus

Introduction

Neuronal cell loss is observed in the CA1 of the ME7 infected hippocampus at 160 dpi., Prior to this loss at 100 dpi cytoskeletal damage in the form of dendritic spine loss is observed (Brown et al, 2001), which correlates with axon terminal degeneration and synapse loss (Jeffrey et al, 2000). A progressive spine loss is observed throughout the incubation period of disease and by the terminal stage of disease the CA1 neurons become distorted, losing most of their dendritic spines and forming abnormal swellings within the apical dendrites (Belichenko et al, 2000; Brown et al, 2001).

In this chapter the role of the cytoskeleton in the neuronal cell loss observed in the CA1 sector of the hippocampus will be investigated and the role that it plays in the synapse loss in these neurons determined.

5.1 Cytoskeleton

The term cytoskeleton is used to denote a system of filamentous intracellular proteins of different shapes and sizes which form a complex often interconnected network throughout the cytoplasm. The cytoskeleton serves such functions as: establishing cell shape, providing mechanical strength, locomotion, chromosome separation in mitosis and meiosis and intracellular transport of organelles. The cytoskeleton is made up of three major kinds of protein filaments: actin filaments, intermediate filaments and microtubules (Auinger & Small, 2008) (Figure 1).

Actin filaments

Actin filaments are well defined filaments with a width of 6-8nm and are the thinnest of the cytoskeletal filaments. Actin filaments form a band just beneath the plasma membrane that provides mechanical strength to the cell, links transmembrane proteins (e.g. cell surface receptors) to cytoplasmic proteins, anchors the centrosomes at opposite poles of the cell during mitosis (Karsenti & Nedelec, 2004), and generates locomotion in cells such as white blood cells and interacts with myosin (thick) filaments in skeletal muscle fibres to provide muscular contraction (Gunst & Zhang, 2008). A wide variety of actin-binding proteins exist and these can modulate the form that actin takes within the cell. Such interactions are fundamental to the structure of the cytoplasm and to cell shape since they regulate cytoplasmic viscosity, connect filaments together in large groups and cause bundles to extend or contract (Gunst & Zhang, 2008). Actin is the main cytoskeletal protein found within dendritic spines, which contributes to the motility and plasticity observed in this structure (Sekino et al, 2007).

Intermediate filaments

Intermediate filaments include a family of protein filaments about 10nm thick, found in different cell types and often present in large numbers where structural strength is needed. There are several types of intermediate filaments, each constructed from one or more proteins characteristic of it:-

Cytokeratins are found in epithelial cells, nuclear **lamins** form a meshwork that stabilises the inner membrane of the nuclear envelope (Gruenbaum et al, 2005), **neurofilaments** strengthen the long axons of neurons and **vimentins** provide mechanical strength to muscle and other cells . Glial fibrillary acid protein and peripherin are two well characterised intermediate filaments; glial fibrillary acid

protein is found abundantly in astrocytes and peripherin is found within peripheral axons in the peripheral nervous system (Perrot et al, 2008). Neurofilaments occur in three different molecular weight groups, some of which are located in the neuronal cell body rather than the axon. Neurofilaments are the most abundant cytoskeletal component of large myelinated axons in the adult central and peripheral nervous system. The disruption to the cytoskeleton of axons due to alterations in neurofilament assembly is observed in the large motor neurons of patients suffering from motor neurone disease (Lee & Cleveland, 1996; Lin & Schlaepfer, 2006)

Microtubules

Microtubules are polymeric fibres with hollow cylinders about 24nm in diameter, and of varying length, some up to 70μm in spermatozoan flagella (Inaba, 2003; Jouannet & Serres, 1998). They are present in most cell types, but particularly abundant in neurons, leucocytes, blood platelets and in the mitotic spindles of dividing cells (Papakonstanti & Stournaras, 2008). Microtubules are polymers of tubulin. There are two major forms of this protein, α- and β-tubulin, which before assembly occur together as dimers (Soifer, 1986) with a combined molecular weight of 100kDa. Microtubules are built by the assembly of both dimers of α and β tubulin, which grow at each end by the polymerization of the tubulin dimers, powered by the hydrolysis of GTP, and shrink at each end by the release of tubulin dimers (depolymerisation) (Beghin et al, 2007; Hammond et al, 2008). Both processes always occur more rapidly at one end, called the plus end, the other less active end is the minus end. Microtubules participate in a wide variety of cell activities, most involving motion. The motion is provided by protein "motors" that use the energy of ATP to move along the microtubule (Hirokawa & Noda, 2008; Kolomeisky & Fisher, 2007). There are two major groups of microtubule motors: kinesins (most of these move towards the

plus end of the microtubule) and dyneins (which move towards the minus end). The rapid transport of organelles, like vesicles and mitochondria, along the axons of neurons takes place along microtubles with their plus ends pointed toward the end of the axon (Caviston & Holzbaur, 2006).One cause of the rare disorder Charcot-Marie-Tooth disease is an inherited mutated gene for one of the kinesins. In these patients, axonal transport is defective (Shy, 2004).

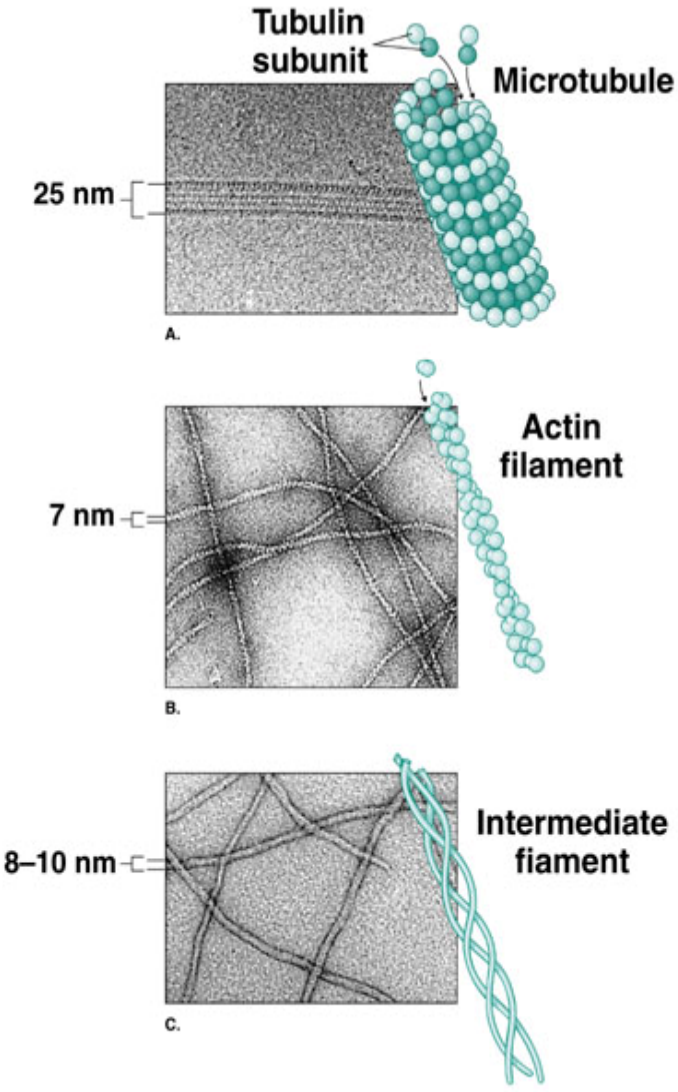

Figure 1. structure of the cytoskeleton. The cytoskeleton consists of three main filament types : (A) Microtubules (B) Actin filaments and (C) Intermediate filaments

5.1.1 Neuronal cytoskeleton

Neurons share many structural features in common with other cells, but they are distinguished by their highly asymmetric shapes and by the existence of dendrites and axons. The cytoskeleton is an important part of a neuron and is a heterogeneous network of filamentous structures which includes microfilaments, neurofilaments and microtubules (Figure 2). The neuronal cytoskeleton is essential for establishing the cells shape and for axonal transport. The axon of a neuron conducts the transmission of action potentials from the cell body to the synapse. The axon also provides a physical conduit for the transport of essential biological materials between the cell body and the synapse that are required for the function and viability of the neuron (Cingolani & Goda, 2008). Disruption of the cytoskeleton within the axon can lead to defects in axonal transport and death of the neuron (Lin & Schlaepfer, 2006), therefore a candidate for examining neurodegenerative mechanisms.

The cytoskeleton of the neuronal dendrite consists of microtubules and microtubule associated proteins, which play a role in maintaining the shape of the dendrite and neuronal transport. Attached to these dendrites are small protrusions called dendritic spines. Actin is the major cytoskeletal protein found within dendritic spines. A compartmentalisation of the cytoskeleton in dendrites occurs, with microtubule proteins limited to the dendritic shaft, whereas actin is concentrated in dendritic spines (Kaech et al, 2001) Many syndromes associated with mental retardation are characterised by cortical dendritic anomalies. Patients suffering from Rett syndrome (Kaufmann et al, 2000), schizophrenia (Benitez-King et al, 2004) and fragile-X syndrome (Zalfa & Bagni, 2004) show a reduction in dendritic arborisation, and a loss of the dendritic microtubule associated protein, MAP-2. Dendritic abnormalities are also observed in Alzheimer's disease (AD), mainly due to the

deposition of hyperphosphorylated microtuble associated protein, tau (Anderton et al, 1998).

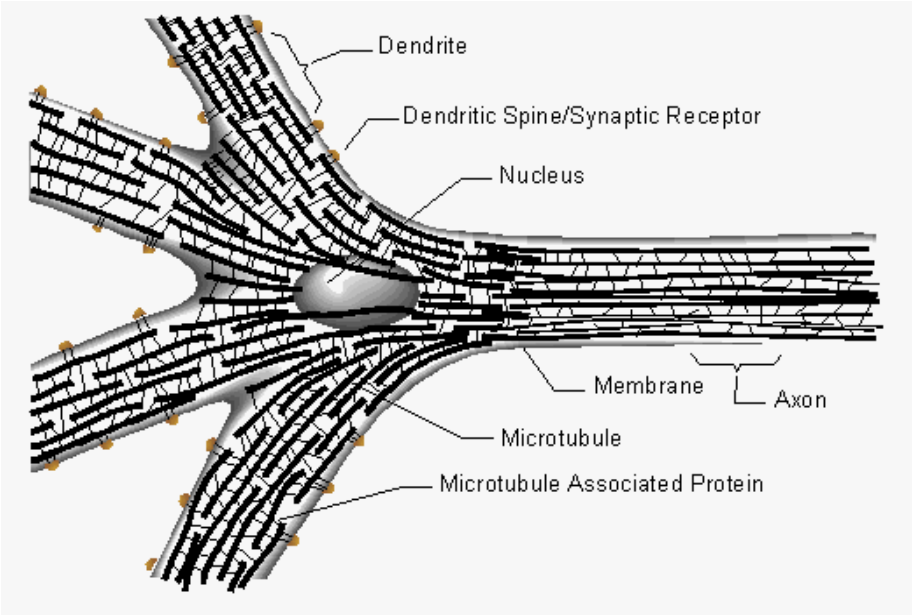

Figure 2. Cytoskeleton of a neuron

5.1.2 Cytoskeletal proteins

Within the cytoplasm or attached to the walls of microtubules are various small proteins that can bind to assembled tubulins, which may be either structural or associated with motility. These proteins are called microtubule associated proteins (MAPs). The MAPs form cross bridges between adjacent microtubules (Figure 2) or between microtubules and other structures such as intermediate filaments, mitochondria and the plasma membrane. MAPs are implicated in various aspects of microtubule biology, including their formation, maintenance and demolition (Moores, 2008).

MAP-2 historically has been perceived primarily as a static, structural protein, necessary along with other cytoskeletal protein to maintain neuroarchitecture. This

protein is in fact quite dynamic and is sensitive to many inputs and has been shown to be involved in the growth, differentiation, and plasticity of neurons, with key roles in neuronal responses to growth factors, neurotransmitters, synaptic activity and neurotoxins (Johnson & Jope, 1992). Its involvement in neurodegeneration will be discussed below.

5.1.3 The cytoskeleton and neurodegeneration

MAP-2

MAP-2 is one of the microtubule associated proteins observed in the mammalian brain, with an important role in neurite outgrowth and in neuronal plasticity. MAP-2 isoforms are split into 2 groups : high molecular weight MAPs (HMWT MAP-2) which includes MAP-2A&B with molecular weights of 280 & 270 kDa, and low molecular weight MAPs (LMWT MAP-2) which includes MAP-2 C&D with molecular weights of 70 &75 kDa (Sanchez et al, 2000). In the central nervous system HMWT MAP-2 is specifically expressed in neurons (Caceres et al, 1984; Huber & Matus, 1984) while LMWT MAP-2 is present in glial cells (Rosser et al, 1997);(Vouyiouklis & Brophy, 1995) HMWT MAP-2 is mainly located in neuronal cell bodies and dendrites where it is associated with microtubules (Caceres et al, 1986). MAP-2 proteins are highly phosphorylated *in vivo*, phosphorylation at distinct sites on the molecule differentially affects MAP-2 function, modulating its interaction with microtubules and its stabilization capacity (Brugg & Matus, 1991; Itoh et al, 1997).

The loss of Map-2 expression, possibly due to the activation of calpain mediated proteolysis, is an early indicator of ischaemia-induced neurodegeneration in several animal models (Ballough et al, 1995; Raley-Susman & Murata, 1995;

Schmidt-Kastner et al, 1998). Cytoskeletal abnormalities involving the disruption of microtubules have also been observed in the hippocampus in schizophrenia. Deficits in MAP-2 and MAP-1 were observed in the hippocampus and entorhinal cortex of brains from schizophrenics compared with controls (Arnold et al, 1991). Abnormal patterns of MAP-2 expression have been observed in neurons of the substantia nigra in Parkinson's disease. MAP-2 co-localises with α-synuclein and ubiquitin in cytoplasmic Lewy bodies of neurons, and has been detected within fibrous aggregates and crystal like structures in neuronal nuclei (D'Andrea et al, 2001). These alterations in MAP-2 morphology and distribution suggest that impaired neuronal transport may be involved in the neuronal loss observed in the brains of patients with Parkinson's disease.

The involvement of MAP-2 in the neuronal cytoskeletal damage observed in TSE diseases has not been well documented. Golgi studies in CJD diseased brains and rodent models of TSE (Hogan et al, 1987), have shown cytoskeletal abnormalities within pyramidal neurons of the cortex, with large varicosities being observed within the dendrites and axons of these neurons (Kim & Manuelidis, 1989; Landis et al, 1981; Machado-Salas, 1986) The involvement of cytoskeletal proteins in the damage observed in these cortical pyramidal neurons has yet to be determined. However the expression levels of MAP-2 has been used successfully to analyse dendritic abnormalities in CA1 neurons in the hippocampus in animal models of HIV (Montgomery et al, 1999), experimental depression (Reines et al, 2004) and chronic hypoxia (Raman et al, 2008). Therefore MAP-2 was used to assess the extent of cytoskeletal disruption within the dendrites of CA1 neurons infected with ME7.

Tau

Tau is a microtubule associated protein that becomes both functionally and structurally altered in several neurodegenerative diseases, collectively known as tauopathies (Williams, 2006). Tauopathies encompass more than 20 clinicopathological entities, including Alzheimer's disease , progressive supranuclear palsy, Pick's disease, and corticobasal degeneration. Common to all these diseases is the deposition of abnormal tau aggregates in the brain (Brandt et al, 2005). Tau is a collection of microtubule associated proteins (MAPs) (Cleveland et al, 1977) expressed from a single gene on chromosome 17 (Andreadis et al, 1992; Neve et al, 1986). In the adult human brain, 6 isoforms ranging between 352 and 441 amino acids in length are produced as a result of alternative RNA splicing (Goedert et al, 1989a; Goedert et al, 1989b). Tau is preferentially found in neurons (Binder et al, 1985; Migheli et al, 1988) but can also be detected in some oligodendrocytes and astrocytes (LoPresti et al, 1995; Migheli et al, 1988; Papasozomenos & Binder, 1987; Tashiro et al, 1997). The normal biological activity of tau, in promoting assembly and stability of microtubles, is regulated by its degree of phosphorylation. In tauopathies, such as AD, tau is abnormally hyperphosphorylated and accumulates with cross-linked microtubules, as intraneuronal tangles of paired helical filaments (Figure 3A). This abnormality is an important process leading to cell death, the severity of which correlates with dementia in AD patients (Iqbal et al, 2005). Pharmacological modulation of tau hyperphosphorylation might represent a valid and feasible therapeutic strategy in tauopathies. Studies designing inhibitors for the most relevant kinases affecting tau hyperphosphorylation – GSK3beta, CDK5 and ERK2 are underway and show much promise (Mazanetz & Fischer, 2007)

The abnormal hyperphosphorylation of tau was observed in the brains of transgenic mice overexpressing bovine PrP. Abnormal tau accumulation was observed in both neurons and glial cells of mice infected with BSE (Bautista et al, 2006). Studies in the 87V/VM scrapie mouse model revealed tau deposition surrounding amyloid plaques observed within the brain (Brion et al, 1987). The deposition of tau within the brain of murine mouse models was predominantly observed in those models where accumulation of PrP^{Sc} was observed in the form of plaques (Figure 3B). In the ME7/CV mouse model in which PrP^{Sc} deposition is mainly observed as the diffuse synaptic type, tau deposition was not prominent. The tau accumulation observed in the BSE mouse model was located in the same areas as PrP deposition, and may be related to the overexpression of PrP in this model. Tau accumulates in dystrophic neurites surrounding amyloid plaques in AD, and has also been identified in neurites surrounding amyloid plaques in human TSEs (Sikorska et al, 2008)

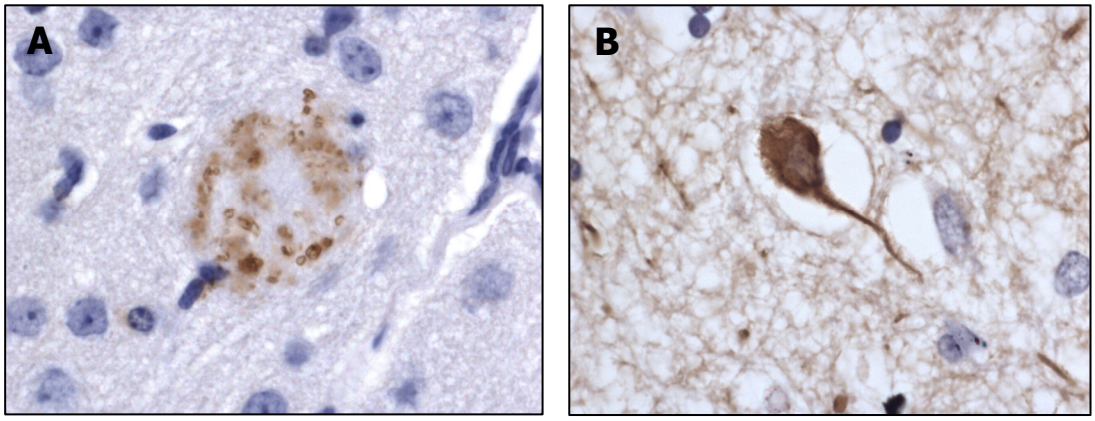

Figure 3. Tau deposition in the 87V/VM scrapie mouse model and an Alzheimer's diseased brain. (A) Tau deposition observed in neurites around an amyloid plaque in the cortex of an 87V infected mouse brain. (B) Tau labeling observed in a neuron from an Alzheimer's patient showing a characteristic neurofibrillary tangle.

5.1.4 The cytoskeleton and TSEs

The association between disruption of the neuronal cytoskeleton and TSE disease is unclear. In two contrasting hippocampal neuronal loss mouse models of TSE : the ME7/CV mouse model where neuronal loss is targeted to the CA1 sector of the hippocampus, and the 87V/VM mouse model where neurodegeneration targets the CA2 sector, cytoskeletal damage was observed. Analysis of Lucifer yellow microinjected CA1 neurons in the ME7 infected hippocampus revealed a loss of dendritic spines early in the incubation period of disease. The Lucifer yellow microinjection technique was an excellent technique to use in order to identify single pyramidal cell neurons within the hippocampus and was used to pick up subtle changes in the morphology of ME7 infected neurons. This technique identified early changes observed in the primary dendrites of scrapie infected neurons. Quantification of confocal images of Lucifer yellow microinjected neurons revealed the initial loss of dendritic spines from primary dendrites infected with ME7 at 109 days post injection, by 126 days 51% of spines are lost (Figure 5&6). By the terminal stage of disease these neurons where grossly altered, losing most if not all of their dendritic spines. Apical and primary dendrites were thin and irregular in shape, contained varicosities and swellings resembling vacuoles (Figure 4B&D) (Belichenko et al, 2000; Brown et al, 2001). In CA2 hippocampal neurons in the 87V/VM model, cytoskeletal abnormalities were observed as early as 70 days of a 320 day incubation period. Dendritic swellings similar to those observed in the CA1 neurons in the ME7/CV model were observed, increasing in numbers by the terminal stage of disease (Jamieson et al, 2001b). Golgi impregnation studies of neurons from the brains of hamsters infected with scrapie (Hogan et al, 1987) and patients suffering from CJD (Landis et al, 1981) revealed similar cytoskeltal abnormalities.

The dendritic spine plays a major role in the cytoskeletal damage observed in TSE infected neurons. In the ME7/CV scrapie mouse model the loss of dendritic spines is the first cytoskeletal abnormality observed within the ME7 infected CA1 neuron.

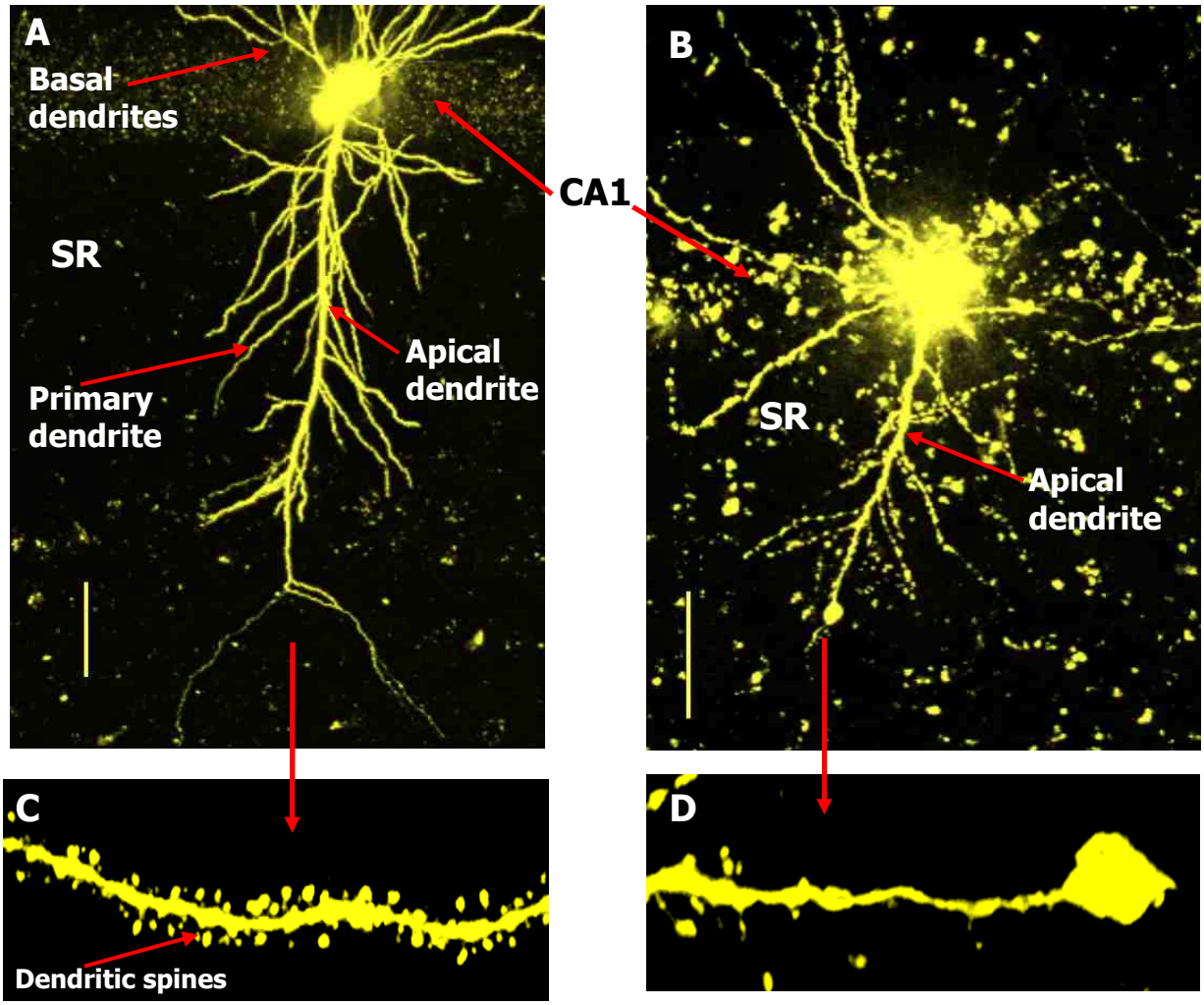

Figure 4. Confocal images of lucifer yellow microinjected CA1 neurons in the hippocampus of a normal brain injected control (A) and a ME7 infected brain (B) at the terminal stage of disease. (A) CA1 pyramidal neuron from a normal brain injected control showing characteristic morphology, long apical dendrite stretching the length of the stratum radiatum (SR), and branching primary dendrites with many dendritic spines (C) The ME7 infected CA1 neurons morphology has changed dramatically. Showing a loss of primary dendrites (B) and dendritic spines from the apical dendrite (D) also observed are large varicosities within the apical shaft and primary dendrites. All images were produced using a Biorad MRC-500 CLSM serial optical scanning (z-series) was performed of all images. (A) & (B) were both taken with an x20 objective and the zoom at 1.5 (C) & (D) were produced using a x60 oil immersion lens and the zoom at 4. Scale bar in (A) = 25µm & (B) = 50µm (Brown et al, 2001).

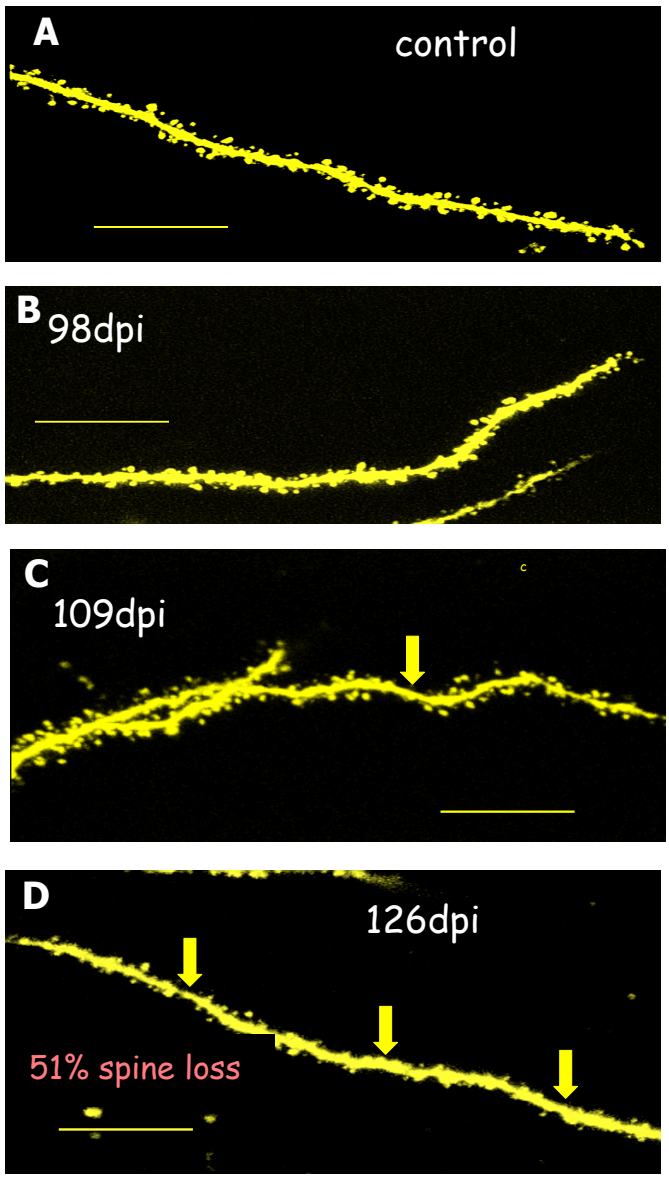

Figure 5. Quantification of dendritic spines Primary dendrites from (A) normal pyramidal cell neuron showing characteristic dendritic spines. (B) ME7 infected pyramidal cell neuron at 98 dpi showing no spine loss looking similar to the control in (A). (C) ME7 infected pyramidal cell neuron at 109dpi showing some gaps with no spines (yellow arrow). (D) ME7 infected pyramidal cell neuron at 126 dpi showing loss of dendritic spines (arrows). Scale bars = 10µm

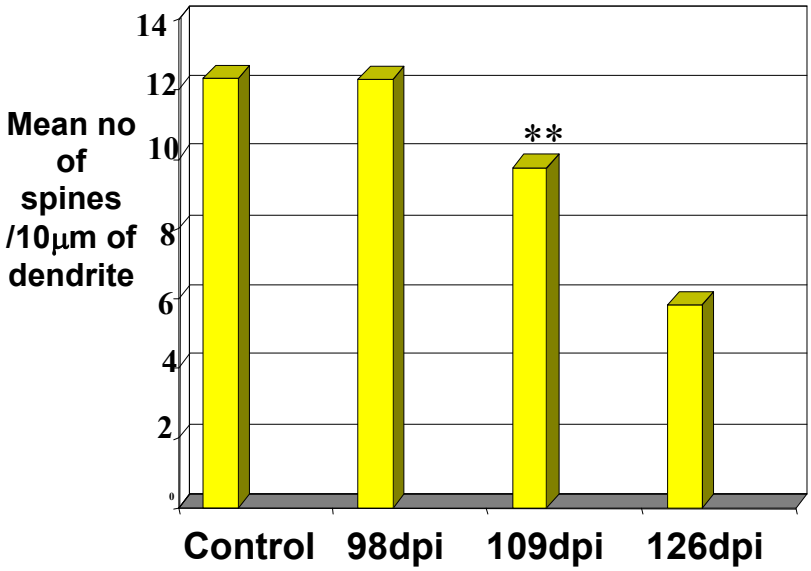

Figure 6. Quantification of dendritic spine loss Bar graph of mean number of spines counted per 10μm of primary dendrite in normal pyramidal cell neurons (control) and ME7 infected pyramidal cell neurons at 98, 109 and 126 dpi. First significant spine loss observed at 109 dpi.

5.1.5 The dendritic spine and the cytoskeleton

Dendritic spines are specialised protrusions from dendritic shafts that receive the vast majority of excitatory input in the central nervous system. Within these spines are neurotransmitter receptors, ion channels, scaffolding proteins, actin cytoskeletal proteins and intracellular signaling molecules (Figure 7). Dendritic spine loss and abnormal spine morphology is observed in many neurological disorders accompanied by cognitive deficits, such as Alzheimer's disease, Down's syndrome, and the fragile-X syndrome (Fiala et al, 2002). Dendritic spines have been proposed as the primary sites of neuronal synaptic plasticity. Actin filaments, which consist of actin molecules and actin-binding proteins, form cytoskeletal networks within dendritic spines and play critical roles in spine maintenance and plasticity. Actin is present in monomeric form (G-actin; globular actin) and a filamentous (F-actin) form in living cells. High

concentrations of F-actin are observed within dendritic spines. The regulation and organization of F-actin is controlled by actin binding proteins. Many actin-binding proteins have been identified in dendritic spines; one of these proteins, drebrin, is thought to be involved in synaptic plasticity (Imamura et al, 1992).

Drebrin is an F-actin binding protein that has a role in regulating assembly and disassembly of actin filaments within the dendritic spine. Drebrin was originally isolated from embryonic chicken brains as developmentally regulated brain proteins that were expressed in the development of neurons (Shirao & Obata, 1985; Shirao & Obata, 1986). There are two major drebrin isoforms, drebrins E and A (Kojima et al, 1988; Shirao et al, 1988). Drebrin E is a ubiquitous isoform, and predominates in the developing brain (Shirao & Obata, 1986), and drebrin A is a neuron-specific isoform, and predominates in the adult brain (Aoki et al, 2005; Kojima et al, 1993). Transfection experiments have demonstrated that drebrin A expressed in mature cultured neurons accumulates spontaneously in dendritic spines (Hayashi & Shirao, 1999). Therefore, the actin cytoskeleton of dendritic spines is distinguished from that of dendritic shafts by its association with drebrin. This phenomenon makes drebrin an ideal protein for analysis of dendritic spines, and the role they may play in the cytoskeletal damage observed in CA1 neurons infected with ME7.

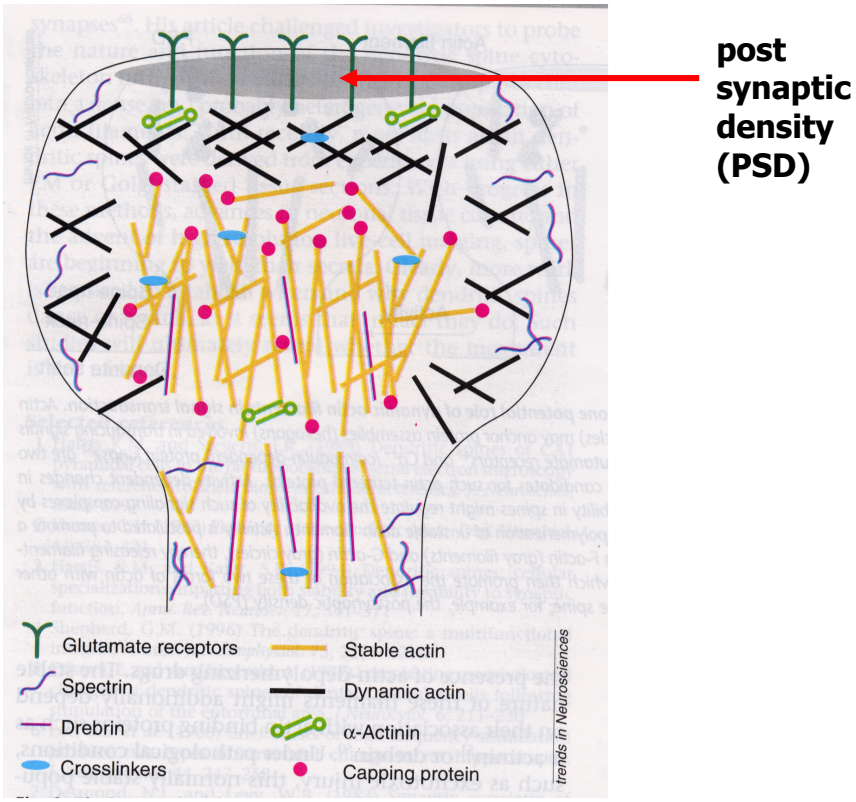

Figure 7. Structure of a dendritic spine. As shown the spine head contains actin and multiple actin binding proteins including spectrin, drebrin and alpha-actinin. The PSD is a compact matrix that lies just beneath the post synaptic membrane, it contains scaffolding molecules i.e. PSD-95 which connect to glutamate receptors and recruit signaling complexes (e.g. protein kinases).

5.2 The Synapse

Synapses are functional connections between neurons, or between neurons and other cell types. A typical neuron gives rise to several thousand synapses, although there are some types that make fewer. Most synapses connect axons to dendrites, but there are also other types of connections, including axon-to-cell-body, axon-axon, and dendrite-to-dendrite. Synapses are generally too small to be recognised using a light microscope, but their cellular elements can be visualised clearly using an electron microscope (Chen et al, 2008) (Figure 8).

Chemical synapses pass information directionally from a pre-synaptic cell to a post-synaptic cell and are therefore asymmetric in structure and function. The pre-synaptic terminal, or synaptic bouton, is a specialised area within the axon of the pre-synaptic cell that contains neurotransmitters enclosed in small membrane-bound spheres called synaptic vesicles (Triller & Choquet, 2008). Synaptic vesicles are docked at the pre-synaptic plasma membrane at regions called active zones. Immediately opposite is a region of the postsynaptic cell containing neurotransmitter receptors; for synapses between two neurons the postsynaptic region may be found on the dendrites or cell body. Behind the postsynaptic membrane is an elaborate complex of interlinked proteins called the postsynaptic density (PSD) (Okabe, 2007) (Figure 9)

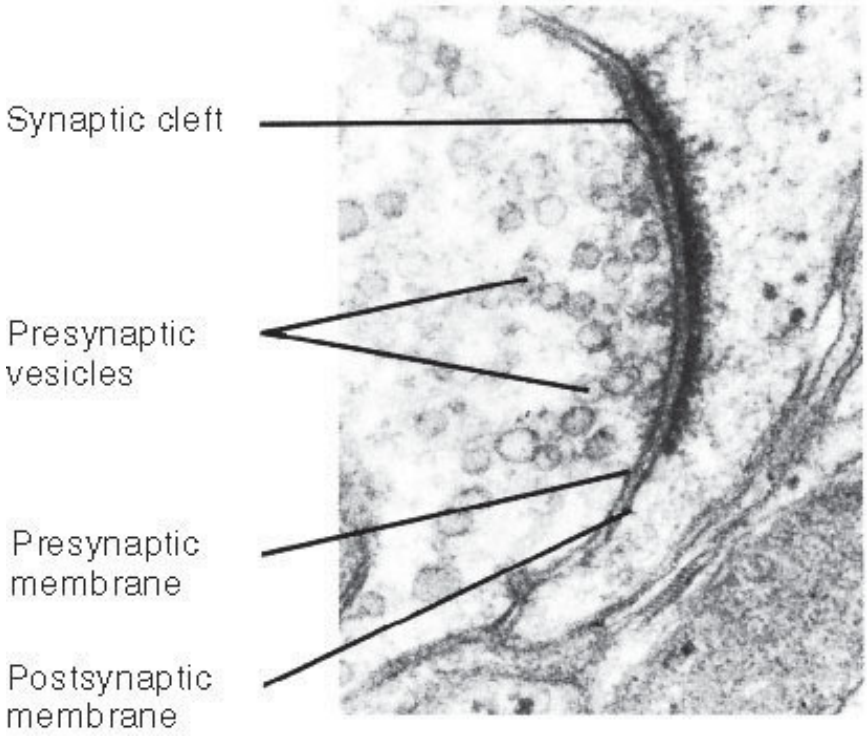

Figure 8. Electron micrograph image of a synapse

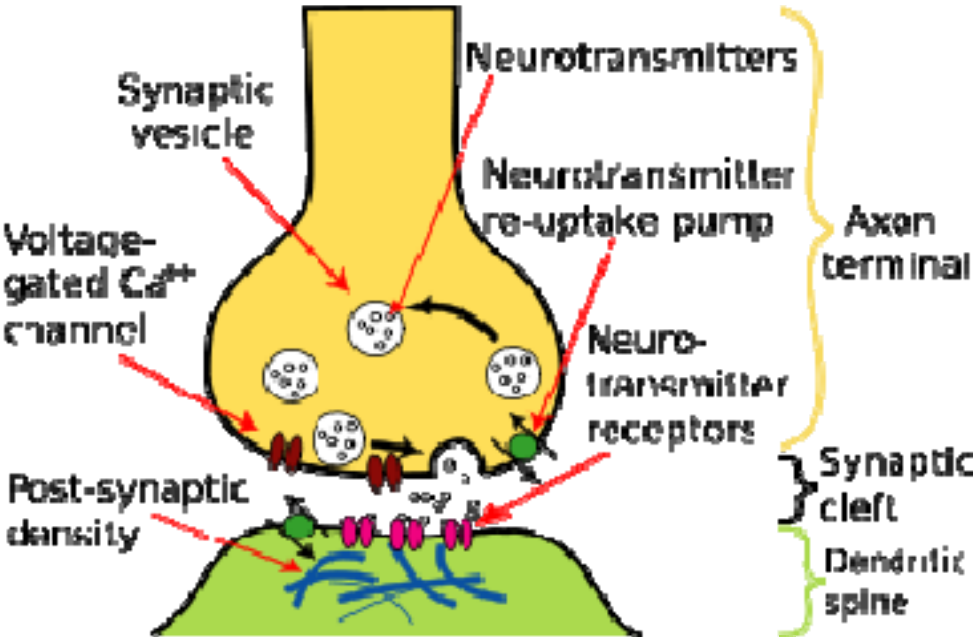

Figure 9. Post- and pre-synaptic structure of a synapse

5.2.1. Synapse loss and TSEs

Synapses appear to be primary pathological targets in TSE disease. Abnormal PrP accumulates in synaptic regions, and preclinical synaptic degeneration has been observed in the brains of patients suffering from CJD (Clinton et al, 1993; Kitamoto et al, 1992) and in mouse models of disease (Jeffrey et al, 2000; Siso et al, 2002).In a mouse model similar to the one used in this study a reduction in pre-synaptic synaptophysin levels correlates with disruptions in neurally driven behaviours such as burrowing and nesting (Cunningham et al, 2003), demonstrating the functional importance of synapse loss for the development of behavioural symptoms in TSE disease.

In an electron microscopic study in the ME7/CV mouse model, synapse loss is observed in the CA1 neurons of the hippocampus from 84 dpi approximately 80 days before the loss of these neurons (Jeffrey et al, 2000) . Prior to this synapse loss is the deposition of abnormal PrP in the stratum radiatum of the hippocampus. In both these mouse models synaptic deficits precede the appearance of gross neuronal degeneration by several weeks, suggesting that synapse loss may be the fundamental lesion in TSE disease. This hypothesis is supported by the experiments attempting to alleviate neurological symptoms in the Tg(PG14) transgenic mouse model of inherited TSE disease through deletion of the pro-apoptotic factor Bax (Chiesa et al, 2005). These mice develop a progressive neurological disorder characterised by ataxia and cerebellar atrophy, with massive apoptotic degeneration of granule neurons. Bax deletion rescued cerebellar granule neurons from apoptosis, but the onset and severity of neurological symptoms were not altered. Quantification of the numbers of synaptophysin positive synaptic endings in the cerebellum showed that synapse loss proceeds even when apoptotic pathways in the rest of the neuron are blocked.

The trigger for the synaptic loss and subsequent neuronal loss observed in the ME7/CV mouse model appears to be the deposition of PrP^{Sc}. However ultrastructural studies analysing the subcellular accumulation of PrP^{Sc} has found no evidence for PrP^{Sc} deposition at synaptic junctions or in synaptic vesicles (Godsave et al, 2008), therefore it appears unlikely that PrP^{Sc} acts directly on synapses. Increasing evidence suggests that oligomeric forms of PrP^{Sc} are those that are likely to be more neurotoxic (Sokolowski et al, 2003) (Baskakov et al, 2002; Baskakov et al, 2001; Simoneau et al, 2007), although little is known about the subcellular location of these oligomeric forms.

5.3 Aims of Chapter

The principal aims of the work in this chapter are to investigate the role of the neuronal cytoskeleton and synaptic changes in the loss of CA1 neurons in the ME7 infected hippocampus.

In the study performed here using the ME7/CV scrapie mouse model the role that the pre- and post-synaptic elements of the synapse play in the synaptic loss observed in CA1 neurons will be analysed and related to the cytoskeletal damage observed in these neurons.

The expression of pre-synaptic protein synaptophysin and post-synaptic protein PSD-95 will be analysed throughout the incubation period of disease.

The cytoskeletal changes observed within both the dendrite and dendritic spines of CA1 sector neurons in the hippocampus will be compared. MAP-2 and alpha tubulin expression, cytoskeletal proteins found within the dendrites of CA1 neurons, will be analysed throughout the incubation period of disease and compared with the expression of drebrin an F-actin binding protein observed only within dendritic spines.

Specific aims

- To analyse the expression of dendritic cytoskeletal proteins tubulin and MAP-2 in the CA1 sector (ME7) and CA2 sector (87V) neurons of the hippocampus at the terminal stage of disease.
- To identify at which time point in the disease progression in the ME7/CV scrapie mouse model changes in the expression of MAP-2 first appear.
- To analyse and compare the expression of drebrin (dendritic spine protein) and tubulin (dendrite protein) in the CA1 sector neurons of the ME7 infected hippocampus throughout the course of the disease.
- To analyse the expression of pre- and post-synaptic proteins synaptophysin and PSD-95.

5.4 Materials and methods

Initial studies analysing the cytoskeletal proteins MAP-2 and alpha tubulin were performed on terminally infected animals from both the ME7/CV and 87V/VM scrapie mouse models (see chapter 1 for description of models). Further studies concentrated on the ME7/CV scrapie mouse model and the role of the cytoskeleton in the loss of CA1 sector neurons in this model.

5.4.1 Immunohistochemical labelling of cytoskeletal proteins

MAP-2 a+b

Immunohistochemical labelling of microtubule associated protein 2 (MAP 2) was performed using an antibody raised to MAP2 a+b. This antibody specifically labels dendrites and soma of neurons and was used to analyse cytoskeletal changes in both the pyramidal neurons of the CA1 (ME7) and the CA2 (87V) sectors of the

hippocampus. Initially this antibody was used on brains from mice at the terminal stage of disease in both mouse models at the suggested concentration (1μg/ml) on the data sheet. Labelling worked well at this concentration therefore the time course study was performed at the same concentration.

Tubulin

Microtubules consist of subunits of alpha and beta tubulin. Initially immunolabelling for both the α and β forms of tubulin was performed on mouse brains from animals at the terminal stage of disease. On analysis of this immunolabelling β tubulin did not label the dendrites of the hippocampal pyramidal neurons and therefore was not used in these studies. Alpha tubulin was used to immunolabel the dendrites of both CA1(ME7) and CA2 (87V) sector pyramidal neurons. The antibody was used successfully at the concentration suggested on the data sheet (2μg/ml). Alpha tubulin labelling was not performed on the ME7 time course series as it gave similar results to the MAP2 immunolabelling.

Drebrin

Ideally the drebrin antibody used in these studies should have been raised to the neuron specific form of drebrin, drebrin A. Unfortunately no commercially produced antibodies are available that recognise only the A form of drebin, therefore an antibody raised to both the neuron specific (A) and embryonic forms (E) was used. This antibody was chosen from MBL international corporation as it had been used successfully in studies analysing human Alzheimer cases (Shim & Lubec, 2002). Initial trials with this antibody were performed on sections from mice at the terminal stage of disease, both ME7 and normal brain controls were analysed. The antibody worked well at the suggested concentration of 10μg/ml on the data sheet therefore labelling of the time course study was performed at this concentration.

5.4.2 Western blot analysis of Tubulin, Drebrin, PSD-95 and synaptophysin

Western blot analysis of Drebrin was performed with the same antibody as that used for the immunohistochemistry (see above and appendix 2 list 2.2). Drebrin was used at 10μg/ml overnight at 4^{o}C. Expression of Drebrin was reduced at 160dpi ME7 confirming the IHC results.

Western blot analysis of alpha tubulin was performed with the same antibody used for IHC. This protein was also used as a loading control for both the cytoskeletal and synapse proteins.

The antibodies used for western blot anlaysis of synaptophysin and PSD-95 where purchased from synaptic systems. Initially the PSD-95 antibody used for the IHC (Abcam) was used in western blot analysis but did not give good results. The antibody from synaptic systems was successfully used at the concentration suggested on the data sheet. The synaptophysin antibody worked well at the suggested concentration on the data sheet (see appendix 2 list 2.2 for western blot technique and antibody concentrations).

5.5 Results - Cytoskeleton

5.5.1 Decrease in MAP2 labelling was observed in the CA2 of the hippocampus in 87V infected scrapie brains and in the CA1 of the hippocampus in the ME7 infected scrapie brains at the terminal stage of disease.

The microtubule associated protein, MAP-2 functions as a stabiliser of microtubules within the neuronal cytoskeleton. MAP-2 a and b are the predominant types found within the dendrites and soma of neurons.

MAP-2 a and b expression was decreased in both the CA2 neurons of the 87V infected hippocampus and the CA1 neurons of the ME7 infected hippocampus (Figure 10 C&D). Total loss of this cytoskeletal protein was observed in the CA2 sector of the 87V infected hippocampus, but in the ME7 infected hippocampus MAP-2 expression was still observed in the few damaged CA1 neurons surviving (Figure 10D).

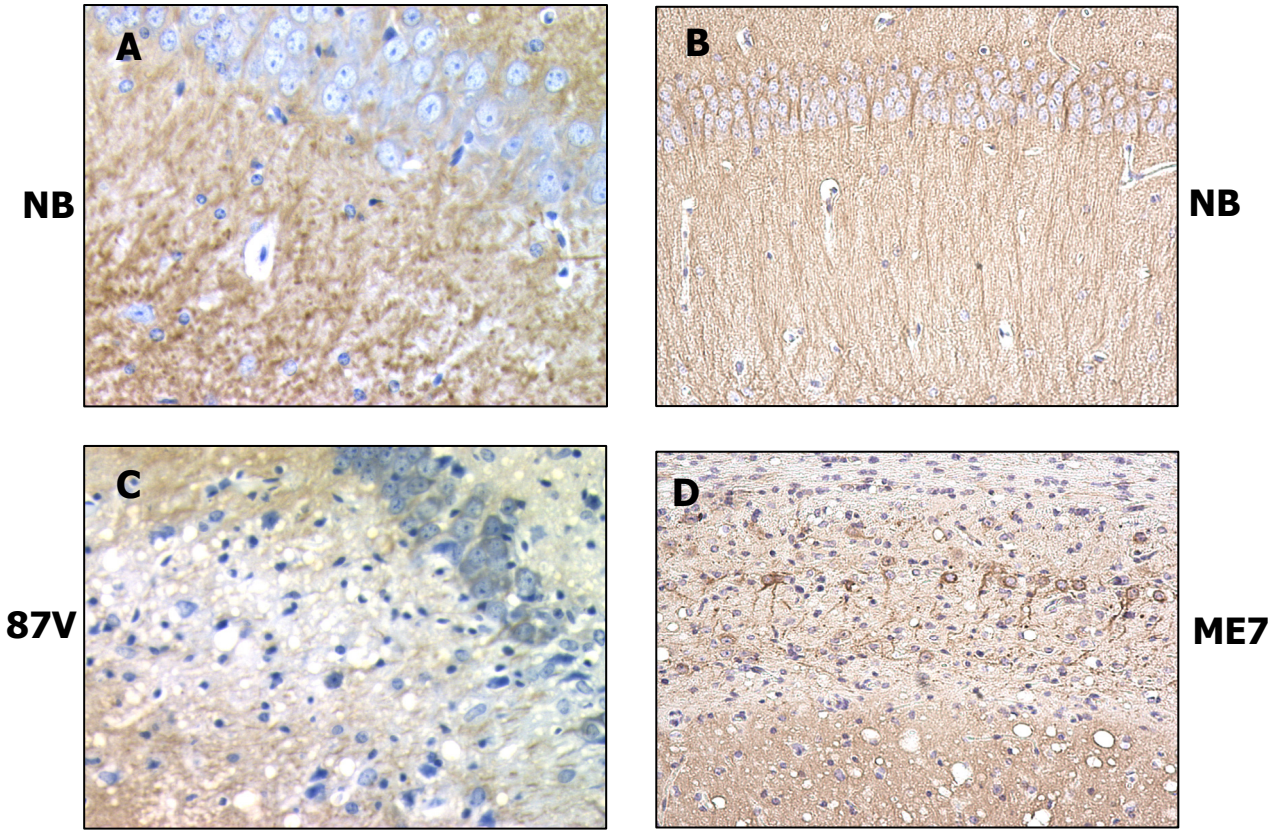

Figure 10. MAP-2 a and b expression in the 87V/VM and ME7/CV scrapie mouse models at the terminal stage of disease. (A) Normal brain VM control mouse showing expression of MAP-2 in the CA2 neurons of the hippocampus and (C) Loss of MAP-2 expression observed in the 87V infected CA2 neurons. (B) CA1 neurons from a normal brain CV control showing MAP-2 expression in the dendrites of these neurons, and (D) Loss of MAP-2 expression in the ME7 infected CA1 neurons. Note the marked neuronal loss also observed in the CA1 sector. Magnifications (A)&(C) x40, (B)&(D) x20

5.5.2. Decrease in tubulin expression observed in both the ME7 infected CA1 neurons and the 87V infected CA2 neurons

Within the cytoskeleton microtubles consist of subunits of both α and β tubulin. To determine the role that tubulin may play in the cytoskeletal disruption observed in both the CA1 (ME7) and CA2 (87V) neurons in the hippocampus, α tubulin expression was analysed. Alpha tubulin expression was decreased in both the CA1 (ME7) (Figure 11C) and the CA2 (87V) (Figure 11D) neurons of the scrapie infected hippocampus. The morphology of the CA1 neurons infected with ME7 looks similar to those injected with lucifer yellow (Figure 5B), showing shrinkage and contortion of the apical dendrites. In the 87V infected CA2 neurons total loss of tubulin is observed in the stratum radiatum, with a loss of apical dendrites, similar to the results obtained labelling these neurons with MAP-2 (Figure 10C).

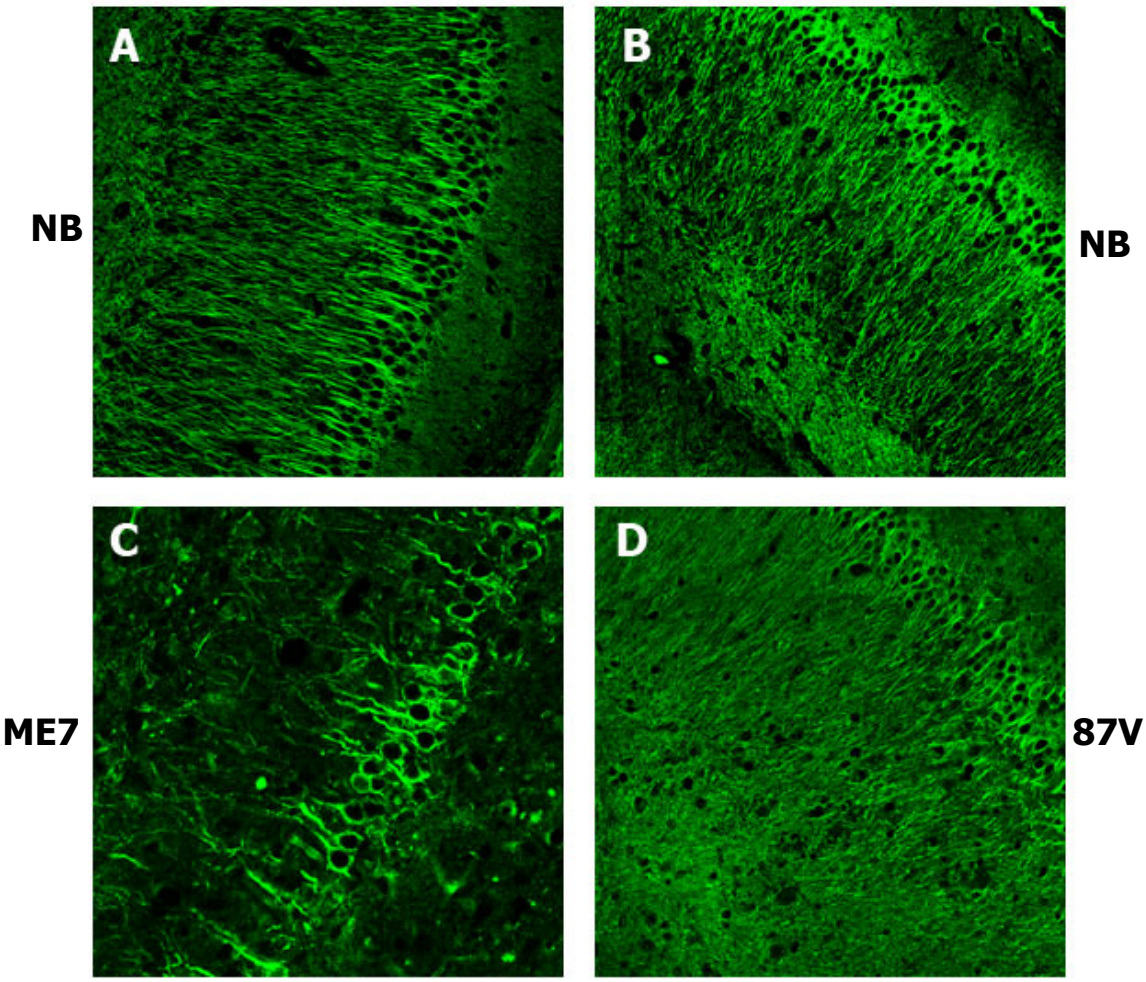

Figure 11. Alpha tubulin expression observed in the CA1 (ME7/CV model) and CA2 (87V/VM model) of the hippocampus. (A) CA1 of a normal brain infected CV control showing expression of alpha tubulin within dendrites of the CA1 neurons. (C) ME7 infected CV brain demonstrating loss of alpha tubulin expression and shrinkage of apical dendrites within the CA1 of the hippocampus. (B) CA2 of a normal brain infected VM control showing alpha tubulin expression in the dendrites of CA2 neurons. (D) 87V infected VM brain showing loss of alpha tubulin expression in the dendrites of the CA2 neurons. Magnification x60 oil immersion

5.5.3 MAP-2 expression is decreased in CA1 neurons of the hippocampus from 160dpi ME7 infection.

The results observed analysing both dendritic proteins MAP-2 and alpha tubulin were similar, therefore Map-2 was used as a marker to analyse the dendritic changes in the ME7 infected neurons throughout the course of disease.

A time course study of the expression of MAP-2a+b in CA1 sector neurons in the ME7 infected hippocampus was performed. MAP-2a+b is expressed in both the soma and dendrites of neurons and was used to analyse the involvement of microtubles in the cytoskeletal damage observed in the dendrites of ME7 infected CA1 sector neurons (Figure 5B&D). A decrease in MAP2a+b expression was observed from 160dpi in the ME7 infected hippocampus (Figure 12D), this loss increased with the extent of neuronal loss observed in the hippocampus. By the terminal stage of disease, where there is marked neuronal loss observed in the CA1 cell layer, almost total loss of MAP-2a+b expression is observed (Figure 12 F)

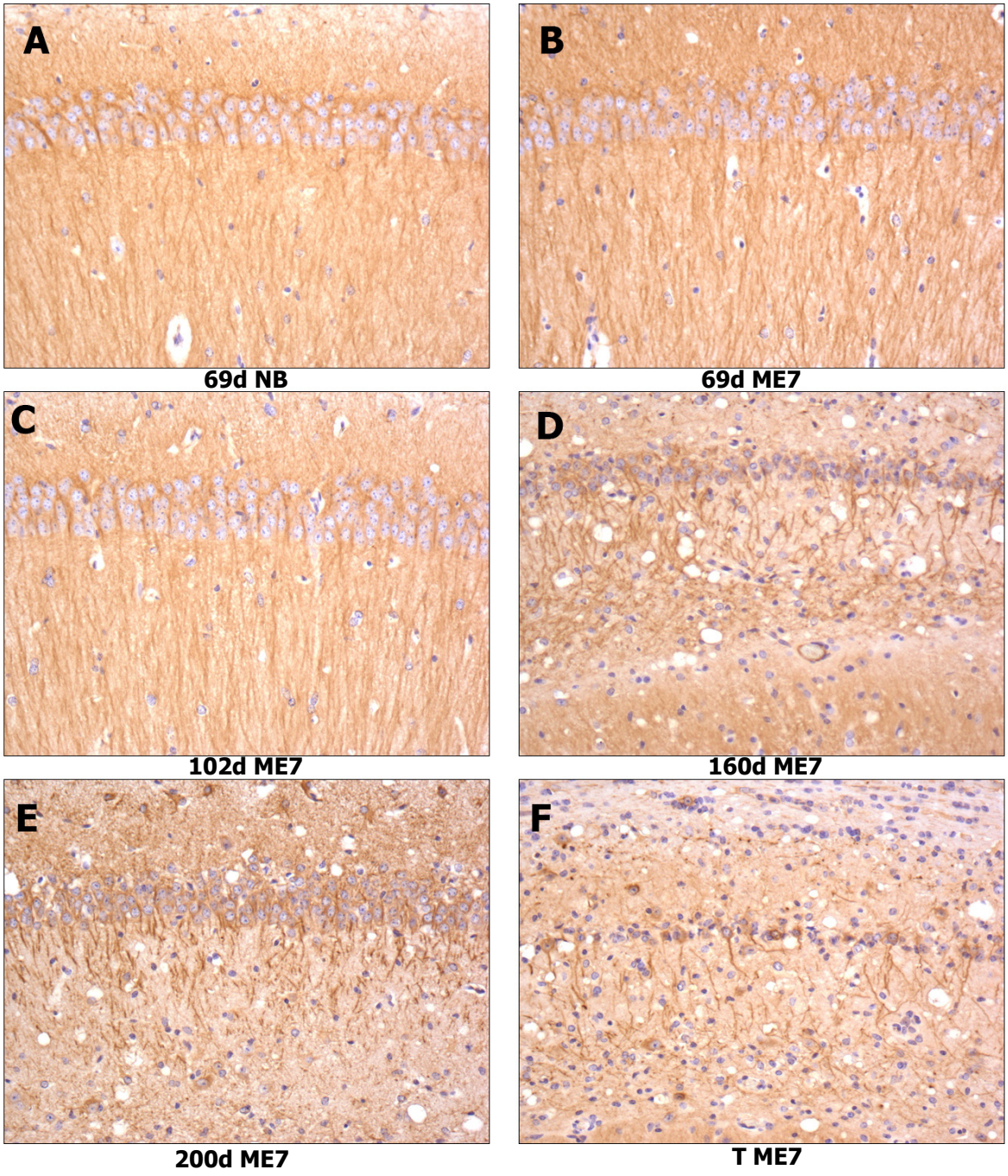

Figure 12. Time course study of MAP-2 expression in the hippocampus of the ME7/CV scrapie mouse model. Dendritic MAP-2 expression observed in the CA1 sector of the hippocampus in (A) 69dpi NB (B) 69dpi ME7 and (C) 102dpi ME7. Disruption and loss of MAP-2 expression observed in (D) 160dpi ME7, (E) 200dpi ME7 and (F) ME7 terminal. MAP-2 expression decreases with the loss of CA1 neurons.

5.5.4 Immunohistochemical analysis of drebrin expression revealed a decrease in the ME7 infected hippocampus from 160 dpi.

A time course study of the expression of drebrin in CA1 neurons in the ME7 infected hippocampus was performed. Drebrin is an F-actin binding protein that is expressed within the dendritic spines of neurons. Immunohistochemistry was used to analyse the role of the dendritic spine in the cytoskeletal damage observed in the ME7 infected CA1 sector neurons of the hippocampus. Any changes observed will be compared with the results analysing the dendritic proteins Map-2 and tubulin. Drebrin expression was decreased in the CA1 sector neurons of the hippocampus from 160dpi., although the loss of expression of this protein was variable at this time point and correlates with the extent of neuronal loss observed in the CA1 sector. This loss was specifically targeted to the CA1 of the hippocampus, slight loss was observed in the CA3 sector mossy fibres (Figure 13C). By the terminal stage of disease total loss of drebrin expression was observed in both the CA1 and CA3 sectors of the hippocampus (Figure 13D), partial loss of drebrin expression was observed in the CA2 sector (Figure 14B) with no loss of expression in the dentate gyrus (Figure 14C). The loss of drebrin correlates with the neuronal loss observed in the CA1 sector of the hippocampus.

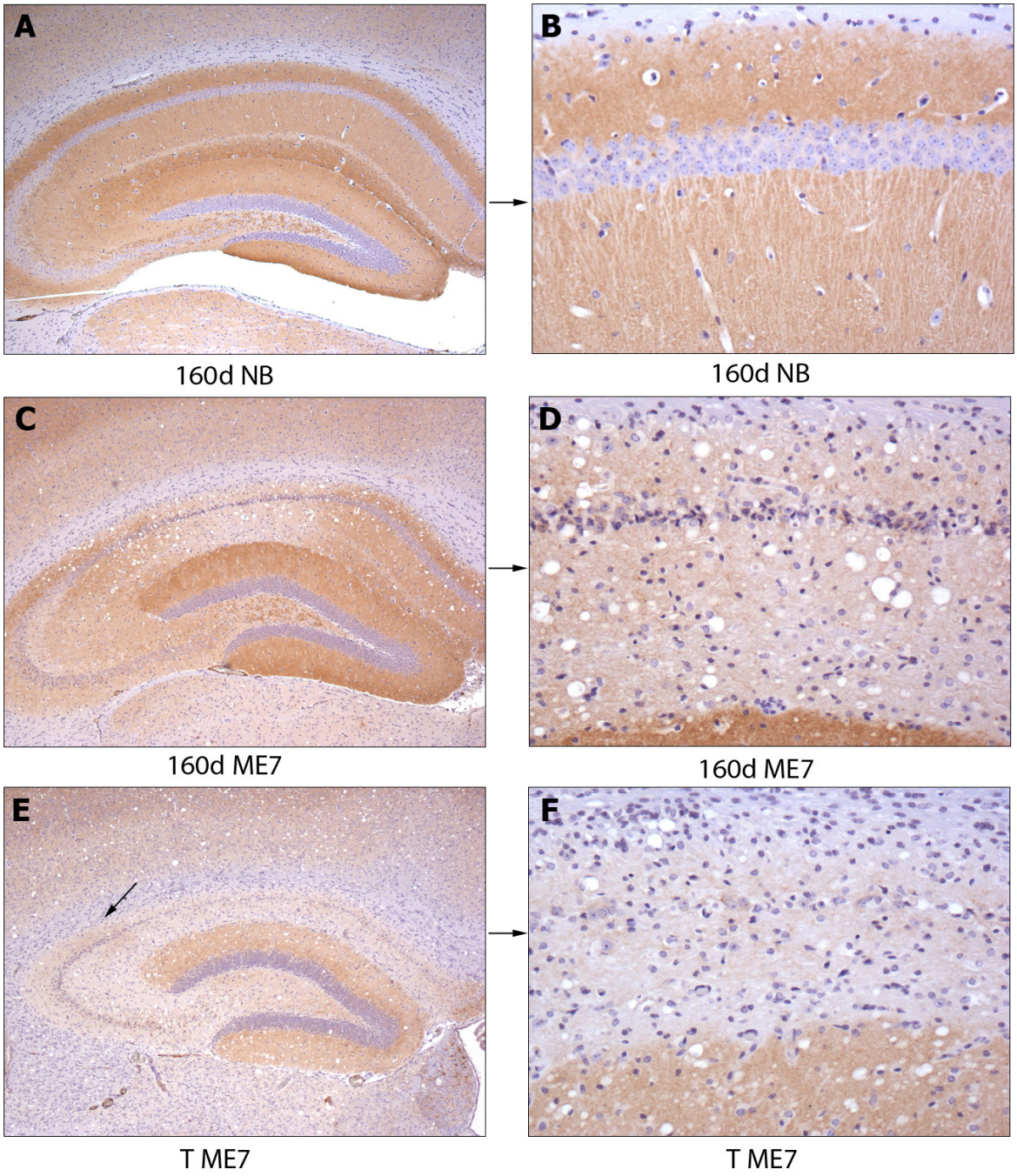

Figure 13. Drebrin immunolabelling in the hippocampus (A) normal brain (NB) control showing widespread labelling throughout the hippocampus. (B) CA1 from NB control widespread labelling observed in the stratum oriens and stratum radiatum of the hippocampus. (C) 160dpi ME7 infected hippocampus showing loss of drebrin labelling in the CA1 sector of the hippocampus. (D) 160dpi CA1 of the hippocampus showing almost total loss of drebrin labelling. (E) ME7 infected hippocampus at the terminal stage of disease showing total loss of drebrin labelling in the CA1 and CA3 sectors of the hippocampus. Intense drebrin labelling still observed in the dentate gyrus of the hippocampus, and in the CA2 sector of the hippocampus (arrow) (see Figure 9). Magnification A,C&E x4 B,D&F x20

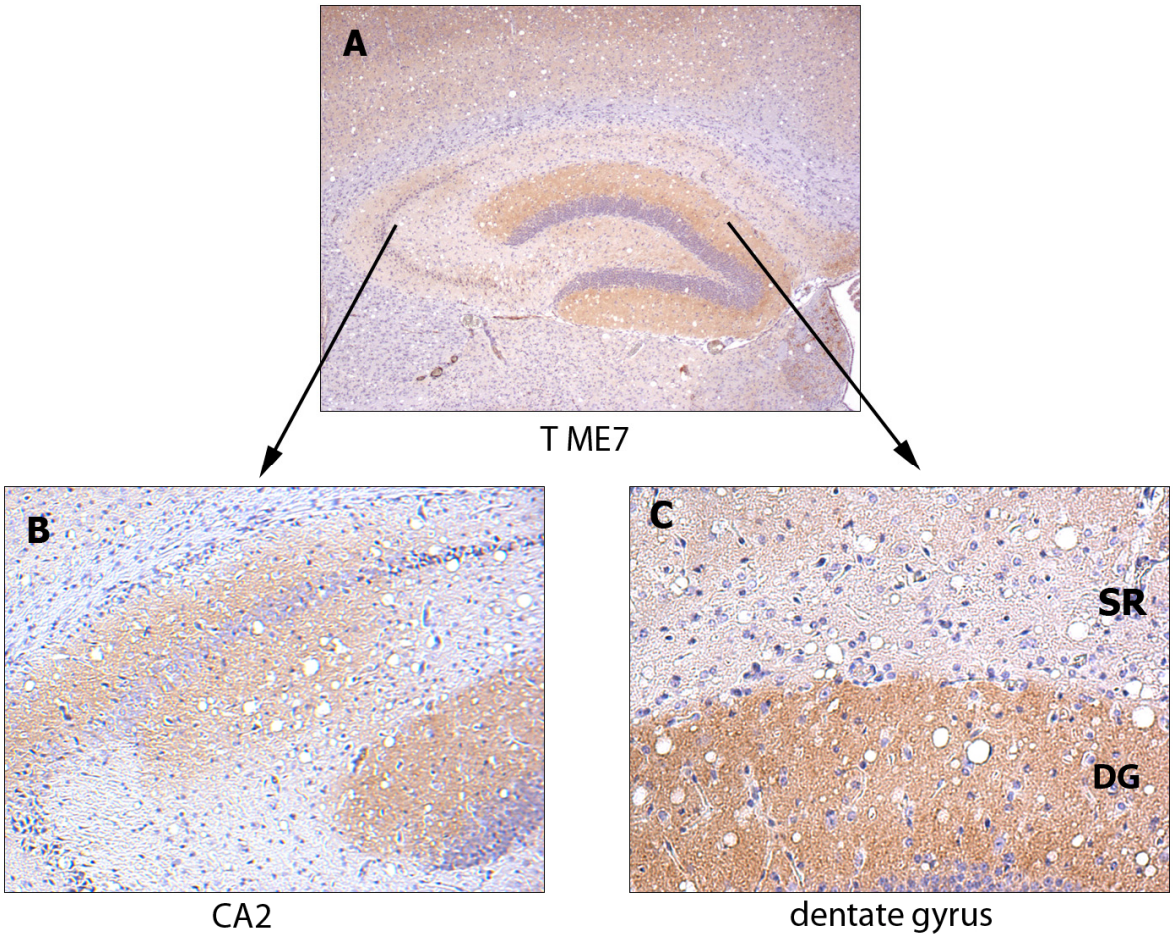

Figure 14. Drebrin immunolabelling in the CA2 and the dentate gyrus (DG) of the ME7 infected hippocampus at the terminal stage of disease (A) drebrin labelling in the ME7 infected hippocampus at the terminal stage of disease, intense labelling still observed in the DG with partial loss in the CA2 sector. (B) drebrin labelling in the CA2 sector of the hippocampus. (C) intense drebrin labelling in the DG, no labelling observed in the stratum radiatum (SR) of the CA1 sector. Magnification A x4, B x20, C x40

5.5.5 Western blot analysis of drebrin, alpha tubulin and PSD-95 expression in the ME7 infected hippocampus revealed a loss of drebrin from 160dpi but no difference in the expression of both alpha tubulin and PSD-95

The antibody used to detect drebrin expression recognises both the embryonic (E) (116 kDa) and the adult (A) (125kDa) form of the protein. In the hippocampus of the developing rat brain drebrin E expression gradually decreased and was not detected in adulthood (Aoki et al, 2005) In the ME7/CV mouse model drebrin E expression disappeared from 160dpi in both the normal and ME7 infected hippocampus, mice in this study were injected at 12 weeks of age therefore the embryonic form disappeared in the mouse hippocampus at 244 days of age. Surprisingly a faint band of drebrin E expression was observed in all four of the aged matched terminal normal brains at 324 days old. Western blot analysis of the expression of the dendritic spine protein, drebrin, revealed loss of this protein from 160 dpi. (Figure 15D). Semi-quantitative densitometry analysis confirmed this loss (Figure 17). At the 160dpi time point only one of the two infected samples showed a significant decrease in drebrin levels in comparison to the normal brain control, therefore more samples will have to be assessed at this time point in order to check the significance of this result. The results observed here in the western blot analysis correlates with the immunohistochemical results in Figure 13.

No differences where observed in the expression of both alpha tubulin and PSD-95 throughout the incubation period of disease. The expression of alpha tubulin assessed by western blot was constant throughout (Figure 15), this did not correlate with the IHC results which revealed loss of alpha tubulin in the CA1 neurons at the terminal stage of disease (Figure 11C). Western blot analysis of synatophysin was not performed on hippocampal lysates from the time series as no difference was observed at the terminal stages of disease using this method and immunohistochemical analysis was the preferred method used to analyse this protein. In light of the results obtained analysing PSD-95,

this would also seem to be the case for this protein. Western blot analysis was not the preferred method of choice to analyse subtle changes in alpha tubulin, synaptophysin and PSD-95 expression. Immunohistochemistry did reveal subtle changes in these proteins that was not observed using western blot analysis (Figure 11, 18 & 19).

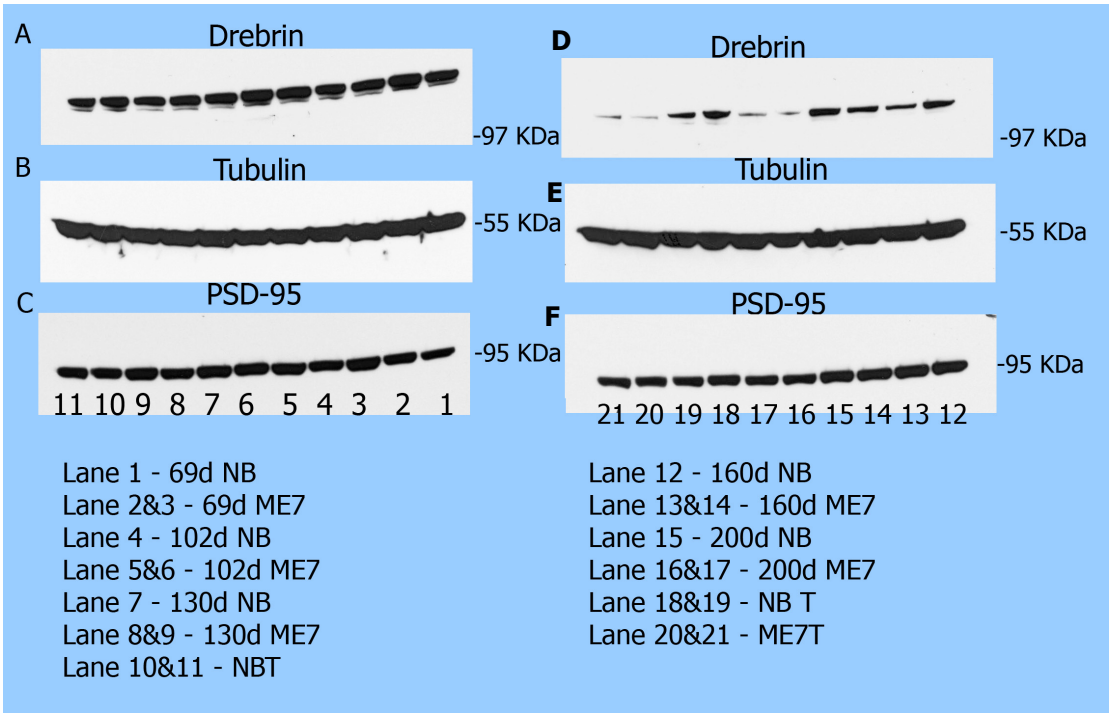

Figure 15. Western blot analysis of Drebrin, Tubulin and PSD-95 on ME7 time series. Time course study of drebrin, tubulin and PSD-95 in dissected hippocampi from normal (NB) and ME7 infected brains. One normal and two infected brains analysed at each time point. (A)&(D) Drebrin expression observed in ME7 time series, top band = drebrin A (125KDa), bottom band = drebrin E (116 KDa). Both bands expressed in infected and controls brains in blot (A) expression of bottom band, embryonic form of drebrin, lost in all samples except NB terminals in blot (D) Expression of drebrin A decreased from 160dpi ME7 infection (D), (B)&(E) No difference in alpha tubulin expression observed throughout the time series. (C)&(F) No difference in PSD-95 expression observed throughout the time series.

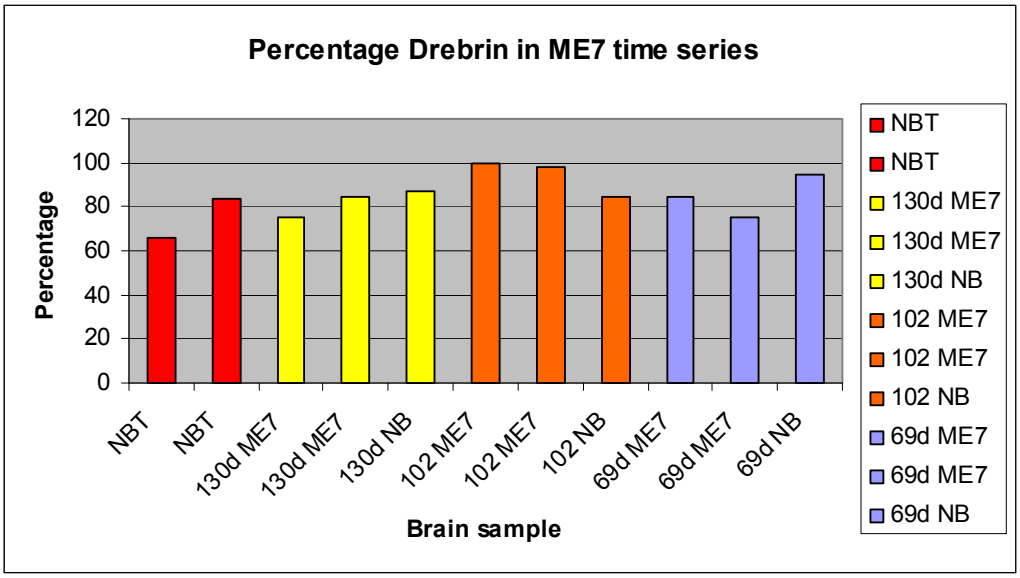

Figure 16. Semi-quantification of percentage drebrin A expression from lanes 1-11 in figure 12 calculated using densitometry. Percentage expression of each band measured as a percentage of the thickest band on the gel (102d ME7 lane 6). No significant difference observed in drebrin expression in the infected samples.

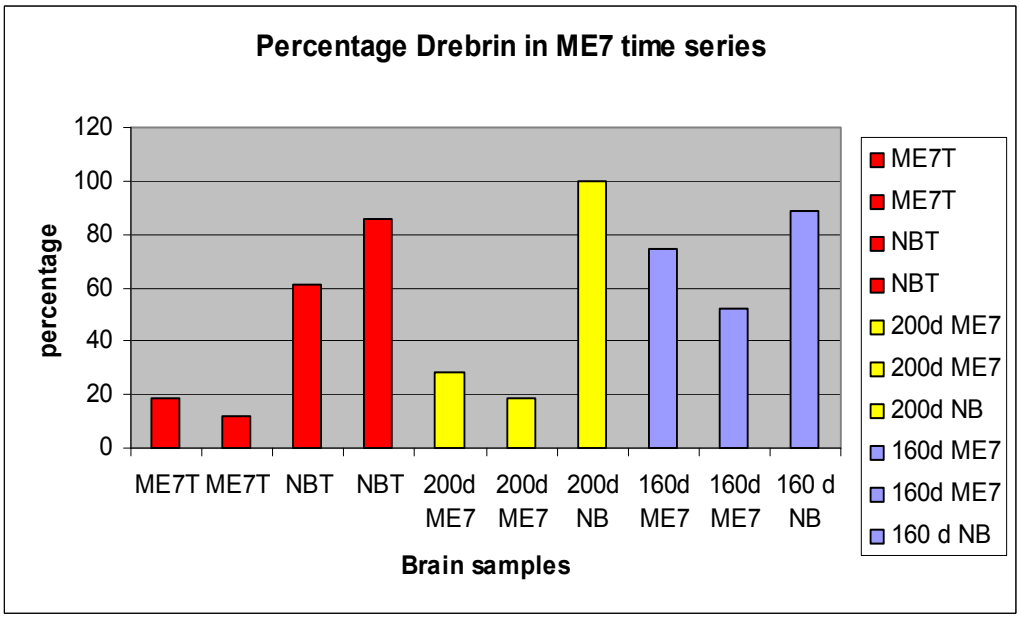

Figure 17. Semi-quantification of percentage drebrin A expression from lanes 12-21 in figure 12 calculated using densitometry. Percentage expression of each band measured as a percentage of the thickest band on the gel (200d NB lane 4). First difference was observed in one sample at 160dpi and showing a dramatic decrease from 200dpi.

5.6 Results – synapse loss

5.6.1. Loss of intensity of synaptophysin observed from 200dpi ME7

A time course study of the expression of synaptophysin in CA1 sector neurons in the ME7 infected hippocampus was performed. Synaptophysin is a synaptic protein found within pre-synaptic terminals. This marker was used to assess the role of the pre-synaptic synapse in the synapse loss observed in the ME7 infected CA1 sector neurons. Deposition of synaptophysin was observed in the ME7 infected hippocampus throughout the incubation period of disease (Figure 18). The distribution of this protein was altered in the ME7 infected brain at 160dpi (Figure 18 D) in comparison to the 102 dpi (Figure 18C), although the intensity of the staining in both brains was similar. The intensity of synaptophysin expression decreased from 200dpi (Figure 18E), although the distribution stayed the same as that observed in the 160day infected brain. By the terminal stage of disease an obvious decrease in intensity can be observed (Figure 18F). Despite this change, there is still a marked labelling of synaptophysin observed in the stratum radiatum of the hippocampus at the end stage of disease (Figure 18F).

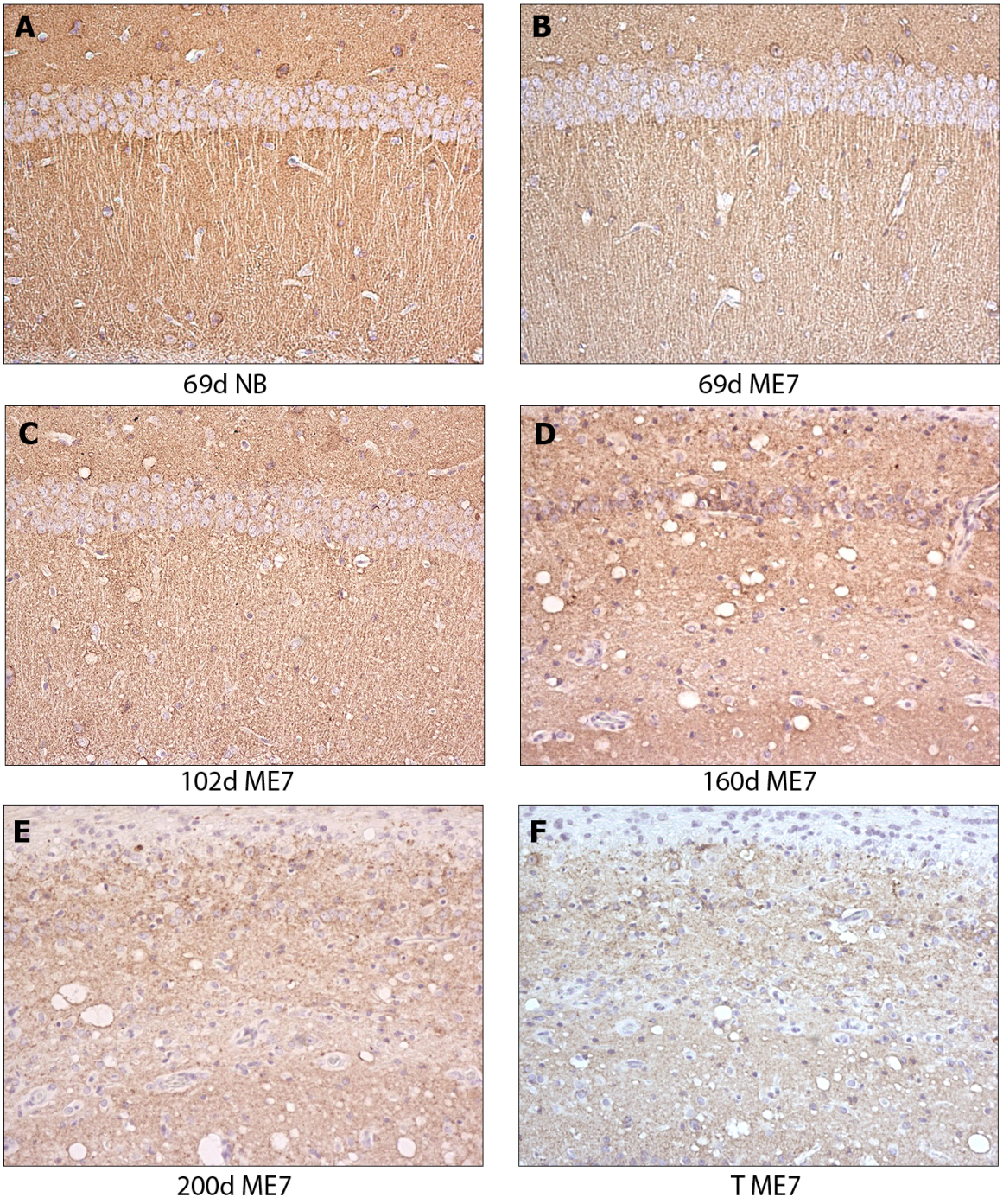

Figure 18. Time series study of synaptophysin labelling in the hippocampus of the ME7/CV scrapie mouse model. No difference in synaptophysin labelling observed from 69 dpi to 130dpi (A) CA1 sector of the hippocampus in a 69dpi NB injected animal and (B) a 69dpi ME7 infected animal.(C)102 dpi ME7 infected animal. (D). Intensity of labelling decreased by 200dpi (E) and by the terminal stage of disease (F). Magnification x20

5.6.2 Loss of intensity of PSD-95 labelling observed in the CA1,CA2 and CA3 sectors of the hippocampus at the terminal stage of disease.

In order to compare the pre- and post-synaptic density a time course study of the expression of post synaptic density -95 (PSD-95) protein in CA1 neurons in the ME7 infected hippocampus was performed. This post-synaptic protein was used to assess the role of the post-synaptic synapse in the loss of CA1 neurons observed in the ME7 infected hippocampus. No change was observed in PSD-95 expression in the time course study until the terminal stage of disease (Figure 19E&F). At the terminal stage of disease PSD-95 expression was decreased in the CA1,CA2 and CA3 sectors of the hippocampus, although marked expression was still observed in the dentate gyrus (Figure 19E). Trypsin was used as a pretreatment at the recommended dilution and time scale, unfortunately it digested some of the sections causing some neuronal cell bodies to disappear in both the CA1 (Figure 19B) and dentate gyrus (Figure 19E) of the hippocampus. This is a common artefact often observed after pretreatment with trypsin, where over digestion of the cell membrane can lead to cell loss from tissue sections (Ugolev & De Laey, 1973).

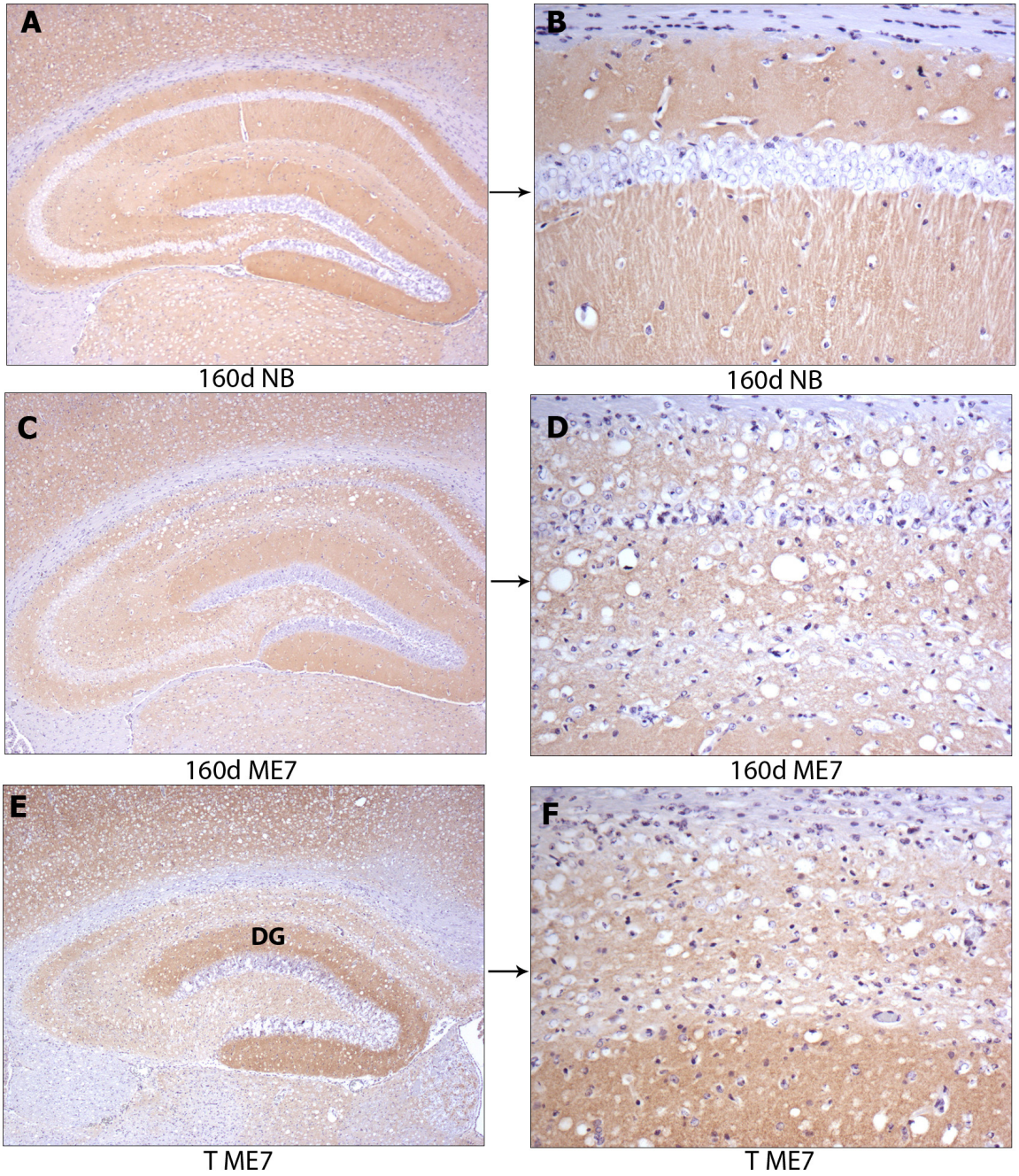

Figure 19. PSD-95 immunolabelling in the hippocampus. (A) normal brain control with widespread PSD-95 labelling throughout the hippocampus. (B) PSD-95 labelling in the CA1 sector, trypsin digestion created an artefact, resulting in loss of cell bodies from the CA1 (C) 160dpi ME7 infected hippocampus PSD-95 labelling still observed although neuronal loss is evident. (D) 160dpi CA1 showing PSD-95 labelling. (E) ME7 infected hippocampus at the terminal (T) stage of disease showing loss of PSD-95 in CA1-CA3 of hippocampus, intense labelling still observed in the dentate gyrus (DG). (F) ME7 T CA1 sector showing loss of PSD-95 labelling. Magnification A,C&E x 4, B,D&F x20

5.6.3 No difference observed in the protein expression of synaptophysin or PSD-95 at the terminal stage of disease.

Using immunohistochemical analysis a decrease in the expression of both synaptophysin (Figure 18F) and PSD-95 (Figure 19E) in the ME7 infected hippocampus at the terminal stages of disease was observed. Could the decrease in expression of these proteins also be detected by western blot analysis of dissected hippocampus?

Western blot analysis of synaptophysin and PSD-95 expression in the hippocampus at the terminal stage of disease showed no differences between the normal brain controls and ME7 infected brains (Figure 20). Ten mice were compared, three control and seven ME7 infected homogenates from dissected hippocampus were analysed. Each blot was stripped and reprobed with alpha tubulin, which revealed no changes between the infected and control samples.

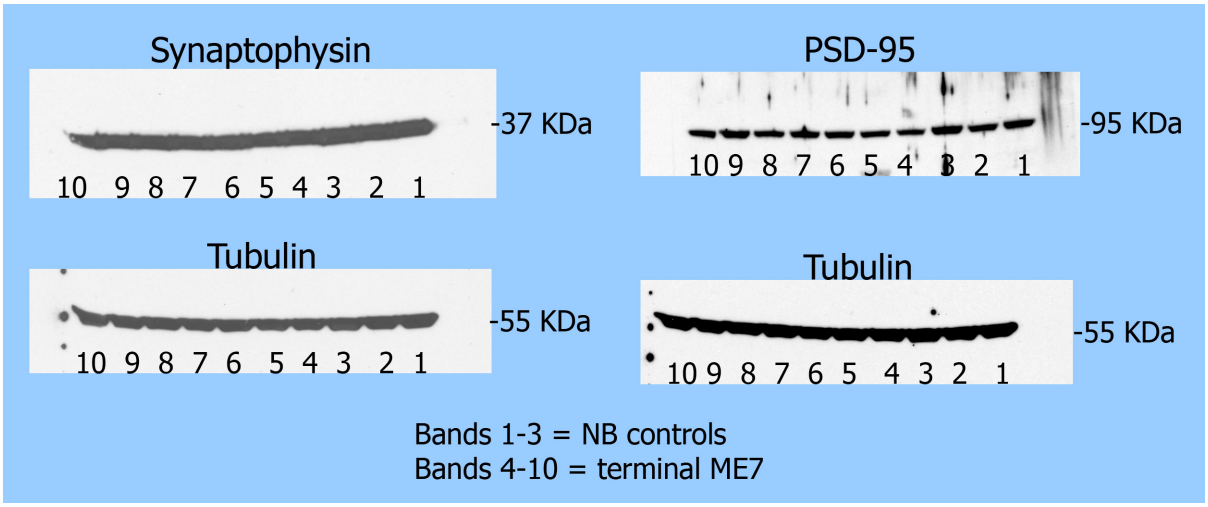

Figure 20. Western blot analysis of Synaptophysin and PSD-95 in ME7 terminal and aged matched normal brain controls. No difference observed between the ME7 infected and the NB controls in both the expression of synaptophysin and PSD-95. Blot was stripped and reprobed with alpha tubulin which revealed no difference between infected and control samples.

5.7 Discussion

The role of the dendritic cytoskeleton in the events leading to neurodegeneration was analysed using the dendritic cytoskeletal proteins MAP-2 and alpha tubulin. A loss of both proteins was observed at the terminal stage of disease in both CA1(ME7) and CA2(87V) scrapie infected neurons. A total loss of MAP-2 expression was observed in the CA2 sector of the 87V infected hippocampus revealing dramatic changes within the dendritic cytoskeleton of these neurons. Previous studies in this model revealed cytoskeletal damage in CA2 neurons as early as 70 days observed as varicosities within the apical dendrites (Jamieson et al, 2001b). In this study by the terminal stage of disease at 320dpi a total loss of MAP-2 expression is observed in the dendritic compartment of these neurons, although expression is still observed in the few remaining cell bodies. In the ME7 infected hippocampus at the terminal stage of disease only a few cell bodies remain in the pyramidal cell layer, MAP-2 immunohistochemistry reveals a total loss of neuronal dendrites. MAP-2 plays a major role in stabilising microtubules and their role in neuronal transport. The loss of MAP-2 and damage to the microtubules within both the scrapie infected CA1 and CA2 neurons may contribute to impaired neuronal transport and subsequent death of these neurons.

A time course study of the expression of MAP-2 within the dendrites of ME7 infected CA1 neurons revealed the initial disruption to the dendritic cytoskeleton at 160dpi, a time point at which neurons are known to be lost in this model (Jeffrey et al, 2000). The loss of expression of MAP-2 and dendritic damage within ME7 infected CA1 neurons is observed late in the progression of the disease. Earlier cytoskeletal changes in these neurons, i.e. the loss of dendritic spines, may initiate the disruption to the dendritic cytoskeleton and the eventual loss of MAP-2 within these neurons.

The initial loss of the expression of the dendritic spine protein, drebrin, within the ME7 infected CA1 neurons was observed at 160dpi, at a time point in the disease where dendritic cytoskeletal damage is first observed. Quantification of dendritic spine loss in ME7 infected CA1 neurons injected with Lucifer yellow revealed a much earlier loss of these spines, at 109 dpi. (Brown et al, 2001) The Lucifer yellow microinjection of CA1 neurons was a more sensitive technique that detected earlier changes observed in the dendritic spines of these neurons. In this study drebrin expression was used as a marker to analyse and compare the role of the dendritic spine cytoskeleton with that of the dendrite. A specific targeted loss of this protein was observed in the CA1 sector of the hippocampus at 160dpi. This loss was observed in both the stratum radiatum and the stratum oriens of the hippocampus revealing cytoskeletal abnormalities within the spines of both the apical and basal dendrites of the CA1 neurons. Intense drebrin expression was observed throughout the other sectors of the hippocampus, at the terminal stage of disease, expression was still observed in the dentate gyrus and CA2 sector of the hippocampus. Similar expression patterns of drebrin were observed in the brains of Alzheimer's disease patients, where a loss of drebrin expression was observed throughout the hippocampal formation, with some slight staining remaining in the dentate gyrus (Harigaya et al, 1996). This loss of drebrin reflects the loss of dendritic spines observed in hippocampal neurons in mouse models of Alzheimers disease (Grutzendler et al, 2007; Knobloch & Mansuy, 2008; Moolman et al, 2004; Scheff et al, 2007). The loss of drebrin expression observed in the CA1 sector also reflects the targeted neuronal damage observed in the hippocampus of the ME7/CV scrapie mouse model.

The CA1 neurons are connected to the CA3 neurons through the Shaffer collateral pathway, and the axons of the CA3 neurons have synaptic connections with

the apical dendrites of CA1 neurons (Spruston, 2008). Therefore the loss of drebrin and damage to the CA3 neurons observed at the terminal stage of disease may be related to the initial damage and spine loss observed in the apical dendrites of CA1 neurons. In immunohistochemical analysis the initial loss of drebrin expression at 160dpi correlates with the loss of MAP-2 and dendritic damage observed in ME7 infected CA1 neurons, suggesting that cytoskeletal changes occur at the same time within dendritic spines and the dendritic shaft. However, the previous lucifer yellow studies show that damage to dendritic spines appears over 50 days earlier. The results observed in this study demonstrated that disruption of the dendritic spine cytoskeleton plays a role in the cytoskeletal damage observed in the CA1 neurons, but what initiates this damage is still to be determined.

To analyse the role of the pre- and post-synaptic synapse in the synaptic loss observed in the ME7/CV mouse model the expression of synaptophysin and the post synaptic density protein PSD-95, were analysed.

Synaptophysin labels a component of the synaptic vesicle membrane and is found predominantly within axon terminals. In the immunohistochemical time series study of synaptophysin labelling in the ME7 infected hippocampus the intensity of synaptophysin labelling was reduced at the terminal stage of disease, a slight reduction was observed in the 200 day group. Although the intensity of synaptophysin was decreased in the stratum radiatum of the ME7 infected hippocampus a marked labelling was still observed. Previous immunohistochemical studies quantifying the loss of synaptophysin at the terminal stage of disease in the ME7/CV model, revealed a significant loss in both the apical and basal dendrites of CA1 sector neurons (Belichenko et al, 2000). Both the basal and apical dendrites of CA1 sector neurons receive innervation from the CA3 sector neurons in the hippocampus. The presynaptic

axon terminals from CA3 neurons make connections with postsynaptic dendritic spines on basal and apical dendrites of CA1 neurons (Spruston, 2008). The loss of synaptophysin labelling observed at the terminal stage of disease in both the basal and apical dendrites is suggestive of a loss of innervation from the CA3 neurons at the end stage of disease.

Ultrastructural studies in the stratum radiatum of the ME7 infected hippocampus revealed early axon terminal degeneration (Jeffrey et al, 2000). Although these axons have degenerated the synaptic vesicles and their contents are still detectable, this may be due to a compensatory role played by the damaged axon. These results were similar to a previous study analysing the mechanisms involved in the neuronal loss observed in the scrapie infected dorsal lateral geniculate nucleus (dLGN). In mice injected intraocularly with the ME7 strain of scrapie, neuronal loss was observed in the dorsal lateral geniculate nucleus (dLGN) (Fraser et al, 1995). Synaptophysin labelling was decreased in the dLGN of mice terminally infected with ME7, but no loss of synaptophysin was detected on or before 150days of a 240 day incubation, suggesting that neuronal loss in this area was not the result of deafferentation.

Excitatory synapses are characterised by an electron-dense thickening of the post synaptic membrane, termed the post synaptic density (Figure 4). PSD-95 is a scaffolding protein enriched in the post-synaptic density, which binds and brings into close proximity, neurotransmitter receptors, signalling molecules and regulators of the actin cytoskeleton. Most excitatory synapses in the mammalian CNS occur on dendritic spines (Fiala et al, 2002; Hering & Sheng, 2001). Dendritic spines are complex structures that have at their surface a post synaptic density.

In the ME7/CV scrapie mouse model dendritic spine and synapse loss is observed early in the incubation period. What role, if any does the post synaptic density, and the scaffolding protein PSD-95, play in this loss?

Using immunohistochemical techniques the loss of expression of PSD-95 in the hippocampus was not observed until the terminal stage of disease, when this deficit was found in all of the hippocampal formation, except for the dentate gyrus .The ultrastructural studies involved in the counting of synapses lost in ME7 infected CA1 neurons reflect the loss of postsynaptic densities. The synapse counts in the ME7/CV model were performed between 84 and 181 dpi ME7 infection. Analysis of the actual numbers of synapses counted at each individual time point does not show a severe decline in numbers of synapses lost, although there is an overall significant loss. If synapse numbers relate to the intensity of PSD-95 labelling, a major difference might not be observed. The intensity of PSD-95 immunostaining observed in the hippocampus may be a true reflection of how much of the PSDs that are actually still intact in the synaptic disruption observed in the ME7 infected CA1 neurons. PSD-95 can also be moved around the cell in a preassembled package as a PDZ-based membrane bound complex. These complexes are transported along microtubule tracts by Kinesin motor proteins. Therefore PSD-95 expression may accumulate in dendritic shafts contributing to the expression levels observed in the ME7 infected hippocamapus. (Kim & Sheng, 2004).

The role of the post-synaptic density and PSD-95 in the synaptic loss observed in TSE disease has not yet been determined. PSD-95 plays a role in synaptic plasticity and in the clustering of the NMDA and AMPA receptors at the PSD and is involved in the maintenance of a form of synaptic plasticity know as long-term potentiation (LTP). In the mouse model studied here the maintenance of LTP in ME7

CA1 neurons was disturbed from 100dpi. Studies analysing the role of the NMDA receptor in this disruption have shown that this receptor complex was not compromised in scrapie infection, and that altered potassium currents rather than increased calcium entry via voltage-sensitive calcium channels or the NMDA receptor complex may be the mechanism involved in scrapie induced neurodegeneration (Johnston et al, 1998a).

In summary, the data from the present study together with previous observations show that synaptic dysfunction plays a role in the loss of CA1 sector neurons, although the mechanisms involved and the trigger for the synaptic loss have still to be determined.

The first neuropathological change observed in the hippocampus of the ME7 infected brain, is the deposition of PrP^{Sc}. The deposition of PrP^{Sc} has been observed on synapses in CJD (Kitamoto et al, 1992; Kovacs et al, 2005) and rodent models of disease (Fournier et al, 2000; Haeberle et al, 2000) suggesting a role for this abnormal protein in the synaptic degeneration observed in TSE disease. A more recent publication analysing the subcellular location of PrP^{Sc} in the stratum radiatum of the RML infected murine hippocampus revealed that there was no evidence for deposition of PrP^{Sc} at synaptic junctions or associated with synaptic vesicles, it therefore appears unlikely that PrP^{Sc} acts directly on synapses.

Astrocytes are known to play a role in synaptic plasticity, they ensure normal neuronal excitability, and participate in glutamate and potassium reuptake from the synaptic region (Seth & Koul, 2008). In the ME7 infected hippocampus astrocytes are activated early in the disease progression increasing in numbers by the terminal stage of disease. Disruption to the normal function of astrocytes and a build

up of glutamate in the surrounding neuropil may contribute to the synaptic degeneration and subsequent synaptic loss observed in CA1 neurons.

The results obtained in this chapter analysing the role of the cytoskeleton and the synaptic loss in the ME7 infected CA1 neuron will be compared with the results observed in Chapters 3 and 4 analysing the neuropathological changes and the mechanism of cell death involved in the neurodegeneration observed in the ME7 infected hippocampus. This will be discussed fully in chapter 6

Chapter 6: Final discussion and future work

The aims of this research were to investigate the mechanisms of neurodegeneration and subsequent neuronal cell loss observed in TSEs. In this study two contrasting scrapie mouse models were used : the ME7/CV model, and the 87V/VM model in which neuronal loss is targeted to different areas of the hippocampus, the CA1, and CA2 respectively. Detailed studies of the progression of neurodegenerative changes in the ME7/CV scrapie mouse model revealed that the initial pathological change observed in the hippocampus was the deposition of PrP^{Sc} followed by a glial response, spongiform change and subsequent neuronal degeneration. The role of the cytoskeleton and synaptic dysfunction in the neuronal damage observed in the CA1 of the ME7 infected hippocampus was investigted. The results observed in these studies suggest that cytoskeletal disruption in the post-synaptic dendritic spine plays a major role in the neuronal dysfunction observed in ME7 infected CA1 neurons, although the post-synaptic density does not seem to be involved. Pre-synaptic changes and disruption to the innervation of CA1 neurons occur relatively late in the disease process as a consequence of earlier degenerative changes in the TSE infected neuron.

One of the main aims of this thesis was to investigate the mechanism of cell death involved in the neuronal loss observed in the CA1 of the ME7 infected hippocampus. Apoptosis is the suggested mechanism of cell death associated with TSE-induced neuronal loss. This research was designed to address the mechanisms leading to the activation of and also subsequent execution of cell death through an apoptotic mechanism. The findings in this study have revealed that the mechanisms of neuronal loss in TSEs may follow different biochemical pathways, which might not necessarily involve an apoptotic mechanism.

The trigger for the cytoskeletal disruption, synaptic dysfunction and subsequent neuronal loss may be the early deposition of PrP^{Sc} in the extracellular space, but the precise mechanisms involved are still to be elucidated. Recent studies analysing the role of PrP^{Sc} in the synapse loss observed in the ME7/C57BL scrapie mouse model correlate with the results obtained in this study and show that presynaptic indices were not compromised (Asuni *et al*, 2008). Although it has been suggested that PrP^{c} may play an important role in the maintenance and function of synapses (Westergard *et al*, 2007) the precise role of PrP^{Sc} at the synapse has still to be determined. The studies in the ME7/CV scrapie mouse model would suggest that the increase in PrP^{Sc} plays a role in the damage to the post-synaptic element of the synapse, the dendritc spine, most likely involving changes in actin dynamics within the spine head. However recent ultrastructural studies have revealed that PrP^{Sc} was not deposited on synapses (Godsave *et al,* 2008) and therefore may not play a significant role in synaptic dysfunction.

The role of PrP^{Sc} and glial activation in the synaptic dysfunction observed in the ME7 infected CA1 neurons is unclear. Glial cells have many functions in the CNS and are known to actively contribute to neurotransmission, neuronal excitability, and several forms of synaptic plasticity, such as long term potentiation (LTP) (Bains & Oliet, 2007; Volterra & Meldolesi, 2005); (Vesce et al, 1999). The deposition of Aβ oligomers in combination with Aβ-mediated activation of microglia and astrocytes in Alzheimer diseased brains results in disruption of both hippocampal LTP and the memory of learned behaviours (Klyubin et al, 2005; Walsh & Selkoe, 2004a; Walsh & Selkoe, 2004b). The deposition of PrP^{Sc} in combination with a marked glial response may play a role in the early disruption of LTP (Johnston et al, 1998b) observed in ME7 infected CA1 neurons.

LTP is a post-synaptic phenomenon involved in synaptic plasticity. Actin dynamics within dendritic spines are known to play a major role in synaptic function (Calverley *et al*, 1990). Disruption to the cytoskeleton and the loss of the F-actin binding protein, drebrin, may contribute to the synaptic dysfunction observed in the ME7 infected CA1 neurons. Surprisingly, the post-synaptic density (PSD) is not involved in the cytoskeltal disruption observed within dendritic spines. This may be due to the fact that different components show a differential dependence on F-actin for localisation within the spine. Although the PSD is a core component observed within the dendritic spine it is known to function independently of conventional cytoskeletal elements (Allison et al, 2000), and therefore may not play a major role in the cytoskeletal disruption observed in the dendritic spine.

The work involved in this study was initiated to obtain a better understanding of the mechanisms involved in the characteristic neurodegeneration and resulting neuronal loss observed in TSEs. Although apoptosis cannot be categorically ruled out the results obtained in this study do not support this type of programmed cell death as the main mechanism by which neurons die in TSEs. Also other mechanisms of apoptosis not studied in this thesis may play a role in the cell death observed in TSEs. Another apoptotic pathway suggested to play a role in the cell death observed in TSEs involves the induction of endoplasmic reticulum (ER) stress. Protein aggregation in the ER triggers the activation of an ER-resident caspase, caspase-12 (Nakagawa et al, 2000). Active caspase-12 and the ER stress inducible chaperon protein Grp58 was shown to be upregulated in the brains of mice infected with the 139A strain of scrapie at the terminal stage of disease (Hetz et al, 2003). However, scrapie infection of mice deficient in caspase-12 showed no differences in behaviour, pathology and incubation time of disease in comparison with wild type mice (Steele *et al*, 2007a), suggesting

that caspase-12 is not necessary for mediating the toxic effects of prion protein misfolding.

Autophagy is another form of cell death that has been observed in TSE diseases. Most of the data to support autophagy as a mechanism of cell death in TSEs comes from electron microscopic studies (Liberski et al, 2008; Liberski et al, 2002b; Liberski et al, 2004; Liberski et al, 1990; Sikorska et al, 2007. Autophagy, or cellular self digestion, is a lysosome mediated cellular pathway involved in protein and organelle degradation. Autophagy is thought to be a cell survival mechanism and growing evidence reveals that alterations in autophagy occur in neurodegenerative diseases, and has been shown to play a role in degredation of disease-related mutant proteins {Mizushima, 2008). Transmission electron microscopy (TEM) is very labour intensive and more recently useful protein markers of autophagy have been discovered. The molecular mechanisms of the autophagy pathway has been well defined, and a subset of genes, denoted as ATGs (autophagy related) (Figure 1), is conserved from yeast to human (Huang & Klionsky, 2002; Ohsumi, 2001).The expression levels of the microtubule associated protein light chain 3 (LC3), one of the mammalian Atg8 homologues, is localised to the autophagosomal membrane and can be used to estimate the abundance of autophagosomes before they are degraded by lysosomal hydrolases (Kabeya et al, 2000).

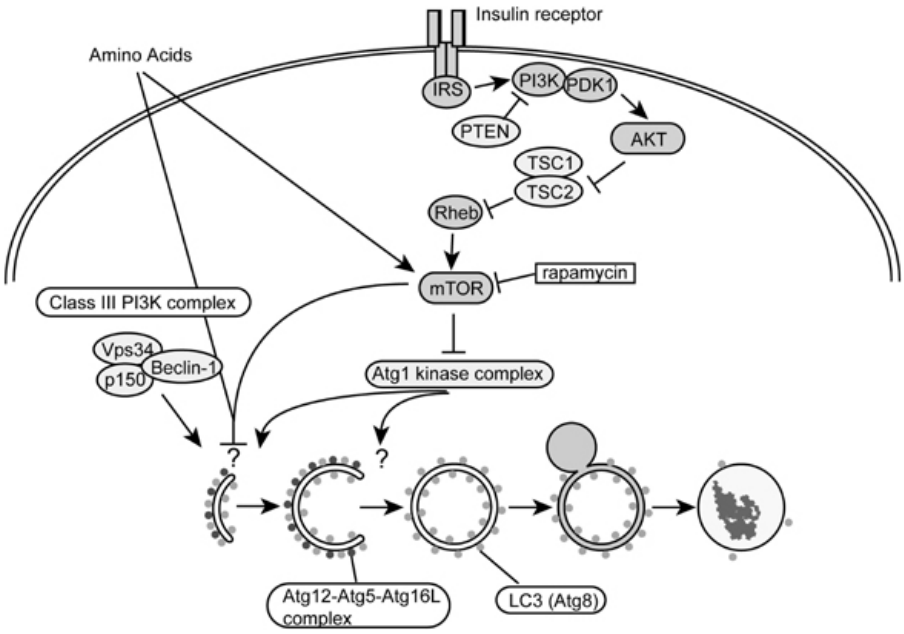

Figure 1. Autophagy pathway In the presence of adequate nutrients, growth factors are able to activate the class 1 P13K proteins which in turn signal via the AKT pathway to activate mTOR. This leads to the inhibition of ATG1- the key signal in autophagy induction. Inadequate nutrients or the presence of mTOR inhibitors (rapamycin) activates ATG1 leading to the induction of the autophagy pathway. Figure from Abcam datasheet.

The role of both PrP^{c} and PrP^{Sc} in the autophagy pathway has been investigated. The expression levels of LC3 by monitoring the conversion from LC3-I into LC3-II, was increased in *Prnp*$^{-/-}$ hippocampal neuronal cells in comparison to wild type cells under serum deprivation. Interestingly, this up-regulated autophagic activity was retarded by the introduction of PrP^{c} into *Prnp*$^{-/-}$ cells but not by the introduction of PrP^{c} lacking the octapeptide repeat region, suggesting a role for the octapeptide repeat region of PrP^{c} in the control of autophagy (Oh et al, 2008). Autophagy induction by trehalose, a known inducer of autophagy, significantly reduced PrP^{Sc} in neuronal cells *in vitro* and delayed appearance of PrP^{Sc} in the spleen of intraperitoneally TSE infected mice but did not result in prolongation of incubation times (Aguib et al, 2009).

In addition scrapie responsive gene 1(scrg1), a gene shown to have increased expression levels in the brains of mice infected with scrapie and BSE and patients with CJD, was associated with autophagy (Dron et al, 2006). The scrg1 protein was observed in autophagic vacuoles within neurones in the scrapie infected mouse brain. Although no significant difference was observed in the disease progression of ME7 infected transgenic mice specifically expressing Scrg1 in neurons (Dron *et al*, 2005). A decrease in mRNA levels of Beclin1 and Atg5 two autophagy related genes, was observed in mice infected with the 139A strain of scrapie, although autophagosome formation was unchanged (Mok et al, 2007). The role of autophagy in the neuronal cell death in TSEs is still to be determined, it may play a role in degrading and removing abnormal forms of the prion protein (Aguib et al, 2009; Heiseke et al, 2009). Future studies analysing the role of autophagy in the neuronal loss observed in the CA1 of the ME7 infected hippocampus could utilise some of the markers of autophagy mentioned above. Expression levels of scrg1 have been observed *in vivo* in brains of mice infected with scrapie and would be an ideal candidate to analyse the role of autophagy in the loss of CA1 neurons in the ME7 infected hippocampus.

TSEs or prion diseases fall into the category of protein misfolding diseases. One of the characterisitc pathological changes observed in the brain in these diseases is the deposition and accumulation of PrP^{Sc} in different forms. In protein misfolding diseases many studies have been performed in order to find the toxic component of the protein. There is growing evidence that in brain amyloidoses, such as Alzheimers disease, prefibrillar soluble protein aggregates, rather than insoluble fibrils, are toxic (Cerpa et al, 2008; Haass & Selkoe, 2007. In mouse models of Alzheimer's disease oligomers of Aβ protein have been shown to impair synaptic plasticity, disrupt LTP and produce changes in dendritic spine shape in CA1 neurons {Shankar, 2008 ; Kayed

et al, 2003; Selkoe, 2008; Stefani & Dobson, 2003; Taylor et al, 2002; Viola et al, 2008). Recently, oligomers of PrP^{Sc} have been shown to be neurotoxic and produce neuronal loss in the CA1 of the mouse hippocampus, while monomeric and fibrillar forms of PrP did not (Simoneau et al, 2007). In the ME7/CV scrapie mouse model diffuse, non-fibrillar forms of PrP^{Sc} accumulate in the ME7 infected hippocampus, in contrast in the 87V/VM scrapie mouse model the main form of PrP observed is in the form of amyloid palques. Further studies are required to compare and analyse the different forms of PrP deposited in the brains of these mice, to determine which forms are neurotoxic. Antibodies raised to the oligomeric form of Aβ have been shown to react with oligomeric forms of PrP (Kayed et al, 2003) which include the hydrophobic PrP106-126 domain of PrP^{Sc} , and could be used in IHC studies to identify the neurotoxic form of PrP.

The identification of the key events involved in the mechanisms of neruodegeneration in TSE diseases may lead to development of therapeutic strategies to inhibit the neurodegenerative process. The fundamental research within this thesis contributes towards understanding the mechanisms involved in the neuronal degeneration observed in the TSE infected brain and may contribute to the development of potential therapeutic strategies for TSEs. This research may also have wider implications for the treatment of other neurodegenerative diseases associated with hippocampal pathology, such as Alzheimer's disease.

The data in this thesis has been presented at local, national and international meetings. I have attended the Edinburgh Neuroscience day every year for the past 10 years were different aspects of the work within this thesis has been presented in poster format. I have presented the work within this thesis at the TSE joint funders meeting held in Warwick. Internationally the work has been presented at the Cell death

meeting in Luxombourg in 2005 and at the FENS meeting in Geneva in 2008. The data within this thesis is in preparation for publication.

Bibliography

Adams D H, Caspary E,A, (1968) The incorporation of nucleic acid and polysaccharide precursors into a post-ribosomal fraction of scrapie-affected mouse brain. *Biochemical journal* **108:** 38p

Agrimi U, Nonno R, Dell'Omo G, Di Bari MA, Conte M, Chiappini B, Esposito E, Di Guardo G, Windl O, Vaccari G, Lipp HP (2008) Prion protein amino acid determinants of differential susceptibility and molecular feature of prion strains in mice and voles. *PLoS Pathog* **4:** e1000113

Aguib Y, Heiseke A, Gilch S, Riemer C, Baier M, Schatzl HM, Ertmer A (2009) Autophagy induction by trehalose counteracts cellular prion infection. *Autophagy* **5**

Allison DW, Chervin AS, Gelfand VI, Craig AM (2000) Postsynaptic scaffolds of excitatory and inhibitory synapses in hippocampal neurons: maintenance of core components independent of actin filaments and microtubules. *J Neurosci* **20:** 4545-4554

Alper T, Cramp WA, Haig DA, Clarke MC (1967) Does the agent of scrapie replicate without nucleic acid? *Nature* **214:** 764-766

Alper T, Haig DA, Clarke MC (1966) The exceptionally small size of the scrapie agent. *Biochem Biophys Res Commun* **22:** 278-284

Alpers M (1965) Epidemiological changes in Kuru, 1957 to 1963. NINDB *monograph no 2 slow, latent and temperate virus infections, National Institute of Neurological Diseases and Blindness, Bethesda, MD, USA*. 65-82

Alpers M, Rail L (1971) Kuru and Creutzfeldt-Jakob disease: clinical and aetiological aspects. *Proc Aust Assoc Neurol* **8:** 7-15

Anderton BH, Callahan L, Coleman P, Davies P, Flood D, Jicha GA, Ohm T, Weaver C (1998) Dendritic changes in Alzheimer's disease and factors that may underlie these changes. *Prog Neurobiol* **55:** 595-609

Andreadis A, Brown WM, Kosik KS (1992) Structure and novel exons of the human tau gene. *Biochemistry* **31:** 10626-10633

Andreoletti O, Lacroux C, Chabert A, Monnereau L, Tabouret G, Lantier F, Berthon P, Eychenne F, Lafond-Benestad S, Elsen JM, Schelcher F (2002) PrP(Sc) accumulation in placentas of ewes exposed to natural scrapie: influence of foetal PrP genotype and effect on ewe-to-lamb transmission. *J Gen Virol* **83:** 2607-2616

Angers RC, Browning SR, Seward TS, Sigurdson CJ, Miller MW, Hoover EA, Telling GC (2006) Prions in skeletal muscles of deer with chronic wasting disease. *Science* **311:** 1117

Ankarcrona M, Dypbukt JM, Bonfoco E, Zhivotovsky B, Orrenius S, Lipton SA, Nicotera P (1995) Glutamate-induced neuronal death: a succession of necrosis or apoptosis depending on mitochondrial function. *Neuron* **15:** 961-973

Aoki C, Sekino Y, Hanamura K, Fujisawa S, Mahadomrongkul V, Ren Y, Shirao T (2005) Drebrin A is a postsynaptic protein that localizes in vivo to the submembranous surface of dendritic sites forming excitatory synapses. *J Comp Neurol* **483:** 383-402

Aoki T, Kobayashi K, Isaki K (1999) Microglial and astrocytic change in brains of Creutzfeldt-Jakob disease: an immunocytochemical and quantitative study. *Clin Neuropathol* **18:** 51-60

Arnold SE, Lee VM, Gur RE, Trojanowski JQ (1991) Abnormal expression of two microtubule-associated proteins (MAP2 and MAP5) in specific subfields of the hippocampal formation in schizophrenia. *Proc Natl Acad Sci U S A* **88:** 10850-10854

Arsac JN, Andreoletti O, Bilheude JM, Lacroux C, Benestad SL, Baron T (2007) Similar biochemical signatures and prion protein genotypes in atypical scrapie and Nor98 cases, France and Norway. *Emerg Infect Dis* **13:** 58-65

Auinger S, Small JV (2008) Correlated light and electron microscopy of the cytoskeleton. *Methods Cell Biol* **88:** 257-272

Awasthi A, Matsunaga Y, Yamada T (2005) Amyloid-beta causes apoptosis of neuronal cells via caspase cascade, which can be prevented by amyloid-beta-derived short peptides. *Exp Neurol* **196:** 282-289

Bains JS, Oliet SH (2007) Glia: they make your memories stick! *Trends Neurosci* **30:** 417-424

Baker CA, Lu ZY, Zaitsev I, Manuelidis L (1999) Microglial activation varies in different models of Creutzfeldt-Jakob disease. *J Virol* **73:** 5089-5097

Baldauf E, Beekes M, Diringer H (1997) Evidence for an alternative direct route of access for the scrapie agent to the brain bypassing the spinal cord. *J Gen Virol* **78 (Pt 5):** 1187-1197

Ballough GP, Martin LJ, Cann FJ, Graham JS, Smith CD, Kling CE, Forster JS, Phann S, Filbert MG (1995) Microtubule-associated protein 2 (MAP-2): a sensitive marker of seizure-related brain damage. *J Neurosci Methods* **61:** 23-32

Barlow RM (1972) Transmissible mink encephalopathy: pathogenesis and nature of the aetiological agent. *J Clin Pathol Suppl (R Coll Pathol)* **6:** 102-109

Barlow RM, Rennie JC (1970) Transmission experiments with a scrapie-like encephalopathy of mink. *J Comp Pathol* **80:** 75-79

Barmada S, Piccardo P, Yamaguchi K, Ghetti B, Harris DA (2004) GFP-tagged prion protein is correctly localized and functionally active in the brains of transgenic mice. *Neurobiol Dis* **16:** 527-537

Baron T, Biacabe AG, Arsac JN, Benestad S, Groschup MH (2007) Atypical transmissible spongiform encephalopathies (TSEs) in ruminants. *Vaccine* **25:** 5625-5630

Barr JB, Somerville RA, Chung YL, Fraser JR (2004) Microdissection: a method developed to investigate mechanisms involved in transmissible spongiform encephalopathy pathogenesis. *BMC Infect Dis* **4:** 8

Barron RM, Campbell SL, King D, Bellon A, Chapman KE, Williamson RA, Manson JC (2007) High titers of transmissible spongiform encephalopathy infectivity associated with extremely low levels of PrPSc in vivo. *J Biol Chem* **282:** 35878-35886

Bartz JC, Marsh RF, McKenzie DI, Aiken JM (1998) The host range of chronic wasting disease is altered on passage in ferrets. *Virology* **251:** 297-301

Baskakov IV, Legname G, Baldwin MA, Prusiner SB, Cohen FE (2002) Pathway complexity of prion protein assembly into amyloid. *J Biol Chem* **277:** 21140-21148

Baskakov IV, Legname G, Prusiner SB, Cohen FE (2001) Folding of prion protein to its native alpha-helical conformation is under kinetic control. *J Biol Chem* **276:** 19687-19690

Basu A, Castle VP, Bouziane M, Bhalla K, Haldar S (2006) Crosstalk between extrinsic and intrinsic cell death pathways in pancreatic cancer: synergistic action of estrogen metabolite and ligands of death receptor family. *Cancer Res* **66:** 4309-4318

Bautista MJ, Gutierrez J, Salguero FJ, Fernandez de Marco MM, Romero-Trevejo JL, Gomez-Villamandos JC (2006) BSE infection in bovine PrP transgenic mice leads to hyperphosphorylation of tau-protein. *Vet Microbiol* **115:** 293-301

Baylis M, Chihota C, Stevenson E, Goldmann W, Smith A, Sivam K, Tongue S, Gravenor MB (2004) Risk of scrapie in British sheep of different prion protein genotype. *J Gen Virol* **85:** 2735-2740

Baylis M, Goldmann W (2004) The genetics of scrapie in sheep and goats. *Curr Mol Med* **4:** 385-396

Beck E, Daniel PM, Alpers M, Gajdusek DC, Gibbs CJ, Jr. (1966) Experimental "kuru" in chimpanzees. A pathological report. *Lancet* **2:** 1056-1059

Beekes M, Baldauf E, Diringer H (1996) Sequential appearance and accumulation of pathognomonic markers in the central nervous system of hamsters orally infected with scrapie. *J Gen Virol* **77 (Pt 8):** 1925-1934

Beekes M, McBride PA (2000) Early accumulation of pathological PrP in the enteric nervous system and gut-associated lymphoid tissue of hamsters orally infected with scrapie. *Neurosci Lett* **278:** 181-184

Beekes M, McBride PA, Baldauf E (1998) Cerebral targeting indicates vagal spread of infection in hamsters fed with scrapie. *J Gen Virol* **79 (Pt 3):** 601-607

Beghin A, Galmarini CM, Dumontet C (2007) Tubulin folding pathways: implication in the regulation of microtubule dynamics. *Curr Cancer Drug Targets* **7:** 697-703

Belichenko PV, Brown D, Jeffrey M, Fraser JR (2000) Dendritic and synaptic alterations of hippocampal pyramidal neurones in scrapie-infected mice. *Neuropathol Appl Neurobiol* **26:** 143-149

Bendheim PE, Brown HR, Rudelli RD, Scala LJ, Goller NL, Wen GY, Kascsak RJ, Cashman NR, Bolton DC (1992) Nearly ubiquitous tissue distribution of the scrapie agent precursor protein. *Neurology* **42:** 149-156

Benestad SL, Arsac JN, Goldmann W, Noremark M (2008) Atypical/Nor98 scrapie: properties of the agent, genetics, and epidemiology. *Vet Res* **39:** 19

Benitez-King G, Ramirez-Rodriguez G, Ortiz L, Meza I (2004) The neuronal cytoskeleton as a potential therapeutical target in neurodegenerative diseases and schizophrenia. *Curr Drug Targets CNS Neurol Disord* **3:** 515-533

Bertrand E, Brouillet E, Caille I, Bouillot C, Cole GM, Prochiantz A, Allinquant B (2001) A short cytoplasmic domain of the amyloid precursor protein induces apoptosis in vitro and in vivo. *Mol Cell Neurosci* **18:** 503-511

Betmouni S, Perry VH, Gordon JL (1996) Evidence for an early inflammatory response in the central nervous system of mice with scrapie. *Neuroscience* **74:** 1-5

Biacabe AG, Laplanche JL, Ryder S, Baron T (2004) Distinct molecular phenotypes in bovine prion diseases. *EMBO Rep* **5:** 110-115

Binder LI, Frankfurter A, Rebhun LI (1985) The distribution of tau in the mammalian central nervous system. *J Cell Biol* **101:** 1371-1378

Boccellino M, Cuccovillo F, Napolitano M, Sannolo N, Balestrieri C, Acampora A, Giovane A, Quagliuolo L (2003) Styrene-7,8-oxide activates a complex apoptotic response in neuronal PC12 cell line. *Carcinogenesis* **24:** 535-540

Boellaard JW, Kao M, Schlote W, Diringer H (1991) Neuronal autophagy in experimental scrapie. *Acta Neuropathol (Berl)* **82:** 225-228

Boellaard JW, Schlote W, Tateishi J (1989) Neuronal autophagy in experimental Creutzfeldt-Jakob's disease. *Acta Neuropathol (Berl)* **78:** 410-418

Bolton DC, McKinley MP, Prusiner SB (1982) Identification of a protein that purifies with the scrapie prion. *Science* **218:** 1309-1311

Bonetti B, Pohl J, Gao YL, Raine CS (1997) Cell death during autoimmune demyelination: effector but not target cells are eliminated by apoptosis. *J Immunol* **159:** 5733-5741

Borchelt DR, Scott M, Taraboulos A, Stahl N, Prusiner SB (1990) Scrapie and cellular prion proteins differ in their kinetics of synthesis and topology in cultured cells. *J Cell Biol* **110:** 743-752

Bossers A, Harders FL, Smits MA (1999) PrP genotype frequencies of the most dominant sheep breed in a country free from scrapie. *Arch Virol* **144:** 829-834

Bounhar Y, Zhang Y, Goodyer CG, LeBlanc A (2001) Prion protein protects human neurons against Bax-mediated apoptosis. *J Biol Chem* **276:** 39145-39149

Bowen S, Ateh DD, Deinhardt K, Bird MM, Price KM, Baker CS, Robson JC, Swash M, Shamsuddin W, Kawar S, El-Tawil T, Roos J, Hoyle A, Nickols CD, Knowles CH, Pullen AH, Luthert PJ, Weller RO, Hafezparast M, Franklin RJ, Revesz T, King RH, Berninghausen O, Fisher EM, Schiavo G, Martin JE (2007) The phagocytic capacity of neurones. *Eur J Neurosci* **25:** 2947-2955

Bradley R (1996) *Bovine spongiform encephalopathy : distribution and update on some transmission and decontamination studies. In: Bovine Spongiform Encephalopathy: the BSE dilemna.*, New York: Springer-Verlag.

Brandner S, Whitfield J, Boone K, Puwa A, O'Malley C, Linehan JM, Joiner S, Scaravilli F, Calder I, M PA, Wadsworth JD, Collinge J (2008) Central and peripheral pathology of kuru: pathological analysis of a recent case and comparison with other forms of human prion disease. *Philos Trans R Soc Lond B Biol Sci* **363:** 3755-3763

Brandt R, Hundelt M, Shahani N (2005) Tau alteration and neuronal degeneration in tauopathies: mechanisms and models. *Biochim Biophys Acta* **1739:** 331-354

Brazier MW, Lewis V, Ciccotosto GD, Klug GM, Lawson VA, Cappai R, Ironside JW, Masters CL, Hill AF, White AR, Collins S (2006) Correlative studies support lipid peroxidation is linked to PrP(res) propagation as an early primary pathogenic event in prion disease. *Brain Res Bull* **68:** 346-354

Brion JP, Fraser H, Flament-Durand J, Dickinson AG (1987) Amyloid scrapie plaques in mice, and Alzheimer senile plaques, share common antigens with tau, a microtubule-associated protein. *Neurosci Lett* **78:** 113-118

Brown AR, Webb J, Rebus S, Walker R, Williams A, Fazakerley JK (2003a) Inducible cytokine gene expression in the brain in the ME7/CV mouse model of scrapie is highly restricted, is at a strikingly low level relative to the degree of gliosis and occurs only late in disease. *J Gen Virol* **84:** 2605-2611

Brown D, Belichenko P, Sales J, Jeffrey M, Fraser JR (2001) Early loss of dendritic spines in murine scrapie revealed by confocal analysis. *Neuroreport* **12:** 179-183

Brown DA, Bruce ME, Fraser JR (2003b) Comparison of the neuropathological characteristics of bovine spongiform encephalopathy (BSE) and variant Creutzfeldt-Jakob disease (vCJD) in mice. *Neuropathol Appl Neurobiol* **29:** 262-272

Brown DR (2001) Copper and prion disease. *Brain Res Bull* **55:** 165-173

Brown DR, Mohn CM (1999) Astrocytic glutamate uptake and prion protein expression. *Glia* **25:** 282-292

Brown DR, Qin K, Herms JW, Madlung A, Manson J, Strome R, Fraser PE, Kruck T, von Bohlen A, Schulz-Schaeffer W, Giese A, Westaway D, Kretzschmar H (1997) The cellular prion protein binds copper in vivo. *Nature* **390:** 684-687

Brown DR, Schmidt B, Kretzschmar HA (1996) Role of microglia and host prion protein in neurotoxicity of a prion protein fragment. *Nature* **380:** 345-347

Brown KL, Stewart K, Ritchie DL, Mabbott NA, Williams A, Fraser H, Morrison WI, Bruce ME (1999) Scrapie replication in lymphoid tissues depends on prion protein-expressing follicular dendritic cells. *Nat Med* **5:** 1308-1312

Brown P, Brandel JP, Preece M, Sato T (2006) Iatrogenic Creutzfeldt-Jakob disease: the waning of an era. *Neurology* **67:** 389-393

Brown P, Rohwer RG, Dunstan BC, MacAuley C, Gajdusek DC, Drohan WN (1998) The distribution of infectivity in blood components and plasma derivatives in experimental models of transmissible spongiform encephalopathy. *Transfusion* **38:** 810-816

Browning SR, Mason GL, Seward T, Green M, Eliason GA, Mathiason C, Miller MW, Williams ES, Hoover E, Telling GC (2004) Transmission of prions from mule deer and elk with chronic wasting disease to transgenic mice expressing cervid PrP. *J Virol* **78:** 13345-13350

Bruce ME (1996) *Strain typing studies of scrapie and BSE. In : Methods in molecular medicine:Prion Diseases* Humana Press Inc.

Bruce ME (2003) TSE strain variation. *Br Med Bull* **66:** 99-108

Bruce ME, Dickinson, A.G., Fraser, H. (1976) Cerebral amyloidosis in scrapie in the mouse: effect of agent strain and mouse genotype. *Neuropathol Appl Neurobiol* **2:** 471-478

Bruce ME, Fraser H (1991) Scrapie strain variation and its implications. *Curr Top Microbiol Immunol* **172:** 125-138

Bruce ME, McBride PA, Farquhar CF (1989) Precise targeting of the pathology of the sialoglycoprotein, PrP, and vacuolar degeneration in mouse scrapie. *Neurosci Lett* **102:** 1-6

Bruce ME, McBride PA, Jeffrey M, Scott JR (1994) PrP in pathology and pathogenesis in scrapie-infected mice. *Mol Neurobiol* **8:** 105-112

Bruce ME, McConnell I, Fraser H, Dickinson AG (1991) The disease characteristics of different strains of scrapie in Sinc congenic mouse lines: implications for the nature of the agent and host control of pathogenesis. *J Gen Virol* **72 (Pt 3):** 595-603

Bruce ME, Will RG, Ironside JW, McConnell I, Drummond D, Suttie A, McCardle L, Chree A, Hope J, Birkett C, Cousens S, Fraser H, Bostock CJ (1997) Transmissions to mice indicate that 'new variant' CJD is caused by the BSE agent. *Nature* **389:** 498-501

Brugg B, Matus A (1991) Phosphorylation determines the binding of microtubule-associated protein 2 (MAP2) to microtubules in living cells. *J Cell Biol* **114:** 735-743

Bueler H, Fischer M, Lang Y, Bluethmann H, Lipp HP, DeArmond SJ, Prusiner SB, Aguet M, Weissmann C (1992) Normal development and behaviour of mice lacking the neuronal cell-surface PrP protein. *Nature* **356:** 577-582

Burwinkel M, Riemer C, Schwarz A, Schultz J, Neidhold S, Bamme T, Baier M (2004) Role of cytokines and chemokines in prion infections of the central nervous system. *Int J Dev Neurosci* **22:** 497-505

Buschmann A, Biacabe AG, Ziegler U, Bencsik A, Madec JY, Erhardt G, Luhken G, Baron T, Groschup MH (2004) Atypical scrapie cases in Germany and France are identified by discrepant reaction patterns in BSE rapid tests. *J Virol Methods* **117:** 27-36

Buschmann A, Gretzschel A, Biacabe AG, Schiebel K, Corona C, Hoffmann C, Eiden M, Baron T, Casalone C, Groschup MH (2006) Atypical BSE in Germany--proof of transmissibility and biochemical characterization. *Vet Microbiol* **117:** 103-116

Caboclo LO, Huang N, Lepski GA, Livramento JA, Buchpiguel CA, Porto CS, Nitrini R (2002) Iatrogenic Creutzfeldt-Jakob disease following human growth hormone therapy: case report. *Arq Neuropsiquiatr* **60:** 458-461

Caceres A, Banker GA, Binder L (1986) Immunocytochemical localization of tubulin and microtubule-associated protein 2 during the development of hippocampal neurons in culture. *J Neurosci* **6:** 714-722

Caceres A, Binder LI, Payne MR, Bender P, Rebhun L, Steward O (1984) Differential subcellular localization of tubulin and the microtubule-associated protein MAP2 in brain tissue as revealed by immunocytochemistry with monoclonal hybridoma antibodies. *J Neurosci* **4:** 394-410

Cammermeyer J (1961) The importance of avoiding dark neurons in experimental neuropathology. *Act Neuropathologica (Berlin)* **1:** 245-270

Capobianco R, Casalone C, Suardi S, Mangieri M, Miccolo C, Limido L, Catania M, Rossi G, Di Fede G, Giaccone G, Bruzzone MG, Minati L, Corona C, Acutis P, Gelmetti D, Lombardi G, Groschup MH, Buschmann A, Zanusso G, Monaco S,

Caramelli M, Tagliavini F (2007) Conversion of the BASE prion strain into the BSE strain: the origin of BSE? *PLoS Pathog* **3:** e31

Carimalo J, Cronier S, Petit G, Peyrin JM, Boukhtouche F, Arbez N, Lemaigre-Dubreuil Y, Brugg B, Miquel MC (2005) Activation of the JNK-c-Jun pathway during the early phase of neuronal apoptosis induced by PrP106-126 and prion infection. *Eur J Neurosci* **21:** 2311-2319

Carleton A, Tremblay P, Vincent JD, Lledo PM (2001) Dose-dependent, prion protein (PrP)-mediated facilitation of excitatory synaptic transmission in the mouse hippocampus. *Pflugers Arch* **442:** 223-229

Carp RI, Ye X, Kascsak RJ, Rubenstein R (1994) The nature of the scrapie agent. Biological characteristics of scrapie in different scrapie strain-host combinations. *Ann N Y Acad Sci* **724:** 221-234

Casalone C, Zanusso G, Acutis P, Ferrari S, Capucci L, Tagliavini F, Monaco S, Caramelli M (2004) Identification of a second bovine amyloidotic spongiform encephalopathy: molecular similarities with sporadic Creutzfeldt-Jakob disease. *Proc Natl Acad Sci U S A* **101:** 3065-3070

Cassarino DS, Bennett JP, Jr. (1999) An evaluation of the role of mitochondria in neurodegenerative diseases: mitochondrial mutations and oxidative pathology, protective nuclear responses, and cell death in neurodegeneration. *Brain Res Brain Res Rev* **29:** 1-25

Castilla J, Morales R, Saa P, Barria M, Gambetti P, Soto C (2008) Cell-free propagation of prion strains. *Embo J* **27:** 2557-2566

Castilla J, Saa P, Hetz C, Soto C (2005) In vitro generation of infectious scrapie prions. *Cell* **121:** 195-206

Caughey B, Brown K, Raymond GJ, Katzenstein GE, Thresher W (1994) Binding of the protease-sensitive form of PrP (prion protein) to sulfated glycosaminoglycan and congo red [corrected]. *J Virol* **68:** 2135-2141

Caughey B, Kocisko DA, Raymond GJ, Lansbury PT, Jr. (1995) Aggregates of scrapie-associated prion protein induce the cell-free conversion of protease-sensitive prion protein to the protease-resistant state. *Chem Biol* **2:** 807-817

Caviston JP, Holzbaur EL (2006) Microtubule motors at the intersection of trafficking and transport. *Trends Cell Biol* **16:** 530-537

Cerpa W, Dinamarca MC, Inestrosa NC (2008) Structure-function implications in Alzheimer's disease: effect of Abeta oligomers at central synapses. *Curr Alzheimer Res* **5:** 233-243

Chaitanya GV, Babu PP (2008) Multiple apoptogenic proteins are involved in the nuclear translocation of Apoptosis Inducing Factor during transient focal cerebral ischemia in rat. *Brain Res* **1246:** 178-190

Chandler R L (1961) Encephalopathy in mice produced by inoculation with scrapie brain material. *Lancet* **1:** 1378-1379

Chen X, Winters CA, Reese TS (2008) Life inside a thin section: tomography. *J Neurosci* **28:** 9321-9327

Chesebro B (1998) BSE and prions: uncertainties about the agent. *Science* **279:** 42-43

Chiesa R, Piccardo P, Dossena S, Nowoslawski L, Roth KA, Ghetti B, Harris DA (2005) Bax deletion prevents neuronal loss but not neurological symptoms in a transgenic model of inherited prion disease. *Proc Natl Acad Sci U S A* **102:** 238-243

Cho BB, Toledo-Pereyra LH (2008) Caspase-independent programmed cell death following ischemic stroke. *J Invest Surg* **21:** 141-147

Cho HJ (1976) Is the scrapie agent a virus? *Nature* **262:** 411-412

Choi SI, Ju WK, Choi EK, Kim J, Lea HZ, Carp RI, Wisniewski HM, Kim YS (1998) Mitochondrial dysfunction induced by oxidative stress in the brains of hamsters infected with the 263 K scrapie agent. *Acta Neuropathol* **96:** 279-286

Christophe M, Nicolas S (2006) Mitochondria: a target for neuroprotective interventions in cerebral ischemia-reperfusion. *Curr Pharm Des* **12:** 739-757

Cingolani LA, Goda Y (2008) Actin in action: the interplay between the actin cytoskeleton and synaptic efficacy. *Nat Rev Neurosci* **9:** 344-356

Cleveland DW, Hwo SY, Kirschner MW (1977) Purification of tau, a microtubule-associated protein that induces assembly of microtubules from purified tubulin. *J Mol Biol* **116:** 207-225

Clinton J, Forsyth C, Royston MC, Roberts GW (1993) Synaptic degeneration is the primary neuropathological feature in prion disease: a preliminary study. *Neuroreport* **4:** 65-68

Cohen FE (1999) Protein misfolding and prion diseases. *J Mol Biol* **293:** 313-320

Cohen GM (1997) Caspases: the executioners of apoptosis. *Biochem J* **326 (Pt 1):** 1-16

Colling SB, Khana M, Collinge J, Jefferys JG (1997) Mossy fibre reorganization in the hippocampus of prion protein null mice. *Brain Res* **755:** 28-35

Collinge J, Sidle KC, Meads J, Ironside J, Hill AF (1996) Molecular analysis of prion strain variation and the aetiology of 'new variant' CJD. *Nature* **383:** 685-690

Collinge J, Whitfield J, McKintosh E, Beck J, Mead S, Thomas DJ, Alpers MP (2006) Kuru in the 21st century--an acquired human prion disease with very long incubation periods. *Lancet* **367:** 2068-2074

Collinge J, Whittington MA, Sidle KC, Smith CJ, Palmer MS, Clarke AR, Jefferys JG (1994) Prion protein is necessary for normal synaptic function. *Nature* **370:** 295-297

Colm H, knight R (2002) Clinical features of variant Creutzfeldt-Jakob disease. *Rev Med Virol* **12:** 143-150

Cordery RJ, Hall M, Cipolotti L, Al-Sarraj S, O'Donovan DG, Davidson L, Adlard P, Rossor MN (2003) Early cognitive decline in Creutzfeldt-Jakob disease associated with human growth hormone treatment. *J Neurol Neurosurg Psychiatry* **74:** 1412-1416

Corsaro A, Thellung S, Villa V, Principe DR, Paludi D, Arena S, Millo E, Schettini D, Damonte G, Aceto A, Schettini G, Florio T (2003) Prion protein fragment 106-126 induces a p38 MAP kinase-dependent apoptosis in SH-SY5Y neuroblastoma cells independently from the amyloid fibril formation. *Ann N Y Acad Sci* **1010:** 610-622

Cosseddu GM, Agrimi U, Pinto J, Schudel AA (2007) Advances in scrapie research. *Rev Sci Tech* **26:** 657-668

Coulpier M, Messiaen S, Hamel R, Fernandez de Marco M, Lilin T, Eloit M (2006) Bax deletion does not protect neurons from BSE-induced death. *Neurobiol Dis* **23:** 603-611

Creutzfeldt HG (1920) Uber eine eigenartige herdformige Erkrankung des Zentralnervensystems. . *Z Ges Neurol Psychiat* **57:** 1-18

Criado JR, Sanchez-Alavez M, Conti B, Giacchino JL, Wills DN, Henriksen SJ, Race R, Manson JC, Chesebro B, Oldstone MB (2005) Mice devoid of prion protein have cognitive deficits that are rescued by reconstitution of PrP in neurons. *Neurobiol Dis* **19:** 255-265

Croes EA, Jansen GH, Lemstra AW, Frijns CJ, van Gool WA, van Duijn CM (2001) The first two patients with dura mater associated Creutzfeldt-Jakob disease in the Netherlands. *J Neurol* **248:** 877-880

Cuille' J, Chelle PL (1936) La maladie dite tremblante du mouton, est-elle inoculable? *Comptes rendu de l'Academie des Sciences* **203:** 1552-1554

Cuille' J, Chelle PL (1939) Experimental transmission of trembling to the goat. *CR Seances Acad Sci* **208:** 1058-1060

Cunningham AA, Kirkwood JK, Dawson M, Spencer YI, Green RB, Wells GA (2004) Bovine spongiform encephalopathy infectivity in greater kudu (Tragelaphus strepsiceros). *Emerg Infect Dis* **10:** 1044-1049

Cunningham C, Deacon R, Wells H, Boche D, Waters S, Diniz CP, Scott H, Rawlins JN, Perry VH (2003) Synaptic changes characterize early behavioural signs in the ME7 model of murine prion disease. *Eur J Neurosci* **17:** 2147-2155

D'Andrea MR, Ilyin S, Plata-Salaman CR (2001) Abnormal patterns of microtubule-associated protein-2 (MAP-2) immunolabeling in neuronal nuclei and Lewy bodies in Parkinson's disease substantia nigra brain tissues. *Neurosci Lett* **306:** 137-140

Dawson M, Hoinville LJ, Hosie BD, Hunter N (1998) Guidance on the use of PrP genotyping as an aid to the control of clinical scrapie. Scrapie Information Group. *Vet Rec* **142:** 623-625

Detwiler LA, Baylis M (2003) The epidemiology of scrapie. *Rev Sci Tech* **22:** 121-143

Diarra-Mehrpour M, Arrabal S, Jalil A, Pinson X, Gaudin C, Pietu G, Pitaval A, Ripoche H, Eloit M, Dormont D, Chouaib S (2004) Prion protein prevents human breast carcinoma cell line from tumor necrosis factor alpha-induced cell death. *Cancer Res* **64:** 719-727

Dickinson AG, Fraser H (1969) Genetical control of the concentration of ME7 scrapie agent in mouse spleen. *J Comp Pathol* **79:** 363-366

Dickinson AG, Fraser H, Outram GW (1975) Scrapie incubation time can exceed natural lifespan. *Nature* **256:** 732-733

Dickinson AG, Meikle VM, Fraser H (1968) Identification of a gene which controls the incubation period of some strains of scrapie agent in mice. *J Comp Pathol* **78:** 293-299

Dickinson AG, Outram GW (1979) *Slow Transmissible Diseases of the Nervous System*
Vol. 1, New York: Academic Press.

Dickinson AG, Outram GW (1988) Genetic aspects of unconventional virus infections: the basis of the virino hypothesis. *Ciba Found Symp* **135:** 63-83

Dickinson AG, Taylor DM (1978) Resistance of scrapie agent to decontamination. *N Engl J Med* **299:** 1413-1414

Diedrich JF, Bendheim PE, Kim YS, Carp RI, Haase AT (1991) Scrapie-associated prion protein accumulates in astrocytes during scrapie infection. *Proc Natl Acad Sci U S A* **88:** 375-379

Diener TO (1973) Similarities between the scrapie agent and the agent of the potato spindle tuber disease. *Ann Clin Res* **5:** 268-278

Diringer H (1984) Sustained viremia in experimental hamster scrapie. Brief report. *Arch Virol* **82:** 105-109

Doherr MG (2003) Bovine spongiform encephalopathy (BSE)--infectious, contagious, zoonotic or production disease? *Acta Vet Scand Suppl* **98:** 33-42

Dorandeu A, Wingertsmann L, Chretien F, Delisle MB, Vital C, Parchi P, Montagna P, Lugaresi E, Ironside JW, Budka H, Gambetti P, Gray F (1998) Neuronal apoptosis in fatal familial insomnia. *Brain Pathol* **8:** 531-537

Dron M, Bailly Y, Beringue V, Haeberle AM, Griffond B, Risold PY, Tovey MG, Laude H, Dandoy-Dron F (2006) SCRG1, a potential marker of autophagy in transmissible spongiform encephalopathies. *Autophagy* **2:** 58-60

Eckroade RJ, ZuRhein GM, Hanson RP (1973) Transmissible mink encephalopathy in carnivores: clinical, light and electron microscopic studies in raccons, skunks and ferrets. *J Wildl Dis* **9:** 229-240

Ehlers B, Rudolph R, Diringer H (1984) The reticuloendothelial system in scrapie pathogenesis. *J Gen Virol* **65 (Pt 2):** 423-428

Eklund CM, Kennedy RC, Hadlow WJ (1967) Pathogenesis of scrapie virus infection in the mouse. *J Infect Dis* **117:** 15-22

Elliott EJ, MacAuley C, D'Addio V, Rohwer RG (2005) Transfusion via the carotid artery in the hamster. *Contemp Top Lab Anim Sci* **44:** 28-30

Ellis RE, Yuan JY, Horvitz HR (1991) Mechanisms and functions of cell death. *Annu Rev Cell Biol* **7:** 663-698

Ermonval M, Mouillet-Richard S, Codogno P, Kellermann O, Botti J (2003) Evolving views in prion glycosylation: functional and pathological implications. *Biochimie* **85:** 33-45

Ersdal C, Simmons MM, Gonzalez L, Goodsir CM, Martin S, Jeffrey M (2004) Relationships between ultrastructural scrapie pathology and patterns of abnormal prion protein accumulation. *Acta Neuropathol* **107:** 428-438

Fabrizi C, Silei V, Menegazzi M, Salmona M, Bugiani O, Tagliavini F, Suzuki H, Lauro GM (2001) The stimulation of inducible nitric-oxide synthase by the prion protein fragment 106--126 in human microglia is tumor necrosis factor-alpha-dependent and involves p38 mitogen-activated protein kinase. *J Biol Chem* **276:** 25692-25696

Fairbairn DW, Carnahan KG, Thwaits RN, Grigsby RV, Holyoak GR, O'Neill KL (1994) Detection of apoptosis induced DNA cleavage in scrapie-infected sheep brain. *FEMS Microbiol Lett* **115:** 341-346

Farfara D, Lifshitz V, Frenkel D (2008) Neuroprotective and neurotoxic properties of glial cells in the pathogenesis of Alzheimer's disease. *J Cell Mol Med* **12:** 762-780

Farquhar CF, Dornan J, Somerville RA, Tunstall AM, Hope J (1994) Effect of Sinc genotype, agent isolate and route of infection on the accumulation of protease-resistant PrP in non-central nervous system tissues during the development of murine scrapie. *J Gen Virol* **75 (Pt 3):** 495-504

Ferreiro E, Costa R, Marques S, Cardoso SM, Oliveira CR, Pereira CM (2008) Involvement of mitochondria in endoplasmic reticulum stress-induced apoptotic cell death pathway triggered by the prion peptide PrP(106-126). *J Neurochem* **104:** 766-776

Ferreiro E, Eufrasio A, Pereira C, Oliveira CR, Rego AC (2007) Bcl-2 overexpression protects against amyloid-beta and prion toxicity in GT1-7 neural cells. *J Alzheimers Dis* **12:** 223-228

Ferrer I (2002) Synaptic pathology and cell death in the cerebellum in Creutzfeldt-Jakob disease. *Cerebellum* **1:** 213-222

Ferrer I, Friguls B, Dalfo E, Justicia C, Planas AM (2003) Caspase-dependent and caspase-independent signalling of apoptosis in the penumbra following middle cerebral artery occlusion in the adult rat. *Neuropathol Appl Neurobiol* **29:** 472-481

Ferri KF, Kroemer G (2001) Organelle-specific initiation of cell death pathways. *Nat Cell Biol* **3:** E255-263

Fiala JC, Spacek J, Harris KM (2002) Dendritic spine pathology: cause or consequence of neurological disorders? *Brain Res Brain Res Rev* **39:** 29-54

Filonova LH, Bozhkov PV, Brukhin VB, Daniel G, Zhivotovsky B, von Arnold S (2000) Two waves of programmed cell death occur during formation and development of somatic embryos in the gymnosperm, Norway spruce. *J Cell Sci* **113 Pt 24:** 4399-4411

Ford MJ, Burton LJ, Li H, Graham CH, Frobert Y, Grassi J, Hall SM, Morris RJ (2002a) A marked disparity between the expression of prion protein and its message by neurones of the CNS. *Neuroscience* **111:** 533-551

Ford MJ, Burton LJ, Morris RJ, Hall SM (2002b) Selective expression of prion protein in peripheral tissues of the adult mouse. *Neuroscience* **113:** 177-192

Foster J, McKenzie C, Parnham D, Drummond D, Goldmann W, Stevenson E, Hunter N (2006) Derivation of a scrapie-free sheep flock from the progeny of a flock affected by scrapie. *Vet Rec* **159:** 42-45

Foster JD, Parnham DW, Hunter N, Bruce M (2001) Distribution of the prion protein in sheep terminally affected with BSE following experimental oral transmission. *J Gen Virol* **82:** 2319-2326

Fournier JG, Escaig-Haye F, Grigoriev V (2000) Ultrastructural localization of prion proteins: physiological and pathological implications. *Microsc Res Tech* **50:** 76-88

Frankfurt OS, Krishan A (2001) Identification of apoptotic cells by formamide-induced dna denaturation in condensed chromatin. *J Histochem Cytochem* **49:** 369-378

Fraser H (1976) The pathology of a natural and experimental scrapie. *Front Biol* **44:** 267-305

Fraser H (1982) Neuronal spread of scrapie agent and targeting of lesions within the retino-tectal pathway. *Nature* **295:** 149-150

Fraser H (1993) Diversity in the neuropathology of scrapie-like diseases in animals. *Br Med Bull* **49:** 792-809

Fraser H, Bruce, M.E., Davies, D., Farquhar, C.F., McBride, P.A. (1992) The lymphoreticular system in the pathogenesis of scrapie. In *Prion diseases of Humans and Animals*, S.B. Prusiner JC, J. Powell, and B. Anderton (ed), pp 308-317. Chichester: Ellis Horwood

Fraser H, Dickinson AG (1967) Distribution of experimentally induced scrapie lesions in the brain. *Nature* **216:** 1310-1311

Fraser H, Dickinson AG (1978) Studies of the lymphoreticular system in the pathogenesis of scrapie: the role of spleen and thymus. *J Comp Pathol* **88:** 563-573

Fraser J, Jeffrey M, Halliday W, Fowler N, Goodsir C, Brown D (1995) Early loss of neurons and axon terminals in scrapie-affected mice revealed by morphometry and immunocytochemistry. *Mol Chem Neuropathol* **24:** 245-249

Fraser JR (2002) What is the basis of transmissible spongiform encephalopathy induced neurodegeneration and can it be repaired? *Neuropathol Appl Neurobiol* **28:** 1-11

Freund TF (2002) Changes in the views of neuronal connectivity and communication after Cajal: examples from the hippocampus. *Prog Brain Res* **136:** 203-213

Gajdusek DC (1963) Kuru. *Trans R Soc Trop Med Hyg* **57:** 151-169

Gajdusek DC, Alpers, M. (1966) Kuru in childhood: Disappearance of the disease in the younger age group. *The journal of pediatrics* **69:** 886-887

Gajdusek DC, Gibbs CJ (1964) Attempts to Demonstrate a Transmissible Agent in Kuru, Amyotrophic Lateral Sclerosis, and Other Sub-Acute and Chronic Nervous System Degenerations of Man. *Nature* **204:** 257-259

Gajdusek DC, Gibbs CJ, Alpers M (1966) Experimental transmission of a Kuru-like syndrome to chimpanzees. *Nature* **209:** 794-796

Gajdusek DC, Zigas V (1957) Degenerative disease of the central nervous system in New Guinea; the endemic occurrence of kuru in the native population. *N Engl J Med* **257:** 974-978

Gambetti P, Kong Q, Zou W, Parchi P, Chen SG (2003) Sporadic and familial CJD: classification and characterisation. *Br Med Bull* **66:** 213-239

Gibbs ME, Hutchinson D, Hertz L (2008) Astrocytic involvement in learning and memory consolidation. *Neurosci Biobehav Rev* **32:** 927-944

Giese A, Brown DR, Groschup MH, Feldmann C, Haist I, Kretzschmar HA (1998) Role of microglia in neuronal cell death in prion disease. *Brain Pathol* **8:** 449-457

Giese A, Groschup MH, Hess B, Kretzschmar HA (1995) Neuronal cell death in scrapie-infected mice is due to apoptosis. *Brain Pathol* **5:** 213-221

Giovanni A, Keramaris E, Morris EJ, Hou ST, O'Hare M, Dyson N, Robertson GS, Slack RS, Park DS (2000) E2F1 mediates death of B-amyloid-treated cortical neurons in a manner independent of p53 and dependent on Bax and caspase 3. *J Biol Chem* **275:** 11553-11560

Glatzel M, Abela E, Maissen M, Aguzzi A (2003) Extraneural pathologic prion protein in sporadic Creutzfeldt-Jakob disease. *N Engl J Med* **349:** 1812-1820

Glenner GG, Eanes ED, Bladen HA, Linke RP, Termine JD (1974) Beta-pleated sheet fibrils. A comparison of native amyloid with synthetic protein fibrils. *J Histochem Cytochem* **22:** 1141-1158

Godsave SF, Wille H, Kujala P, Latawiec D, DeArmond SJ, Serban A, Prusiner SB, Peters PJ (2008) Cryo-immunogold electron microscopy for prions: toward identification of a conversion site. *J Neurosci* **28:** 12489-12499

Goedert M, Spillantini MG, Jakes R, Rutherford D, Crowther RA (1989a) Multiple isoforms of human microtubule-associated protein tau: sequences and localization in neurofibrillary tangles of Alzheimer's disease. *Neuron* **3:** 519-526

Goedert M, Spillantini MG, Potier MC, Ulrich J, Crowther RA (1989b) Cloning and sequencing of the cDNA encoding an isoform of microtubule-associated protein tau containing four tandem repeats: differential expression of tau protein mRNAs in human brain. *Embo J* **8:** 393-399

Gohel C, Grigoriev V, Escaig-Haye F, Lasmezas CI, Deslys JP, Langeveld J, Akaaboune M, Hantai D, Fournier JG (1999) Ultrastructural localization of cellular prion protein (PrPc) at the neuromuscular junction. *J Neurosci Res* **55:** 261-267

Goldfarb LG, Brown P, McCombie WR, Goldgaber D, Swergold GD, Wills PR, Cervenakova L, Baron H, Gibbs CJ, Jr., Gajdusek DC (1991) Transmissible familial Creutzfeldt-Jakob disease associated with five, seven, and eight extra octapeptide coding repeats in the PRNP gene. *Proc Natl Acad Sci U S A* **88:** 10926-10930

Goldmann W (2008) PrP genetics in ruminant transmissible spongiform encephalopathies. *Vet Res* **39:** 30

Gorham J. (1991) Viral and bacterial diseases of mink in Soviet Union. *Fur Rancher* **71:** 10-11

Gray F, Chretien F, Adle-Biassette H, Dorandeu A, Ereau T, Delisle MB, Kopp N, Ironside JW, Vital C (1999) Neuronal apoptosis in Creutzfeldt-Jakob disease. *J Neuropathol Exp Neurol* **58:** 321-328

Green KM, Castilla J, Seward TS, Napier DL, Jewell JE, Soto C, Telling GC (2008) Accelerated high fidelity prion amplification within and across prion species barriers. *PLoS Pathog* **4:** e1000139

Griffith JS (1967) Self-replication and scrapie. *Nature* **215:** 1043-1044

Griffiths RE, Heesom KJ, Anstee DJ (2007) Normal prion protein trafficking in cultured human erythroblasts. *Blood* **110:** 4518-4525

Groschup MH, Weiland F, Straub OC, Pfaff E (1996) Detection of scrapie agent in the peripheral nervous system of a diseased sheep. *Neurobiol Dis* **3:** 191-195

Gruenbaum Y, Margalit A, Goldman RD, Shumaker DK, Wilson KL (2005) The nuclear lamina comes of age. *Nat Rev Mol Cell Biol* **6:** 21-31

Grutzendler J, Helmin K, Tsai J, Gan WB (2007) Various dendritic abnormalities are associated with fibrillar amyloid deposits in Alzheimer's disease. *Ann N Y Acad Sci* **1097:** 30-39

Guentchev M, Voigtlander T, Haberler C, Groschup MH, Budka H (2000) Evidence for oxidative stress in experimental prion disease. *Neurobiol Dis* **7:** 270-273

Gunst SJ, Zhang W (2008) Actin cytoskeletal dynamics in smooth muscle: a new paradigm for the regulation of smooth muscle contraction. *Am J Physiol Cell Physiol* **295:** C576-587

Haass C, Selkoe DJ (2007) Soluble protein oligomers in neurodegeneration: lessons from the Alzheimer's amyloid beta-peptide. *Nat Rev Mol Cell Biol* **8:** 101-112

Hadlow WJ (1959) Scrapie and Kuru. *Lancet* **ii:** 289-290

Hadlow WJ, Kennedy RC, Race RE (1982) Natural infection of Suffolk sheep with scrapie virus. *J Infect Dis* **146:** 657-664

Hadlow WJ, Race RE, Kennedy RC (1987) Temporal distribution of transmissible mink encephalopathy virus in mink inoculated subcutaneously. *J Virol* **61:** 3235-3240

Haeberle AM, Ribaut-Barassin C, Bombarde G, Mariani J, Hunsmann G, Grassi J, Bailly Y (2000) Synaptic prion protein immuno-reactivity in the rodent cerebellum. *Microsc Res Tech* **50:** 66-75

Hafiz FB, Brown DR (2000) A model for the mechanism of astrogliosis in prion disease. *Mol Cell Neurosci* **16:** 221-232

Hainfellner JA, Brantner-Inthaler S, Cervenakova L, Brown P, Kitamoto T, Tateishi J, Diringer H, Liberski PP, Regele H, Feucht M, et al. (1995) The original Gerstmann-

Straussler-Scheinker family of Austria: divergent clinicopathological phenotypes but constant PrP genotype. *Brain Pathol* **5:** 201-211

Hall DH, Gu G, Garcia-Anoveros J, Gong L, Chalfie M, Driscoll M (1997) Neuropathology of degenerative cell death in Caenorhabditis elegans. *J Neurosci* **17:** 1033-1045

Hammond JW, Cai D, Verhey KJ (2008) Tubulin modifications and their cellular functions. *Curr Opin Cell Biol* **20:** 71-76

Harigaya Y, Shoji M, Shirao T, Hirai S (1996) Disappearance of actin-binding protein, drebrin, from hippocampal synapses in Alzheimer's disease. *J Neurosci Res* **43:** 87-92

Hariri M, Millane G, Guimond MP, Guay G, Dennis JW, Nabi IR (2000) Biogenesis of multilamellar bodies via autophagy. *Mol Biol Cell* **11:** 255-268

Harris DA, Lele P, Snider WD (1993) Localization of the mRNA for a chicken prion protein by in situ hybridization. *Proc Natl Acad Sci U S A* **90:** 4309-4313

Hartsough GR, Burger D (1965) Encephalopathy of mink. I. Epizootiologic and clinical observations. *J Infect Dis* **115:** 387-392

Hayashi K, Shirao T (1999) Change in the shape of dendritic spines caused by overexpression of drebrin in cultured cortical neurons. *J Neurosci* **19:** 3918-3925

Head MW, Ritchie D, Smith N, McLoughlin V, Nailon W, Samad S, Masson S, Bishop M, McCardle L, Ironside JW (2004) Peripheral tissue involvement in sporadic, iatrogenic, and variant Creutzfeldt-Jakob disease: an immunohistochemical, quantitative, and biochemical study. *Am J Pathol* **164:** 143-153

Heiseke A, Aguib Y, Riemer C, Baier M, Schatzl HM (2009) Lithium induces clearance of protease resistant prion protein in prion-infected cells by induction of autophagy. *J Neurochem*

Hering H, Sheng M (2001) Dendritic spines: structure, dynamics and regulation. *Nat Rev Neurosci* **2:** 880-888

Hetz C, Russelakis-Carneiro M, Maundrell K, Castilla J, Soto C (2003) Caspase-12 and endoplasmic reticulum stress mediate neurotoxicity of pathological prion protein. *Embo J* **22:** 5435-5445

Hill AF, Antoniou M, Collinge J (1999a) Protease-resistant prion protein produced in vitro lacks detectable infectivity. *J Gen Virol* **80 (Pt 1):** 11-14

Hill AF, Butterworth RJ, Joiner S, Jackson G, Rossor MN, Thomas DJ, Frosh A, Tolley N, Bell JE, Spencer M, King A, Al-Sarraj S, Ironside JW, Lantos PL, Collinge J (1999b) Investigation of variant Creutzfeldt-Jakob disease and other human prion diseases with tonsil biopsy samples. *Lancet* **353:** 183-189

Hill AF, Desbruslais M, Joiner S, Sidle KC, Gowland I, Collinge J, Doey LJ, Lantos P (1997) The same prion strain causes vCJD and BSE. *Nature* **389:** 448-450, 526

Hilton DA, Fathers E, Edwards P, Ironside JW, Zajicek J (1998) Prion immunoreactivity in appendix before clinical onset of variant Creutzfeldt-Jakob disease. *Lancet* **352:** 703-704

Hirokawa N, Noda Y (2008) Intracellular transport and kinesin superfamily proteins, KIFs: structure, function, and dynamics. *Physiol Rev* **88:** 1089-1118

Hogan RN, Baringer JR, Prusiner SB (1987) Scrapie infection diminishes spines and increases varicosities of dendrites in hamsters: a quantitative Golgi analysis. *J Neuropathol Exp Neurol* **46:** 461-473

Hornabrook RW, Moir DJ (1970) Kuru: epidemiological trends. *Lancet* **2:** 1175-1179

Horonchik L, Tzaban S, Ben-Zaken O, Yedidia Y, Rouvinski A, Papy-Garcia D, Barritault D, Vlodavsky I, Taraboulos A (2005) Heparan sulfate is a cellular receptor for purified infectious prions. *J Biol Chem* **280:** 17062-17067

Houston F, McCutcheon S, Goldmann W, Chong A, Foster J, Siso S, Gonzalez L, Jeffrey M, Hunter N (2008) Prion diseases are efficiently transmitted by blood transfusion in sheep. *Blood* **112:** 4739-4745

http://www.cjd.ed.ac.uk/.

Huang WP, Klionsky DJ (2002) Autophagy in yeast: a review of the molecular machinery. *Cell Struct Funct* **27:** 409-420

Huber G, Matus A (1984) Differences in the cellular distributions of two microtubule-associated proteins, MAP1 and MAP2, in rat brain. *J Neurosci* **4:** 151-160

Hundt C, Peyrin JM, Haik S, Gauczynski S, Leucht C, Rieger R, Riley ML, Deslys JP, Dormont D, Lasmezas CI, Weiss S (2001) Identification of interaction domains of the prion protein with its 37-kDa/67-kDa laminin receptor. *Embo J* **20:** 5876-5886

Hunter N (1997) PrP genetics in sheep and the applications for scrapie and BSE. *Trends Microbiol* **5:** 331-334

Hunter N, Cairns D, Foster JD, Smith G, Goldmann W, Donnelly K (1997a) Is scrapie solely a genetic disease? *Nature* **386:** 137

Hunter N, Foster J, Chong A, McCutcheon S, Parnham D, Eaton S, MacKenzie C, Houston F (2002) Transmission of prion diseases by blood transfusion. *J Gen Virol* **83:** 2897-2905

Hunter N, Goldmann W, Foster JD, Cairns D, Smith G (1997b) Natural scrapie and PrP genotype: case-control studies in British sheep. *Vet Rec* **141:** 137-140

Hunter N, Moore L, Hosie BD, Dingwall WS, Greig A (1997c) Association between natural scrapie and PrP genotype in a flock of Suffolk sheep in Scotland. 140 Thesis, Vet Rec,

Ierna M, Farquhar CF, Outram GW, Bruce ME (2006) Resistance of neonatal mice to scrapie is associated with inefficient infection of the immature spleen. *J Virol* **80:** 474-482

Iizuka T, Sasaki M, Koike M (2006) Apoptosis in lactating rat mammary tissue using TUNEL method. In *Short and long term effects of breast feeding on child health* Vol. 478, pp 369-370. USA: Springer US

Imamura K, Shirao T, Mori K, Obata K (1992) Changes of drebrin expression in the visual cortex of the cat during development. *Neurosci Res* **13:** 33-41

Inaba K (2003) Molecular architecture of the sperm flagella: molecules for motility and signaling. *Zoolog Sci* **20:** 1043-1056

Iqbal K, Alonso Adel C, Chen S, Chohan MO, El-Akkad E, Gong CX, Khatoon S, Li B, Liu F, Rahman A, Tanimukai H, Grundke-Iqbal I (2005) Tau pathology in Alzheimer disease and other tauopathies. *Biochim Biophys Acta* **1739:** 198-210

Isomura H, Shinagawa M, Ikegami Y, Sasaki K, Ishiguro N (1991) Morphological and biochemical evidence that scrapie-associated fibrils are derived from aggregated amyloid-like filaments. *Virus Res* **18:** 191-201

Itoh TJ, Hisanaga S, Hosoi T, Kishimoto T, Hotani H (1997) Phosphorylation states of microtubule-associated protein 2 (MAP2) determine the regulatory role of MAP2 in microtubule dynamics. *Biochemistry* **36:** 12574-12582

Jakob A (1921) Uber eigenartige Erkrankungen des Zentralnervensystems mit bemerkenswertem anatomischem Befunde (spastiche Pseudo-sklerose-Encephalomyelopathie mit disseminier-ten Degenerationsherden). *Dtsch Z Nervenheilk* **70:** 132-146

Jamieson E, Jeffrey M, Ironside JW, Fraser JR (2001a) Activation of Fas and caspase 3 precedes PrP accumulation in 87V scrapie. *Neuroreport* **12:** 3567-3572

Jamieson E, Jeffrey M, Ironside JW, Fraser JR (2001b) Apoptosis and dendritic dysfunction precede prion protein accumulation in 87V scrapie. *Neuroreport* **12:** 2147-2153

Jeffrey M, Fraser JR, Halliday WG, Fowler N, Goodsir CM, Brown DA (1995a) Early unsuspected neuron and axon terminal loss in scrapie-infected mice revealed by morphometry and immunocytochemistry. *Neuropathol Appl Neurobiol* **21:** 41-49

Jeffrey M, Goodbrand IA, Goodsir CM (1995b) Pathology of the transmissible spongiform encephalopathies with special emphasis on ultrastructure. *Micron* **26:** 277-298

Jeffrey M, Goodsir CM, Bruce M, McBride PA, Scott JR, Halliday WG (1994a) Correlative light and electron microscopy studies of PrP localisation in 87V scrapie. *Brain Res* **656:** 329-343

Jeffrey M, Goodsir CM, Bruce ME, McBride PA, Scott JR (1994b) Infection-specific prion protein (PrP) accumulates on neuronal plasmalemma in scrapie-infected mice. *Ann N Y Acad Sci* **724:** 327-330

Jeffrey M, Goodsir CM, Race RE, Chesebro B (2004) Scrapie-specific neuronal lesions are independent of neuronal PrP expression. *Ann Neurol* **55:** 781-792

Jeffrey M, Halliday WG, Bell J, Johnston AR, MacLeod NK, Ingham C, Sayers AR, Brown DA, Fraser JR (2000) Synapse loss associated with abnormal PrP precedes neuronal degeneration in the scrapie-infected murine hippocampus. *Neuropathol Appl Neurobiol* **26:** 41-54

Jeffrey M, Halliday WG, Goodsir CM (1992a) A morphometric and immunohistochemical study of the vestibular nuclear complex in bovine spongiform encephalopathy. *Acta Neuropathol (Berl)* **84:** 651-657

Jeffrey M, Martin S, Barr J, Chong A, Fraser JR (2001) Onset of accumulation of PrPres in murine ME7 scrapie in relation to pathological and PrP immunohistochemical changes. *J Comp Pathol* **124:** 20-28

Jeffrey M, Scott JR, Fraser H (1991) Scrapie inoculation of mice: light and electron microscopy of the superior colliculi. *Acta Neuropathol (Berl)* **81:** 562-571

Jeffrey M, Scott JR, Williams A, Fraser H (1992b) Ultrastructural features of spongiform encephalopathy transmitted to mice from three species of bovidae. *Acta Neuropathol* **84:** 559-569

Jesionek-Kupnicka D, Buczynski J, Kordek R, Liberski PP (1999) Neuronal loss and apoptosis in experimental Creutzfeldt-Jakob disease in mice. *Folia Neuropathol* **37:** 283-286

Jesionek-Kupnicka D, Buczynski J, Kordek R, Sobow T, Kloszewska I, Papierz W, Liberski PP (1997) Programmed cell death (apoptosis) in Alzheimer's disease and Creutzfeldt-Jakob disease. *Folia Neuropathol* **35:** 233-235

Jesionek-Kupnicka D, Kordek R, Buczynski J, Liberski PP (2001) Apoptosis in relation to neuronal loss in experimental Creutzfeldt-Jakob disease in mice. *Acta Neurobiol Exp (Wars)* **61:** 13-19

Johnson GV, Jope RS (1992) The role of microtubule-associated protein 2 (MAP-2) in neuronal growth, plasticity, and degeneration. *J Neurosci Res* **33:** 505-512

Johnston AR, Fraser JR, Jeffrey M, MacLeod N (1998a) Alterations in potassium currents may trigger neurodegeneration in murine scrapie. *Exp Neurol* **151:** 326-333

Johnston AR, Fraser JR, Jeffrey M, MacLeod N (1998b) Synaptic plasticity in the CA1 area of the hippocampus of scrapie-infected mice. *Neurobiol Dis* **5:** 188-195

Jouannet P, Serres C (1998) [The movement of the human spermatozoon]. *Bull Acad Natl Med* **182:** 1025-1034; discussion 1034-1026

Kabeya Y, Mizushima N, Ueno T, Yamamoto A, Kirisako T, Noda T, Kominami E, Ohsumi Y, Yoshimori T (2000) LC3, a mammalian homologue of yeast Apg8p, is localized in autophagosome membranes after processing. *Embo J* **19:** 5720-5728

Kaech S, Parmar H, Roelandse M, Bornmann C, Matus A (2001) Cytoskeletal microdifferentiation: a mechanism for organizing morphological plasticity in dendrites. *Proc Natl Acad Sci U S A* **98:** 7086-7092

Kanaani J, Prusiner SB, Diacovo J, Baekkeskov S, Legname G (2005) Recombinant prion protein induces rapid polarization and development of synapses in embryonic rat hippocampal neurons in vitro. *J Neurochem* **95:** 1373-1386

Karsenti E, Nedelec F (2004) The mitotic spindle and actin tails. *Biol Cell* **96:** 237-240

Kaufmann WE, MacDonald SM, Altamura CR (2000) Dendritic cytoskeletal protein expression in mental retardation: an immunohistochemical study of the neocortex in Rett syndrome. *Cereb Cortex* **10:** 992-1004

Kayed R, Head E, Thompson JL, McIntire TM, Milton SC, Cotman CW, Glabe CG (2003) Common structure of soluble amyloid oligomers implies common mechanism of pathogenesis. *Science* **300:** 486-489

Kiechle T, Dedeoglu A, Kubilus J, Kowall NW, Beal MF, Friedlander RM, Hersch SM, Ferrante RJ (2002) Cytochrome C and caspase-9 expression in Huntington's disease. *Neuromolecular Med* **1:** 183-195

Kim E, Sheng M (2004) PDZ domain proteins of synapses. *Nat Rev Neurosci* **5:** 771-781

Kim JH, Manuelidis EE (1983) Ultrastructural findings in experimental Creutzfeldt-Jakob disease in guinea pigs. *J Neuropathol Exp Neurol* **42:** 29-43

Kim JH, Manuelidis EE (1986) Serial ultrastructural study of experimental Creutzfeldt-Jacob disease in guinea pigs. *Acta Neuropathol* **69:** 81-90

Kim JH, Manuelidis EE (1989) Neuronal alterations in experimental Creutzfeldt-Jakob disease: a Golgi study. *J Neurol Sci* **89:** 93-101

Kim JI, Choi SI, Kim NH, Jin JK, Choi EK, Carp RI, Kim YS (2001) Oxidative stress and neurodegeneration in prion diseases. *Ann N Y Acad Sci* **928:** 182-186

Kimberlin RH (1982) Scrapie agent: prions or virinos? *Nature* **297:** 107-108

Kimberlin RH, and Walker, C.A. (1993) Invasion of the CNS by scrapie agent and its spread to different parts of the brain. In *Virus non conventionels et affections du systeme nerveux central*, F. CLAC (ed), pp 17-33. Paris: Masson

Kimberlin RH, Cole S, Walker CA (1987) Pathogenesis of scrapie is faster when infection is intraspinal instead of intracerebral. *Microb Pathog* **2:** 405-415

Kimberlin RH, Field HJ, Walker CA (1983a) Pathogenesis of mouse scrapie: evidence for spread of infection from central to peripheral nervous system. *J Gen Virol* **64 Pt 3:** 713-716

Kimberlin RH, Hall SM, Walker CA (1983b) Pathogenesis of mouse scrapie. Evidence for direct neural spread of infection to the CNS after injection of sciatic nerve. *J Neurol Sci* **61:** 315-325

Kimberlin RH, Walker CA (1979) Pathogenesis of mouse scrapie: dynamics of agent replication in spleen, spinal cord and brain after infection by different routes. *J Comp Pathol* **89:** 551-562

Kimberlin RH, Walker CA (1980) Pathogenesis of mouse scrapie: evidence for neural spread of infection to the CNS. *J Gen Virol* **51:** 183-187

Kimberlin RH, Walker CA (1982) Pathogenesis of mouse scrapie: patterns of agent replication in different parts of the CNS following intraperitoneal infection. *J R Soc Med* **75:** 618-624

Kimberlin RH, Walker CA (1986) Pathogenesis of scrapie (strain 263K) in hamsters infected intracerebrally, intraperitoneally or intraocularly. *J Gen Virol* **67 (Pt 2):** 255-263

Kimberlin RH, Walker CA (1989) The role of the spleen in the neuroinvasion of scrapie in mice. *Virus Res* **12:** 201-211

Kimberlin RH, Walker, C.A. (1988) Pathogenesis of experimental scrapie. In *Novel infectious agents and the central nervous system (Ciba Foundation Symposium vol 135)*, G. Bock RM (ed), pp 37-62. Chichester: Wiley

Kirkwood JK, Wells GA, Wilesmith JW, Cunningham AA, Jackson SI (1990) Spongiform encephalopathy in an arabian oryx (Oryx leucoryx) and a greater kudu (Tragelaphus strepsiceros). *Vet Rec* **127:** 418-420

Kitamoto T, Shin RW, Doh-ura K, Tomokane N, Miyazono M, Muramoto T, Tateishi J (1992) Abnormal isoform of prion proteins accumulates in the synaptic structures of the central nervous system in patients with Creutzfeldt-Jakob disease. *Am J Pathol* **140:** 1285-1294

Klatzo I, Gajdusek DC, Zigas V (1959) Pathology of Kuru. *Lab Invest* **8:** 799-847

Kluck RM, Bossy-Wetzel E, Green DR, Newmeyer DD (1997) The release of cytochrome c from mitochondria: a primary site for Bcl-2 regulation of apoptosis. *Science* **275:** 1132-1136

Klyubin I, Walsh DM, Lemere CA, Cullen WK, Shankar GM, Betts V, Spooner ET, Jiang L, Anwyl R, Selkoe DJ, Rowan MJ (2005) Amyloid beta protein immunotherapy neutralizes Abeta oligomers that disrupt synaptic plasticity in vivo. *Nat Med* **11:** 556-561

Knobloch M, Mansuy IM (2008) Dendritic spine loss and synaptic alterations in Alzheimer's disease. *Mol Neurobiol* **37:** 73-82

Kojima N, Kato Y, Shirao T, Obata K (1988) Nucleotide sequences of two embryonic drebrins, developmentally regulated brain proteins, and developmental change in their mRNAs. *Brain Res* **464:** 207-215

Kojima N, Shirao T, Obata K (1993) Molecular cloning of a developmentally regulated brain protein, chicken drebrin A and its expression by alternative splicing of the drebrin gene. *Brain Res Mol Brain Res* **19:** 101-114

Kolomeisky AB, Fisher ME (2007) Molecular motors: a theorist's perspective. *Annu Rev Phys Chem* **58:** 675-695

Kong Q, Huang S, Zou W, Vanegas D, Wang M, Wu D, Yuan J, Zheng M, Bai H, Deng H, Chen K, Jenny AL, O'Rourke K, Belay ED, Schonberger LB, Petersen RB, Sy MS, Chen SG, Gambetti P (2005) Chronic wasting disease of elk: transmissibility to humans examined by transgenic mouse models. *J Neurosci* **25:** 7944-7949

Kosco MH, Pflugfelder E, Gray D (1992) Follicular dendritic cell-dependent adhesion and proliferation of B cells in vitro. *J Immunol* **148:** 2331-2339

Kovacs GG, Preusser M, Strohschneider M, Budka H (2005) Subcellular localization of disease-associated prion protein in the human brain. *Am J Pathol* **166:** 287-294

Kovacs GG, Trabattoni G, Hainfellner JA, Ironside JW, Knight RS, Budka H (2002) Mutations of the prion protein gene phenotypic spectrum. *J Neurol* **249:** 1567-1582

Kramer ML, Kratzin HD, Schmidt B, Romer A, Windl O, Liemann S, Hornemann S, Kretzschmar H (2001) Prion protein binds copper within the physiological concentration range. *J Biol Chem* **276:** 16711-16719

Krasnianski A, Bartl M, Sanchez Juan PJ, Heinemann U, Meissner B, Varges D, Schulze-Sturm U, Kretzschmar HA, Schulz-Schaeffer WJ, Zerr I (2008) Fatal familial insomnia: Clinical features and early identification. *Ann Neurol* **63:** 658-661

Kretzschmar HA (1993) Neuropathology of human prion diseases (spongiform encephalopathies). *Dev Biol Stand* **80:** 71-90

Kretzschmar HA, Honold G, Seitelberger F, Feucht M, Wessely P, Mehraein P, Budka H (1991) Prion protein mutation in family first reported by Gerstmann, Straussler, and Scheinker. *Lancet* **337:** 1160

Kretzschmar HA, Prusiner SB, Stowring LE, DeArmond SJ (1986) Scrapie prion proteins are synthesized in neurons. *Am J Pathol* **122:** 1-5

Kurschner C, Morgan JI (1995) The cellular prion protein (PrP) selectively binds to Bcl-2 in the yeast two-hybrid system. *Brain Res Mol Brain Res* **30:** 165-168

Kurschner C, Morgan JI (1996) Analysis of interaction sites in homo- and heteromeric complexes containing Bcl-2 family members and the cellular prion protein. *Brain Res Mol Brain Res* **37:** 249-258

Laine J, Marc ME, Sy MS, Axelrad H (2001) Cellular and subcellular morphological localization of normal prion protein in rodent cerebellum. *Eur J Neurosci* **14:** 47-56

Landis DM, Williams RS, Masters CL (1981) Golgi and electronmicroscopic studies of spongiform encephalopathy. *Neurology* **31:** 538-549

Lasmezas CI, Deslys JP, Robain O, Jaegly A, Beringue V, Peyrin JM, Fournier JG, Hauw JJ, Rossier J, Dormont D (1997) Transmission of the BSE agent to mice in the absence of detectable abnormal prion protein. *Science* **275:** 402-405

Lee MK, Cleveland DW (1996) Neuronal intermediate filaments. *Annu Rev Neurosci* **19:** 187-217

Lee SJ, Zhou T, Choi C, Wang Z, Benveniste EN (2000) Differential regulation and function of Fas expression on glial cells. *J Immunol* **164:** 1277-1285

Legname G, Baskakov IV, Nguyen HO, Riesner D, Cohen FE, DeArmond SJ, Prusiner SB (2004) Synthetic mammalian prions. *Science* **305:** 673-676

Leist M, Single B, Castoldi AF, Kuhnle S, Nicotera P (1997) Intracellular adenosine triphosphate (ATP) concentration: a switch in the decision between apoptosis and necrosis. *J Exp Med* **185:** 1481-1486

Liao YC, Lebo RV, Clawson GA, Smuckler EA (1986) Human prion protein cDNA: molecular cloning, chromosomal mapping, and biological implications. *Science* **233:** 364-367

Liberski PP (2004) Spongiform change--an electron microscopic view. *Folia Neuropathol* **42 Suppl B:** 59-70

Liberski PP, Bratosiewicz-Wasik J, Gajdusek DC, Brown P (2002a) Ultrastructural studies of experimental scrapie and Creutzfeldt-Jakob disease in hamsters. I. Alterations of myelinated axons. *Acta Neurobiol Exp (Wars)* **62:** 121-129

Liberski PP, Brown DR, Sikorska B, Caughey B, Brown P (2008) Cell death and autophagy in prion diseases (transmissible spongiform encephalopathies). *Folia Neuropathol* **46:** 1-25

Liberski PP, Gajdusek DC, Brown P (2002b) How do neurons degenerate in prion diseases or transmissible spongiform encephalopathies (TSEs): neuronal autophagy revisited. *Acta Neurobiol Exp (Wars)* **62:** 141-147

Liberski PP, Sikorska B, Bratosiewicz-Wasik J, Gajdusek DC, Brown P (2004) Neuronal cell death in transmissible spongiform encephalopathies (prion diseases) revisited: from apoptosis to autophagy. *Int J Biochem Cell Biol* **36:** 2473-2490

Liberski PP, Yanagihara R, Asher DM, Gibbs CJ, Jr., Gajdusek DC (1990) Reevaluation of the ultrastructural pathology of experimental Creutzfeldt-Jakob disease. Serial studies of the Fujisaki strain of Creutzfeldt-Jakob disease virus in mice. *Brain* **113 (Pt 1):** 121-137

Lin H, Schlaepfer WW (2006) Role of neurofilament aggregation in motor neuron disease. *Ann Neurol* **60:** 399-406

Liu WG, Brown DA, Fraser JR (2003) Immunohistochemical comparison of anti-prion protein (PrP) antibodies in the CNS of mice infected with scrapie. *J Histochem Cytochem* **51:** 1065-1071

Lledo PM, Tremblay P, DeArmond SJ, Prusiner SB, Nicoll RA (1996) Mice deficient for prion protein exhibit normal neuronal excitability and synaptic transmission in the hippocampus. *Proc Natl Acad Sci U S A* **93:** 2403-2407

Lo RY, Shyu WC, Lin SZ, Wang HJ, Chen SS, Li H (2007) New molecular insights into cellular survival and stress responses: neuroprotective role of cellular prion protein (PrPC). *Mol Neurobiol* **35:** 236-244

LoPresti P, Szuchet S, Papasozomenos SC, Zinkowski RP, Binder LI (1995) Functional implications for the microtubule-associated protein tau: localization in oligodendrocytes. *Proc Natl Acad Sci U S A* **92:** 10369-10373

Lucassen PJ, Williams A, Chung WC, Fraser H (1995) Detection of apoptosis in murine scrapie. *Neurosci Lett* **198:** 185-188

Lyahyai J, Bolea R, Serrano C, Monleon E, Moreno C, Osta R, Zaragoza P, Badiola JJ, Martin-Burriel I (2006) Correlation between Bax overexpression and prion deposition in medulla oblongata from natural scrapie without evidence of apoptosis. *Acta Neuropathol* **112:** 451-460

Lyahyai J, Bolea R, Serrano C, Vidal E, Pumarola M, Badiola JJ, Zaragoza P, Martin-Burriel I (2007) Differential expression and protein distribution of Bax in natural scrapie. *Brain Res* **1180:** 111-120

Mabbott NA, Farquhar CF, Brown KL, Bruce ME (1998) Involvement of the immune system in TSE pathogenesis. *Immunol Today* **19:** 201-203

Mabbott NA, MacPherson GG (2006) Prions and their lethal journey to the brain. *Nat Rev Microbiol* **4:** 201-211

Machado-Salas JP (1986) Dendritic and axonal spherules in the neocortex of a patient with Creutzfeldt-Jakob disease (CJD): Golgi and electron-microscopical investigation--neurobiological significance. *Clin Neuropathol* **5:** 176-184

Manson J, West JD, Thomson V, McBride P, Kaufman MH, Hope J (1992) The prion protein gene: a role in mouse embryogenesis? *Development* **115:** 117-122

Manson JC, Clarke AR, McBride PA, McConnell I, Hope J (1994) PrP gene dosage determines the timing but not the final intensity or distribution of lesions in scrapie pathology. *Neurodegeneration* **3:** 331-340

Manson JC, Hope, J. Clarke, A.R., Johnston, A., Black, C., MacLeod, N. (1995) PrP gene dosage and long term potentiation. *Neurodegeneration 4***:** 113-114

Marques CP, Cheeran MC, Palmquist JM, Hu S, Lokensgard JR (2008) Microglia are the major cellular source of inducible nitric oxide synthase during experimental herpes encephalitis. *J Neurovirol* **14:** 229-238

Marsh RF, Hadlow WJ (1992) Transmissible mink encephalopathy. *Rev Sci Tech* **11:** 539-550

Martin JB (1999) Molecular basis of the neurodegenerative disorders. *N Engl J Med* **340:** 1970-1980

Martin LJ (2001) Neuronal cell death in nervous system development, disease, and injury (Review). *Int J Mol Med* **7:** 455-478

Martins VR (1999) A receptor for infectious and cellular prion protein. *Braz J Med Biol Res* **32:** 853-859

Mathews JD, Glasse R, Lindenbaum S (1968) Kuru and cannibalism. *Lancet* **2:** 449-452

Mazanetz MP, Fischer PM (2007) Untangling tau hyperphosphorylation in drug design for neurodegenerative diseases. *Nat Rev Drug Discov* **6:** 464-479

Mazumder S, Plesca D, Almasan A (2008) Caspase-3 activation is a critical determinant of genotoxic stress-induced apoptosis. *Methods Mol Biol* **414:** 13-21

McBride PA, Eikelenboom P, Kraal G, Fraser H, Bruce ME (1992) PrP protein is associated with follicular dendritic cells of spleens and lymph nodes in uninfected and scrapie-infected mice. *J Pathol* **168:** 413-418

McBride PA, Schulz-Schaeffer WJ, Donaldson M, Bruce M, Diringer H, Kretzschmar HA, Beekes M (2001) Early spread of scrapie from the gastrointestinal tract to the

central nervous system involves autonomic fibers of the splanchnic and vagus nerves. *J Virol* **75:** 9320-9327

McGowan. J (1922) Scrapie in sheep. 5 Thesis, Scottish Journal of Agriculture,

McKinley MP, Bolton DC, Prusiner SB (1983) A protease-resistant protein is a structural component of the scrapie prion. *Cell* **35:** 57-62

McLennan NF, Brennan PM, McNeill A, Davies I, Fotheringham A, Rennison KA, Ritchie D, Brannan F, Head MW, Ironside JW, Williams A, Bell JE (2004) Prion protein accumulation and neuroprotection in hypoxic brain damage. *Am J Pathol* **165:** 227-235

Mensah-Brown EP, Shahin A, Garey LJ, Lukic ML (2005) Neuroglial response after induction of experimental allergic encephalomyelitis in susceptible and resistant rat strains. *Cell Immunol* **233:** 140-147

Merz PA, Somerville RA, Wisniewski HM, Iqbal K (1981) Abnormal fibrils from scrapie-infected brain. *Acta Neuropathol (Berl)* **54:** 63-74

Merz PA, Somerville RA, Wisniewski HM, Manuelidis L, Manuelidis EE (1983) Scrapie-associated fibrils in Creutzfeldt-Jakob disease. *Nature* **306:** 474-476

Meyer RK, McKinley MP, Bowman KA, Braunfeld MB, Barry RA, Prusiner SB (1986) Separation and properties of cellular and scrapie prion proteins. *Proc Natl Acad Sci U S A* **83:** 2310-2314

Migheli A, Butler M, Brown K, Shelanski ML (1988) Light and electron microscope localization of the microtubule-associated tau protein in rat brain. *J Neurosci* **8:** 1846-1851

Milhavet O, Lehmann S (2002) Oxidative stress and the prion protein in transmissible spongiform encephalopathies. *Brain Res Brain Res Rev* **38:** 328-339

Miller MW, Williams ES (2003) Prion disease: horizontal prion transmission in mule deer. *Nature* **425:** 35-36

Miller MW, Williams ES, Hobbs NT, Wolfe LL (2004) Environmental sources of prion transmission in mule deer. *Emerg Infect Dis* **10:** 1003-1006

Mironov A, Jr., Latawiec D, Wille H, Bouzamondo-Bernstein E, Legname G, Williamson RA, Burton D, DeArmond SJ, Prusiner SB, Peters PJ (2003) Cytosolic prion protein in neurons. *J Neurosci* **23:** 7183-7193

Mohan J, Brown KL, Farquhar CF, Bruce ME, Mabbott NA (2004) Scrapie transmission following exposure through the skin is dependent on follicular dendritic cells in lymphoid tissues. *J Dermatol Sci* **35:** 101-111

Mohan J, Bruce ME, Mabbott NA (2005) Neuroinvasion by scrapie following inoculation via the skin is independent of migratory Langerhans cells. *J Virol* **79:** 1888-1897

Mok SW, Riemer C, Madela K, Hsu DK, Liu FT, Gultner S, Heise I, Baier M (2007) Role of galectin-3 in prion infections of the CNS. *Biochem Biophys Res Commun* **359:** 672-678

Montgomery MM, Dean AF, Taffs F, Stott EJ, Lantos PL, Luthert PJ (1999) Progressive dendritic pathology in cynomolgus macaques infected with simian immunodeficiency virus. *Neuropathol Appl Neurobiol* **25:** 11-19

Montrasio F, Frigg R, Glatzel M, Klein MA, Mackay F, Aguzzi A, Weissmann C (2000) Impaired prion replication in spleens of mice lacking functional follicular dendritic cells. *Science* **288:** 1257-1259

Moolman DL, Vitolo OV, Vonsattel JP, Shelanski ML (2004) Dendrite and dendritic spine alterations in Alzheimer models. *J Neurocytol* **33:** 377-387

Moore RC, Hope J, McBride PA, McConnell I, Selfridge J, Melton DW, Manson JC (1998) Mice with gene targetted prion protein alterations show that Prnp, Sinc and Prni are congruent. *Nat Genet* **18:** 118-125

Moore RC, Redhead NJ, Selfridge J, Hope J, Manson JC, Melton DW (1995) Double replacement gene targeting for the production of a series of mouse strains with different prion protein gene alterations. *Biotechnology (N Y)* **13:** 999-1004

Moores C (2008) Studying microtubules by electron microscopy. *Methods Cell Biol* **88:** 299-317

Moser M, Colello RJ, Pott U, Oesch B (1995) Developmental expression of the prion protein gene in glial cells. *Neuron* **14:** 509-517

Moya KL, Sales N, Hassig R, Creminon C, Grassi J, Di Giamberardino L (2000) Immunolocalization of the cellular prion protein in normal brain. *Microsc Res Tech* **50:** 58-65

Muramoto T, Kitamoto T, Tateishi J, Goto I (1993) Accumulation of abnormal prion protein in mice infected with Creutzfeldt-Jakob disease via intraperitoneal route: a sequential study. *Am J Pathol* **143:** 1470-1479

Nakagawa T, Zhu H, Morishima N, Li E, Xu J, Yankner BA, Yuan J (2000) Caspase-12 mediates endoplasmic-reticulum-specific apoptosis and cytotoxicity by amyloid-beta. *Nature* **403:** 98-103

Nakamitsu S, Miyazawa T, Horiuchi M, Onoe S, Ohoba Y, Kitagawa H, Ishiguro N (2006) Sequence variation of bovine prion protein gene in Japanese cattle (Holstein and Japanese Black). *J Vet Med Sci* **68:** 27-33

Neve RL, Harris P, Kosik KS, Kurnit DM, Donlon TA (1986) Identification of cDNA clones for the human microtubule-associated protein tau and chromosomal localization of the genes for tau and microtubule-associated protein 2. *Brain Res* **387:** 271-280

Oesch B, Westaway D, Walchli M, McKinley MP, Kent SB, Aebersold R, Barry RA, Tempst P, Teplow DB, Hood LE, et al. (1985) A cellular gene encodes scrapie PrP 27-30 protein. *Cell* **40:** 735-746

Oh JM, Shin HY, Park SJ, Kim BH, Choi JK, Choi EK, Carp RI, Kim YS (2008) The involvement of cellular prion protein in the autophagy pathway in neuronal cells. *Mol Cell Neurosci* **39:** 238-247

Ohsumi Y (2001) Molecular dissection of autophagy: two ubiquitin-like systems. *Nat Rev Mol Cell Biol* **2:** 211-216

Okabe S (2007) Molecular anatomy of the postsynaptic density. *Mol Cell Neurosci* **34:** 503-518

Outram GW, Dickinson AG, Fraser H (1973) Developmental maturation of susceptibility to scrapie in mice. *Nature* **241:** 536-537

Ouyang YB, Giffard RG (2004) Changes in astrocyte mitochondrial function with stress: effects of Bcl-2 family proteins. *Neurochem Int* **45:** 371-379

Pan KM, Baldwin M, Nguyen J, Gasset M, Serban A, Groth D, Mehlhorn I, Huang Z, Fletterick RJ, Cohen FE, et al. (1993) Conversion of alpha-helices into beta-sheets features in the formation of the scrapie prion proteins. *Proc Natl Acad Sci U S A* **90:** 10962-10966

Papakonstanti EA, Stournaras C (2008) Cell responses regulated by early reorganization of actin cytoskeleton. *FEBS Lett* **582:** 2120-2127

Papasozomenos SC, Binder LI (1987) Phosphorylation determines two distinct species of Tau in the central nervous system. *Cell Motil Cytoskeleton* **8:** 210-226

Park SK, Choi SI, Jin JK, Choi EK, Kim JI, Carp RI, Kim YS (2000) Differential expression of Bax and Bcl-2 in the brains of hamsters infected with 263K scrapie agent. *Neuroreport* **11:** 1677-1682

Pattison IH, Millson GC (1961) Scrapie produced experimentally in goats with special reference to the clinical syndrome. *J Comp Pathol* **71:** 101-109

Pattison IH, Smith K (1963) EXPERIMENTAL SCRAPIE IN GOATS: A MODIFICATION OF INCUBATION PERIOD AND CLINICAL RESPONSE FOLLOWING PRE-TREATMENT WITH NORMAL GOAT BRAIN. *Nature* **200:** 1342-1343

Perez M, Rojo AI, Wandosell F, Diaz-Nido J, Avila J (2003) Prion peptide induces neuronal cell death through a pathway involving glycogen synthase kinase 3. *Biochem J* **372:** 129-136

Perrot R, Berges R, Bocquet A, Eyer J (2008) Review of the multiple aspects of neurofilament functions, and their possible contribution to neurodegeneration. *Mol Neurobiol* **38:** 27-65

Perry VH, Cunningham C, Holmes C (2007) Systemic infections and inflammation affect chronic neurodegeneration. *Nat Rev Immunol* **7:** 161-167

Piccardo P, Manson JC, King D, Ghetti B, Barron RM (2007) Accumulation of prion protein in the brain that is not associated with transmissible disease. *Proc Natl Acad Sci U S A* **104:** 4712-4717

Porto-Carreiro I, Fevrier B, Paquet S, Vilette D, Raposo G (2005) Prions and exosomes: from PrPc trafficking to PrPsc propagation. *Blood Cells Mol Dis* **35:** 143-148

Provini F, Cortelli P, Montagna P, Gambetti P, Lugaresi E (2008) Fatal insomnia and agrypnia excitata: sleep and the limbic system. *Rev Neurol (Paris)* **164:** 692-700

Prusiner SB (1982) Novel proteinaceous infectious particles cause scrapie. *Science* **216:** 136-144

Prusiner SB, Bolton DC, Groth DF, Bowman KA, Cochran SP, McKinley MP (1982) Further purification and characterization of scrapie prions. *Biochemistry* **21:** 6942-6950

Prusiner SB, McKinley MP, Bowman KA, Bolton DC, Bendheim PE, Groth DF, Glenner GG (1983) Scrapie prions aggregate to form amyloid-like birefringent rods. *Cell* **35:** 349-358

Puig B, Ferrer I (2001) Cell death signaling in the cerebellum in Creutzfeldt-Jakob disease. *Acta Neuropathol* **102:** 207-215

Qin K, Yang DS, Yang Y, Chishti MA, Meng LJ, Kretzschmar HA, Yip CM, Fraser PE, Westaway D (2000) Copper(II)-induced conformational changes and protease resistance in recombinant and cellular PrP. Effect of protein age and deamidation. *J Biol Chem* **275:** 19121-19131

Race RE, Fadness LH, Chesebro B (1987) Characterization of scrapie infection in mouse neuroblastoma cells. *J Gen Virol* **68 (Pt 5):** 1391-1399

Raeber AJ, Race RE, Brandner S, Priola SA, Sailer A, Bessen RA, Mucke L, Manson J, Aguzzi A, Oldstone MB, Weissmann C, Chesebro B (1997) Astrocyte-specific expression of hamster prion protein (PrP) renders PrP knockout mice susceptible to hamster scrapie. *Embo J* **16:** 6057-6065

Rainov NG, Kramm CM, Banning U, Riemann D, Holzhausen HJ, Heidecke V, Burger KJ, Burkert W, Korholz D (2000) Immune response induced by retrovirus-mediated HSV-tk/GCV pharmacogene therapy in patients with glioblastoma multiforme. *Gene Ther* **7:** 1853-1858

Raivich G (2005) Like cops on the beat: the active role of resting microglia. *Trends Neurosci* **28:** 571-573

Raley-Susman KM, Murata J (1995) Time course of protein changes following in vitro ischemia in the rat hippocampal slice. *Brain Res* **694:** 94-102

Raman L, Hamilton KL, Gewirtz JC, Rao R (2008) Effects of chronic hypoxia in developing rats on dendritic morphology of the CA1 subarea of the hippocampus and on fear-potentiated startle. *Brain Res* **1190:** 167-174

Reines A, Cereseto M, Ferrero A, Bonavita C, Wikinski S (2004) Neuronal cytoskeletal alterations in an experimental model of depression. *Neuroscience* **129:** 529-538

Reix S, Mechawar N, Susin SA, Quirion R, Krantic S (2007) Expression of cortical and hippocampal apoptosis-inducing factor (AIF) in aging and Alzheimer's disease. *Neurobiol Aging* **28:** 351-356

Rezaie P, Lantos PL (2001) Microglia and the pathogenesis of spongiform encephalopathies. *Brain Res Brain Res Rev* **35:** 55-72

Ritchie DL, Brown, K.L., Bruce, M.E. (1999) Visualisation of PrP protein and follicular dendritic cells in uninfected and scrapie infected spleen. *journal of cell pathology* **1:** 3-10

Rosser AE, Tyers P, ter Borg M, Dunnett SB, Svendsen CN (1997) Co-expression of MAP-2 and GFAP in cells developing from rat EGF responsive precursor cells. *Brain Res Dev Brain Res* **98:** 291-295

Rubenstein R, Merz PA, Kascsak RJ, Scalici CL, Papini MC, Carp RI, Kimberlin RH (1991) Scrapie-infected spleens: analysis of infectivity, scrapie-associated fibrils, and protease-resistant proteins. *J Infect Dis* **164:** 29-35

Saa P, Castilla J, Soto C (2006) Ultra-efficient replication of infectious prions by automated protein misfolding cyclic amplification. *J Biol Chem* **281:** 35245-35252

Saborio GP, Permanne B, Soto C (2001) Sensitive detection of pathological prion protein by cyclic amplification of protein misfolding. *Nature* **411:** 810-813

Sakaguchi S, Katamine S, Nishida N, Moriuchi R, Shigematsu K, Sugimoto T, Nakatani A, Kataoka Y, Houtani T, Shirabe S, Okada H, Hasegawa S, Miyamoto T, Noda T (1996) Loss of cerebellar Purkinje cells in aged mice homozygous for a disrupted PrP gene. *Nature* **380:** 528-531

Sales N, Hassig R, Rodolfo K, Di Giamberardino L, Traiffort E, Ruat M, Fretier P, Moya KL (2002) Developmental expression of the cellular prion protein in elongating axons. *Eur J Neurosci* **15:** 1163-1177

Salvesen GS, Dixit VM (1997) Caspases: intracellular signaling by proteolysis. *Cell* **91:** 443-446

Sanchez C, Diaz-Nido J, Avila J (2000) Phosphorylation of microtubule-associated protein 2 (MAP2) and its relevance for the regulation of the neuronal cytoskeleton function. *Prog Neurobiol* **61:** 133-168

Satoh J, Obayashi S, Misawa T, Sumiyoshi K, Oosumi K, Tabunoki H (2009) Protein microarray analysis identifies human cellular prion protein interactors. *Neuropathol Appl Neurobiol* **35:** 16-35

Sattler T, Mayer A (2000) Cell-free reconstitution of microautophagic vacuole invagination and vesicle formation. *J Cell Biol* **151:** 529-538

Scheff SW, Price DA, Schmitt FA, DeKosky ST, Mufson EJ (2007) Synaptic alterations in CA1 in mild Alzheimer disease and mild cognitive impairment. *Neurology* **68:** 1501-1508

Schmalzbauer R, Eigenbrod S, Winoto-Morbach S, Xiang W, Schutze S, Bertsch U, Kretzschmar HA (2008) Evidence for an association of prion protein and sphingolipid-mediated signaling. *J Neurochem* **106:** 1459-1470

Schmidt-Kastner R, Zhao W, Truettner J, Belayev L, Busto R, Ginsberg MD (1998) Pixel-based image analysis of HSP70, GADD45 and MAP2 mRNA expression after focal cerebral ischemia: hemodynamic and histological correlates. *Brain Res Mol Brain Res* **63:** 79-97

Schulz-Schaeffer WJ, Fatzer R, Vandevelde M, Kretzschmar HA (2000) Detection of PrP(Sc) in subclinical BSE with the paraffin-embedded tissue (PET) blot. *Arch Virol Suppl***:** 173-180

Schwab C, McGeer PL (2008) Inflammatory aspects of Alzheimer disease and other neurodegenerative disorders. *J Alzheimers Dis* **13:** 359-369

Scott JR, Fraser H (1984) Degenerative hippocampal pathology in mice infected with scrapie. *Acta Neuropathol (Berl)* **65:** 62-68

Sekino Y, Kojima N, Shirao T (2007) Role of actin cytoskeleton in dendritic spine morphogenesis. *Neurochem Int* **51:** 92-104

Selkoe DJ (2008) Soluble oligomers of the amyloid beta-protein impair synaptic plasticity and behavior. *Behav Brain Res* **192:** 106-113

Seth P, Koul N (2008) Astrocyte, the star avatar: redefined. *J Biosci* **33:** 405-421

Shankar GM, Li S, Mehta TH, Garcia-Munoz A, Shepardson NE, Smith I, Brett FM, Farrell MA, Rowan MJ, Lemere CA, Regan CM, Walsh DM, Sabatini BL, Selkoe DJ (2008) Amyloid-beta protein dimers isolated directly from Alzheimer's brains impair synaptic plasticity and memory. *Nat Med* **14:** 837-842

Shim KS, Lubec G (2002) Drebrin, a dendritic spine protein, is manifold decreased in brains of patients with Alzheimer's disease and Down syndrome. *Neurosci Lett* **324:** 209-212

Shirao T, Kojima N, Kato Y, Obata K (1988) Molecular cloning of a cDNA for the developmentally regulated brain protein, drebrin. *Brain Res* **464:** 71-74

Shirao T, Obata K (1985) Two acidic proteins associated with brain development in chick embryo. *J Neurochem* **44:** 1210-1216

Shirao T, Obata K (1986) Immunochemical homology of 3 developmentally regulated brain proteins and their developmental change in neuronal distribution. *Brain Res* **394:** 233-244

Shy ME (2004) Charcot-Marie-Tooth disease: an update. *Curr Opin Neurol* **17:** 579-585

Sigurdson CJ, Williams ES, Miller MW, Spraker TR, O'Rourke KI, Hoover EA (1999) Oral transmission and early lymphoid tropism of chronic wasting disease PrPres in mule deer fawns (Odocoileus hemionus). *J Gen Virol* **80 (Pt 10):** 2757-2764

Sikorska B, Liberski PP, Brown P (2007) Neuronal autophagy and aggresomes constitute a consistent part of neurodegeneration in experimental scrapie. *Folia Neuropathol* **45:** 170-178

Sikorska B, Liberski PP, Giraud P, Kopp N, Brown P (2004) Autophagy is a part of ultrastructural synaptic pathology in Creutzfeldt-Jakob disease: a brain biopsy study. *Int J Biochem Cell Biol* **36:** 2563-2573

Sikorska B, Liberski PP, Sobow T, Budka H, Ironside JW (2008) Ultrastructural study of florid plaques in variant Creutzfeldt-Jakob disease: a comparison with amyloid plaques in kuru, sporadic Creutzfeldt-Jakob disease and Gerstmann-Straussler-Scheinker disease. *Neuropathol Appl Neurobiol*

Simoneau S, Rezaei H, Sales N, Kaiser-Schulz G, Lefebvre-Roque M, Vidal C, Fournier JG, Comte J, Wopfner F, Grosclaude J, Schatzl H, Lasmezas CI (2007) In vitro and in vivo neurotoxicity of prion protein oligomers. *PLoS Pathog* **3:** e125

Siso S, Gonzalez L, Houston F, Hunter N, Martin S, Jeffrey M (2006) The neuropathologic phenotype of experimental ovine BSE is maintained after blood transfusion. *Blood* **108:** 745-748

Siso S, Puig B, Varea R, Vidal E, Acin C, Prinz M, Montrasio F, Badiola J, Aguzzi A, Pumarola M, Ferrer I (2002) Abnormal synaptic protein expression and cell death in murine scrapie. *Acta Neuropathol (Berl)* **103:** 615-626

Slee EA, Adrain C, Martin SJ (1999) Serial killers: ordering caspase activation events in apoptosis. *Cell Death Differ* **6:** 1067-1074

Slezak M, Pfrieger FW, Soltys Z (2006) Synaptic plasticity, astrocytes and morphological homeostasis. *J Physiol Paris* **99:** 84-91

Soifer D (1986) Factors regulating the presence of microtubules in cells. *Ann N Y Acad Sci* **466:** 1-7

Sokolowski F, Modler AJ, Masuch R, Zirwer D, Baier M, Lutsch G, Moss DA, Gast K, Naumann D (2003) Formation of critical oligomers is a key event during conformational transition of recombinant syrian hamster prion protein. *J Biol Chem* **278:** 40481-40492

Somerville RA (1999) Host and transmissible spongiform encephalopathy agent strain control glycosylation of PrP. *J Gen Virol* **80 (Pt 7):** 1865-1872

Somerville RA, Chong A, Mulqueen OU, Birkett CR, Wood SC, Hope J (1997) Biochemical typing of scrapie strains. *Nature* **386:** 564

Soto C, Anderes L, Suardi S, Cardone F, Castilla J, Frossard MJ, Peano S, Saa P, Limido L, Carbonatto M, Ironside J, Torres JM, Pocchiari M, Tagliavini F (2005) Pre-symptomatic detection of prions by cyclic amplification of protein misfolding. *FEBS Lett* **579:** 638-642

Sparkes RS, Simon M, Cohn VH, Fournier RE, Lem J, Klisak I, Heinzmann C, Blatt C, Lucero M, Mohandas T, et al. (1986) Assignment of the human and mouse prion protein genes to homologous chromosomes. *Proc Natl Acad Sci U S A* **83:** 7358-7362

Spruston N (2008) Pyramidal neurons: dendritic structure and synaptic integration. *Nat Rev Neurosci* **9:** 206-221

Stahelin BJ, Marti U, Solioz M, Zimmermann H, Reichen J (1998) False positive staining in the TUNEL assay to detect apoptosis in liver and intestine is caused by endogenous nucleases and inhibited by diethyl pyrocarbonate. *Mol Pathol* **51:** 204-208

Steele AD, King OD, Jackson WS, Hetz CA, Borkowski AW, Thielen P, Wollmann R, Lindquist S (2007) Diminishing apoptosis by deletion of Bax or overexpression of Bcl-2 does not protect against infectious prion toxicity in vivo. *J Neurosci* **27:** 13022-13027

Stefani M, Dobson CM (2003) Protein aggregation and aggregate toxicity: new insights into protein folding, misfolding diseases and biological evolution. *J Mol Med* **81:** 678-699

Stobart MJ, Parchaliuk D, Simon SL, Lemaistre J, Lazar J, Rubenstein R, Knox JD (2007) Differential expression of interferon responsive genes in rodent models of transmissible spongiform encephalopathy disease. *Mol Neurodegener* **2:** 5

Susin SA, Lorenzo HK, Zamzami N, Marzo I, Snow BE, Brothers GM, Mangion J, Jacotot E, Costantini P, Loeffler M, Larochette N, Goodlett DR, Aebersold R, Siderovski DP, Penninger JM, Kroemer G (1999) Molecular characterization of mitochondrial apoptosis-inducing factor. *Nature* **397:** 441-446

Syntichaki P, Tavernarakis N (2002) Death by necrosis. Uncontrollable catastrophe, or is there order behind the chaos? *EMBO Rep* **3:** 604-609

Taber KH, Hurley RA (2008) Astroglia: not just glue. *J Neuropsychiatry Clin Neurosci* **20:** iv-129

Tashiro K, Hasegawa M, Ihara Y, Iwatsubo T (1997) Somatodendritic localization of phosphorylated tau in neonatal and adult rat cerebral cortex. *Neuroreport* **8:** 2797-2801

Taylor DM (2000) Inactivation of transmissible degenerative encephalopathy agents: A review. *Vet J* **159:** 10-17

Taylor DM (2004) Resistance of transmissible spongiform encephalopathy agents to decontamination. *Contrib Microbiol* **11:** 136-145

Taylor DM, Dickinson AG, Fraser H, Marsh RF (1986) Evidence that transmissible mink encephalopathy agent is biologically inactive in mice. *Neuropathol Appl Neurobiol* **12:** 207-215

Taylor DM, McConnell I, Fraser H (1996) Scrapie infection can be established readily through skin scarification in immunocompetent but not immunodeficient mice. *J Gen Virol* **77 (Pt 7):** 1595-1599

Taylor DR, Hooper NM (2006) The prion protein and lipid rafts. *Mol Membr Biol* **23:** 89-99

Taylor JP, Hardy J, Fischbeck KH (2002) Toxic proteins in neurodegenerative disease. *Science* **296:** 1991-1995

Terry LA, Marsh S, Ryder SJ, Hawkins SA, Wells GA, Spencer YI (2003) Detection of disease-specific PrP in the distal ileum of cattle exposed orally to the agent of bovine spongiform encephalopathy. *Vet Rec* **152:** 387-392

Theodosis DT, Poulain DA, Oliet SH (2008) Activity-dependent structural and functional plasticity of astrocyte-neuron interactions. *Physiol Rev* **88:** 983-1008

Tobler I, Gaus SE, Deboer T, Achermann P, Fischer M, Rulicke T, Moser M, Oesch B, McBride PA, Manson JC (1996) Altered circadian activity rhythms and sleep in mice devoid of prion protein. *Nature* **380:** 639-642

Todorova-Balvay D, Simon S, Creminon C, Grassi J, Srikrishnan T, Vijayalakshmi MA (2005) Copper binding to prion octarepeat peptides, a combined metal chelate affinity and immunochemical approaches. *J Chromatogr B Analyt Technol Biomed Life Sci* **818:** 75-82

Tokuda E, Ono S, Ishige K, Watanabe S, Okawa E, Ito Y, Suzuki T (2007) Dysequilibrium between caspases and their inhibitors in a mouse model for amyotrophic lateral sclerosis. *Brain Res* **1148:** 234-242

Triller A, Choquet D (2008) New concepts in synaptic biology derived from single-molecule imaging. *Neuron* **59:** 359-374

Tuzi NL, Cancellotti E, Baybutt H, Blackford L, Bradford B, Plinston C, Coghill A, Hart P, Piccardo P, Barron RM, Manson JC (2008) Host PrP glycosylation: a major factor determining the outcome of prion infection. *PLoS Biol* **6:** e100

Tuzi NL, Gall E, Melton D, Manson JC (2002) Expression of doppel in the CNS of mice does not modulate transmissible spongiform encephalopathy disease. *J Gen Virol* **83:** 705-711

Ugolev AM, De Laey P (1973) Membrane digestion. A concept of enzyme hydrolysis on cell membranes. *Biochim Biophys Acta* **300:** 105-128

Ullian EM, Christopherson KS, Barres BA (2004) Role for glia in synaptogenesis. *Glia* **47:** 209-216

Van Everbroeck B, Dewulf E, Pals P, Lubke U, Martin JJ, Cras P (2002) The role of cytokines, astrocytes, microglia and apoptosis in Creutzfeldt-Jakob disease. *Neurobiol Aging* **23:** 59-64

Van Keulen LJ, Schreuder BE, Meloen RH, Mooij-Harkes G, Vromans ME, Langeveld JP (1996) Immunohistochemical detection of prion protein in lymphoid tissues of sheep with natural scrapie. *J Clin Microbiol* **34:** 1228-1231

van Keulen LJ, Vromans ME, Dolstra CH, Bossers A, van Zijderveld FG (2008) Pathogenesis of bovine spongiform encephalopathy in sheep. *Arch Virol* **153:** 445-453

Vassallo N, Herms J, Behrens C, Krebs B, Saeki K, Onodera T, Windl O, Kretzschmar HA (2005) Activation of phosphatidylinositol 3-kinase by cellular prion protein and its role in cell survival. *Biochem Biophys Res Commun* **332:** 75-82

Veerhuis R, Hoozemans JJ, Janssen I, Boshuizen RS, Langeveld JP, Eikelenboom P (2002) Adult human microglia secrete cytokines when exposed to neurotoxic prion protein peptide: no intermediary role for prostaglandin E2. *Brain Res* **925:** 195-203

Vesce S, Bezzi P, Volterra A (1999) The highly integrated dialogue between neurons and astrocytes in brain function. *Sci Prog* **82 (Pt 3):** 251-270

Viles JH, Cohen FE, Prusiner SB, Goodin DB, Wright PE, Dyson HJ (1999) Copper binding to the prion protein: structural implications of four identical cooperative binding sites. *Proc Natl Acad Sci U S A* **96:** 2042-2047

Viola KL, Velasco PT, Klein WL (2008) Why Alzheimer's is a disease of memory: the attack on synapses by A beta oligomers (ADDLs). *J Nutr Health Aging* **12:** 51S-57S

Volterra A, Meldolesi J (2005) Astrocytes, from brain glue to communication elements: the revolution continues. *Nat Rev Neurosci* **6:** 626-640

Vouyiouklis DA, Brophy PJ (1995) Microtubule-associated proteins in developing oligodendrocytes: transient expression of a MAP2c isoform in oligodendrocyte precursors. *J Neurosci Res* **42:** 803-817

Wadsworth JD, Joiner S, Hill AF, Campbell TA, Desbruslais M, Luthert PJ, Collinge J (2001) Tissue distribution of protease resistant prion protein in variant Creutzfeldt-Jakob disease using a highly sensitive immunoblotting assay. *Lancet* **358:** 171-180

Walker NI, Harmon BV, Gobe GC, Kerr JF (1988) Patterns of cell death. *Methods Achiev Exp Pathol* **13:** 18-54

Walsh DM, Selkoe DJ (2004a) Deciphering the molecular basis of memory failure in Alzheimer's disease. *Neuron* **44:** 181-193

Walsh DM, Selkoe DJ (2004b) Oligomers on the brain: the emerging role of soluble protein aggregates in neurodegeneration. *Protein Pept Lett* **11:** 213-228

Weber P, Giese A, Piening N, Mitteregger G, Thomzig A, Beekes M, Kretzschmar HA (2007) Generation of genuine prion infectivity by serial PMCA. *Vet Microbiol* **123:** 346-357

Weise J, Crome O, Sandau R, Schulz-Schaeffer W, Bahr M, Zerr I (2004) Upregulation of cellular prion protein (PrPc) after focal cerebral ischemia and influence of lesion severity. *Neurosci Lett* **372:** 146-150

Weissmann C (1991) A 'unified theory' of prion propagation. *Nature* **352:** 679-683

Wells GA, Hawkins SA, Austin AR, Ryder SJ, Done SH, Green RB, Dexter I, Dawson M, Kimberlin RH (2003) Studies of the transmissibility of the agent of bovine spongiform encephalopathy to pigs. *J Gen Virol* **84:** 1021-1031

Wells GA, Hawkins SA, Green RB, Austin AR, Dexter I, Spencer YI, Chaplin MJ, Stack MJ, Dawson M (1998) Preliminary observations on the pathogenesis of experimental bovine spongiform encephalopathy (BSE): an update. *Vet Rec* **142:** 103-106

Wells GAH SA, Johnson CT,Gunning RF,Hancock RD,Jeffrey M,Dawson M,Bradley R (1987) A novel progressive encephalopathy in cattle. *Vet Rec* **135:** 40-41

White AR, Guirguis R, Brazier MW, Jobling MF, Hill AF, Beyreuther K, Barrow CJ, Masters CL, Collins SJ, Cappai R (2001) Sublethal concentrations of prion peptide PrP106-126 or the amyloid beta peptide of Alzheimer's disease activates expression of proapoptotic markers in primary cortical neurons. *Neurobiol Dis* **8:** 299-316

White CA, McCombe PA, Pender MP (1998) The roles of Fas, Fas ligand and Bcl-2 in T cell apoptosis in the central nervous system in experimental autoimmune encephalomyelitis. *J Neuroimmunol* **82:** 47-55

Wilesmith JW, Ryan JB, Atkinson MJ (1991) Bovine spongiform encephalopathy: epidemiological studies on the origin. *Vet Rec* **128:** 199-203

Wilesmith JW, Ryan JB, Hueston WD, Hoinville LJ (1992) Bovine spongiform encephalopathy: epidemiological features 1985 to 1990. *Vet Rec* **130:** 90-94

Williams A, Lucassen PJ, Ritchie D, Bruce M (1997a) PrP deposition, microglial activation, and neuronal apoptosis in murine scrapie. *Exp Neurol* **144:** 433-438

Williams A, Van Dam AM, Ritchie D, Eikelenboom P, Fraser H (1997b) Immunocytochemical appearance of cytokines, prostaglandin E2 and lipocortin-1 in the CNS during the incubation period of murine scrapie correlates with progressive PrP accumulations. *Brain Res* **754:** 171-180

Williams AE, Lawson LJ, Perry VH, Fraser H (1994) Characterization of the microglial response in murine scrapie. *Neuropathol Appl Neurobiol* **20:** 47-55

Williams DR (2006) Tauopathies: classification and clinical update on neurodegenerative diseases associated with microtubule-associated protein tau. *Intern Med J* **36:** 652-660

Williams ES, Mille, M.W. (2000) Pathogenesis of chronic wasting disease in orally exposed mule deer (Odocoileus hemionus): preliminary results. *Proc 49th Wildl Dis Assoc Conf 2000:29*

Williams ES, Miller MW (2002) Chronic wasting disease in deer and elk in North America. *Rev Sci Tech* **21:** 305-316

Williams ES, Young S (1980) Chronic wasting disease of captive mule deer: a spongiform encephalopathy. *J Wildl Dis* **16:** 89-98

Williams ES, Young S (1992) Spongiform encephalopathies in Cervidae. *Rev Sci Tech* **11:** 551-567

Wisniewski HM, Bruce ME, Fraser H (1975) Infectious etiology of neuritic (senile) plaques in mice. *Science* **190:** 1108-1110

Wisniewski HM, Vorbrodt AW, Wegiel J, Morys J, Lossinsky AS (1990) Ultrastructure of the cells forming amyloid fibers in Alzheimer disease and scrapie. *Am J Med Genet Suppl* **7:** 287-297

Wyllie AH, Kerr JF, Currie AR (1980) Cell death: the significance of apoptosis. *Int Rev Cytol* **68:** 251-306

Xue L, Fletcher GC, Tolkovsky AM (1999) Autophagy is activated by apoptotic signalling in sympathetic neurons: an alternative mechanism of death execution. *Mol Cell Neurosci* **14:** 180-198

Yakovlev AG, Faden AI (2001) Caspase-dependent apoptotic pathways in CNS injury. *Mol Neurobiol* **24:** 131-144

Yamakawa Y, Hagiwara K, Nohtomi K, Nakamura Y, Nishijima M, Higuchi Y, Sato Y, Sata T (2003) Atypical proteinase K-resistant prion protein (PrPres) observed in an apparently healthy 23-month-old Holstein steer. *Jpn J Infect Dis* **56:** 221-222

Yang J, Liu X, Bhalla K, Kim CN, Ibrado AM, Cai J, Peng TI, Jones DP, Wang X (1997) Prevention of apoptosis by Bcl-2: release of cytochrome c from mitochondria blocked. *Science* **275:** 1129-1132

Ye X, Scallet AC, Carp RI (1997) The 139H scrapie agent produces hypothalamic neurotoxicity and pancreatic islet histopathology: electron microscopic studies. *Neurotoxicology* **18:** 533-545

Ye X, Scallet AC, Kascsak RJ, Carp RI (1998) Astrocytosis and amyloid deposition in scrapie-infected hamsters. *Brain Res* **809:** 277-287

Zalfa F, Bagni C (2004) Molecular insights into mental retardation: multiple functions for the Fragile X mental retardation protein? *Curr Issues Mol Biol* **6:** 73-88

Zigas V, Gajdusek DC (1957) Kuru: clinical study of a new syndrome resembling paralysis agitans in natives of the Eastern Highlands of Australian New Guinea. *Med J Aust* **44:** 745-754

Zlotnik I, Rennie JC (1965) EXPERIMENTAL TRANSMISSION OF MOUSE PASSAGED SCRAPIE TO GOATS, SHEEP, RATS AND HAMSTERS. *J Comp Pathol* **75:** 147-157

Zou H, Li Y, Liu X, Wang X (1999) An APAF-1.cytochrome c multimeric complex is a functional apoptosome that activates procaspase-9. *J Biol Chem* **274:** 11549-11556

Appendix 1. Immunohistochemistry methods and reagents

1.1 ABC method for immunolabelling

1. Take sections to water i.e. remove paraffin wax by immersion in xylene, graded alcohols (IMS 99) and water – 10mins
2. Antigen retrieval steps – depends on antibody used see table of antibodies
3. Wash in water.
4. Block with 1% hydrogen peroxide (H_2O_2) in methanol 10mins.
5. Wash in water then 1 x 5 mins in PBS/BSA.
6. Block with normal goat serum 1/20 for 15 mins.
7. Tap off serum and apply primary antibody.
8. Wash in 3 x 5 min in wash buffer.
9. Apply secondary antibody – either goat anti mouse biotinylated (for mouse monoclonals) or goat anti rabbit (for rabbit polyclonals) at 1/600 - 1 hr.
   For fluorescent labelling of alpha tubulin a goat anti mouse Alexa 488 secondary was used.

NB: At this point make up Avidin-Biotin-Complex (ABC) - 10µl A + 10µl B in 1ml PBS/BSA buffer. This must be prepared at least 30mins before use.

10. Wash 3 x 5 min in PBS/BSA.
11. Incubate in ABC for 30 mins.
12. Wash 3x5 mins in PBS/BSA.
13. Incubate in DAB for 5-10 mins.
14. Counterstain in haematoxylin 1min and blue in scotts tap water.
15. Dehydrate in alcohol, clear in xylene and mount in dpx.

1.2. List of antibodies used in IHC in this thesis

Antibody	Antibody type	pretreatment	Conc. / time temp	Commercial source or reference
6H4	Mouse Monoclonal	Autoclave 121°C 15mins 98% formic acid 10 mins	1/1000 overnight at 4°C	Prionics, Switzerland
GFAP	Rabbit Polyclonal	none	1/400 1hr at room temp	Dako
Iba1	Rabbit Polyclonal	0.1M citrate buffer 10 mins microwave	1/1000 1hr at room temp	Wako,USA
Active caspase-3	Rabbit Polyclonal	none	0.03µg/ml for 1hr at room temp	R&D systems
Active caspase-3	Rabbit Polyclonal	0.1M citrate buffer 10 mins microwave	20µg/ml for 1.5hr at room temp	Oncogene
Fas receptor (A20)	Rabbit Polyclonal	none	1/600 overnight at 4°C	Santa Cruz
Fas receptor (C20)	Rabbit Polyclonal	0.1M citrate buffer 10 mins microwave	1/100 for 1hr at room temp	Santa Cruz
Cytochrome C	Mouse Monoclonal	0.1M citrate buffer 10 mins microwave	1µg/ml for 30 mins at room temp	Biocarta
Bax	Rabbit Polyclonal	0.1M citrate buffer 10 mins microwave	1/100 for 1hr at room temp	Upstate
Bcl-2	Mouse Monoclonal	0.1M citrate buffer 10 mins microwave	1/40 for 1hr at room temp	Upstate
Alpha tubulin	Mouse Monoclonal	none	2µg/ml for 30mins at room temp	Lab Vision
Drebrin	Mouse Monoclonal	0.1M citrate buffer 10 mins microwave	10µg/ml for 1hr at room temp	MBL International
PSD-95	Goat polyclonal	0.5% Trypsin digestion 10mins at 37°C	10µg/ml for 30mins at 37°C	Abcam
Synaptophysin	Rabbit polyclonal	Dako antigen retrieval solution 10mins microwave	Ready to use for IHC	Dako
MAP-2 a+b	Mouse Monoclonal	0.1M citrate buffer 10 mins microwave	1µg/ml 30mins at room temp	Abcam

1.3 Immunolabelling Reagents

PBS/BSA wash buffer

Dissolve 5g BSA (bovine serum albumin) in 250mls stock PBS (10x PBS) top up to 2500ml with distilled water

10x PBS

400g Sodium Chloride

10g Potassium Chloride

57.5g DiSodium Hydrogen Orthophosphate

10g Potassium DiHydrogen Orthophosphate

5 litres of deionised water

1% PBS/BSA – antibody diluent

1g BSA in 100mls PBS (1x PBS tablet in 200ml distilled water)

Methanol/H_2O_2

1% - 232mls methanol + 8mls H_2O_2

0.3% - 198mls methanol + 20mls H_2O_2

DAB chromagen

Stock solution :- 1g 3,4,3,4, Tetra amino biphenyl hydrochloride + 40ml distilled water. Frozen in 1ml aliquots

Working solution :- dissolve 2ml of stock DAB solution in 200ml PBS, add 200µl 30% H_2O_2 prior to use.

Scotts Tap Water

8.75g Sodium Hydrogen Carbonate

50g Magnesium Sulphate

2500ml tap water

0.1M Citrate Buffer

0.1M Citric Acid :- 1.92g citric acid anhydrous in 100ml distilled water

0.1M Sodium Citrate dihydrate :- 14.7g Na citrate in 500ml distilled water

Citrate buffer working solution :-

9.0 ml of 0.1M citric acid

41.0 ml of 0.1M Na citrate

Bring to 500ml total volume with distilled water and PH to 6.0 with 5N sodium hydroxide

1.4 TUNEL method- Intergen APOPTAG TUNEL kit protocol

1. REHYDRATE – 5 mins xylene, 3 mins per alcohol (Make sure all xylenes and alcohols are fresh)

2. PICRIC ACID – 2mins in saturated solution, thorough water washes until all acid removed.

3. 5 min PBS wash, ring round section with PAP pen.

4. PK : Try 15 mins at 10 ,5 and 2.5µg/ml - 100µl per slide @ RT

5. Wash in 2 changes of distilled water 2x2mins.

6. QUENCH - in 3% H_2O_2 in PBS for 5mins. 36mls PBS + 4ml H_2O_2

7. Wash 2 x 5min in PBS.

8. EQUILIBRATION BUFFER supplied in kit - apply 75µl per slide for at least 10 secs. Slides may be left in equilibration buffer for 60mins at 4^{o}C as a stopping point.

9. TdT ENZYME - No washes tap off excess liquid add 55µl per slide

-ve control RB + water instead of TdT enzyme.

77µl Reaction Buffer (RB)	38µl RB
33µl TdT	11µl TdT
110µl total enough for 2 slides	5µl Dnase free water
	54µl total for 1 slide

apply for 1 hour @ 37^{o}C cover sections with plastic coverslips

10. STOP BUFFER supplied in kit - agitate for 15 secs, incubate for 10 mins

1ml stop buffer stock(freezer) + 34 ml dist. water

11. Wash 3x 1 min in PBS. Take out an aliquot of anti-digoxigenin enough for number of slides and let warm up to room temp.

12. ANTI-DIGOXIGENIN : tap off excess liquid, apply 65µl per slide, coverslip and leave for 30 mins at room temp.

13. Wash 4x2mins in PBS.

14. DAB 5-10 mins – prepare as for ABC methods in immunohistochemistry

15. COUNTERSTAIN – 0.5% methyl green for 5-10 mins. Then wash specimens in three changes of dist. water leaving in last one for 30 secs. Then in 3 changes of 100% n-butanol leave in last one for 30 secs (all done in coplin jars) then take straight to xylene. This will prevent methyl green coming out of the section.

16. Mount in d.p.x.

1.5 Solutions for use with APOPTAG protocol

- Dnase free water – from biochemistry, in autoclaved bottle, 1x 400ml and two small bottles.
- PK buffer – make up in autoclaved bottle : 500ml
  30g TRIS (Bor min)
  9.25g EDTA
  Dnase free water
  PH7.6 with HCL

- PK – Stock in freezer @ 1000µg/ml a 1/50 dilution gives 20µg/ml double diluting for 10,5 etc
- PBS – 3 PBS tablets in 600ml distilled water.

Coplin jars and bottles all autoclaved, -ve control : no TdT.

Appendix 2: Western blot analysis

2.1 western blot method

1. Use Invitrogen 4-12% Bis-Tris gels, MES running buffer and appropriate transfer buffer and sample buffer for these gels.
2. After sample preparation add 20ul sample, 8ul sea blue 2 standard and appropriate amount of positive control to gel. 12 well 4-12% Bis-Tris gels are used.
3. Prepare running buffer as per Bis-Tris method book, run samples on gel at 200v for approx 45 mins until both sample buffer and protein has run to bottom of gel.
4. Remove gels and transfer to PVDF membrane as per instructions in Bis-Tris method book.
5. Remove pvdf membrane from transfer block wash in methanol and rinse in tap water.
6. Place in blocking solution - 3% non fat milk in TBS for approx 2 hours.
7. Add primary antibody diluted in blocking solution at appropriate concentration, leave in fridge overnight.
8. 3x5min washes in TBST (TBS with 0.05% tween 20)
9. Block 10mins in blocking solution.
10. Add appropriate secondary antibody diluted in blocking solution. Use at 1/30,000 dilution and leave on at room temp for 1 hour.
11. Copious washes in TBST- 6x10mins.
12. 2x 5min washes in water.

    Chemmiluminescent visualisation using solutions A and B from upstate kit. For two blots add 500ul A + 1000ul B vortex to mix cover with foil and let warm up to room temp before use.
13. Add chemmiluminescent solution to blot for 5mins.

14. Develop blot using Kodak imager, monitoring development of protein bands.

Semi-quantitative analysis of amounts of protein observed on gel is performed.

2.2 List of antibodies used in western blot analysis

Antibody	**Antibody type**	**Conc./time**	**Source**
Synaptophysin	Rabbit polyclonal	1/1000 overnight at 4^{o}C	Synaptic systems
Drebrin	Mouse monoclonal	10µg/ml overnight at 4^{o}C	MBL international
PSD-95	Rabbit polyclonal	1/1000 overnight at 4^{o}C	Synaptic systems
Active caspase-3	Rabbit polyclonal	0.5µg/ml overnight at 4^{o}C	R&D systems
Active caspase-3	Rabbit polyclonal	1/2000,1/4000 overnight at 4^{o}C	pharmingen
Active caspase-3	Rabbit polyclonal	1/700 overnight at 4^{o}C	Cell signalling technology
Active caspase-8	Mouse monoclonal	1/1000 overnight at 4^{o}C	Cell signalling technology
Active caspase-9	Rabbit polyclonal	1/1000 overnight at 4^{o}C	Cell signalling technology
Alpha tubulin	Mouse monoclonal	1/2000 overnight at 4^{o}C	Lab vision
Bcl-2	Mouse monoclonal	0.5µg/ml overnight at 4^{o}C	Upstate
Bax	Rabbit polyclonal	0.5µg/ml overnight at 4^{o}C	Upstate

Appendix 3: FACS analysis method

3.1 FACS analysis method

1. Remove brain and place into growth medium without buffers, RPMI or HBSS can be used.
2. Incubate all tissue on ice.
3. Brain dissected into three pieces the front, mid and hind brain and placed into dissociation medium (sigma) for 15mins at 37^{o}C. Remove after 15 mins and gently suck the tissue up in a syringe and expel back into dissociation medium and leave in incubator for a further 15mins.
4. Pour tissue and dissociation medium into a 100µm sieve and gently strain tissue through sieve using a 1ml syringe containing HBSS.
5. Centrifuge at 1500-2000 rpm for 5-10mins at 4^{o}C.
6. Resuspend cells in 1ml FACS buffer (see below).
7. Perform cell count using trypan blue and haemocytometer and calculate number of cells/ml and add 1x10^{6} cells to 50µl of FACS buffer.
8. Add cells to microtitre plate and incubate with appropriate primary antibody (for microglia – F4/80 FITC conjugated, neurons- NeuN mouse monoclonal), incubate on ice for 40mins
9. wash x3 in FACS buffer, spin microtitre plate at 1500rpm/5mins at 4^{o}C and resuspend cells in fresh buffer.
10. Incubate with appropriate secondary antibody if needed. For NeuN used goat anti mouse FITC.
11. Wash x3 in FACS buffer then analyse on the FACS machine.

3.2 Solutions for FACS analysis

FACS buffer 10x

di-sodium hydrogen orthophosphate	25.6g
sodium chloride	74.8g
potassium di-hydrogen orthophosphate	3.88g
potassium chloride	2.01g

make up to 1litre with distilled water

FACS buffer working solution

For 1 litre
100ml of 10x made up to 1litre in distilled water add:

Sodium azide	1g
BSA	1g
EDTA	0.2g